Nitrogen cycling in a calcareous fen peatland: stresses, controls, and variability

A thesis submitted for the degree of Doctor of Philosophy

Department of Geography and Environmental Science

Phillip Agredazywczuk

March 2023

Declaration

I confirm that this is my own work and that the use of all material from other sources has been properly and fully acknowledged.

Phillip Agredazywzcuk

The maps throughout this thesis were created using Esri's ArcGIS® software. ArcGIS® and ArcMap™ are the intellectual property of Esri and are used here under licence. Copyright Esri. All rights reserved. For more information on the Esri® software, visit www.esri.com.

Abstract

This thesis describes nitrogen (N) cycling in Greywell Fen (38-ha) - a calcareous, nitrate-enriched groundwater-fed peatland in the Loddon catchment in the south of England. Peatlands are important environments for N cycling, and Greywell Fen is of particular interest because of plans to abate further ecological degradation by ceasing groundwater abstraction; essentially, this would involve rewetting the site with the nitrate-enriched groundwater. This is the first study to quantify the N dynamics in Greywell Fen. A year-long intensive monitoring programme was carried out, focussing on fortnightly measurement of the hydrochemistry and hydrology of fen porewaters, groundwater, and surface waters. Analysis of N concentrations and water table heights established that groundwater abstraction had a relatively limited effect on the fen water table and that nitrate concentrations in the fen varied spatially more than temporally, where discrete nitrate-rich porewater sites existed. Multivariate statistical analysis of N and dissolved solutes demonstrated that the hydrological transfer and cycling of nitrate in the fen were controlled mainly by discrete inflows of nitrate-enriched groundwater, which was regulated by the thickness of a clay layer dividing the fen and the Chalk aquifer. The effects of soil rewetting were then investigated through a laboratory experiment. Intact soil columns, extracted from the fen, were rewetted with nitrate-enriched water, and the porewater hydrochemistry and nitrous oxide gas emissions were measured. Higher nitrate concentrations at the peat surface and nitrous oxide release were both observed in soil columns with a thinner clay layer, particularly during partially and fully water saturated conditions. In terms of site management, the research demonstrated that groundwater abstraction shutdown may not be necessary to prevent further ecological degradation of the fen. In a broader context, the research demonstrates the importance of considering hydrogeology when restoring peatlands for the specific use of nitrate buffering, as well as the risk of nitrate saturation and increased nitrous oxide release resulting from direct nitrate-enriched groundwater inflow.

Acknowledgements

Contents

6.0 Nitrogen and Hydrochemical Transfer and Cycling in Nitrate-enriched Calcareous

7.0 Nitrogen Buffering Capacity and Nitrous Oxide Release in Nitrate-enriched Fen Peat

ix

List of Figures

List of Tables

Glossary of Abbreviations

Total Aluminium	Al
Ammonium	NH_4-N
Anaerobic ammonium oxidation	ANAMMOX
Bicarbonate	HCO_3
Calcium	Ca^{2+}
Carbon/nitrogen ratio	C:N
Carbonate	CO_3
Carbon dioxide	CO_2
Chalk groundwater sampling site	CG
Chloride	Cl^-
Complete ammonium oxidation	COMAMMOX
Concentration-Based Estimated Deposition	CBED
Diffusion gradient in thin films	DGT
Dissimilatory nitrate reduction to ammonium	DNRA
Dissolved organic carbon	DOC
Dissolved organic nitrogen	DON
Groundwater springs	GS
Hierarchal cluster analysis	HCA
Hydrological monitoring site	GF
Inorganic nitrogen	IN
Ion exchange membranes	IEM
Magnesium	Mg^{2+}
Magnesium/calcium ratio	Mg:Ca
Methane	CH_4
Metres Above Ordnance Datums	mAOD

Nitrogen	N
Nitrate	NO_3-N
Nitric Oxide	NO
Nitrogen gas	N_2
Nitrogen isotope	$\delta^{15}N$
Nitrous Oxide	N_2O
Oxygen isotope	$\delta^{18}O$
Oxygen	O_2
Phosphorus	P
Polyethersulfone	PES
Polyvinyl chloride	PVC
Porewater sampling site	PW
Potassium	K^+
Principal component analysis	PCA
Rhizon soil moisture samplers	Rhizon SMS
Shallow groundwater sampling site	SG
Silicon	SiO_2
Sodium	Na^+
Special Site of Scientific Interest	SSSI
Strontium/calcium ratio	Sr:Ca
Sulphate	SO_4^{2-}
Surface water sampling site	SW/PS
Total dissolved solids	TDS
Total iron	Fe
Total nitrogen	TN

1.0 Introduction

Peatlands are unique environments, which are globally important for carbon storage and sequestration, drinking water, biogeochemical cycling, and biodiversity (Verhoeven, et al., 2006; Acreman, et al., 2011; Zomeren, et al., 2012; Ramsar Convention on Wetlands, 2018). Peatlands are found in a variety of climates, from tropical to polar, covering approximately 4.23 million km^2 of the world's surface (Xu, et al., 2018). The United Kingdom is estimated to contain between 9 and 15% (46,000 to 77,000 km^2) of European peatlands. However, estimates suggest that 80% of UK peatlands are in a damaged or deteriorating state (IUCN, 2018). Peatlands can be divided into two main environments: bogs and fens (Joosten, et al., 2016). Bogs are ombrotrophic, receiving water and nutrients exclusively through precipitation (Charman, 2003), while fens can be either minerotrophic (synonymous *rich fens*) or mesotrophic (synonymous *poor fens*). Rich fens receive mineral-enriched calcareous waters via groundwater and/or overland flow (Bridgham et al., 2001); whereas, in hydrochemical terms, poor fens are intermediate between minerotrophic and ombrotrophic (Paulissen, et al., 2004). Fen peatland loss or degradation is associated with a change in land use, for example, a change to farmland through drainage ditches or drinking water abstraction, resulting in lower groundwater tables (Beltman, et al., 1996; Rückauf, et al., 2004). In the UK, peatlands are linked to many socioeconomic activities, such as drinking water provision (Bain, et al., 2019).

In addition to fen peatland degradation, nitrogen (N) pollution in groundwater and surface water has increased globally over the last few decades (Galloway, et al., 2003). In general, this can be attributed to intensive agricultural practices (Ardón, et al., 2010). It is well known that N derived from agriculture, for example, nitrate (NO_3-N), can leach into waterways and cause freshwater and marine eutrophication episodes (Lewis, et al., 2011; Hou, et al., 2015; Wang, et al., 2016). Eutrophication is the increase in nutrients in a freshwater or marine area that can occur naturally or be human-induced, for example, nitrate-enriched hydrological inputs (Jonge, et al., 2002). Toxic algal blooms can occur in response to these inputs, which

can result in major ecological and socioeconomic damage; however, the intensity of the bloom is also linked to water residence time, temperature, and light as much as nutrient concentrations (Howarth & Marino, 2006; Lewis, et al., 2011; Moal, et al., 2019). Furthermore, NO_3-N can negatively affect human and animal health (Ward, et al., 2018). It should be noted that phosphorus (P) is also a nutrient that can induce eutrophication (Beltman, et al., 1996; Pieterse, et al., 2005; Boomer & Bedford, 2008); however, throughout this investigation, P concentrations were near or below the detection limits (Section 6.2.1), and therefore not considered for the research.

NO_3-N pollution is difficult to control as it generally occurs through diffuse or non-point sources (Ardón, et al., 2010). Furthermore, as a highly soluble ion, NO_3-N travels easily with water flow, and therefore, can easily leach into waterways and groundwaters (Forster, et al., 1982; Almasri & Kaluarachchi, 2007). Consequently, there has been significant interest in the capacity of peatlands to control NO_3-N pollution (for example, Brix, 1994; Hoffmann et al., 2011; Lind, et al., 2012; Kleimeier et al., 2018; Mwagona, et al., 2019; Han, et al., 2020). The inundation and biogeochemical characteristics of peatlands are suitable for the retention and removal of NO_3-N through various microbial and biogeochemical processes (Fisher & Acreman, 2004; Cabezas, et al., 2012; Kleimeier, et al., 2017). Despite this, peatlands can reach a critical load or N saturation, which can result in vegetation change, loss of biodiversity, reduced N removal, and increased N leaching as the assimilation capacity of the system is reached (Hanson, et al., 1994; Verhoeven, et al., 2006; Hefting, et al., 2006; Cusell, et al., 2013). Furthermore, NO_3-N enrichment in peatlands has been shown to increase nitrous oxide release, a strong greenhouse gas (Lohila, et al., 2010; Lind, et al., 2013; Leroy, et al., 2019).

Degraded or managed fen peatlands with lower groundwater tables can result in profound biogeochemical changes, as the subsurface conditions change from anoxic to oxic. The introduction of oxygen into the system activates oxidation and hydrolytic enzymes in the peat layer (Freeman, et al., 2001), thus increasing the decomposition of organic substances. These

processes contribute to peat degradation, nutrient export, greenhouse gas release, and internal eutrophication, where nutrient release can result in vegetation changes and biodiversity loss (Smolders, et al., 2007; Zak & Gelbrecht, 2007; Macrae, et al., 2013). Essentially, lower water tables reduce the effectiveness of net N removal.

With increased awareness of the importance of peatlands and associated problems, restoration projects have increased (Zak, et al., 2011), and are considered a valid method to reduce the NO_3-N enrichment of waters (Haycock, et al., 1993; Trepel & Palmeri, 2002). Restoration involves rewetting the system, for example, removing drainage ditches or restoring natural groundwater levels. These management interventions aim to return the biogeochemical environment to its original anoxic state (Wheeler, et al., 1995; Venterin, et al., 2002; Rückauf, et al., 2004). However, the return to an anoxic state causes a rapid change in redox conditions, possibly inducing nutrient release, internal eutrophication, and vegetation changes (Venterin, et al., 2002; Cabezas, et al., 2012; Riet, et al., 2013; Koskinen, et al., 2017).

Restoration of fen peatlands with nitrate-enriched groundwater, after a period of managed water table drawdown, can alter the biogeochemical nature of the peat environment (Cabezas, et al., 2012; Cusell, et al., 2013). For example, rewetting previously drained fens with high NO_3-N loads have been shown to increase ammonium (NH_4-N) and dissolved organic nitrogen (DON) export (Cabezas, et al., 2012). Furthermore, NO_3-N retention across a peatland is highly variable over space and time, adding further complexity to investigations (Tiemeyer, et al., 2007; Johnes, et al., 2020). In general, few studies have explored the effect of rewetting fens with nitrate-enriched groundwater (Rückauf, et al., 2004; Cabezas, et al., 2012), with no studies particularly focussing on groundwater-fed fens with water tables managed by groundwater abstraction. Considering this, the inflow of nitrate-enriched groundwater into managed fen peatlands remains relatively ambiguous.

Greywell Fen, in Hampshire, southern England, is a minerotrophic peatland that receives calcareous and nitrate-enriched (eutrophic) groundwater and is adjacent to the River Whitewater, a tributary of the River Loddon (Davies, 2012; South East Water, 2019). The fen is characterised by porewater with an alkaline pH, high concentrations of Ca^{2+} and CO_3, and high diversity of plant species (Davies, 2012; Low, et al., 2012; South East Water, 2020). In general, fens are associated with the richness of plant species, since they transcend the terrestrial and aquatic environment. Consequently, Greywell Fen is a Site of Special Scientific Interest (SSSI) (Natural England, 1984). However, the fen has been designated in an ecologically unfavourable – declining condition (Natural England, 2018), with previous hydrological reports suggesting that the local groundwater abstraction site (currently operated and managed by South East Water Ltd) lowers groundwater tables and therefore negatively affects plant species in the fen (Low, et al., 2012; Jacobs, 2019). As a result, the decision has been taken to cease groundwater abstraction at Greywell Fen soon, raising concerns that this could lead to increased NO_3-N enrichment of the fen due to an increase in the (nitrate-enriched) groundwater table. However, since the groundwater abstraction shutdown has not yet occurred, there is a requirement to simulate the shutdown. Therefore, the potential effect of rewetting with nitrate-enriched groundwater will be investigated through laboratory simulations of groundwater behaviour; these controlled experiments will complement the field observations, as detailed in the Thesis Structure (Section 1.1).

This thesis aims to evaluate the N dynamics in a managed calcareous rich fen peatland fed by nitrate-enriched groundwater. Furthermore, the study assesses the impacts of groundwater restoration and proposes mitigation options, if necessary. Greywell Fen will be used as a case study. Specifically, the objectives are to (1) monitor groundwater table height and N concentrations in the fen and related water sources over space and time; (2) determine the hydrochemical transfer and cycling of N in the fen and related water sources; (3) quantify the porewater N cycling and nitrous oxide release in rewetted nitrate-enriched fen peat; and (4) if

necessary, propose mitigation measures to prevent the fen from increased NO_3-N enrichment resulting from a groundwater abstraction shutdown.

1.1 Thesis Structure

   This thesis is structured in a paper-style format. Each of the results chapters (Chapters 5 – 7) is presented in the style of a research paper, with the view of these being submitted for publication during 2023-2024. The thesis consists of a general introduction, a literature review, two technical sections outlining the study site and methodologies for continuous field monitoring, followed by three paper-style study chapters prepared for future publication, and finally, a conclusion chapter summarising the research findings and wider implications. As a result, there is some repetition in the chapters, particularly in the introduction and methodological sections. This thesis is structured as follows:

Chapter 1 – General introduction outlines the importance of rich fen peatlands and the effects of human-induced issues, particularly water table management and NO_3-N enrichment on a global and local scale.

Chapter 2 - Review of NO_3-N contamination in calcareous groundwater and N cycling in fen peatlands, particularly with a focus on the effects of drying-rewetting and NO_3-N enrichment. This chapter also presents a technical review of NO_3-N tracking methods and experimental designs; these were completed to find novel methods and knowledge gaps for investigating N cycling in these dynamic systems.

Chapter 3 – Technical description of the study site, Greywell Fen. This includes descriptions of the general study area, geology, ecology, hydrogeology, human management, and N inputs.

Chapter 4 – Technical description of the field sampling methodologies and laboratory analytical techniques used for continuous site monitoring, directly related to Chapters 5 and 6.

Chapter 5 – Monitoring programme on groundwater table movement and N concentrations in the fen and related water sources over space and time. This was essential to understand the effects of water table management and NO_3-N enrichment on lowland peatlands in the real environment, providing context to the N status at this unique study site.

This chapter - 'Nitrogen Concentrations in a Calcareous Nitrate-enriched Fen across Space and Time' - aims to assess the N status of groundwater-fed calcareous peatlands impacted by nitrate-enriched groundwater and groundwater abstraction. The following objectives were established to achieve this aim: (1) identify the N variability in the fen porewater and related water sources throughout space and time; (2) investigate the impact of groundwater abstraction on (a) water table heights and (b) porewater N; and (3) asses the processes that can be attributed to the observed N variability in the fen porewater.

Chapter 6 – The application of multivariate statistical analysis for solute chemistry analysis in the study of hydrological transfer and cycling of N in the fen. Hydrological transport of dissolved substances can have a particularly important effect on biogeochemical cycling, especially in fens, which can have high hydrological connectivity to groundwater and surface waters.

This chapter - 'Nitrogen and Hydrochemical Transfer and Cycling in a Nitrate-enriched Calcareous Fen' - undertakes a rigorous multivariate approach to understand N transfer and cycling as a result of hydrology and hydrogeochemistry in a calcareous nitrogen-enriched peatland. The following objectives were established to achieve this aim: (1) determine the

6

hydrological connectivity of the fen porewater with the other site water sources; (2) evaluate the transfer of N in the system through the porewater and other site water sources; and (3) determine where and how N cycling may occur as a result of hydrological connectivity and hydrochemical controls.

Chapter 7 – Laboratory simulation of fen peat restoration with nitrate-enriched water. This provided an opportunity to investigate porewater and gaseous N cycling at high spatial and temporal resolutions, and further examine and complement the observations made in Chapters 5 and 6.

This chapter - 'Nitrogen Buffering Capacity and Nitrous Oxide Release in Nitrate-enriched Fen Peat' - aims to evaluate the nature of porewater NO_3-N cycling and nitrous oxide release in nitrogen-enriched peat at different water table heights. Based on the key findings from Chapters 5 and 6, the hypothesis for this chapter was the following:

NO_3-N concentrations in the porewaters and nitrous oxide release will be higher during (1) high nitrate-enriched water tables and (2) in nitrate-rich porewater sites due to hydrogeological factors.

The following objectives were established to achieve this aim: (1) simulate the effect of groundwater abstraction shutdown at two fen sites with contrasting NO_3-N concentrations; (2) determine the effect of water table height and NO_3-N enrichment on N dynamics; (3) determine the effect of different water table heights and NO_3-N enrichment on nitrous oxide release; and (4) investigate the influence of DOC and Fe chemistry on N dynamics.

Chapter 8 – A synthesis of the key research findings, proposing an evidence-based conceptual model of N cycling in Greywell Fen. The chapter concludes with a critical

commentary on the current research's local and broader implications for understanding N

cycling in fen peatlands.

2.0 Literature Review

2.1 Introduction

This literature review provides additional context for the research. It builds on the challenges presented in Chapter 1, develops the research justification, and identifies the major knowledge gaps to be addressed in the thesis. Section 2.2 establishes the context of N contamination in Chalk aquifers in the United Kingdom. Section 2.3 provides a general overview of N cycling in peatlands and reviews the literature on this topic, focussing on water table dynamics and NO_3-N enrichment. Furthermore, Sections 2.4 and 2.5 review previous methodologies that have been used to further investigate N cycling in the environment and peatlands, specifically tracking waterborne NO_3-N and subsequent cycling reactions in a system, and previous experimental designs of peat mesocosms. Lastly, Section 2.6 provides a summary of the justification and knowledge gaps identified from the reviewed literature.

2.2 Nitrogen Contamination in Chalk Aquifers

In north-western Europe, Chalk aquifers provide an important source of drinking water, providing up to 55% of drinkable groundwater in the United Kingdom (Haria, et al., 2003; Sorensen, et al., 2015). In lowland areas, Chalk aquifers are commonly unconfined, where surface water can flow directly through the unsaturated zone of the aquifer and replenish it, known as groundwater recharge (MacDonald & Allen, 2001). Groundwater recharge is defined as water that travels from the unsaturated zone to the saturated zone of the aquifer; the water table defines the boundary between these two zones (Ireson & Butler, 2011). This process is an important control of pollution transfer and is influenced by geological characteristics. Chalk aquifers have a dual porosity structure, where water flows through the matrix (piston flow) or more rapidly through fractures (preferential flow), which influences the dilution, attenuation,

and degradation of a pollutant (Gooddy, et al., 2007; Sorensen, et al., 2015). N transport in Chalk aquifers is essential to understand NO_3-N enrichment in calcareous systems.

Generally, the application of N fertilisers to agricultural soils exceeds plant demand and N cycling capacity; this often leads to N leaching, particularly in the NO_3-N form, which is a highly mobile, water-soluble ion (Forster, et al., 1982; Almasri & Kaluarachchi, 2007). Eventually, the leaching of NO_3-N through the unsaturated zone will reach the saturated zone of the aquifer and groundwater. This occurs over years to decades because the soil-aquifer-groundwater system is complex (Lee, et al., 2006). In the unsaturated zone, waterborne NO_3-N is subject to either the aforementioned piston or preferential flow (Wellings & Bell, 1980). Generally, piston flow is the dominant flow type, whereas preferential flow only occurs when the matrix is fully saturated, for example, during rainfall events (British Geological Survey, 1999; Price, et al., 2000; Haria, et al., 2003). The slow movement of NO_3-N in the unsaturated zone results in long-term storage. For example, Foster & Bath (1983) found NO_3-N concentrations of 1100 kg N ha^{-1} in the upper 8 m of the Chalk profile, with concentrations of up to 75 mg N l^{-1} leaching to the saturated zone. Furthermore, Sorensen (2015) found leaching rates of 0.3 to 1.4 m yr^{-1} in a Chalk aquifer. NO_3-N removal by denitrification is limited in Chalk aquifers due to low organic carbon concentrations, an important electron donor in the reaction (Forster, et al., 1982; Wang, et al., 2016). Consequently, NO_3-N contamination in Chalk aquifers is common (Table 2.1), known as 'legacy nitrate storage'. Wang et al. (2016) reported that 16 of 28 Chalk aquifers in the UK showed increasing concentration trends of NO_3-N, which was likely to continue for decades.

NO_3-N contamination in Chalk aquifers is important because it can have significant impacts on the health of aquatic or groundwater-dependent ecosystems (for example, Feast et al., 1997; Jarvie, et al., 2005; Howden & Burt, 2008; Howden, et al., 2010; Allen, et al., 2010; Wexler, et al., 2012; House, et al., 2015; Stuart & Lapworth, 2016). Jarvie et al. (2005) found that NO_3-N concentrations in rivers and groundwater in an English Chalk catchment were

similar, averaging 1.24 and 1.21 mg NO_3-N l^{-1}, with NO_3-N contamination causing habitat deterioration in the spring-fed river. This illustrated the significant impact groundwater quality can have on surface waters. Allen et al. (2010) found that NO_3-N concentrations in gravel, groundwater, and river water in a calcareous riparian peatland were 6.60 mg NO_3-N l^{-1}, 6.13 mg NO_3-N l^{-1}, and 7.13 mg NO_3-N l^{-1}, respectively. This demonstrated the high level of hydrological connectivity in these systems and the presence of nitrate-enriched groundwater in different water sources of the system.

Groundwater and surface water are valuable water resources, which require management policies to reduce N loading from intensive agriculture practices, but due to the limited in situ removal of NO_3-N and the high amount of NO_3-N storage in Chalk aquifers, the benefits of N management policies will not be apparent for decades (Hansen, et al., 2017). In southeast England, many Chalk aquifers are located in lowland catchments, resulting in groundwater upwelling. Fen peatlands are suitable for restoring nitrate-enriched surface and groundwater, as they are water saturated throughout the year, providing ideal conditions for denitrification, an important NO_3-N removal process. NO_3-N removal studies in surface and groundwater in riparian lowland peatlands or wetlands are extensive (for example, Haycock & Pinay, 1993; Hanson, et al., 1994; Correll, et al., 1997; Spruill, 2004; Hill, 2019). Haycock & Pinay (1993) compared two riparian zones for their NO_3-N retention capacity. The poplar tree zone showed a higher retention capacity, 99% compared to 84% in the grass-vegetated riparian zone. This difference was due to the different NO_3-N loading rates and organic carbon concentrations at the two sites. Hanson et al. (1994) reported a NO_3-N removal rate of 40 kg N ha^{-1} yr^{-1} in a nitrate-enriched riparian wetland, which was up to 50% of the NO_3-N in the subsurface flow. However, uncertainties remain about the inflow of nitrate-enriched groundwater and the effectiveness of fen peatlands as NO_3-N buffers (Hill, 2019). In general, peatlands are complex systems, where N cycling is affected by a variety of factors (Section 2.3), for example, hydrology, hydrogeology, and hydrochemistry. More research is required to better understand the uncertainties of N cycling in peatlands, particularly over space and time.

Table 2.1: Summary of the concentrations of N species in groundwater and rivers in unconfined Chalk aquifers. All N species concentrations were reported as N-nitrogen. The symbol '–' represents below the detection limit. A portion of the information was adapted from Stuart & Lapworth (2016).

Water source	Location	NO$_2$-N (mg l^{-1})			NO$_3$-N (mg l^{-1})			NH$_4$-N (mg l^{-1})			Reference
		Min.	Mean	Max.	Min.	Mean	Max.	Min.	Mean	Max.	
Groundwater	Norfolk					0.00					Feast et al. (1997)
	Hampshire				0.001	1.21	8.79				Jarvie et al. (2005)
	Berkshire					6.13					Allen et al. (2010)
	Norfolk										
	Deep					-					
	Shallow					9.81					Wexler et al. (2012)
	Berkshire					5.65					House et al. (2015)
	Yorkshire/Humber	< 0.01	6.00	0.27	< 0.50	9.50	33.20	< 0.003	20.00		Smedley et al. (2004)
	North Norfolk	0.002	0.09	4.07	0.001	0.090	21.80	0.001	0.001	0.010	Ander et al. (2006)
	Great Ouse	< 0.001	0.019	0.101	0.29	10.30	38.40	< 0.003	0.011	0.170	Ander et al. (2004)
	Colne/Lee	< 0.001	0.006	0.053	3.20	6.40	11.20	< 0.003	0.017	0.150	Shand et al. (2003)
	North Downs	< 0.003		0.008	0.20		28.20	< 0.009		12.00	Smedley et al. (2003)
	Hampshire	< 0.001	0.002	0.01	< 0.050	6.58	12.60	< 0.005	0.009	0.066	Stuart & Smedley (2009)
River	Hampshire				0.016	1.24	6.35				Jarvie et al. (2005)
	West Dorset										
	River Frome				0.053	0.018	0.10				
	River Piddle				0.11	0.031	0.18				Howden & Burt (2008)
	West Dorset										
	River Frome	0.01	0.05	3.94	0.16	4.80	12.14	0.01	0.05	0.30	
	River Piddle	0.01	0.05	0.67	0.41	5.37	29.44	0.01	0.07	2.84	Howden et al. (2010)
	Berkshire					1.61					Allen et al. (2010)
	Norfolk					8.40					Wexler et al. (2012)

2.3 Peatland Nitrogen Cycle

N accounts for around 80% of the atmosphere as nitrogen gas (N_2). Despite this, the bioavailable N for plants and microbes in soils is limited, either as NH_4-N or NO_3-N (Wetzel, 2001; Jain & Singh, 2003). The availability of soil N depends on prokaryote N fixation, which is the reduction of nitrogen gas to NH_4-N. Furthermore, organic matter mineralisation in soils can be an internal source of N, which is the microbial-mediated release of NH_4-N from organically bound N (Rascio & Rocca, 2008; Hagemann, et al., 2016). The latter reaction can occur in both the aerobic and anaerobic zones of a peatland, but mainly in the aerobic zone. Organic matter mineralisation is influenced by oxygen concentrations (O_2), temperature, microbial activity, and the carbon/nitrogen (C:N) ratio (Roy & White, 2013; Stefanakis, et al., 2014). NH_4-N produced from these reactions can be cycled through various N cycling reactions, presented in Figure 2.1.

NH_4-N accumulates in the inundated anaerobic soil layer and diffuses to the oxidised soil layer or the water column, where it is subject to nitrification (Lindau, et al., 1999), an oxidative stepwise reaction from NH_4-N to NO_3-N, with nitrite (NO_2-N) as an intermediate. The reaction is limited by oxygen concentrations (Sandrin, et al., 2009). NO_3-N diffuses to the anaerobic layer, where it is cycled by denitrification, a stepwise reduction reaction from NO_3-N or NO_2-N to N_2, including the intermediates nitric oxide (NO) and nitrous oxide (N_2O) (Martens, 2005). Under certain conditions, denitrification can be disrupted, releasing intermediates NO or N_2O, two strong greenhouse gases (Rückauf, et al., 2004). This is considered mainly controlled by soil pH and moisture content (Šimek, et al., 2004; Harris, et al., 2021). The aerobic requirement of nitrification conserves N in peatlands, preventing complete N removal. Therefore, denitrification is limited by NO_3-N availability, as well as organic carbon and oxygen concentrations (Rivett, et al., 2008). Nitrification and denitrification are important peatland N cycling reactions; however, other reactions, such as dissimilatory nitrate reduction to ammonium (DNRA), anaerobic ammonium oxidation (ANAMMOX), and complete ammonium

oxidation (COMAMMOX), can contribute to N cycling in peatlands. Dissimilatory nitrate reduction to ammonium is an anaerobic reaction, but its relative importance in peatlands and wetlands has been shown to vary widely (D'Angelo & Reddy, 1993; Pan, et al., 2020). Anaerobic ammonium oxidation is an anaerobic stepwise reaction that converts ammonium to nitrogen gas via nitrite reduction. Hou et al. (2015) estimated that the reaction accounted for approximately 3.8 to 10.7% of the total reactive N removal in a coastal marsh. Complete ammonium oxidation is a recently discovered one-step conversion of NH_4-N to NO_3-N; the details of its activity in peatlands are uncertain, but recent studies have suggested that it could occur in freshwater systems (Daims, et al., 2015). In general, oxygen concentrations are the main control of N cycling reactions in fen peatlands, which is mainly controlled by the groundwater table height, which acts as a boundary between the aerobic and anaerobic zones. Therefore, the water table height is an important predictor of N speciation in peatland soils. Additionally, peat soil has a particularly unique structure that can also influence N cycling.
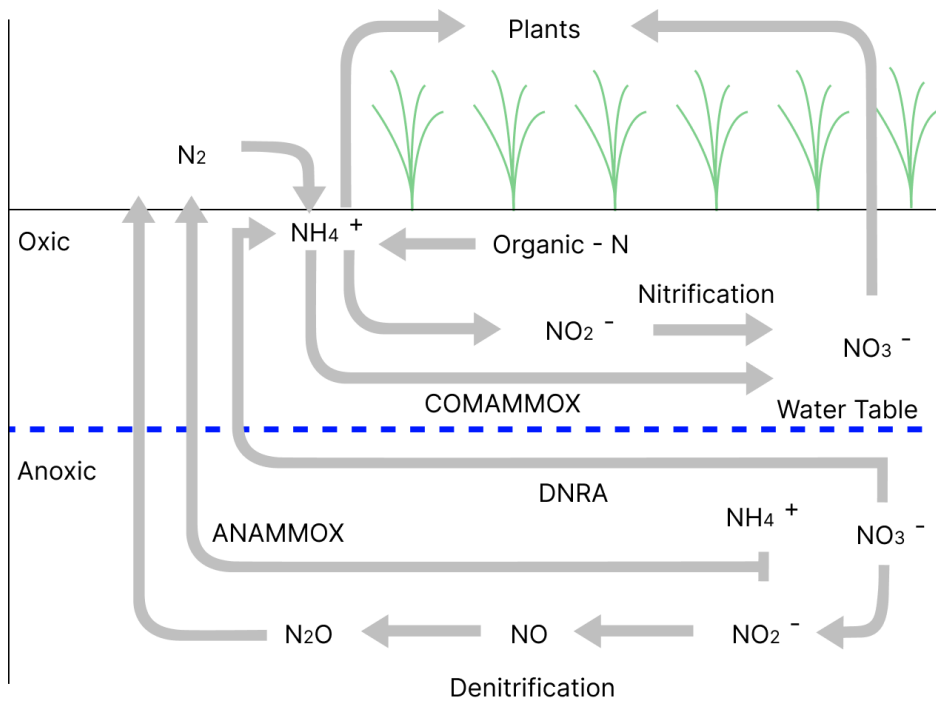
Figure 2.1: General peatland N cycle.

2.3.1 Porewater Nitrogen Cycling

Peat soil has a dual porosity structure, which refers to two regions of permeability; a 'mobile region' where water flow is high and an 'immobile region' where water flow is close to none (Rezanezhad, et al., 2012; Rezanezhad, et al., 2017). Peat has a high porosity (approximately 90%), where water is contained in large interparticle pores (active porosity) (Boelter, 1968), and the remaining water is contained in small closed pores that are immobile (inactive porosity) (Hoag & Price, 1997; Quinton, et al., 2000). As a result, solutes can exchange between mobile and immobile regions through diffusion, advection in the open and connected (active) pores, and matrix diffusion in and out of the immobile pores (Rezanezhad, et al., 2016). The exchange of solutes through the 'active' and 'inactive' pores can control the rate of biogeochemical reactions. For example, an increase in 'active porosity' can accelerate NO_3-N delivery to denitrifying microorganisms present in small 'inactive' pores (Watt, et al., 2006; Rezanezhad, et al., 2017). Furthermore, peat permeability decreases with depth, where the 'active porosity' is reduced as the peat becomes more humified, which is the degree of organic material decomposition (Klavins, et al., 2008). This separates porewaters between the immobile and mobile regions, limiting the exchange from the surface to the atmosphere (Caron, et al., 2015; Rezanezhad, et al., 2016). However, water table lowering can alter the peat structure through decomposition and degradation, which can further influence solute transport and biogeochemical reactions. Peat decomposition can be inferred using C:N ratios (Bridgham, et al., 1998). As a result, N variability and N speciation can vary over space and time due to the variability of water table height and peat heterogeneity (Duren & Pegtel, 2000).

2.3.2 Peatland Nitrogen Cycling Response to Water Tables

It should be noted that an N cycling rate is a relatively ambiguous term that can represent several different calculation methods, depending on the specific N cycling reaction or the study medium, that is, static soil or flowing water (Tietema, et al., 1993; Lind, et al., 2013; Yao, et al., 2018). For example, Tietema et al. (1993) calculated the nitrification rate as the difference in NO_3-N concentration over a period and the net N mineralisation rate as the difference in total inorganic N concentrations over a period. These were then converted from mg N kg^{-1} to kg N ha^{-1} yr^{-1} using an incubation period and the mean dry weight of the soil samples. While Lind et al. (2012) first calculated a NO_3-N flux (mg m^{-2} d^{-1}) using measured NO_3-N concentrations and flow rates through soil columns, and the NO_3-N cycling rate was calculated as the difference in the NO_3-N flux between the inlet and outlet of the soil columns. Therefore, an N cycling rate can be defined as the difference in the mass or concentration of an N species over a period that is scaled to an areal estimate using a unit converter, such as the dry weight of a soil sample or a flow rate.

Peatland and wetland responses to water table lowering are well known, resulting in increased N mineralisation, lower denitrification rates, increased nitrification rates, and N export (De Mars, et al., 1996; Venterink, et al., 2002; Mettrop, et al., 2014). De Mars et al. (1996) found that drainage considerably changed the chemical composition of the surface peat layer, increasing the risk of vegetation change, as well as increased drought vulnerability due to decreased capillary capacity. Mettrop et al. (2014) reported a considerable pH decrease after drainage, possibly due to the oxidation of reduced sulphur to sulphuric acid in the peat, increasing the risk of vegetation change. Venterink et al. (2002) found that the primary control of N cycling rates in soil cores was the water table height and pore space saturation. Dry cores (water pore saturation of approximately 45%) had increased N mineralisation, decreased denitrification, and increased dissolved organic nitrogen compared to wet cores (water pore saturation of 100%). Although Macrae et al. (2013) reported that

lowering the water table resulted in only modest increases in extractable NO_3-N and nitrification rates. Overall, it did not affect the concentrations of extractable inorganic N (IN) (NH_4-N and NO_3-N). As the water table was only 20 cm lower than in the control experiment, the minimal effect on N concentrations was attributed to capillary fringe, where water diffusion saturates peat pores by capillary action. The effects of lowering the water table in peatlands are generally well established. However, further investigation is necessary to understand the effects of drying-rewetting and NO_3-N enrichment in peatlands.

N dynamics after rewetting in lowland peatlands and wetlands is relatively well studied. Hoffmann et al. (2011) found a range of NO_3-N removal efficiencies in four resorted riparian wetlands, ranging from 8 to 95%. This variance was probably influenced by NO_3-N dilution by older, uncontaminated groundwater or NO_3-N leaching to deeper groundwater that bypassed the riparian areas. However, the monitoring periods for each wetland were different, where temporal variation could have affected the removal efficiency of the individual sites. Similarly, Hefting et al. (2006) reported groundwater dilution as a potential reason for the observed NO_3-N removal rates. They found removal rates of 63% and 38% in a rewetted grassland and riparian forest wetland, respectively. The lower removal rate in the forested wetland suggested N saturation, as it received a higher NO_3-N load and had a lower porewater pH, probably affecting denitrification. This N saturation may also have resulted in increased nitrous oxide release, but no gaseous measurements were performed during the study. Dijk et al. (2004) and Cusell et al. (2013) both found that restoring natural mineral-rich groundwater flows increased porewater pH and wetland alkalinity. In general, restoration aims to restore efficient denitrification; however, rewetting can influence other N cycling reactions. For example, Ardón et al. (2010) reported that fen restoration considerably reduced ammonia (NH_3-N) contamination in surface waters, but increased the export of DON and NH_4-N. In this context, removal rate estimates and N balances in peatlands and wetlands do not adequately consider the potential variability of internal N dynamics in peatlands across space and time under different drying-rewetting scenarios, particularly the production of other N species.

Few studies have explored the internal dynamics of N cycling in rewetted peatlands, with research focused primarily on highly degraded agriculture or highly polluted industrial areas. Dijk et al. (2004) found that the rewetting of acidified agricultural land with base-rich groundwater unexpectedly resulted in internal eutrophication. The higher water table increased soil pH and decomposition rates. Unlike decomposition rates, rewetting did not significantly affect net nitrification or net N mineralisation rates, possibly due to an increase in the denitrification rate, but this could not be confirmed. Zak & Gelbrecht (2007) rewetted previously drained peat in a 54-week mesocosm experiment; the water table was maintained 5 cm above the peat surface. They reported high concentrations of NH_4-N in the porewater, particularly in the highly degraded peat layers. This resulted from the increased concentrations of redox-sensitive solutes and decomposable organic matter in highly degraded peat. However, the study did not consider different water table heights, which would be more representative of the environmental conditions after rewetting. Koskinen et al. (2017) found increased concentrations of porewater NH_4-N and DON in restored minerotrophic peatlands over 6 years (2008-2014). The increase in NH_4-N was likely due to the absence of nitrification under restored anoxic conditions. The increase in DON may have resulted from increased mobilisation and leaching of organic compounds. Furthermore, seasonal variation influenced the concentrations of NH_4-N and total N (TN), which both were highest in late summer/autumn and lowest during early spring/summer. In contrast, Hartsock & Bremer (2018) investigated several restored rich fens, reporting low concentrations of NH_4-N and NO_3-N in the porewater, probably due to the lower N mineralisation rates, low nitrification rates, and high denitrification rates. However, the study period was short considering N dynamics over just a few days. Lundin et al. (2017) reported that porewater concentrations of NH_4-N, NO_3-N, and total N were highly variable but predominantly lower than the draining period in two restored peatlands over 15 years. Most studies on rewetting or drying-rewetting cycles in peatlands have overlooked the inflow of nitrate-enriched water, which is essential to consider due to its commonality and the potential of N saturation in peatlands and other biogeochemical issues.

Most of the research has used laboratory mesocosm experiments to investigate the internal N dynamics of peatlands that receive nitrate-enriched water. Rückauf et al. (2004) found that soil moisture conditions primarily influenced N dynamics in a nitrate-enriched rewetting scenario. After 21 days, 80% of the ^{15}N-nitrate was cycled into organic N compounds under dry conditions (water-filled pore space of 31%). Whereas under rewetting conditions (water-filled pore space of 100%), only 1.8% of ^{15}N-nitrate was converted to organic N compounds. Furthermore, total gaseous N represented 77 to 95% of the ^{15}N-nitrate loss, but nitrous oxide production was low under both moisture conditions. Cabezas et al. (2012) investigated the role of temperature, NO_3-N load, and peat decomposition in a 6-week rewetting mesocosm experiment. The experimental conditions were divided into moderately and highly degraded peat, low and high NO_3-N loads (40 kg N ha^{-1} yr^{-1} and 140 kg N ha^{-1} yr^{-1}), and two temperatures (5 °C and 20 °C). The removal efficiencies of dissolved N varied considerably, ranging from 15 to 75%, with the highest removal efficiencies at 20 °C. Peat composition strongly influenced dissolved N cycling, where the highly decomposed peat showed higher net N mineralisation, N microbial immobilisation, and NH_4-N export. Similarly, Kleimeier et al. (2017) reported the influence of peat degradation on N cycling, where degraded peat provided superior denitrification conditions due to increased immobile pores compared to undegraded peat. Lind et al. (2012) investigated the effect of NO_3-N loading (5 mg N l^{-1}) on N dynamics in a 15-day mesocosm experiment. NO_3-N removal reached 95% in the lower soil layers, but decreased with increasing height. Denitrification was the main cycling reaction, although an increase in NH_4-N flux at the experimental outlet indicated the possible occurrence of dissimilatory nitrate reduction to ammonium. Previous research has suggested the importance of dissimilatory nitrate reduction to ammonium in low NO_3-N and high organic carbon environments (Burgin & Hamilton, 2007). Furthermore, Lind et al. (2012) found that nitrous oxide represented 0 to 29% of porewater N removal, which increased due to higher NO_3-N concentrations but generally dissipated before reaching the soil surface. However, under more

dynamic water table conditions, there could be a considerable risk of nitrous oxide release under high NO_3-N loads.

In general, previous studies have failed to address both NO_3-N enrichment and different rewetting scenarios, which can both have considerable impacts on N cycling in peatlands. Han et al. (2020) investigated the effects of NO_3-N loading (20 mg N l^{-1}) and water table fluctuations in a 4-month mesocosm experiment. Three mesocosm conditions were tested: mesocosm A (MA) - high water level (5 cm above the sediment surface) with vegetation, mesocosm B (MB) - low water level (2.5 cm above the sediment surface) with vegetation, and mesocosm C (MC) – high water level without vegetation. NO_3-N reductions were highest in mesocosm A, particularly at depths closest to the plant roots (-20 to -15 cm below the surface). NO_3-N was not detected above -20 cm in mesocosm A, but was detected in mesocosms B and C. NH_4-N was not detected in any of the mesocosms (A, B, or C). Mesocosm experiments like this provide detailed biogeochemical information in a controlled simulated environment. However, the conditions are not the real environment, where variability across space and time is greater; for example, water table height or seasonal variation. Therefore, experimental results must be validated with field observations to ensure that the observed processes occur in the environment. Greywell Fen provides a significant opportunity to investigate the inflow of nitrate-enriched groundwater in a fen with managed water tables.

2.3.3 Peatland Nitrous Oxide Release

Peatlands can be considerable sources of nitrous oxide (N_2O), produced by microbial nitrogenic reactions, such as denitrification and nitrification; however, the increased release has been linked to peatland degradation (Glatzel, et al., 2008; Jørgensen, et al., 2012). Nitrous oxide is an important greenhouse gas with a global warming potential 298 times stronger than carbon dioxide over 100 years (IPCC, 2007). However, the controlling factors of nitrous oxide release can be highly variable over space and time; reactions often occur in unevenly distributed soil pores (Muñoz-Leoz, et al., 2011). Nitrous oxide release rates have been investigated in a range of peatlands under different conditions, such as natural, degraded, and rewetted. Despite this, a comprehensive understanding of nitrous oxide release in peatlands has yet to be achieved, particularly regarding the response to N enrichment, where studies have found conflicting results (Glatzel, et al., 2008; Muñoz-Leoz, et al., 2011; Jørgensen, et al., 2012; Van Zomeren, et al., 2012; Lind, et al., 2013; Riet, et al., 2013; Audet, et al., 2014; Kleimeier, et al., 2018).

In peatlands, denitrification is considered the main source of nitrous oxide (Martens, 2005). In model systems, the contribution may be small (Groffman, et al., 1998), but peatland degradation or water table lowering can disrupt denitrification, increasing nitrous oxide production (Rückauf, et al., 2004). Blicher-Mathiesen & Hoffmann (1999) demonstrated that undisturbed peatlands had high reduction rates of nitrous oxide, acting as sinks rather than sources. Although Audet et al. (2014) reported a range of nitrous oxide emission rates from -44 to 122 ug N_2O-N m^{-2} h^{-1} in four undisturbed riparian peatlands. In a minerotrophic peatland, Jørgensen et al. (2012) found nitrous oxide emission rates ranging from -200 to 300 µg N_2O–N m^{-2} h^{-1} over a growing season (May to October). During near surface periods, emission rates were < 25 µg N_2O–N m^{-2} h^{-1} but increased in response to the lower water tables. However, Chen et al. (2012) found no significant relationship between water tables and nitrous

oxide emissions in a fen, ranging from 0.018 to 0.056 mg N m^{-2} h^{-1} (CV = 311%). Furthermore, Dowrick et al. (1999) determined that moderate mire drought (- 8 cm below the surface) did not significantly affect nitrous oxide emission rates, compared to complete drainage in peat columns. Weller et al. (1994) reported that no soil parameters were correlated with nitrous oxide release in a riparian forest.

Generally, increased nitrous oxide release has been associated with increased N concentrations (Granli & Boeckman, 1994; Regina, et al., 1996). Glatzel et al. (2008) investigated nitrous oxide emission rates in a nitrogen-enriched bog (deposition rate: 22 kg ha^{-1} yr^{-1}). Emission rates ranged from 0 to 574 mg m^{-2} h^{-1}, which was considered higher compared to similar oligotrophic peatlands. Leroy et al. (2019) reported ammonium nitrate (NH_4NO_3) fertilisations (3.2 g N m^{-2} yr^{-1}) increased nitrous oxide emissions in acidic peat columns, ranging from 0.033 to 0.125 g N m^{-2} yr^{-1}. Roobroeck et al. (2010) compared the effect of three N deposition rates (0, 0.1, and 1.0 mg NO_3-N m^{-2}) on nitrous oxide emissions in fen tussocks and hollows, where emissions increased from 2.08 to 2.16 to 2.69 µg N_2O-N m^{-2} hr^{-1} and -3.04 to 16.27 to 3.43 µg N_2O-N m^{-2} hr^{-1}, respectively. This suggested that the physicochemical properties of the tussocks and hollows influenced nitrous oxide emissions. Observations by Lohila et al. (2010) further corroborate the effect of increased N on nitrous oxide, reporting a positive relationship of atmospheric N deposition with nitrous oxide emissions (r^2 = 0.68, n = 5) in a remote boreal fen. Furthermore, Yu et al. (2006) added 25 mg N l^{-1} of ^{15}N-nitrate to a plot in a Louisiana marsh, with up to 30% converted to nitrous oxide. Similarly, Lind et al. (2013) reported a conversion rate of up to 29% at the lower depths of peat columns receiving nitrogen-enriched water (5 mg N l^{-1}). Although surface emissions did not reflect this, this suggested that much of the nitrous oxide dissipated before reaching the surface. This was supported by Šimek et al. (2004), reporting higher porewater concentrations of nitrous oxide than emissions from the surface, which suggested that nitrous oxide can accumulate in porewater. However, some studies have reported contrary findings. For example, Paludan & Blicher-Mathiesen (1996) measured nitrous oxide emissions in a

nitrogen-enriched riparian peatland (9.67 to 16.11 mg NO_3-N l^{-1}), which did not exceed 1 μmol N_2O m^{-2} h^{-1}. This was similar to a nonenriched Wisconsin wet meadow with an emission rate of 1.1 μmol N_2O m^{-2} h^{-1} (Goodroad & Keeney, 1984). Similarly, Leeson et al. (2017) reported that there was no statistically significant response of nitrous oxide to additions of NH_4-N (NH_4Cl) and NO_3-N ($NaNO_3$) of 16, 32 and 64 kg N ha^{-1} y^{-1} over 13 years. Consequently, it has not yet been fully established whether NO_3-N enrichment increases nitrous oxide release in peatlands.

Generally, nitrous oxide release is measured using vented static gas chambers (Hutchinson & Mosier, 1981). Vented gas chambers are simple cylindrical enclosures placed on the soil surface, and the change in nitrous oxide concentration inside the enclosure is measured by taking a gas sample (ml), which is analysed directly by gas chromatography using an electron capture detector (Hutchinson & Mosier, 1981; Smith, et al., 1995). These chambers are considered a low-cost measurement method, as they are inexpensive to manufacture and can be easily transported to remote areas (Flechard, et al., 2007; Hensen, et al., 2013). However, since they require manual sampling and nitrous oxide release is known to be highly variable in space and time, this can lead to methodological bias (Henault, et al., 2012; Hensen, et al., 2013). This problem is particularly acute when employed in the field, where the study site may not be accessible daily or the required labour intensity is too great. However, this can be overcome if vented gas chambers are used in a laboratory setting, where it is easier to achieve high-resolution sampling over time. Although the main disadvantage of this is that the environment is no longer representative of the field, this can be compensated by designing the experiment to achieve maximum representativity.

2.4 Understanding Nitrogen Transfer and Cycling

Hydrology is particularly important in groundwater-fed fens, where high hydrological connectivity can occur between groundwater and surface water, which can influence the transfer and concentration of solutes throughout the system (Paulissen, et al., 2004). Consequently, hydrology can be an important control of N concentrations and cycling in a fen system (Holden, 2005), which can cumulate distinct biogeochemical cycling hotspots (Mitchell & Branfireun, 2005; Morris, et al., 2011). Therefore, it is essential to understand the hydrological and hydrochemical transport in these environments to further improve how N cycling and NO_3-N transfer occur between water sources in fen peatlands.

In general, tracking waterborne NO_3-N in the environment is complicated by the variety of potential sources and the nonconservative behaviour of NO_3-N, and therefore understanding its hydrological transport and cycling in a system can be difficult (Fenech, et al., 2012; Xu, et al., 2016). Several methods can be used to track NO_3-N in the environment, such as export coefficients, agriculture pollution potential indexes, nonpoint source pollution models, dual isotope analysis, or major ion analysis (Xu, et al., 2016; Fenech, et al., 2012; Amano, et al., 2018). However, many of these methods are particularly tailored for NO_3-N source appointment and transport, while dual isotope analysis or major ion analysis are more versatile and can also be used to understand NO_3-N cycling (for example, Babiker, et al., 2004; Fenech, et al., 2012; Jin, et al., 2015; Xu, et al., 2016; Minet, et al., 2017; Moore, et al., 2017; Amano, et al., 2018; Huang, et al., 2018; Biddau, et al., 2019; Li, et al., 2020; Su, et al., 2020).

Dual isotope analysis is based on the principle of isotopic fractionation, where heavy and light isotopes separate disproportionally between reaction substrates and products; identified by different chemical and physical properties (Fenech, et al., 2012). Therefore, an isotopic 'fingerprint' of the N isotope ($\delta^{15}N$) can be used to track NO_3-N and its transformation pathways in the environment (Böttcher, et al., 1990; Cey, et al., 1999; Lehmann, et al., 2004; Fenech,

et al., 2012; Xu, et al., 2016; Bouskill, et al., 2019). However, its singular use is considered ineffective in study areas with many NO_3-N sources and high N cycling as a result of isotopic overlap. Consequently, the dual isotope approach was developed, which uses the oxygen isotope ($\delta^{18}O$) together with $\delta^{15}N$ to reduce the overlapping effect (Fenech, et al., 2012; Xu, et al., 2016; Biddau, et al., 2019). Jin et al. (2015) identified multiple NO_3-N sources and transformation processes in a lake catchment area. Dual isotopes demonstrated that the NO_3-N in surface waters originated mainly from soil N and chemical fertilisers, with $\delta^{15}N_{NO3}$ and $\delta^{18}O_{NO3}$ values ranging from -1.1 to 19.4‰ and −13.1 to 26.9‰, respectively. Although groundwater NO_3-N originated from multiple sources along its flow path, such as soil N, domestic sewage, urban areas, and agricultural activities, with $\delta^{15}N_{NO3}$ and $\delta^{18}O_{NO3}$ values ranging from − 1.7‰ and 35.7‰ and − 13.1‰ and 40.3‰, respectively. Cey et al. (1999) used $\delta^{15}N_{NO3}$ and $\delta^{18}O_{NO3}$ values to indicate groundwater borne NO_3-N flowing into a riparian area originating from manure and inorganic fertilisers, as well as indicating denitrification in subsurface groundwater. Furthermore, Bouskill et al. (2019) demonstrated the disentanglement of seasonal NO_3-N dynamics in the soils of an unconsolidated aquifer. Dual isotope variability indicated and separated the effects of biogeochemical activity and dilution on NO_3-N at depths between 2 and 3 m due to rising and falling water tables. In addition, the researchers were able to attribute the contributing reactions to the observed variability at different depths, for example, denitrification and dilution. However, despite the widespread use of the dual isotope method, there are several limitations. For example, climatic and seasonal changes can influence $\delta^{15}N$ and $\delta^{18}O$ values. Therefore, the isotopic composition of NO_3-N is not constant and can change during transport or vary in different regions, and therefore the unique 'fingerprint' can vary widely (Jin, et al., 2015; Xu, et al., 2016). Furthermore, the analysis of $\delta^{15}N$ and $\delta^{18}O$ requires specialist and expensive equipment, as well as complex time consuming methodologies (Zhang, et al., 2019).

Major ion analysis is an accessible and reliable method based on the hydrochemistry of waters and subsequent interactions related to geography, geology, and pollution (Babiker, et al., 2004; Huang, et al., 2018). The bedrock of a catchment has a particularly important influence on groundwater hydrochemistry (Han & Liu, 2004; Gan, et al., 2018). Chemical weathering occurs as groundwater moves through the bedrock, increasing dissolved solutes in the groundwater that are related to the geochemical characteristics of the rock (Reeder, et al., 1972; Zhang, et al., 1995). For example, in calcareous bedrock, CO_3 dissolution increases dissolved solutes such as CO_3, Ca^{2+}, and Mg^{2+} (Fairchild, et al., 1994). Climatic conditions can also affect groundwater hydrochemistry, controlling weathering and erosion rates through temperature and runoff (Rogora, et al., 2003; West, 2012). Furthermore, anthropogenic activities influence groundwater hydrochemistry through the hydrological actions already discussed in this review (Section 2.2). Therefore, NO_3-N transport and transformations can be indicated by the evolution of hydrochemistry. For example, ionic ratios can be used to identify anthropogenic inputs of NO_3-N in groundwater or the water residence times in a peatland system (Johnes, et al., 2020; Su, et al., 2020). Furthermore, multivariate statistical analyses, for example, hierarchal cluster analysis (HCA) and principal component analysis (PCA), can be used to increase the effectiveness of hydrochemical analysis to classify water sources and suggest the main factors that result in the hydrochemical composition (Amano, et al., 2018; Su, et al., 2020).

Multivariate statistical analyses are quantitative and semiobjective approaches that can use a range of chemical (major, minor, and trace elements), physical, and other related parameters to summarise and simplify potentially complex data matrices (Güler, et al., 2002; Cloutier, et al., 2008; Gan, et al., 2018); indicating associations between samples and variables (Mazlum, et al., 1999; Helena, et al., 2000). There is a distinction between multivariate analysis techniques, with variable directed techniques concerned with relationships between variables, for example, PCA, and individual directed (or sample directed) techniques concerned with relationships between samples, such as HCA (Mazlum,

et al., 1999). PCA is a transformative technique, reducing the dimensionality of data sets and revealing factors affecting sample composition, while HCA is a data classification technique, grouping samples into representative clusters (Cloutier, et al., 2008; Gan, et al., 2018).

Previous literature has commonly used hydrochemical and multivariate statistical analyses to track NO_3-N in groundwater and watersheds (Babiker, et al., 2004; Moore, et al., 2017; Amano, et al., 2018; Li, et al., 2020; Su, et al., 2020). Babiker et al. (2004) analysed the groundwater hydrochemistry of a catchment area in Japan. Groundwater was found to be enriched with NO_3-N, SO_2^{-4}, Ca^{2+}, and Mg^{2+}, which is typical of inorganic fertilisers such as ammonium sulphate $((NH_4)_2SO_4)$ and dolomite $(Ca, Mg)CO_3)$. Furthermore, correlation analysis between these solutes further indicated the similar origin of chemical fertilisers. A negative correlation between NO_3-N and HCO_3 resulted from heterotrophic denitrification, which releases HCO_3 as a byproduct. A study by Moore et al. (2017) identified processes that contributed to the hydrochemistry of five watersheds in the United States. Elevated concentrations of sodium (Na^+) and CO_3 in a watershed indicated plagioclase weathering. Elevated Na^+ and Cl^- in several watersheds suggested the input of road salt. Furthermore, the elevated concentrations of Ca^{2+} and SO_4^{2-} concentrations in certain watersheds were probably due to the weathering of construction materials, for example, concrete or drywall. However, this would only be a concern in highly urbanised watersheds.

Furthermore, Mazlum et al. (1999) identified the hydrochemical influences and biogeochemical processes of surface water quality in Turkey using PCA, for example, domestic waste discharge, industrial waste discharge, nitrification, and the effects of seasonality. While Cloutier et al. (2008) were able to define groundwater groups associated with geochemical regions in a Canadian catchment using HCA and PCA. The analyses distinguished the hydrochemistry resulting from geological formations, hydrogeology, hydraulic gradients, and geochemical processes. Su et al. (2020) investigated groundwater NO_3-N in China, using HCA and PCA. The strength of the effect a variable has on a principal

component is represented by positive and negative loadings (Legendre & Legendre, 1998). HCA grouped the groundwater into three main groups (C1, C2, and C3), and within these groups, PCA was used to identify certain processes that occurred based on the positive or negative loadings of variables. For example, in group C3, high loadings of total dissolved solids, Mg^{2+}, CO_3, Ca^{2+}, Na^+, and pH, coupled with a low loading of NO_3-N, suggested that rainwater was the main source of groundwater NO_3-N. Furthermore, the high positive loading of NH_4-N and the moderate loading of NO_3-N in another principal component suggested that an oxic environment was the main control of groundwater NO_3-N in C3.

In addition, multivariate statistical analyses have been used in hydrochemical studies in peatlands. Reeve et al. (1996) investigated the hydrochemistry of porewater in several bogs and fens in Canada using PCA and HCA. These produced similar results, where the clustering and similar loading of several cations and pH indicated the mineral dissolution of calcite, dolomite, and feldspar transported from nearby mineral soils. In the second principal component, the positive loadings of dissolved organic carbon (DOC), silicon (SiO_2), potassium (K^+), and methane (CH_4) and the negative loadings of alkalinity and pH classified the porewaters between bogs and fens, with the latter influenced by the input of mineral-rich groundwater compared to the bog. Furthermore, several SO_4^{2-} and NO_3-N reducing processes were identified, indicated by positive loadings of DOC, Cl^-, SO_4^{2-}, and NO_3-N, compared to negative loadings of CH_4 and total Fe ($Fe^{2+/3+}$). Griffiths et al. (2019) investigated the variability of porewater hydrochemistry across space and time along a bog and fen gradient. The PCA identified distinct hydrochemical signatures in each peatland at three sample depths, revealing useful comparisons of the hydrochemical and hydrological processes in each peatland. For example, the near surface porewater of the rich fen was distinct from that of the bogs and poor fen, suggesting that the sources, transport, and cycling of solutes diverged with increasing depth.

However, there are several limitations of multivariate statistical analyses; for example, they generally require large data sets, usually no less than 100 samples (Inobeme, et al., 2022). Furthermore, missing or below detection limit values, which are common in environmental data sets, cannot be used in analyses without some form of data processing, as the analyses require a complete data set (Sanford, et al., 1993; Güler, et al., 2002). In particular, HCA is sensitive to both noise and outliers (Saxena, et al., 2017); however, this effect can be reduced by using robust linkage methods, for example, average and Ward's linkage methods (Bu, et al., 2020). Furthermore, several studies have used several preparatory and transformational steps on hydrochemical data sets before using these methods (Güler, et al., 2002; Cloutier, et al., 2008; Gan, et al., 2018). For example, highly positively skewed variables are commonly log transformed, and then all variables are standardised (Mazlum, et al., 1999; Güler, et al., 2002; Cloutier, et al., 2008; Gan, et al., 2018). Although PCA does not assume normality, it is considered improved if the variables are normally distributed (Tabachnick & Fidell, 2007; Mertler, et al., 2021). Additionally, standardisation reduces the influence of variable standard deviations and homogenises the variance of the distribution within a data set (Judd, 1980; Rummel, 1980; Berry, 1996).

In summary, multivariate statistical analysis and dissolved solute correlations can improve the understanding of the hydrology and hydrochemical transfer of NO_3-N in a system, using preexisting and accurate methodologies available in most laboratories. In comparison to dual isotope analysis, which requires more complex methodologies and sophisticated equipment. Furthermore, there was an element of time constraint in this research, due to the effects of the COVID-19 pandemic, reducing the time available for method development.

2.5 Peat Mesocosm Experimental Design

In general, laboratory experiments have been used to investigate N dynamics in peatlands and wetlands over the past two decades, commonly referred to as mesocosm experiments (for example, Venterink, et al., 2002; Zak & Gelbrecht, 2007; Bougon, et al., 2011; Cabezas, et al., 2012; Roy & White, 2012; Cusell, et al., 2013; Riet, et al., 2013; Mettrop, et al., 2014; Zajac & Blodau, 2016). Laboratory mesocosms enable low-cost testing of ecosystem level influences in reproducible, controlled, repeatable, and seminatural conditions, bridging the gap between standardised laboratory experiments and field studies (Giddings & Eddlemon, 1979; Ahn & Mitsch, 2002); results between the two frequently correlate (Clements, et al., 1988). However, there are limitations to their use that influence the results and interpretations of a simulated system. The inherent size limit of a mesocosm is considered to prevent the simulation of complex interactions normally present in natural systems, as well as producing mesocosm artefacts that arise from edge effects due to the experimental vessel and restricted solute mixing (Stephenson, et al., 1984; Szalay, et al., 1996; MacNally, 1997; Ahn & Mitsch, 2002; Alexander, et al., 2016). Therefore, caution must be applied in outright comparison to the simulated system, but laboratory mesocosms can be considered 'model systems' (Teuben & Verhoef, 1992; Ahn & Mitsch, 2002). As a model system, a whole area or environment cannot be represented, and therefore field studies are necessary to validate observations; however, field studies are expensive and difficult to replicate. Therefore, mesocosms are a relevant method to investigate peatland N dynamics. This review investigates the methodologies and experimental designs of previous studies to inform the experimental design in this research.

Generally, peatland and wetland mesocosm research has focused on the impacts of different water tables and drying-rewetting scenarios (for example, Venterink, et al., 2002; Zak & Gelbrecht, 2007; Cusell, et al., 2013; Riet, et al., 2013; Mettrop, et al., 2014), rather than nitrate-enriched water inflow. Note that the + and – symbols represent the water table height

above or below the soil surface. Zak & Gelbrecht (2007) layered degraded peat in square boxes and flooded them (+ 5 cm), simulating rewetting in a drained fen. While Cusell et al. (2013) incorporated three different water table heights in soil columns: a water level at the surface (0 cm), a low water level (− 15 cm), and a high water level (+ 15 cm). These designs are robust in testing different water table heights and rewetting scenarios. However, in this study, a nitrate-enriched water input is required along with different water table heights. Cabezas et al. (2012) compared low and high NO_3-N conditions (1.7 N mg l^{-1} and 5.7 N mg l^{-1}) in two different peat degradations (moderate and high) and rewetted the peat (+ 5 cm). Zajac & Blodau (2016) simulated two water table heights (− 8 cm and − 28 cm) and replicated atmospheric N deposition (16.65 N mg l^{-1}). However, these experiments are not fully representative of groundwater-fed fens, where groundwater migrates upward through the peat to the surface.

Flow-through mesocosm designs are commonly used to investigate the effectiveness of constructed wetlands (for example, Sasikala, et al., 2009; Kleimeier, et al., 2018; Mburu, et al., 2019), where a wetland is constructed specifically to treat polluted surface water or groundwater. Kleimeier et al. (2018) homogenised degraded peat samples, layered in an experimental box with a top inflow and an opposite bottom outflow. Nitrogen-enriched surface water flowed down through the homogenised soil profile, and three NO_3-N conditions were tested: 65, 100, and 150 mg N l^{-1}. Mwagona et al. (2019) investigated the effect of nitrogen-enriched surface runoff on a natural wetland. The intact wetland soil cores enclosed in PVC pipes were subjected to a downward vertical flow of nitrate-enriched water (60 N mg l^{-1}) through inlets and outlets. These mesocosm designs incorporate NO_3-N enrichment and flow simulation, providing valuable design information; however, the water table height is not considered and the experimental water flows downward rather than upward through the soil profile.

Studies by Sasikala et al. (2009) and Han et al. (2020) considered both upward vertical flows and different water table heights. Sasikala et al. (2009) layered PVC tubes with gravel and sand and flushed them with a nitrogen-enriched wastewater solution (NO_3-N: 16.2 ± 2.5 mg N l^{-1} and NH_4-N: 6.80 ± 4.0 mg N l^{-1}). Furthermore, four water tables were tested: a control column with a fixed water table (+ 3 cm), a control column with a fluctuating water table, a planted column with a fixed water table (+ 3 cm), and a planted column with a fluctuating water table. Fluctuating water tables were simulated by drainage valves installed at the bottom of the columns. As a constructed wetland study, the primary focus was on investigating N removal efficiency, so the purpose of the fluctuating water table was to aerate the sediment by complete drainage, which is unrealistic in a natural peatland. Han et al. (2020) simulated the upward flow of nitrate-polluted groundwater (20 mg N l^{-1}) in three acrylic columns layered with gravel, sand, and wetland soil. Furthermore, water table height conditions were tested: a high water table (+ 5 cm) with plants, a low water table (+ 2.5 cm) with plants, and a high water table (+ 5 cm) without plants. This mesocosm design is more realistic for simulating peatland N dynamics. However, in the experimental designs discussed, the sediment or peat has either been constructed or homogenised before experimentation, which is not representative of peat soil and changes the unique structure, influencing N cycling. Few experimental designs combine upward vertical flow and intact peat cores to investigate N dynamics.

Lind et al. (2012) sampled four intact cores from four different peatlands and wetlands in steel cylinders, which doubled as an experimental container. Nitrate-enriched groundwater (5 mg N l^{-1}) was pumped through the cores using a peristaltic pump, with a bottom inflow and a top outflow in the cores; however, variable water tables were not considered. Furthermore, a limitation of the Lind et al. (2012) study was that the inner diameter of the experimental soil cores (6 cm) was thin, increasing the potential of edge effects (Weltzin, et al., 2001; Mulot, et al., 2015). To the author's knowledge, no experiment has subjected intact peat cores to an upward vertical flow of nitrate-enriched water and different water table heights to replicate N dynamics in a nitrogen-enriched environment under different rewetting scenarios.

Furthermore, other experimental design conditions must be considered; for example, the investigation period, temperature, or maintaining surface vegetation. Investigation periods vary considerably between studies. Sasikala et al. (2009) investigated N dynamics for eight months in wetland sediment cores. However, the investigation period is affected by certain logistics in a laboratory, such as space and studies by other researchers, and thus long experimental periods may be infeasible. Typically, experimental periods of three to four months have been used (for example, Riet, et al., 2013; Zajac & Blodau, 2016; Han, et al., 2020). Lind et al. (2012) and Mwagona et al. (2019) used relatively short experimental periods, 15 and 30 days, respectively. This provided a sufficient period to capture N dynamics at high spatial and temporal resolutions. Investigating N dynamics at high spatial and temporal resolutions is an intensive process, which requires a lot of resources and commitment. Therefore, it would be difficult to maintain such intensive sampling over extended periods; for example, over months.

Furthermore, the period in which each water table is tested is also important to consider, as sufficient time must be allocated for the system to equilibrate and capture N dynamics. Han et al. (2020) tested different water tables using individual columns, rather than successive water table height changes. This reduces the complexity of the experiment but is not representative of natural water tables in a peatland. Riet et al. (2013) tested three water table conditions: a high water table, a low water table, and a fluctuating water table. The fluctuating regime consisted of a high water table for the first 40 days and drained conditions for the remaining 70 days. However, Zajac & Blodau (2016) subjected mesocosms to a low water table for 76 days and then raised the water table for the remaining 90 days. Although these water tables allow for a sufficient period to investigate the subsequent effect on N dynamics, they increase the total investigation period.

Temperature is an important control of microbial reaction rates (Birgander, et al., 2018), and therefore must be considered when investigating N dynamics. In the environment,

temperatures vary considerably over seasons compared to constant laboratory temperatures. Temperature controlled rooms are frequently used to maintain experiments at specific temperatures ranging from 10 °C to 16 °C (for example, Zak & Gelbrecht, 2007; Lind, et al., 2012; Riet, et al., 2013; Mwagona, et al., 2019; Han, et al., 2020). Cabezas et al. (2012) investigated the effect of temperature changes (5 °C to 20 °C), the lower temperature decreased NO_3-N removal efficiency and net N mineralisation. However, this adds further complexity to an experiment, introducing another condition variable. Riet et al. (2013) used a constant temperature of 16 °C, removing it as an experimental variable.

2.5.1 In situ Porewater Sampling

Furthermore, a porewater water sampling method must be considered. Many methods can be used to sample peat porewaters, categorised into destructive (or ex situ) and nondestructive (or in situ) (Song, et al., 2003). Ex situ porewater sampling methods include separating particles from fluids by centrifugation or compressing sliced sediments. Ex situ methods are abrasive and require physical changes to the intact columns, which results in a change of the porewater environment; for example, compression or centrifugation. These methods are known to release nutrients and/or gases, affecting the interpretation of the results (Seeberg-Elverfeldt, et al., 2005; Ibánhez & Rocha, 2014). The destructive nature of ex situ methods is unsuitable for this experiment. In situ methods include ion exchange membranes, diffusive gels, and suction samplers that can be inserted directly into the soil (Gao, et al., 2012; Fisher & Reddy, 2013). To characterise biogeochemical variability at high spatial resolution, consistent positioning is required to prevent misinterpretation of spatial heterogeneity (Seeberg-Elverfeldt, et al., 2005; Gao, et al., 2012). Generally, in situ methods provide position reproducibility, but there is no consciousness of the most suitable method (Reynolds, et al., 2004).

Ion exchange membranes (IEMs) are ion sinks, which were first used to measure nutrient concentrations in soils by Pratt (1951) and Amer et al. (1955). Exchange membranes have been extensively used in agricultural science studies (Qian & Schoenau, 2002), but application in peatlands is less common (Kreiling, et al., 2015; Wood, et al., 2015; Hartsock & Bremer, 2018; Wang, et al., 2018). Ion exchange membranes can be used in two forms: bead or sheet. Recently, sheet membranes have been used due to their simplicity in design and definable surface area. The membrane sheet is usually enclosed in a plastic frame, creating a probe that can be inserted directly into the soil (Qian & Schoenau, 2002). However, the sink function of the ion membrane has a limit, and eventually, it can behave as an ion exchanger with the soil or switch between the two throughout an installation period (Miller, et al., 2015). This period, in which the ion exchange membranes can be left in the soil, is affected by several factors, such as moisture, temperature, exchange capacity of the resin, and ion concentration. This dynamic behaviour can cause porewater quality misinterpretation, and it is recommended that incubation periods are limited to two weeks (Qian & Schoenau, 2002). Furthermore, they can only measure ions, which is unsuitable for this experiment, as DOC must be considered as it is an important variable in N dynamics.

Another similar method that has been recently applied in porewater studies is diffusion gradient in thin films (DGTs), a passive, time-integrated sampling technique. It has been commonly used in freshwater environments and less so in soil environments to measure solute concentrations. The DGT probes consist of three parts: a membrane filter, a diffusive layer, and a binding layer, all within a plastic frame. Solutes diffuse across the diffusive layer and are immobilised by the binding layer over a deployment period (Huang, et al., 2016a; Huang, et al., 2016b; Huang, et al., 2016c). Solutes are then eluted from the binding layer, and the mass is determined. The mean solution concentrations are calculated from the solute mass accumulated during the deployment period using a specific DGT equation (Huang, et al., 2016a). This method has many of the same drawbacks as the ion exchange membranes,

where the resin binding capacity is finite and limited to ions. Consequently, both methods are not suitable for long-term in situ N dynamics studies in a laboratory setting.

Rhizon soil moisture samplers (SMS) have been used in numerous mesocosm studies (for example, Argo, et al., 1997; Song, et al., 2003; Seeberg-Elverfeldt, et al., 2005; Sigfusson, et al., 2006; Lind, et al., 2012; Ibánhez & Rocha, 2014; Chen, et al., 2015; Steiner, et al., 2018). Rhizon soil moisture samplers (SMS) consist of a hydrophilic micropore tube (pore size 0.1 µm) supported by a plastic or metal rod, connected to a polyvinyl chloride (PVC) sampling port with a Leur-lock male connector. Typical dimensions are 2.5 mm outer diameter, 1.4 mm inner diameter, and 5 to 10 cm in length. The rhizon sampling principle is based on the hydrodynamic response of a porous substance when negative pressure is applied. Negative pressure can be applied by several instruments, such as syringes, vacuum tubes, or peristaltic pumps (Argo, et al., 1997; Seeberg-Elverfeldt, et al., 2005; Falcon-Suarez, et al., 2014; Ibánhez & Rocha, 2014). The rhizon sampler can measure a range of trace metals, nutrients, and gases as it directly samples the porewater (Seeberg-Elverfeldt, et al., 2005). Seeberg-Elverfeldt (2005) reviewed the use of rhizon samplers in mesocosm studies in intertidal sediments. The researchers highlighted several benefits of rhizon use: low soil structural disturbance (tube diameter: 2.5 mm), low dead volume (0.5 ml including standard tubing), minimal absorption processes in the inert polymer tube, and no degradation during long-term use. Furthermore, the tube pore size (0.1 µm) ensures the extraction of microbial and colloidal-free solutions. The researchers also established the minimum vertical spacing between the rhizons before the suction zones overlap and sampling bias occurs, which was approximately 1 cm per 7 ml of sample.

However, Chen et al. (2015) reported a possible filtration effect on the porewater sample as a result of the membrane pore size (0.1 µm), where the centrifuged samples contained a higher number of large molecules. In addition, studies have disputed the inertness of the polyethersulfone (PES) sampling tube. Ibánhez & Rocha (2014) reported NH_4-N adsorption

on the polyethersulfone membrane, where maximum adsorption was associated with low temperatures (5 °C) and salinity (0 ‰); however, membrane desorption was rapid, affecting only the first millilitres of sample. Van Haesebroeck et al. (1997) noted the potential adsorption of phosphate (PO_4^{3-}) onto the polyethersulfone membranes, although no further investigation was completed. Other studies have also reported tube clogging after repeated suction during sampling, which requires the replacement of the rhizon sampler (Fisher & Reddy, 2013; Falcon-Suarez, et al., 2014). Furthermore, Falcon-Suarez et al. (2014) observed that rhizon insertion into the soil can cause some small scale compaction, which could affect the pore structure surrounding the sampler. Despite these limitations, rhizon samplers allow repeatable, spatially reproducible, in situ, and nonion specific sampling, which corresponds to the requirements of this experimental study.

2.5.2 Intact Peat Column Sampling

Additionally, to sample an intact section of peat to have a representative laboratory mesocosm, a suitable methodology is required, adding a degree of complexity to the sampling process. Several studies have established methodologies and published designs of intact soil column samplers (for example, Jowsey, 1966; Fenton, 1980; Clymo, 1988; Buttler, et al., 1998; Lind, et al., 2012). In this study, the peat columns must be: (1) undisturbed; (2) tall enough for different water tables; (3) cross-sectionally wide enough to decrease the potential of edge effects; and (4) cause the least disturbance to the surrounding area. This final requirement is particularly important, as Greywell Fen is a Special Site of Scientific Interest (SSSI), and previous sampling methods of intact peat columns can result in high amounts of peat excavation, and therefore disturbance (Kenzie, et al., 1997; Clark, et al., 2006; Dowrick, et al., 2006). A study by Buttler et al. (1998) designed an intact peat column methodology and sampler with similar aims, and therefore will be used as a model methodology and design for this experiment. The design, presented in Figure 2.2, is based on a close-fitting tube arrangement. An outer steel tube with serrated teeth acts as a 'peat cutter' and an inner tube

as a 'soil column collecter'. The outer core is applied rotationally to the soil surface, and the resultant core is collected by the inner tube, in a stepwise action. The two-tube design decreases friction and prevents peat compression.
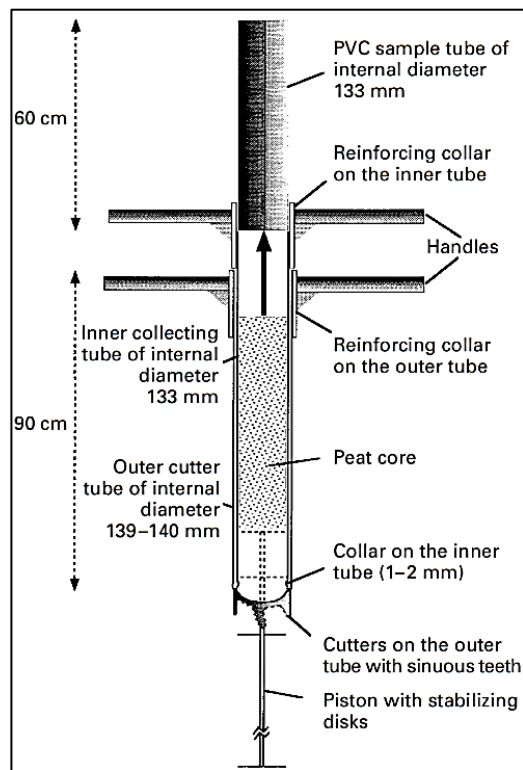
Figure 2.2: Intact peat column sampler design (Buttler, et al., 1998).

2.6 Conclusion

In summary, despite the extensive research on N cycling in peatlands under different water tables and NO_3-N enrichment scenarios, there remain significant knowledge gaps of their effects, particularly in lowland peatlands. Greywell Fen provides a unique opportunity to address these gaps by being subject to managed water tables and a nitrate-enriched groundwater source; these factors enable the investigation of a range of N species in the fen

over space and time as a result of these effects. This study will use multivariate statistical analyses to better understand the processes of hydrological transfer and biogeochemical cycling of NO_3-N that likely explain fen N variability; to date, these approaches have rarely been used in fens, in spite of their potential to offer insightful analysis in systems characterised by high hydrological connectivity with related water sources, such as groundwater and surface water. Fundamentally, multivariate statistical analysis can group a large number of water samples into clusters based on their hydrochemistry and can process a large number of variables, detecting subtle hydrochemical changes that can be overlooked by standard graphical methods. Consequently, this can indicate how NO_3-N is transferred and processed through different water sources, providing a hydrological and biogeochemical overview of the fen, which previous studies may not have captured due to focussing on a limited number of N species or dissolved solutes. To understand the N and hydrochemical variability in a nitrate-enriched fen, water samples will be collected from various water sources at high spatial and temporal resolutions over a year. Furthermore, this research presents a novel simulation of the impact on the peat N dynamics of rewetting with nitrate-enriched groundwater. This simulation of conditions that result from groundwater abstraction cessation will not only further our process-level knowledge of peat solute and gaseous N dynamics, but will also inform the decision making of South East Water Ltd. Previous experiments investigating N dynamics under rewetting with nitrate-enriched groundwater have not always been fully representative of a peatland environment, leading to a potential misinterpretation of processes in response to different management scenarios. Critically, current simulations will provide an opportunity to investigate the impact of water table height management on nitrous oxide release, as well as porewater N chemistry; very few simulations have addressed this combination of crucial parameters in nitrate-enriched fens. To achieve this, large-scale intact columns will be subjected to different water tables and NO_3-N enrichment, measuring porewater and nitrous oxide release at high spatial and temporal resolutions. To the knowledge of the author, no studies have used this approach to investigate N dynamics and nitrous oxide release.

3.0 Study Site Description

Chapter 3 provides a detailed technical description of the study site, Greywell Fen, covering topics related to geology, ecology, past and current human management, a conceptual hydrogeological model, and N inputs. In general, Chapter 3 provides context for the study site and research.

3.1 Study Site

Greywell Fen (51.251°N 0.971°W) is located in Hampshire, United Kingdom (Figure 3.1), within a lowland valley, 80 metres Above Ordnance Datum (mAOD), with western and eastern sloping boundaries rising to 100 mAOD. It is a calcareous groundwater-dependent peatland (pH = 6.5 to 8.3) that covers a 38-ha area and is a designated Site of Special Scientific Interest (SSSI). The River Whitewater borders the fen for a 2 km stretch on the western edge, and the discrete groundwater springs that form the headwaters of the river are located upstream and to the south of the fen (Figure 3.1). Further, multiple discrete groundwater springs are located within the fen, mainly along the eastern edge. The site is surrounded by a mixture of land uses (within a 2 km boundary): permanent calcareous grasslands (31.4%), arable land (21.5%), woodland (12%) and made-made structures (34.9%), for example, farmhouses or concreted areas (Rowland, et al., 2017). This study only considered the south fen section (Figure 3.1), which is the largest section and contains the deepest peat (≤ 3 m). Furthermore, this section is reported to be the largest and best-preserved calcareous fen found in this area of England (Sanderson, 2003). The northern section is different in character from the southern section, being more open and containing less fen vegetation; it contains shallow peat deposits (< 1 m) and calcareous spoil dumps that considerably change the character of plant species (Jacobs, 2019).
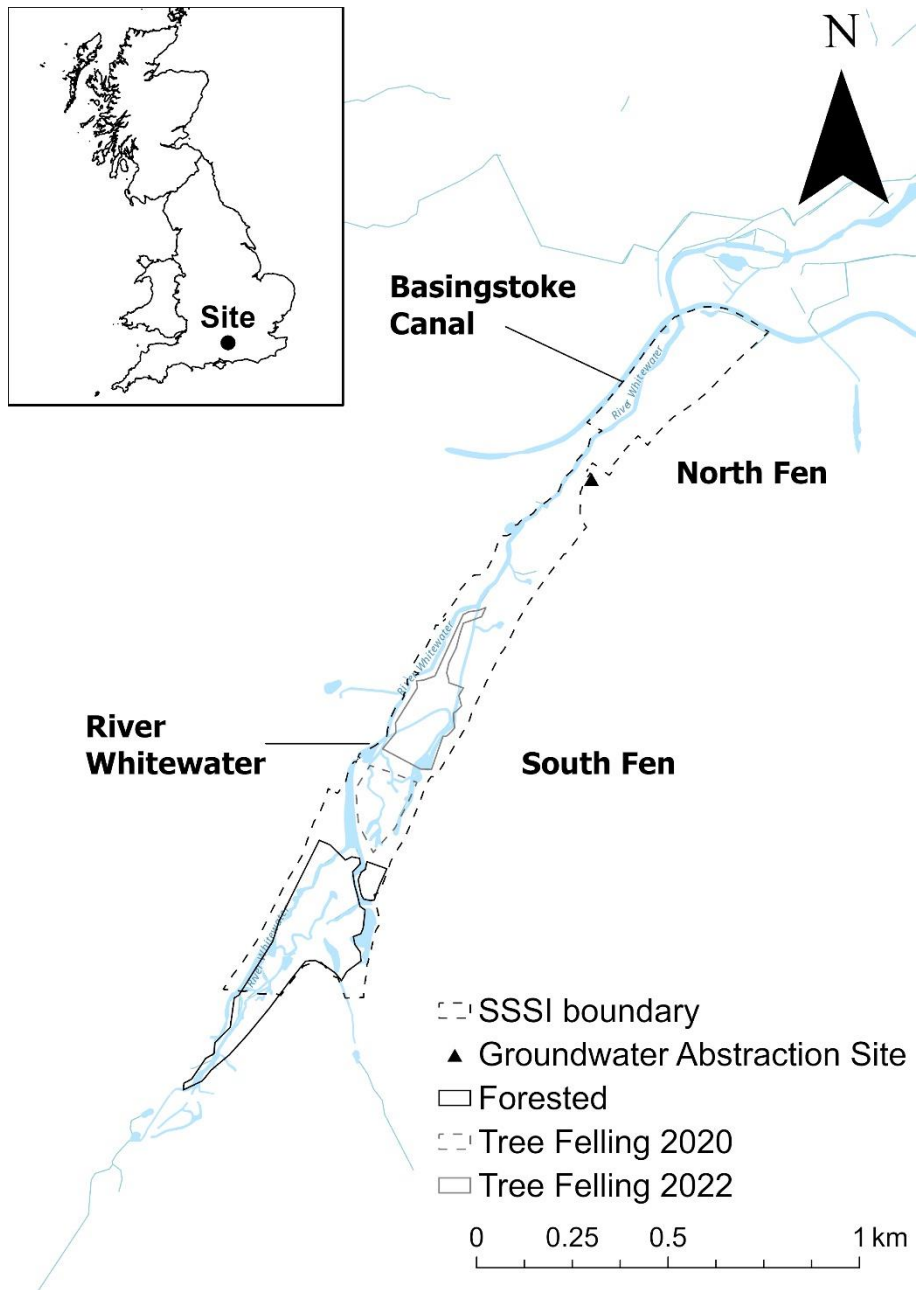
Figure 3.1: Greywell Fen.

3.2 Geology

3.2.1 Bedrock Deposits

   The bedrock geology is dominated by Seaford and Newhaven Chalk formations, which are soft to medium-hard Chalks that contain flint nodules and marl bands. The bedrock declines towards the north-northeast at a 4 to 6 ° slope. The Chalk formations are overlain by impermeable layers of clay formations from the Lambeth and Thames Groups. The Lambeth Group is divided into Upnor and Reading Formations, the former up to a metre thick. The Thames Group consists of London Clay Formations, with a Harwich Formation base. Chalk-Palaeogene contact occurs 100 to 150 m north of the Greywell abstraction site (Farrant, 2012). Table 3.1 provides further information on bedrock geology.

Table 3.1: Geological succession in the Greywell catchment (Jacobs, 2019).

Period	Epoch	Group	Formation	Lithology	Thickness (m)
Palaeogene	Eocene	Thames Group	London Clay	Bioturbated or poorly laminated, blue-grey or grey-brown, slightly calcareous, silty to very silty clay, clayey silt and sometimes silt, with some layers of sandy clay	55 to 100
			Harwich	Typically, it comprises glauconitic, silty, or sandy clays, silts, and fine- to coarse-grained glauconitic sands, some gravelly varying to flint gravel beds. Thin beds of grey clay occur in some parts, as do shell-rich beds and thin beds of argillaceous limestone	3 to 6
	Palaeocene	Lambeth Group	Reading	Vertically and laterally variable sequences mainly of clay, some silty or sandy, with some sands and gravels, minor limestones and lignites and occasional sandstone and conglomerate	18 to 27
			Upnor		1 to 6
Cretaceous	Upper Cretaceous	White Chalk Sub-Group	Seaford Chalk Formation	Firm white chalk with conspicuous semicontinuous nodular and tabular flint seams. Hardgrounds and thin marls are known from the lowest beds. Some flint nodules are large to very large	60 to 100 m (formerly the upper chalk)
			Lewes Nodular Chalk Formation	Hard to very hard nodular chalks and hard grounds with interbedded soft to medium-hard chalks and marls	
			New Pit Chalk Formation	Principally blocky, white firm to moderately hard chalk with numerous marls or paired marl seams. Flint occurs sporadically in the upper part in the deeper basin areas of the Southern Province	65 (formerly the Middle Chalk)
			Holywell Nodular Chalk Formation	Generally hard nodular chalks with thin marls and significant proportions of shell debris in part. Base marked by the interbedded coloured marl and chalk succession characteristic of the Plenus Marls Member (a term applicable in both the Southern and Northern Provinces). The Melbourn Rock Member above the base can be distinguished by its lack of shell material	
		Grey Chalk Sub-Group	Zig-Zag Chalk Formation	Mostly firm, pale grey to off-white blocky chalk with a lower part characterised by rhythmic alternations of marl and marly chalks with firm white chalk. Thin gritty and silty chalk beds act as markers in the sequence.	50 to 80 (formerly the Lower Chalk

3.2.2 Superficial Deposits

The bedrock geology is overlain by superficial deposits of gravel (River Terrace Deposits), clay, and peat. Within the fen, alluvial deposits are up to 10 m thick, including peat deposits up to 3 m thick, overlying flinty sandy gravel, and highly weathered bedrock (Farrant, 2012). Table 3.2 provides further detailed information on the superficial deposit. The fen is located within an elongated basin formed by the accumulation of river terrace gravels enclosed in a cross valley. Valley gravel was likely laid down during the postglacial period, and in lowland areas water may have been dammed within the basin to form a lake or slow water flow, resulting in clay deposits within and over the gravel depositions. Allen Associates (1992) observed remnants of common reed (*Phragmites australis)* accumulation in the deepest peat, providing evidence of a historical water column. Throughout this period, changes in channel formation influenced the distribution of the three-dimensional clay-gravel mixture. Furthermore, fine gravel is distributed throughout the peat and soft clay deposits, which probably represents periodic flooding and overflow from the adjacent River Whitewater. Generally, the thickness of the peat and soft clay increase south within the fen (Table 3.2). In certain areas, the peat is overlain by semifluid peat, which forms a floating/quaking bog (Jacobs, 2019).

Table 3.2: Geological deposits from ground investigations in the southern fen (Jacobs, 2019).

Unit	Primary Description	Secondary Description	Thickness range (m)
Topsoil	Soft brown, slightly sandy clay topsoil	Sometimes with a little subrounded fine flint and chalk gravel. Roots and rootlets	0.10 to 0.80
Peat[1]	Soft/very soft dark brown organic amorphous peat.	Sometimes with a little subrounded fine flint and chalk gravel. Roots and rootlets.	0.07 to 2.00
Clay[1]	Very soft firm cream, cream-grey, light brown, slightly sandy, or dark brown organic clay. Occasionally, locally orange or orange/brown. Some indistinctly laminated.	Often with a little subrounded fine flint and chalk gravel. Occasional roots and rootlets.	0.05 to 1.05
Chalk	Slightly sandy silty structureless Chalk, to slightly gravelly sandy silt. Fine to coarse subrounded gravel with little subrounded cobbles set in a light brown locally cream matrix. Clasts range from very weak to weak and low to medium density.	White with frequent black specs and rounded. Some roots and rootlets.	12.5 to 13.55

[1]Clay and peat thickness were not defined in all locations as some augers did not prove the base of these units.

3.3 Ecology

Greywell Fen has been a designated Site of Special Scientific Interest (SSSI) since 1951 (Ratcliffe, 1977); notable terrestrial plant communities from the national vegetation survey (NVC) include M9 (bottle sedge (*Carex rostrata*) and pointed & giant spear-moss (*Calliergon cuspidatum/giganteum*)), M22 (blunt-flowered rush and marsh thistle (*Juncus subnodulosus and Cirsium palustre*)) (Rodwell, 1991). Other vascular plant species listed in the SSSI citation include lesser tussock sedge (*Carex diandra*), long stalked yellow sedge (*Carex lepidocarpa*), marsh helleborine (*Epipactis helleborine*), and marsh fern (*Thelypteris palustris*). Historically, the listed terrestrial plant communities were more widely distributed throughout the fen. Since the 1940s, the fen has undergone considerable ecological zonation and succession, primarily explained by the absence of management. The colonisation of alder (*Alnus glutinosa)* and willow (*Salix)* has changed the vegetation from open marshland/mire species to wet woodland (Jacobs, 2019). Consequently, 97% of the fen has been designated in an ecologically 'unfavourable - declining condition'. Units 2 and 10 are the only two vegetation units that were designated in an ecologically 'favourable condition' and have never been colonised by alder or willow (Figure 3.2) (Natural England, 2018). A 'favourable condition' is described as 'the situation in which a habitat or species is thriving throughout its natural range and is expected to continue to thrive in the future' (Natural England, 2021).
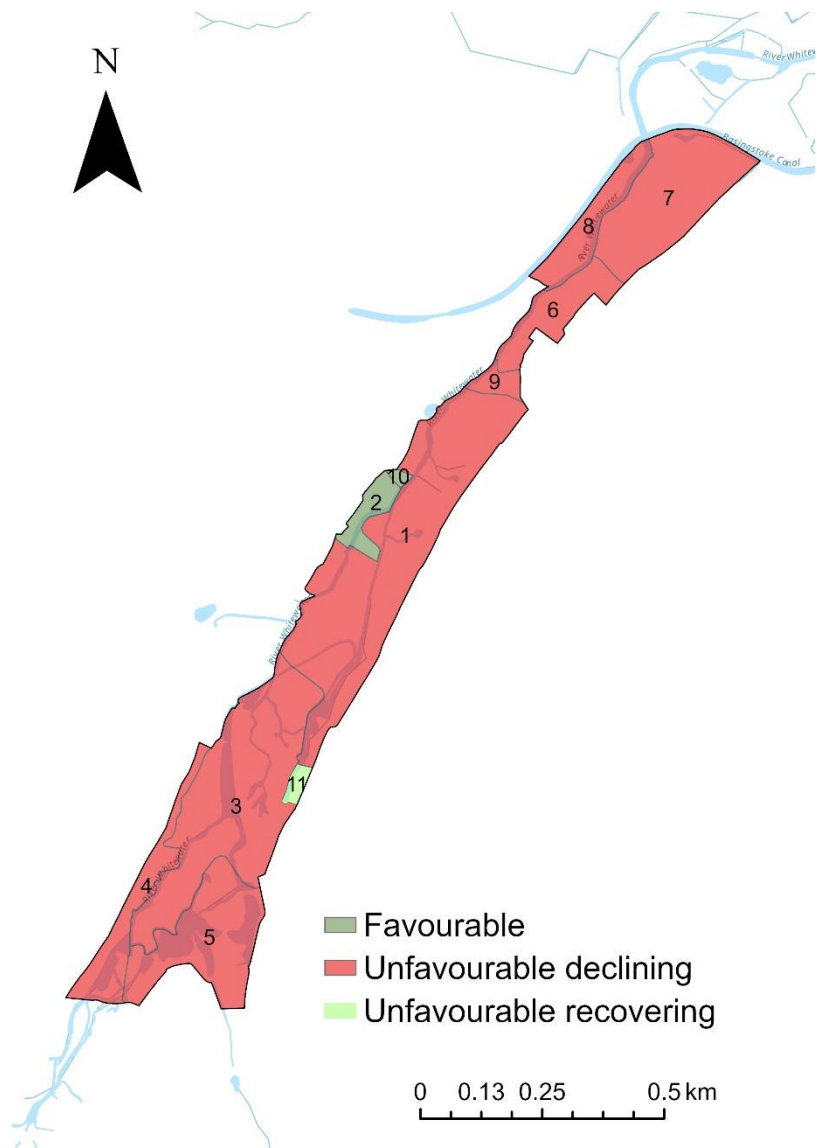
Figure 3.2: Greywell Fen and Natural England condition status. Numbers 1 to 11 represent the vegetation survey units (Natural England, 2018).

3.4 Fen Management

3.4.1 Hydrological - Groundwater Abstraction

The nearby groundwater abstraction site has been operating since 1908. The current abstraction licence holders are South East Water. Groundwater is abstracted through two deep wells (41.5 m deep) at a rate between 5000 and 6400 m^3 d^{-1} (Figure 3.1). In South East Water's Asset Management Plan Period Four (AMP4), the Environmental Agency identified Greywell Fen and the River Whitewater for hydrological investigation due to their ecohydrological importance and potential sensitivity to groundwater abstraction, in response to ecological deterioration (Figure 3.2) (South East Water, 2005). As a result, several ecohydrological monitoring programmes were completed. Low et al. (2012) reported that under nonpumping conditions, water table heights recovery ranged from 0.287 to 0.785 mAOD. Furthermore, Jacobs (2019) found that groundwater abstraction influenced fen water table heights. These findings suggested that groundwater abstraction may have affected the fen ecology through groundwater water table lowering and has led to the decision to cease groundwater abstraction at Greywell Fen by the year 2025.

3.4.2 Ecological Management

The south fen is owned and managed by the Hampshire and Isle of Wight Wildlife Trust (HIWWT). Since 1995, the Hampshire and Isle of Wight Wildlife Trust have introduced ecological management techniques, for example, herd grazing and tree/shrub removal, aiming to restore Greywell Fen to a 'favourable condition' and reduce evapotranspiration rates from forestation. Herd grazing occurs annually from September to March, while major tree clearances have been more sporadic, occurring in autumn-winter 2011/2012, winter 2017/18, spring-summer 2020, and winter 2022 (Figure 3.1).

*It is important to note that the 2022 winter tree clearing included an area where five hydrochemical and two hydrological sampling sites were located, including those installed as part of this thesis (Chapter 4.0).

3.5 Hydrogeology & Nitrogen Inputs

3.5.1 Hydrogeology

The fen hydrology at Greywell Fen is thought to be controlled by the hydrological processes of the Chalk aquifer. Jacobs (2019) is the only conceptual hydrogeological model available, and this model suggests that groundwater leaves the Chalk aquifer in four ways: (1) flow into the confined zone; (2) discharge to the surface through springs and diffuse flows; (3) groundwater abstraction; and (4) discharge to the nearby Basingstoke Canal. The discrete groundwater springs and diffuse flows hydrologically connect the fen to the Chalk aquifer. Within the fen, it is likely that the diffuse flow rate and volume vary spatially, depending on substrate permeability; for example, gravel horizons overlain by peat and alluvium may exhibit higher permeability than purer clay deposits (Figure 3.3). Therefore, vertical diffuse flows may preferentially discharge from the gravel layer to the fen margins, bypassing the alluvium and forming discrete springs on the eastern margin (Figure 3.3). Where the clay-rich gravel mixture is thin or absent, the flow can permeate through the permeable alluvium; however, the hydrological contribution may be small. The Chalk aquifer is considered hydrologically connected to the River Whitewater by two mechanisms: (1) discrete groundwater springs south of the fen; and (2) horizontally through the fen sediment (peat). However, the hydrological connectivity of the hyporheic zone to the fen remains relatively unknown.
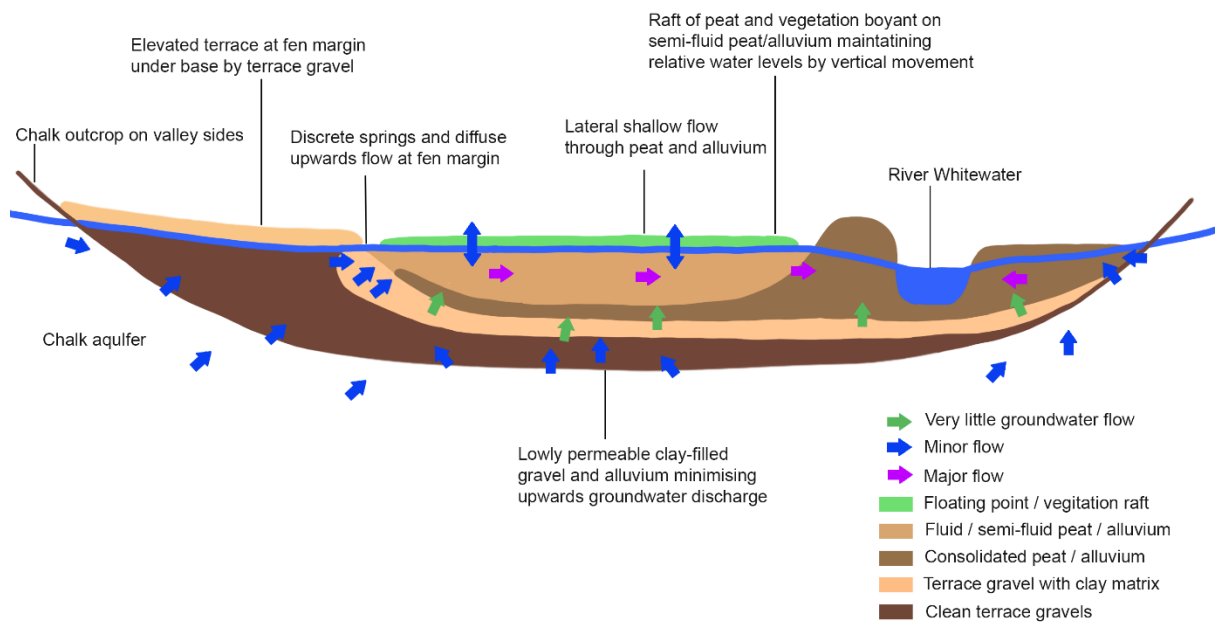
Figure 3.3: Conceptual hydrogeological model of Greywell Fen (Jacobs, 2012).

3.5.2 Nitrogen Inputs

The Chalk aquifer is known to be enriched with NO_3-N concentrations ranging from 6.14 to 9.44 mg NO_3-N l^{-1} (mean = 7.00 mg NO_3-N l^{-1}) measured in the groundwater abstraction boreholes (Figure 3.4), between 1997 and 2021. Furthermore, records suggest that concentrations are increasing (Figure 3.4). NO_3-N contamination is likely the result of 'legacy nitrate storage', common in Chalk aquifers in the United Kingdom (Section 2.1). N deposition is another common problem in the United Kingdom. The UK Centre for Ecology and Hydrology's Concentration Based Estimated Deposition (CBED) data (2016 - 2018) were used to estimate atmospheric N deposition at the site. Using the 5x5 km CBED model, wet and dry N depositions were added together, which were collected at the UK Eutrophying and Acidifying Pollutants (UKEAP) network sites. Subsequently, the summed N depositions were interpolated across the UK, and using annual precipitation maps from the UK Meteorological Office, the deposition rates were calculated (Levy, et al., 2020). N deposition at the site was estimated to be 11.02 kg N ha^{-1} yr^{-1}; the average total N deposition within a 10 km radius was 12.16 kg N ha^{-1} yr^{-1}, ranging from 9.66 kg N ha^{-1} yr^{-1} to 17.92 kg N ha^{-1} yr^{-1}. Currently, the N input from surrounding land use through surface runoff is unknown.
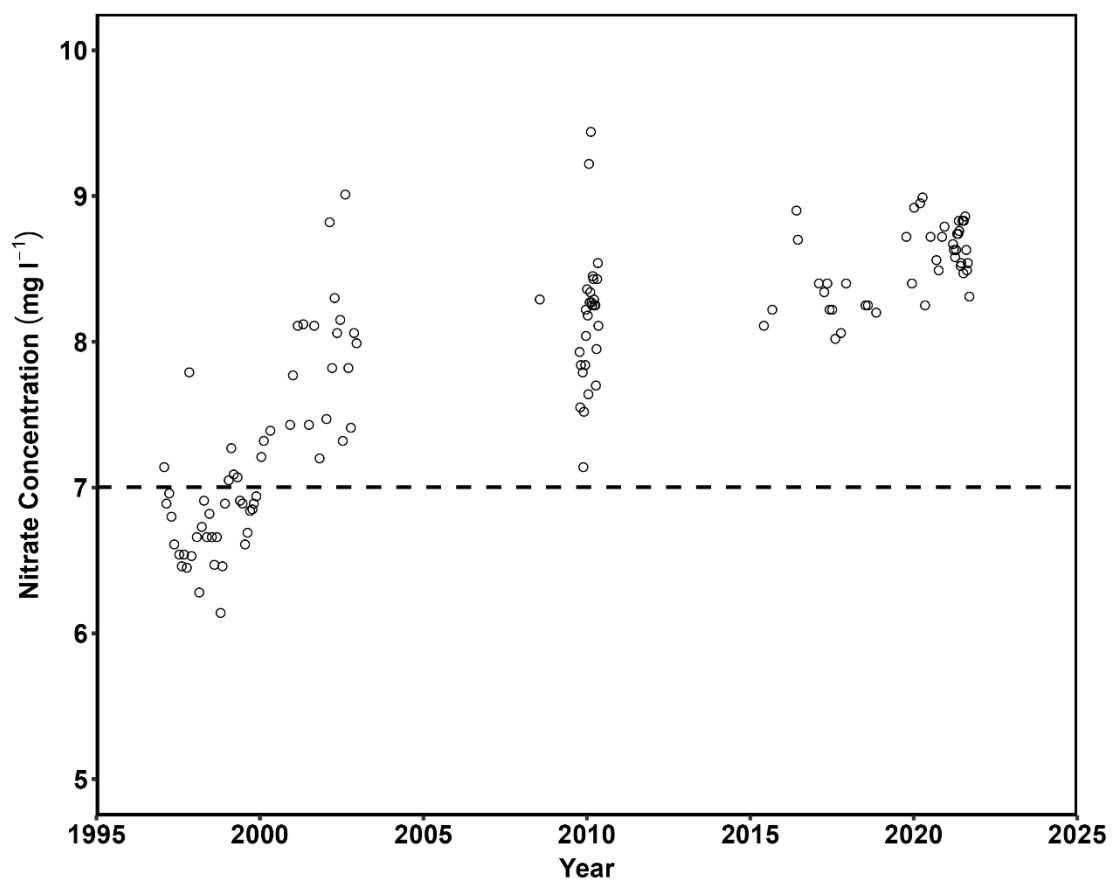
Figure 3.4: NO$_3$-N concentrations measured at the groundwater abstraction site from 1997 to 2021. The dotted line represents the mean concentration during this period. Nitrate data provided by South East Water.

4.0 Continuous Field Monitoring
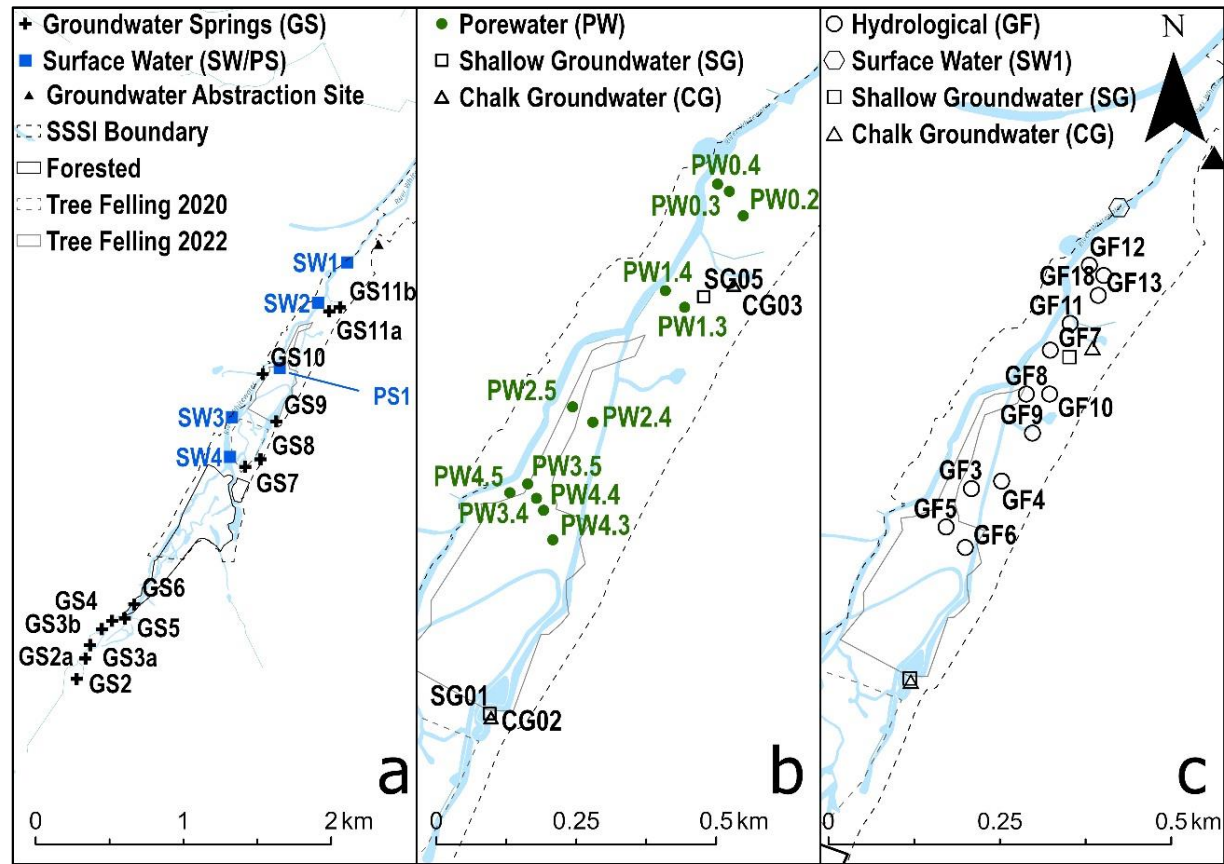
Figure 4.1: Hydrochemical and hydrological monitoring sites located throughout Greywell Fen: a) groundwater springs (GS) and surface water (SW/PS) sites, b) Chalk groundwater (CG), shallow groundwater (SG), and porewater (PW) sites, and c) hydrological monitoring (GF) sites.

This chapter provides a technical description and overview of the soil, hydrochemical, and hydrological sampling sites at Greywell Fen. In addition, methodologies for soil, hydrochemical and hydrological sampling, soil and water laboratory analysis techniques, and hydrological data processing are provided. The information in Chapter 3 (study site description) helped in the decision making regarding sampling locations and water source labels, as well as updating the reader with any changes that occurred at the study site during the investigation.

4.1 Physicochemical Sampling & Analysis

Fourteen soil cores were collected adjacent (< 1 m distance) to each of the following porewater (PW) and hydrological dipwells (GF) in April 2019 and June 2021 (Figures 4.1, b and c): PW0.4, PW1.3, PW1.4, PW2.5, PW3.5, GF3, GF5, GF6, GF7, GF8, GF9, GF10, GF11, and GF12. The cores sampled in April 2019 (PW0.4, PW1.3, PW1.4, PW2.5, and PW3.5) were sampled and analysed by an M.Sc. student; however, the sampling protocol was identical. Core sampling was completed using a Russian corer, with an internal diameter (ID) of 5 cm, to bore to a depth of 100 cm, except at sites where the peat/clay substrate was < 100 cm. Consequently, the core depths ranged from 50 to 100 cm. All soil cores were stored at 4 °C until processing, which began around two weeks after collection. The soil cores were horizontally divided into 10 cm (June 2021) or 25 cm (April 2019) sections. Subsamples of the soil sections were homogenized, air-dried, ground, and sieved (< 2 mm). Further, the peat subsamples were dried (105 °C for 24 hours) and milled (Laval Lab Inc. Planetary Ball Mill Pulverisette 5, Laval, Canada), before determining C:N, total carbon (C_t) and total nitrogen (N_t). The subsamples were analysed with a CN elemental analyser (Thermo Scientific™ Flash 2000 Elemental Analyser, Waltham, MA, US).

4.2 Hydrochemical Monitoring & Analysis

To understand the spatial and temporal variations in the fen of dissolved inorganic and organic N, cations, and DOC, multiple water sources were measured fortnightly from May 2021 to May 2022 (Figure 4.1). The sources were groundwater springs (GS), surface water (SW), Chalk groundwater (CG), shallow groundwater (SG), and fen porewater (PW).

Thirteen spring groundwaters were sampled, seven located upstream of the fen (GS2 to GS6) and six within the fen (GS7 to GS11b) (Figure 4.1). The seven upstream springs are the River Whitewater source. Four surface water sites (SW4 to SW1) were located along the River Whitewater adjacent to the fen, following the northeast direction of the river flow (Figure 4.1). Furthermore, a protostream (PS1) located inside the fen which joined the river was sampled. All groundwater springs and surface water samples were obtained by rinsing followed by submerging a 250 ml HDPE bottle in the water source. Rinsing involved submerging, filling, and emptying the sample bottle with the respective sample site water.

The Chalk groundwater samples (CG02 and CG03) and shallow groundwater samples (SG01 and SG05) were accessed through four steel boreholes (two for each source) within the fen. These were installed at depths of approximately 16 m (Chalk substrate) and 2 m (gravel/clay/peat substrate) for the Chalk and shallow groundwater boreholes (Table 4.1). All boreholes were cased to prevent the influence of water in other geological substrates through which the boreholes passed. The shallow groundwater sites were distinguished from the porewater sites, as they were deeper (2 m compared to 0.5 to 1 m) and the substrate potentially varied from gravel/clay/peat. The samples were collected under suction (operated manually using PVC tubing attached to a thumb wheel pipette pump) and dispensed into 250 ml HDPE bottles.

The twelve porewater sampling sites (PW0.2, PW0.3, etc.) were also located within the fen and were organised into four transects, running perpendicular to the river. However, this was not always possible due to dense vegetation and hazards such as surface water pools and the quaking bog; sometimes, resulting in skewed or overlapping transects. Porewater was sampled using the same suction technique as described for Chalk groundwater and shallow groundwater sites, collected from dipwells installed in April 2019 by an M.Sc. student, the depths of which range between 50 and 100 cm. The dipwells were installed by taking a soil core using a Russian corer (ID = 5 cm) to a depth of 100 cm, except where the soil depth was < 100 cm, followed by inserting perforated PVC tubes (ID = 5 cm) into the hole. All water samples were transported in a freezer box and stored at 4 °C until analysis, which was carried out within 72 hours.

Table 4.1: Depths of Chalk groundwater and shallow groundwater boreholes.

Borehole	Depth (m)	Substrate
CG02	16	Chalk
CG03	15.5	Chalk
SG01	2	Gravel/clay/peat
SG05	2.5	Gravel/clay/peat

In the laboratory, all water samples were filtered (Whatman 41, 20 µm filter) and portioned into subsamples for the analysis of dissolved inorganic and organic N, cations, and dissolved organic carbon (DOC) (Figure 4.2). The samples portioned for the analysis of dissolved organic nitrogen (DON), cations, and DOC were filtered again (Whatman 0.45 µm membrane filter). Ammoniacal-N (NH_3-NH_4-N, measured as NH_3-N), nitrite-nitrate-N (NO_2-NO_3-N, measured as NO_3-N), and phosphorus (P) were measured with an automated colourimetric analyser (Skalar San[++] Continuous Flow Analyser, Breda, The Netherlands), with detection limits of 0.03 to 0.34 mg l^{-1}, 0.13 to 0.49 mg l^{-1}, and 0.02 to 0.024 mg l^{-1} for NH_3-N, NO_3-N, and P, respectively. The range of detection limits was due to the detection limit being calculated for each sample batch. It should be noted that the water samples measured for NH_3-N, NO_3-

N, and P and filtered only through the Whatman 41 (20 µm filter) paper may have led to a slight overestimation of concentrations compared to previous studies that filtered through a Whatman 0.45 µm membrane filter. The filtration protocol ensured continuity throughout the study, as the double filtration of samples was completed from the start. DON was determined using sodium persulfate ($Na_2S_2O_8$) and a digestion oven (CEM MARS 5 Digestion Microwave). The digested samples were analysed with an automated colourimetric analyser (Skalar San[++] Continuous Flow Analyser, Breda, The Netherlands). DON was calculated based on the difference between total dissolved N and total inorganic N (TIN) (DON = TDN – TIN). The cations, calcium (Ca^{2+}), magnesium (Mg^{2+}), potassium (K^+), sodium (Na^+), total iron ($Fe^{2+/3+}$), and aluminium (Al^{3+}), were determined by acidifying samples with concentrated (v/v 5 ‰) nitric acid (HNO_3) and analysed using ICP-OES (Perkin Elmer Optima 7300 ICP-OES, Waltham, Massachusetts, United States). DOC was determined by acidifying the samples with 0.1 ml of concentrated (v/v 15 ‰) hydrochloric acid (HCl) and analysed using a total organic carbon (TOC) analyser (Shimadzu TOC-L, Kyoto, Japan). The analysis methods used here are well-established water quality analysis techniques (Miner, 2006; Neal, et al., 2006).

It should be noted that different pore sizes were used in Chapters 5 and 6 and Chapter 7. In Chapters 5 and 6, pore sizes of 0.45 µm or 20 µm (Figure 4.2) were used for all water samples measured. While Chapter 7 used a nominal pore size of 0.1 µm due to the use of Rhizon samples for pore water sampling in the experiment (Section 7.3.2). This was unlikely to affect the concentrations of dissolved solutes such as NO_3-N and cations (Ca^{2+}, Mg^{2+}, K^+, and Na^+), but may have affected concentrations of analytes with colloidal phases, such as DON, DOC, Fe, and P. Therefore, some caution should be applied to the comparison of the results in these potentially colloidal analytes in Chapters 5 and 6 and Chapter 7.

```
                        Water
                        sample
                          │
                      Whatman 41
                        filter
            ┌─────────────────┴─────────────────┐
                                          0.45 µm
       Colourmetric                       membrane
        Analysis                           filter
            ┌─────────────────────┴─────────────────────┐
       Microwave              ICP-OES                 TOC-L
       Digestion
```
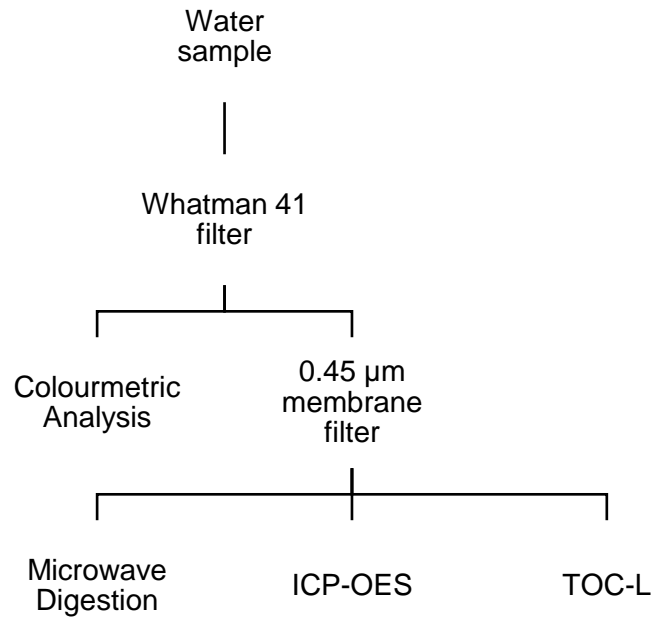
Figure 4.2: Tree diagram of the hydrochemical analysis procedure.

4.3 Hydrological Monitoring & Analysis

Continuous hydrological monitoring was carried out over the same period as the hydrochemistry (Section 4.2, May 2021 to May 2022), including Chalk groundwater (boreholes CG02 and CG03), shallow groundwater (boreholes SG01 and SG05), fen water (GF3, GF4, etc.), and surface water (SW1) (Figure 4.1c). Fen hydrology was monitored using 13 dipwells installed in November 2020 using a similar method as described in Section 4.2. The depths of the dipwells ranged between 30 and 100 cm. All hydrological data collection, quality assurance checks, and calibration were completed by a South East Water Field Scientist, an employee of the water company operating the groundwater abstraction site (Summers 2021, personal communication, 16 July).

Water table heights at all borehole and dipwell sites were measured continuously at 15-minute intervals using pressure transducers (Solinst® M5 Level Loggers, Georgetown, Ontario, Canada). Barometric data were corrected for atmospheric variability using a pressure transducer installed at the groundwater abstraction site (Figure 4.1c - 51.256°N 0.965°W). Barometric data were converted to metres below ground level and then to metres above ordnance datum (mAOD). The mAOD unit was chosen to remove the effect of local ground surface height variation. Quality assurance was completed monthly, manually measuring the water table with an in-situ water level meter, and this measurement was compared to the continuous measurement.

The river water level (m) was continuously monitored at 15-minute intervals using an automated Nivus® PCM4 flowmeter installed on the riverbed, labelled SW1 (Figure 4.1c - 51.256°N 0.967°W). The river water level (m) was converted into mAOD. Quality assurance was completed monthly using manual water level measurements from a water depth gauge board.

Rainfall was monitored using a Casella Tipping Bucket Rain gauge (TBR), located at the groundwater abstraction site with a 0.2 mm tipping spoon. Rainfall was collected within a 400 cm^2 aperture and the data was converted to daily rainfall (mm d^{-1}). Groundwater abstraction volumes were recorded continuously at 15-minute intervals using flow meters installed in the groundwater abstraction boreholes, which were monitored and maintained by South East Water (Earl 2022, personal communication, 28 October). Data were received in the 15-minute interval (water table heights, surface water levels, and groundwater abstraction) and daily rainfall formats.

5.0 Nitrogen Concentrations in a Calcareous Nitrate-enriched Fen across Space and Time

This chapter explores how water table management and NO_3-N enrichment affect the N status of a lowland fen. The chapter presents the results of a year-long continuous monitoring programme at Greywell Fen of both N species and groundwater table behaviour (see Chapter 4.0 for methods and methodology). Consequently, the chapter determined where, when, and how N concentrations varied across the groundwater-fed fen, providing a characterisation of the study site which was used to inform further research topics in Chapters 6 and 7.

5.1 Introduction

In the UK, 80% of peatlands are designated as degraded, which is associated with mismanagement and change in land use (IUCN, 2018). Peatlands are unique habitats that are important for global carbon storage and sequestration, drinking water, biogeochemical cycling, and the cultivation of rare biodiversity (Verhoeven, et al., 2006; Acreman, et al., 2011; Zomeren, et al., 2012; Ramsar Convention on Wetlands, 2018). Groundwater-dependent peatlands, or fens, are particularly vulnerable to changes in land use, being situated in lowland permeable catchments subject to drainage and groundwater-fed pollution. In southern England, groundwater abstraction accounts for 30% of drinking water, predominantly in lowland permeable Chalk catchments (Shand, et al., 2007), where rare calcareous fens are commonly located.

Calcareous fens, or rich fens, are defined by their cation- and carbonate-rich and nutrient-poor porewaters (Bridgham, et al., 2001; Paulissen, et al., 2004), reflecting the hydrochemistry of groundwater inflow. However, many of the Chalk aquifers in the UK are contaminated with nitrate (NO_3-N), a consequence of 'legacy nitrate storage' from intensive agriculture (Stuart &

Lapworth, 2016; Wang, et al., 2016). Previously, calcareous nitrate-enriched groundwater concentrations have been shown to range from 5.7 to 9.0 mg NO_3-N l^{-1} (Allen, et al., 2010; House, et al., 2015; Johnes, et al., 2020), which can lead to nitrogen (N) enrichment; however, groundwater-borne NO_3-N is subject to transformation by a variety of N cycling reactions. N cycling in peatlands is complex, varying over space and time (Hefting, et al., 2006; Frank, et al., 2014; Frei & Peiffer, 2016; Bernard-Jannin, et al., 2017; Rezanezhad, et al., 2017; Johnes, et al., 2020; Zhang & Furman, 2021). Primarily, N dynamics are controlled by water table heights, which determine the aerobic-anaerobic boundary and N transformation (Brix, 1994; Hoffmann, et al., 2011; Lind, et al., 2012; Mwagona, et al., 2019; Han, et al., 2020). Groundwater-fed fens are believed to have stable water tables (Almendinger & Leete, 1998), where N can be cycled by processes such as denitrification and dissimilatory nitrate reduction to ammonium (DNRA) (Reddy & Patrick, 1986; Bachand & Horne, 1999; Martens, 2005; Burgin & Hamilton, 2007; Scott, et al., 2008), as well as N attenuation by plant uptake (Haycock & Pinay, 1993; Kuusemets, et al., 2001; Vincent, et al., 2018; Johnes, et al., 2020). However, if the water table is lowered, N can be made available by nitrification or organic matter mineralisation (Lindau, et al., 1999; Venterink, et al., 2002; Sandrin, et al., 2009).

As a result of the anaerobic nature of peatlands and potentially high N cycling and attenuation, they are considered N limited and N sinks, which can limit vegetation growth (Beltman, et al., 1996; Duren & Pegtel, 2000) However, N concentrations in rich fens are suggested to be greater than other types of peatlands due to higher pH, higher mineral content, and more hydrological inputs (Bridgham, et al., 1996; Bridgham, et al., 1998); however, studies have challenged this finding (Verhoeven & Schmitz, 1991; Mettrop, et al., 2014). Almendinger & Leete (1998) reported average porewater concentrations of 0.50 mg NO_3-N l^{-1} in several unmanaged calcareous peatlands. Although Duval & Waddington (2018) reported lower mean porewater NO_3-N concentrations of < 0.05 mg NO_3-N l^{-1} in three unmanaged calcareous fens. The mean ammonium (NH_4-N) concentrations reported were considerably higher, reaching 0.36 mg NH_4-N l^{-1}. Vitt & Chee (1990) reported that seasonally

variable N, with organic N and NH_4-N highest during autumn in a moderately rich fen, while NO_3-N and NH_4-N were highest during spring in an extremely rich fen; however, the mean concentrations of NO_3-N and NH_4-N were low, < 0.05 mg NO_3-N l^{-1} and < 0.06 mg NH_4-N l^{-1}. The mean concentrations of organic nitrogen were considerably higher, ranging from 1.18 to 2.50 mg l^{-1}. Boomer & Bedford (2008) reported that NO_3-N and NH_4-N concentrations varied spatially, depending on groundwater flow paths in three rich fens.

Low resolution sampling is frequently used to investigate N concentrations, but this does not adequately consider N dynamics across space and time or N speciation. Often, more rigorous sampling regimes identify a more complex biogeochemical system, where N concentrations are highly variable and fluctuate between an N source or sink (Prior & Johnes, 2002; Allen, et al., 2010; House, et al., 2015; Johnes, et al., 2020). Jarvie et al. (2020) reported high NH_4-N release (up to 5.7 mg NH_4-N l^{-1}) between late summer and autumn at the outlet of a lowland wetland pond system, but NO_3-N concentrations remained low. Johnes et al. (2020) reported considerable concentrations of dissolved organic nitrogen (DON) in porewaters (up to 16 mg l^{-1}) during a rain event at the end of autumn, in a calcareous meadow fed by nitrate-enriched groundwater (up to 9 mg NO_3-N l^{-1}). At the same study site, porewater NO_3-N concentrations remained > 2.0 mg NO_3-N l^{-1} throughout a 2-year study, reaching up to 5.0 mg NO_3-N l^{-1} between winter and early spring (Prior & Johnes, 2002). Furthermore, increased N concentrations have been reported in fens impacted by groundwater abstraction (Bart, et al., 2020), where water tables are managed, that is, water table lowering can increase N concentrations in peatlands (De Mars, et al., 1996; Venterink, et al., 2002; Mettrop, et al., 2014). Consequently, comprehensive sampling regimes across space and time and the measurement of multiple N species are required to properly assess N concentrations in fen peatlands, particularly in managed sites where high N concentrations can occur.

This work aims to assess the N status of groundwater-fed calcareous peatlands impacted by nitrate-enriched groundwater and groundwater abstraction. Respectively, the objectives

are to (1) identify the N variability in the fen porewater and related water sources throughout space and time; (2) investigate the impact of groundwater abstraction on (a) water table heights and (b) porewater N; and (3) asses the processes that can be attributed to the observed N variability in the fen porewater. Greywell Fen was used as a case study because it provides a rare opportunity to observe the effects of groundwater abstraction and N enrichment simultaneously.

5.2 Methodology

5.2.1 Study Site Description

Greywell Fen (51.251°N 0.971°W) is located in Hampshire, United Kingdom. It is a calcareous groundwater-dependent peatland (pH = 6.5 to 8.3) that encompasses a 38-ha area and a designated Site of Special Scientific Interest (SSSI), due to its ecological value (Figure 5.1). The surrounding area is used for intensive mixed arable production. The bedrock geology is dominated by Seaford and Newhaven Chalk formations, overlain by permeable and semipermeable superficial deposits of gravel (River Terrace Deposits), clay, and peat. These alluvial deposits (gravel and clay) are up to 10 m deep and the peat deposits are up to 3 m deep. The Chalk groundwater at the site is known to be highly NO_3-N contaminated with mean concentrations of 7.00 mg NO_3-N l^{-1} (between 1997 and 2021). The total rainfall over the study period was 549 mm.

The fen is situated within a lowland valley, 80 meters Above Ordnance Datum (mAOD), with western and eastern sloping boundaries rising to 100 mAOD. Additionally, the River Whitewater runs through the valley, bordering the fen for 2 km along its western edge. It is a typical lowland Chalk stream common in the southeast of England. The river headwaters, discrete groundwater springs, are located south of the fen (Figure 5.1), as well as multiple

discrete groundwater springs scattered throughout the fen, concentrated along its eastern edge.

Greywell Fen has been a designated SSSI since 1951 (Ratcliffe, 1977), notable for bottle sedge (*Carex rostrata*), pointed & giant spear-moss (*Calliergon cuspidatum/giganteum*), blunt-flowered rush (*Juncus subnodulosus*), and marsh thistle (*Cirsium palustre*) species (Rodwell, 1991). However, as a result of ecological zonation, succession, and potential ecohydrological degradation, the fen has been colonised by alder (*Alnus glutinosa*) and willow (*Salix*), shifting vegetation from open marshland/mire species to wet woodland (Jacobs, 2019). Thus, the fen has been actively managed to restrict afforestation through annual herd grazing and tree/shrub removal - which occurred during this study in the spring/summer of 2020 and winter of 2022. Furthermore, the fen is subject to a nearby groundwater abstraction site (Figure 5.1), which has been operational since 1908.
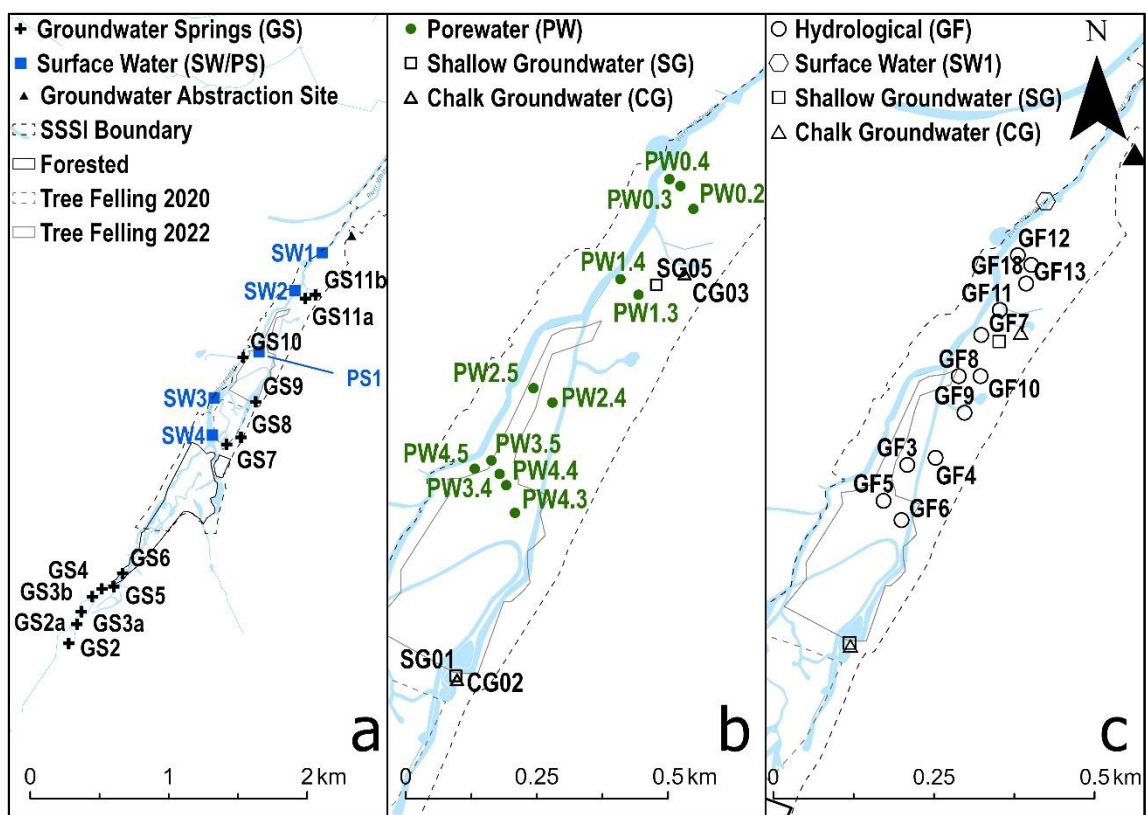
Figure 5.1: Locations of soil, hydrochemical, and hydrological sampling sites in Greywell Fen (further explained in Chapter 4).

5.2.2 Soil Sampling & Analysis

Please refer to Section 4.1 for an explanation of soil sampling & analysis

5.2.3 Nitrogen Monitoring & Analysis

Please refer to Section 4.2 for an explanation of N monitoring & analysis

5.2.4 Hydrological Monitoring & Analysis

Please refer to Section 4.3 for an explanation of hydrological monitoring & analysis

5.2.5 Statistical Analysis

Spearman's rho correlation analysis was used for all correlation analyses, as most of the measured variables did not meet normality. The one-way analysis of variance (Kurskal-Wallis) test was used to evaluate N differences in water sources, and a threshold of 0.05 was used for significance. All data and statistical analyses were performed in RStudio® Version 1.4.1103.

5.3 Results

5.3.1 Hydrological Dynamics

To understand whether the groundwater abstraction affected the groundwater water table, the correlations of mean water table heights with groundwater abstraction site distance (Figure 5.2) and daily water table heights with daily abstraction volume (Figure 5.3) were analysed to identify any drawdown effect. Furthermore, the correlations between hydrological monitoring sites were examined to understand their potential relationship and hydrological connectivity to one another. The correlation of groundwater table heights with groundwater abstraction site distance showed a weak but not statistically significant positive correlation (rho = 0.2, p-value = 0.45), providing weak evidence of a groundwater abstraction effect on the groundwater table height relative to distance (Figure 5.2). Generally, groundwater tables were stable during the study with standard deviations < 0.10 mAOD. The water table heights of Chalk groundwater at CG02 (77.92 ± 0.05 mAOD) and CG03 (77.79 ± 0.05 mAOD) differed, and CG02 had higher groundwater table heights and was further from the groundwater abstraction site. The shallow groundwater site SG05 had the highest and most stable mean groundwater table height in the study (78.04 ± 0.01 mAOD), while SG01 (77.1 ± 0.05 mAOD) showed lower mean groundwater table heights, but was further from the groundwater abstraction site than SG05. It should be noted that sites SG01, CG02, and CG03 were elevated on a grassy bank above the other monitoring sites (SG05 and GF), contributing to the much higher groundwater table heights (Figure 5.2). The mean groundwater table heights of the GF sites were between 77.19 and 77.60 mAOD, but the variability of each site was relatively small, with standard deviations between 0.01 and 0.08 mAOD. The sites GF5, GF12, and GF18 had the highest standard deviations, 0.08 mAOD, 0.06 mAOD, and 0.07 mAOD, respectively, with GF12 and GF18 located closest to the groundwater abstraction site.
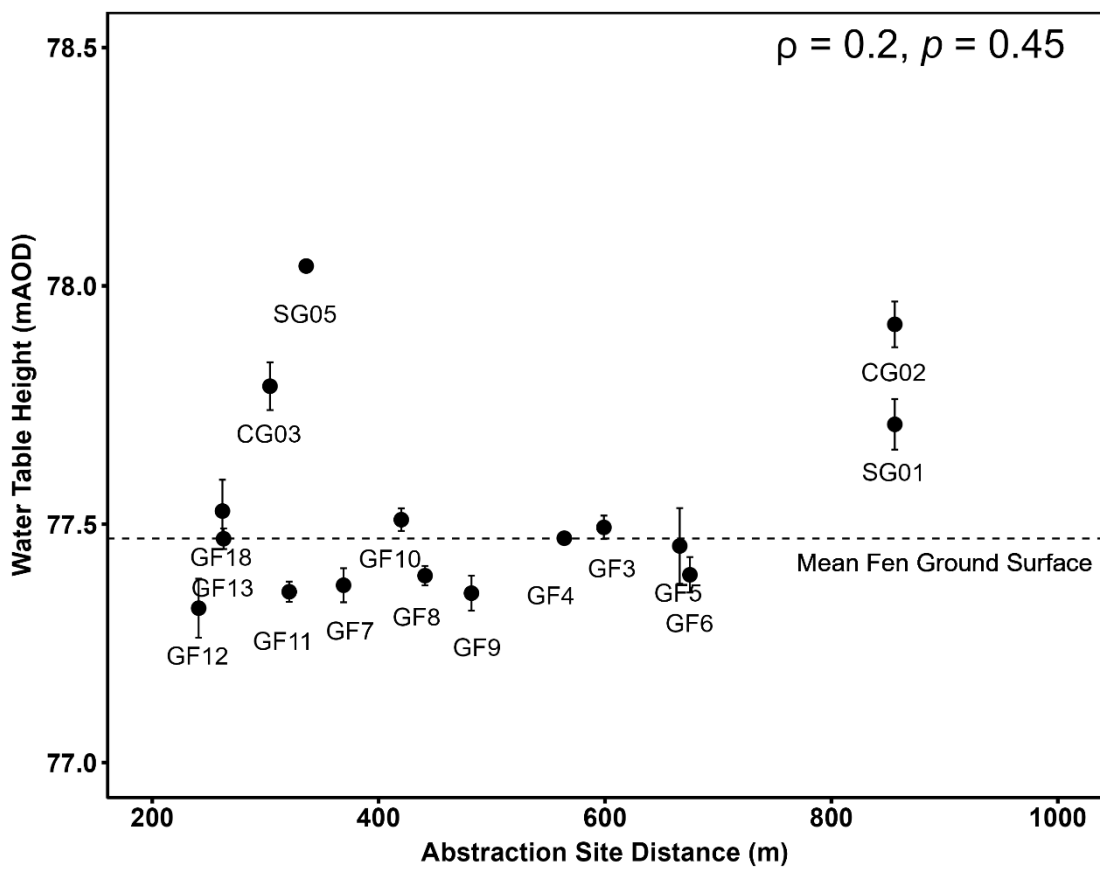
Figure 5.2: Mean groundwater table heights of hydrological monitoring sites compared with their distance from the groundwater abstraction site. The monitoring sites are explained in Chapter 4.0. Spearman's rho correlation was used for the correlation analysis to emphasise any potential drawdown effect by groundwater abstraction. Error bars represent the standard deviation and the dotted line represents the mean fen ground surface level (mAOD) ($n = 3$).

Daily groundwater abstraction volume (GWA) over the study period ranged between 2615 and 5437 m^3. GWA did not correlate strongly with the groundwater table height at any monitoring site (Figure 5.3), indicating that groundwater abstraction variability did not have an acute impact on groundwater table heights. In general, the two CG sites were closely related (rho = 0.71) to each other and to the GF sites (Figure 5.3), suggesting that groundwater table heights within the fen were influenced by hydrological processes in the aquifer; for example, groundwater recharge (Edmunds, et al., 1987; Abesser, et al., 2008). Although there were some variations between the GF sites, they were generally well correlated (Figure 5.3), indicating that the hydrological processes that influenced the groundwater table height in the fen were similar or related. The distance between the GF sites appeared to influence the correlations; for example, GF4 to GF6 were all highly correlated and close to each other. However, there were instances where the GF sites, which were distant from each other, showed high correlations, for example, GF18 and GF5 or GF13 and GF9 (Figure 5.3).

Surface water levels were positively correlated with the shallow groundwater and GF hydrological monitoring sites (Figure 5.3), suggesting a hydraulic gradient from the fen to the river. Interestingly, the GF sites that were more closely correlated with surface water levels were the sites farthest away from the surface water monitoring site (Figure 5.1). In contrast to the GF sites, surface water levels did not correlate well with the Chalk groundwater sites. Furthermore, groundwater abstraction (GWA) had the strongest negative correlation with surface water levels, suggesting a particular impact of groundwater abstraction on surface water levels.
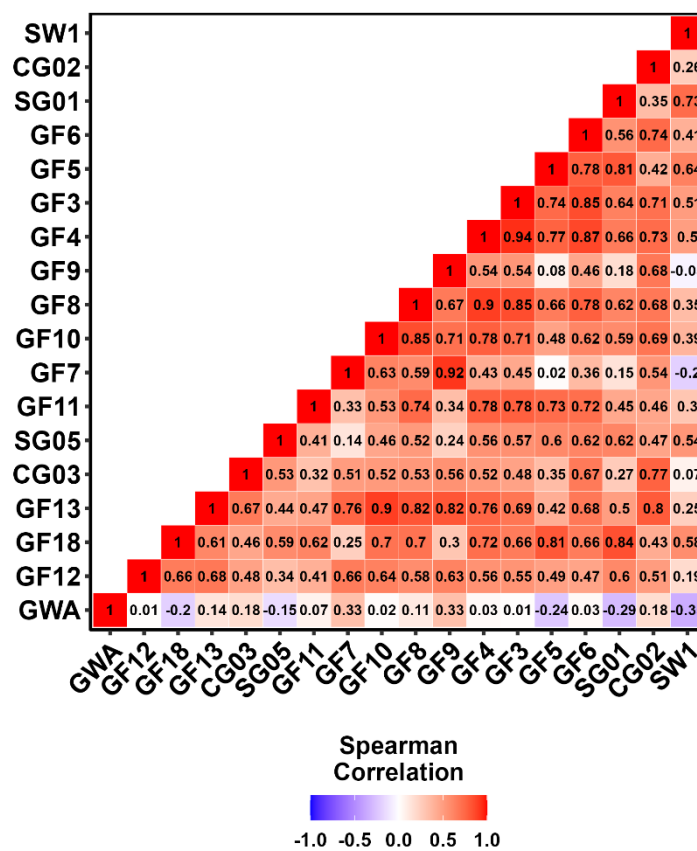
Figure 5.3: Spearman's rho correlation between daily groundwater table heights at the hydrological monitoring sites, surface water levels and daily groundwater abstraction volumes (GWA).

5.3.2 Water Source Nitrogen Concentrations

N concentrations depended on the water source, especially NO_3-N (Table 5.1). NO_3-N was highest in groundwater springs (median = 10.62 ± 3.10 (SD) mg NO_3-N l^{-1}), surface water (8.67 ± 2.25 mg NO_3-N l^{-1}) and Chalk groundwater (7.46 ± 2.06 mg NO_3-N l^{-1}) and lowest in shallow groundwater (1.28 ± 3.05 mg NO_3-N l^{-1}) and porewater (0.40 ± 1.79 mg NO_3-N l^{-1}). NO_3-N differed significantly between groundwater springs, surface water, Chalk groundwater, shallow groundwater, and porewater with all p-values < 0.001. Furthermore, NO_3-N differed significantly from groundwater springs and Chalk groundwater (p-value < 0.001), but there was no significant difference between surface water and Chalk groundwater (p-value $= 0.07$) or surface water and groundwater springs (p-value $= 0.09$).

Spatial patterns in DON concentrations were similar to those of NO_3-N (Table 5.1), being consistently higher than in groundwater springs, surface waters, and Chalk groundwater sites, with median values ranging from 1.19 to 6.81 mg l^{-1} during the study, compared to the shallow groundwater and porewater sites, which ranged from 0.00 to 5.02 mg l^{-1}. Similarly, DON differed significantly between groundwater springs, surface water, Chalk groundwater, and porewater with all p-values < 0.001. Although DON did not differ significantly between groundwater springs, surface water, or Chalk groundwater (p-value $= 0.08$ to 0.58).

NH_3-N was low or below the detection limits in all water sources (Table 5.1), and did not differ significantly between any of the water sources (p-value $= 0.05$ to 0.60).

Table 5.1: Summary of N characteristics for each water source (median concentration in mg l^{-1}). Concentrations in bold or underlined represent the highest and lowest concentrations, respectively, in the water sources (May 2021 - May 2022).

	GS					SW					CG					SG					PW				
	n	Min.	Max.	Med.	SD	*n*	Min.	Max.	Med.	SD	*n*	Min.	Max.	Med.	SD	*n*	Min.	Max.	Med.	SD	*n*	Min.	Max.	Med.	SD
NH₃-N	259	0.03	0.63	0.09	0.07	95	0.03	0.26	<u>0.08</u>	0.05	40	0.03	0.56	<u>0.08</u>	0.09	39	0.03	0.97	**0.11**	0.25	239	0.03	1.35	0.09	0.49
NO₃-N	259	1.53	15.7	**10.62**	3.10	95	0.21	11.03	8.67	2.25	40	0.10	9.29	7.46	2.06	39	0.10	8.18	1.28	3.05	239	0.10	8.67	<u>0.40</u>	1.79
DON	259	0.00	6.81	2.79	1.14	95	0.00	4.10	2.44	0.88	40	0.00	5.89	2.21	1.36	39	0.00	4.50	0.87	1.26	239	0.00	5.02	0.05	0.79

5.3.3 Spatial and Seasonal Nitrate Variability

The groundwater springs outside the fen (OF) (GS2 to GS6), considered the source of the river (Figure 5.4), consistently had the highest median NO_3-N concentrations, between 10.61 and 14.01 mg NO_3-N l^{-1}. NO_3-N concentrations in groundwater springs inside the fen (IF) (GS7 to GS11b), surface water (SW4 to SW1), and Chalk groundwater sites (CG02 and CG03) ranged from 5.55 to 9.11 mg NO_3-N l^{-1}, 8.01 to 10.03 mg NO_3-N l^{-1}, and 7.01 to 7.97 mg NO_3-N l^{-1}, respectively (Figure 5.4). Interestingly, NO_3-N concentrations in groundwater springs outside the fen (OF) differed significantly from groundwater springs inside the fen (IF, p-value < 0.001), surface water (p-value < 0.001) and Chalk groundwater sites (p-value < 0.001).

NO_3-N did not differ significantly between groundwater springs IF, surface water, and Chalk groundwater sites, with p-values ranging from 0.14 to 0.97. The median values showed that surface water NO_3-N decreased downstream from 9.3 ± 0.82 mg NO_3-N l^{-1} (SW4) to 8.44 ± 2.08 mg NO_3-N l^{-1} (SW1). Although PS1, a protostream within the fen, showed median values ranging from 3.90 to 4.83 mg NO_3-N l^{-1} (Figure 5.4). However, the surface water NO_3-N concentrations did not differ significantly downstream (p-values = 1.00) or from those in the protostream, PS1 (p-values = 0.18 to 1.00). In general, the NO_3-N concentrations at shallow groundwater and porewater sites were considerably lower (Figure 5.4). They could be classified into two groups based on NO_3-N concentrations: sites with median NO_3-N > 1 mg NO_3-N l^{-1} (SG01, PW0.2, PW2.4, and PW4.4) and < 1 mg NO_3-N l^{-1} (SG05, PW0.3, PW0.4, PW1.3, PW1.4, PW2.5, PW3.4, PW3.5, PW4.3, and PW4.5).

In general, seasonal variations of NO_3-N concentrations (the median value for each season) were limited at all water source sampling sites (Figure 5.4). Seasonal median concentrations in > 1 mg NO_3-N l^{-1} sites ranged from 1.37 ± 1.12 to 6.86 ± 2.09 mg NO_3-N l^{-1}, compared to < 1 mg NO_3-N l^{-1} sites which were consistently near or below detection limits. In general, > 1 mg NO_3-N l^{-1} sites had seasonal variation, with median values of SG01, PW0.2, PW2.4, and

PW4.4 ranging from 4.74 ± 0.17 to 6.86 ± 2.09 mg NO_3-N l^{-1}, 1.50 ± 1.15 to 5.96 ± 1.36 mg NO_3-N l^{-1}, 1.37 ± 1.12 to 4.26 ± 1.55 mg NO_3-N l^{-1}, and 1.77 ± 2.63 to 6.09 ± 1.34 mg NO_3-N l^{-1}, respectively, highest in winter and spring. However, NO_3-N did not differ significantly between SG01 and SG05 (*p*-value = 0.29) or between any of the porewater sites (*p*-values = 1.00).

2021 - 2022

Spring

Summer
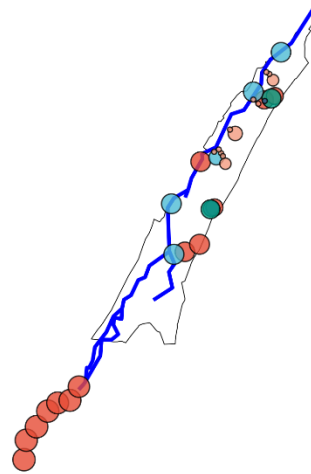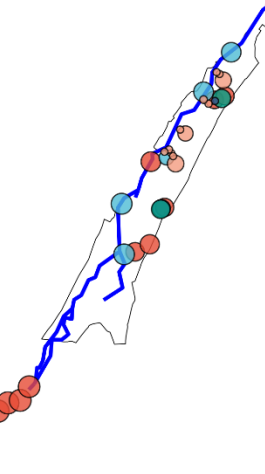
Autumn

Winter
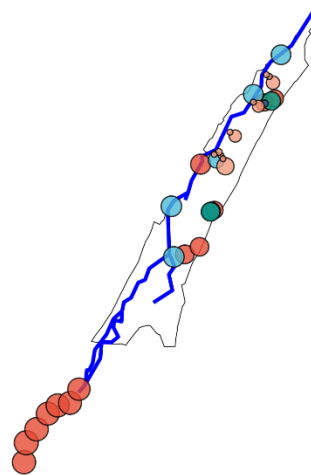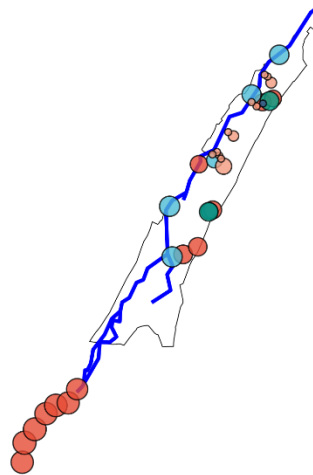
Groundwater Spring • Surface Water
Chalk Groundwater • Shallow Groundwater
Porewater

$NO_3 - N \; (mg \; l^{-1})$

○ 2 ○ 4 ○ 6 ○ 8 ○ 12

Figure 5.4: Seasonal median NO₃-N concentrations of water sources in Greywell Fen (May 2021 - May 2022).

5.3.4 High Nitrate Sources and Sites Temporal Variability

Water sources and sampling sites with high NO_3-N concentrations were further investigated to observe their relationships under higher temporal resolution (Figure 5.5). The NO_3-N concentration in groundwater springs outside (OF) and inside (IF) the fen, the surface water, and Chalk groundwater sites showed similar temporal changes, with a pattern of decreasing concentrations from summer to mid-winter and then increasing from late winter to mid-spring; although, a sudden decrease occurred in early March. The groundwater springs outside the fen (OF) showed similar but weaker temporal NO_3-N concentration trends compared to groundwater springs inside the fen (IF), surface water, and Chalk groundwater.

In general, the temporal NO_3-N concentration trends of shallow groundwater and porewater were relatively similar to those of groundwater springs, surface waters, and Chalk groundwater: decreasing from summer to early autumn, increasing slightly, staying relatively stable throughout autumn and winter, and increasing again from late winter to late spring, although there were differences (Figure 5.5). Sites SG01 and PW4.3 were strongly related to the temporal trends in groundwater springs, surface waters, and Chalk groundwater. Although PW0.2 and T2.4 had relatively weak associations between summer and autumn, they became more associated with the groundwater springs, surface waters, and Chalk groundwater during winter and spring (Figure 5.5).
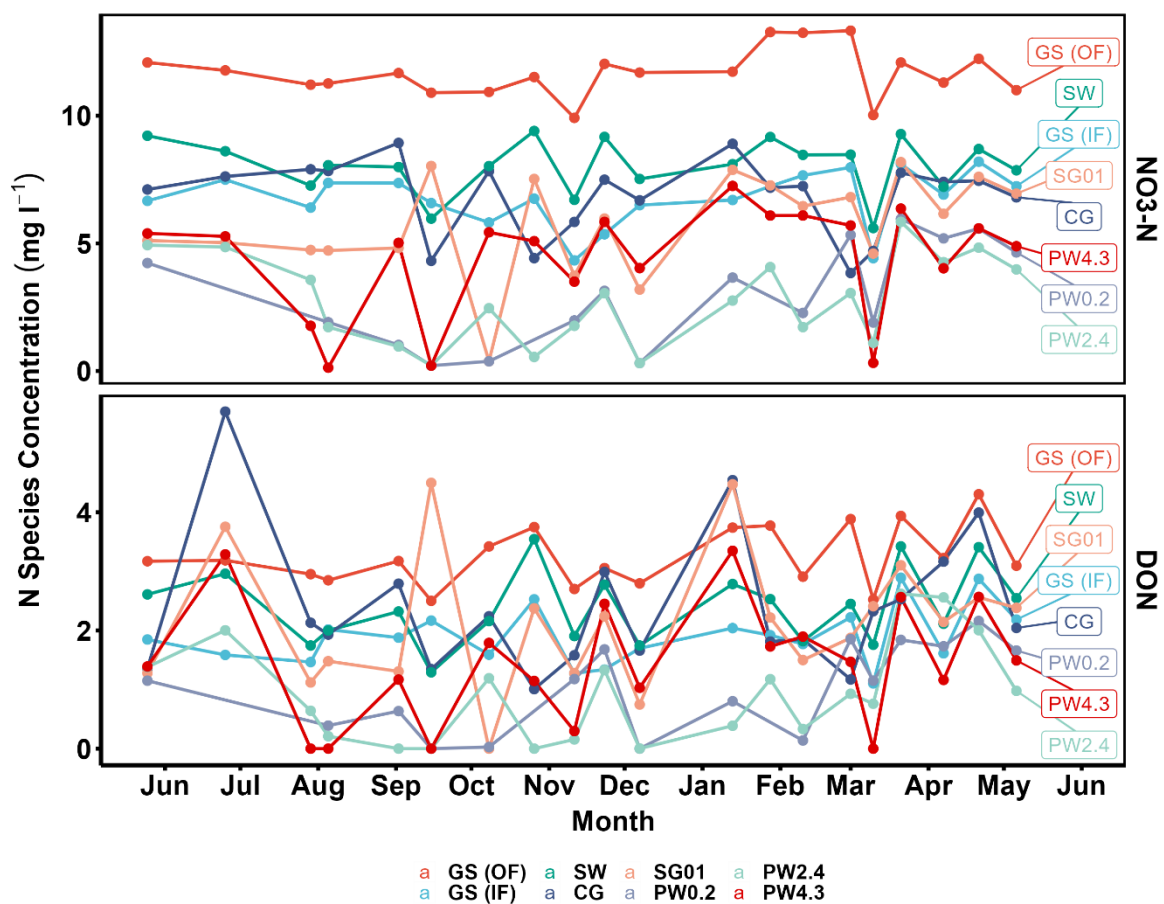
Figure 5.5: N speciation (NO$_3$-N & DON) of water sources and high NO$_3$-N shallow groundwater and porewater sites over the study (May 2021 – May 2022). For water sources, the median value of cumulative sampling sites was used.

5.3.5 Nitrogen Concentrations and Groundwater Table Height Correlation

A correlation analysis of N with groundwater table heights was performed, where possible, to determine the effect of the water table height on N concentrations (Table 5.2). In general, NO_3-N concentrations in peatlands are considered to decrease with increasing water tables, resulting from decreased mineralisation and increased denitrification (Thormann, et al., 1997; Bouskill, et al., 2019). It should be noted that not all PW sites had direct groundwater table measurements; instead, groundwater table measurements from the closest GF sites were used (distance < 5 m), when required. In general, N was not strongly correlated with groundwater table heights (mAOD) when considering all sites. However, individual sites showed stronger positive correlations, particularly SG01, PW4.3, and PW4.4 for NO_3-N.

Table 5.2: Spearman's correlation (rho) between N concentrations and daily groundwater table height at available sites (May 2021 - May 2022).

Sampling Site	n	NH_3-N	NO_3-N	DON
All	160	0.04	0.20	0.27
CG02	20	0.38	0.09	-0.005
CG03	20	-0.36	0.27	0.32
SG01	20	0.14	0.42	0.19
SG05	20	-0.07	0.09	-0.07
PW0.4 (GF12)	20	-0.01	-0.12	0.09
PW1.4 (GF7)	20	0.03	-0.35	-0.59
PW4.3 (GF6)	20	0.17	0.33	0.34
PW4.4 (GF5)	20	-0.08	0.38	0.40

5.3.6 Soil Characteristics

The C:N values of the 18 soil cores sampled across the fen are presented in Table 5.3. Across all depths, the C:N values ranged from 13.7 to 153.0. The median values of the soil cores showed considerably lower variability, ranging from 14.0 to 19.1. Visual inspection showed that the large C:N value resulted from peat to clay substrate shifts in the soil profile. In general, peat substrate C:N values were low and consistent, and peat depths varied from 40 to 100 cm.

Table 5.3: Soil characteristics (C:N values) of certain porewater and hydrological monitoring sites.

Core Site	Depth (cm)	Min.	Max.	Median
PW0.4	100	15.0	26.0	16.3
PW1.3	100	13.9	19.1	16.6
PW1.4	100	18.5	57.1	19.1
PW2.5	100	14.3	15.4	14.8
PW3.5	100	14.5	19.6	15.5
GF3	70	15.0	19.4	17.9
GF5	100	14.7	29.3	16.4
GF6	50	17.1	19.2	17.7
GF7	88	16.4	71.6	18.2
GF8	50	13.7	19.9	16.1
GF9	50	14.3	35.5	16.0
GF10	100	14.0	153.0	18.5
GF11	68	14.0	40.0	15.5
GF12	40	14.0	15.0	14.0

5.4 Discussion

The main study aim was to investigate the NO_3-N concentrations over space and time in a nitrate-enriched groundwater-fed fen subject to groundwater abstraction; specifically, to determine where, when, and how N concentrations varied over the peatland. In general, fen porewater N concentrations were low over space and time, which was comparable to other unmanaged fens (Vitt & Chee, 1990; Almendinger & Leete, 1998; Duval & Waddington, 2018); however, discrete nitrate-rich porewater sites were observed. Interestingly, groundwater abstraction appeared to have a limited effect on groundwater table heights, which contrasts with other reports (De Mars, et al., 1996; Venterink, et al., 2002; Mettrop, et al., 2014). This suggested that N concentrations were controlled by other factors, rather than groundwater table drawdown.

5.4.1 Spatial and Temporal Variation of Groundwater Table Height

Continuous groundwater table height measurements at fen monitoring sites (GF) (Figure 5.2) were within typical ranges reported in other unmanaged fens in the United States (Amon, et al., 2002; Bedford & Godwin, 2003). However, there was spatial variability between the hydrological monitoring sites (77.32 to 77.53 mAOD), which showed a nonsignificant correlation with groundwater abstraction (rho = 0.20, p-value = 0.45), suggesting a weak groundwater table drawdown effect. Furthermore, the two monitoring sites closest to groundwater abstraction, GF12 and GF18, showed the highest groundwater table height fluctuations (Figure 5.2). Groundwater abstraction can create a localised cone of groundwater depression that can affect the areas closest to the groundwater abstraction site (Fojt, 1994). However, the monitoring site GF13, located near GF12 and GF18, showed stable water table heights (Figure 5.2). Bart et al. (2020) reported a nonuniform hydrological effect of groundwater abstraction in calcareous fens, which was highly influenced by small scale

hydrogeological variability (McDermott-Kurtz, et al., 2007), which may explain the groundwater table variability between sites GF13, GF12, and GF18.

Generally, hydrological monitoring sites did not show strong correlations with daily groundwater abstraction volumes (Figure 5.3), suggesting that groundwater table heights did not respond to abstraction volume variability. Furthermore, fen groundwater table heights (GF3 to GF18) showed positive correlations between each other and with the Chalk groundwater sites (Figure 5.3), indicating the influence of groundwater recharge that occurs on a seasonal basis in aquifers (Edmunds, et al., 1987; Abesser, et al., 2008). Fens overlying regional groundwater flow systems are often associated with stable groundwater table heights, particularly where aquifers are large and deep (Roulet, 1990; Hill & Devito, 1997). Previous geological studies of the study area have indicated that the underlying Chalk aquifer was large and probably regional (Section 3.2.1), buffering the effects of groundwater abstraction.

Groundwater abstraction appeared to have a potential effect on surface water levels (rho = -0.35). Interestingly, surface water levels did not correlate with Chalk groundwater sites, suggesting that surface water levels were not directly influenced by the Chalk aquifer underlying the fen and the river. This is contradictory, as there is presumably sufficient hydrological connection between surface water and groundwater abstraction for an effect to occur, but the surface water was disconnected from the Chalk aquifer directly underlying the fen and river. The primary source of the river is several groundwater springs south of the fen (approximately 2 km), suggesting that the springs may be affected by groundwater abstraction; however, this would be unlikely due to the distance from the groundwater abstraction site and the relatively limited effect of groundwater abstraction on hydrological monitoring sites closer to the abstraction site (Figure 5.1). Furthermore, there appeared to be a hydraulic gradient from the fen to the river (Figure 5.3), indicating that the fen supplemented the surface water level affected by groundwater abstraction. It is not known how often this occurs from the river to the fen, but evidence suggests that the fen is better connected to the underlying Chalk

aquifer compared to the river. It is recommended that further studies investigate the hydrological connection between the river and the Chalk aquifer. However, for the scope of this study, groundwater abstraction appeared to have a limited effect on the fen groundwater table height, which was largely near the surface and stable (Figure 5.2).

5.4.2 Spatial and Temporal Variation of Nitrogen

NO_3-N was the dominant N form observed in the study and is, therefore, the primary focus of this discussion. Consistently high NO_3-N concentrations (as well as DON) in groundwater springs, surface waters, and Chalk groundwater suggested that the Chalk aquifer was the main N source for the fen and water sources (Figure 5.4). High hydrological connectivity between aquifer-groundwater-surface water has been reported in similar systems (Abesser, et al., 2008; Lapworth, et al., 2009). DON has previously been reported to be a significant component in groundwater (Lapworth, et al., 2008), particularly in Chalk groundwater (Peach, et al., 2006; Yates, et al., 2022); however, the median concentrations reported here were higher than these previous reports, which may be due to the dominance of agricultural land use surrounding the study site. Yates et al. (2022), for example, reported a significant positive relationship (p-value < 0.001) between DON and agricultural cover (%). It is interesting to note that the NO_3-N concentrations in the groundwater springs outside the fen (OF) differed significantly from the groundwater springs inside the fen (IF, p-value < 0.001), surface water (p-value < 0.001) and Chalk groundwater sites (p-value < 0.001). In addition, the groundwater springs outside the fen (OF) consistently showed the highest NO_3-N values (Figure 5.4). This could represent the stratification of the Chalk aquifer, where different degrees of nitrate-rich groundwater exist simultaneously and flow from different depths (Feast, et al., 1997). However, NO_3-N variability between groundwater springs outside and inside the fen, surface waters, and Chalk groundwater sources may also represent an influence of fen NO_3-N cycling, particularly in the groundwater springs. However, this impact is less likely in the Chalk groundwater, as the boreholes are cased down to the Chalk substrate (16 m deep).

The consistency of NO_3-N concentrations in the groundwater springs, surface water, and Chalk groundwater was generally contrasted with NO_3-N in shallow groundwater and porewater sources (Figure 5.4). Furthermore, the shallow groundwater and porewater NO_3-N varied considerably over space, showing either consistently low or high NO_3-N concentrations. This could have been influenced by numerous physical and biological processes that can vary across space and time (Haycock & Pinay, 1993; Rückauf, et al., 2004; Hefting, et al., 2006; Bouskill, et al., 2019; Johnes, et al., 2020). The shallow groundwater and porewater sites showed NO_3-N concentrations either near or below the detection limits or relatively high concentrations throughout the study. Porewater sites that showed near or below detection limits were comparable to unmanaged fens in the United States (Vitt & Chee, 1990; Almendinger & Leete, 1998; Duval & Waddington, 2018).

Generally, biogeochemical processes that can affect NO_3-N concentrations, such as plant uptake and microbial-mediated cycling, are considered to vary seasonally, fluctuating with changes in seasonal moisture conditions and temperatures (Haycock & Pinay, 1993; Kuusemets, et al., 2001; Potila & Sarjal, 2004; Maslov & Maslova, 2020). The lack of seasonal variation of NO_3-N has been observed in other lowland peatlands and wetlands (Gilliam, 1994; Sabater, et al., 2003). Plant uptake and microbial-mediated NO_3-N cycling can occur under different moisture conditions and temperatures, which could obscure any seasonality (Pinay & Decamps, 1988; Nelson, et al., 1995). Furthermore, the stable groundwater table probably facilitated microbial-mediated NO_3-N cycling throughout the study, buffering any seasonal changes of rainfall, as well as providing a consistent temperature, with groundwater typically around 10 °C in northern Europe (Rivett, et al., 2008); although this cannot be confirmed, as the groundwater temperature was not measured in this study. Dissimilatory nitrate reduction to ammonium and denitrification are important microbial-mediated NO_3-N cycling reactions and reduce NO_3-N concentrations (Tobias, et al., 2001; Rückauf, et al., 2004; Amha & Bohne, 2011; Moon, et al., 2020). Dissimilatory nitrate reduction to ammonium is associated with porewater NH_4-N accumulation (Matheson, et al., 2002; Wang, et al., 2020). However,

porewater NH_3-N was generally near or below the detection limits during the study (Table 5.1), suggesting dissimilatory nitrate reduction to ammonium was minor (Matheson, et al., 2002; Rückauf, et al., 2004). However, the low concentrations of NH_3-N could also be the result of NH_4-N volatilisation, but previous studies have reported that NH_4-N volatilisation only represented 3 to 4% of N loss in nitrogen-enriched minerotrophic (rich) fens (Mugasha & Pluth, 1995).

Low porewater NH_4-N has been reported in several unmanaged minerotrophic (rich) fens in North America (Vitt & Chee, 1990; Duval & Waddington, 2018). Previous reports of limited porewater NH_4-N accumulation in peatlands have indicated high denitrification rates (Lucassen, et al., 2004; Boomer & Bedford, 2008). High denitrification is common in peatlands, which probably contributes to the low NO_3-N concentrations at most porewater sites (Rückauf, et al., 2004; Gutknecht, et al., 2006; Hefting, et al., 2006; Amha & Bohne, 2011; Cabezas, et al., 2012). Mesotrophic and eutrophic peat has been shown to facilitate particularly high denitrification rates (Amha & Bohne, 2011), because they generally have higher rates of decomposition and biological activity compared to other peatlands (Kooijman & Hedenäs, 2009; Calver, et al., 2019). This results in considerably lower C:N values, ranging from 15 to 17 (Koreselamn, et al., 1993; Kooijman & Hedenäs, 2009), which were similar to the C:N values in this study (Table 5.3). As a result, the gaseous loss of N could be considerable; for example, Silvan et al. (2002) reported that nitrogen oxide release accounted for 15% of NO_3-N loss in a minerotrophic nitrogen-enriched fen.

The lack of seasonal variation in the low NO_3-N shallow groundwater and porewater sites probably resulted from plant uptake and denitrification (Sabater, et al., 2003); however, discrete nitrate-rich shallow groundwater and porewater sites existed within the fen (Figure 5.5). The porewater NO_3-N reported at these discrete sites corresponds to NO_3-N concentrations in a calcareous meadow fed by nitrate-enriched groundwater (Prior & Johnes, 2002). Previous reports have shown that porewater NO_3-N > 0.62 mg NO_3-N l^{-1} can represent

oxygenated conditions and lower groundwater table heights (Boomer & Bedford, 2008), leading to nitrification or organic matter decomposition, and increased NO_3-N concentrations (Hoewyk, et al., 2000; Bouskill, et al., 2019). However, the concentrations of NO_3-N in the shallow groundwater and porewater showed a weak positive correlation with the groundwater table (rho = 0.20), which was particularly strong at some sites (SG01, rho = 0.42; PW4.4, rho = 0.38). Only PW1.4 had a negative correlation with groundwater table heights (rho = -0.35); however, this site usually had low porewater NO_3-N (0.40 ± 0.97 mg NO_3-N l^{-1}), but the associated variability may have been caused by groundwater table fluctuations. Overall, the weak positive correlations suggested that the NO_3-N at these sites was not produced in situ due to water table fluctuations. Furthermore, N deposition has been shown to increase porewater N (Wieder, et al., 2019); however, if N deposition was responsible for the increase in porewater NO_3-N, it would probably affect a greater area of the fen rather than the discrete porewater sites observed in this study.

The temporal variation of shallow groundwater and porewater nitrate-rich sites was often associated with the variability of the groundwater springs, surface water, and Chalk groundwater sources (Figure 5.5), particularly SG01 and PW4.3, which showed positive correlations with groundwater table heights (Table 5.3). Despite a temporal pattern similar to that of surface waters, NO_3-N concentrations at these sites were probably not directly influenced by the river, as most of the sites were far from the river banks. Instead, NO_3-N concentrations were probably influenced by the direct and discrete inflows of nitrate-enriched groundwater into the fen. Discrete groundwater inflows have influenced hydrochemistry in other calcareous wetlands (for example, Abesser, et al., 2008; Lapworth, et al., 2009; House, et al., 2015). In particular, House et al. (2015) reported that nitrate-rich porewater sites were associated with nitrate-enriched groundwater inflows in a calcareous meadow, resulting primarily from hydrogeological variability in the substrate underlying the peat. However, additional studies are required to confirm this, particularly with a focus on the hydrological movement and subsequent cycling of NO_3-N. This suggested that these discrete nitrate-rich

sites were NO_3-N saturated, that is, NO_3-N concentrations exceeded the processing capacity (Hanson, et al., 1994; Hefting, et al., 2006).

DON showed a spatial trend similar to that of NO_3-N in the porewater (Figure 5.5), which was generally highest at these nitrate-enriched sites, suggesting that groundwater was also a source of DON for the fen. Similarly, Yates et al. (2022) reported elevated concentrations of DON in Chalk groundwater compared to upland peat catchments. However, concentrations in this study were generally lower than previously reported in minerotrophic (rich) fens (Vitt & Chee, 1990).

Contrary to previous reports suggesting that peatlands reduce adjacent surface water NO_3-N concentrations (Gilliam, 1994; Kull, et al., 2008; Hill, 2019), these results indicated a small and nonsignificant decrease in NO_3-N downstream (*p*-value = 1.00), suggesting a limited interaction between the fen and surface water. Similarly, Prior & Johnes (2002) reported a small, but significant, decrease in surface water NO_3-N located along a calcareous meadow, indicating that the observations probably resulted from instream processes as well. However, continuous hydrological monitoring suggested that there was a hydrological gradient from the fen to the river, where the mostly low NO_3-N fen porewater probably diluted the nitrate-rich surface water. The amount of water movement from the fen to the river is unknown, but it is likely that it is not considerable, resulting from the limited decrease of NO_3-N downstream. However, this study primarily considered baseflow conditions; additional studies are required to properly evaluate fen and surface water interactions during high-flow events, which are known to enhance connectivity between the two (Cirmo & McDonnell, 1997; Johnes, et al., 2020). For example, Johnes et al. (2020) reported that a calcareous meadow released large amounts of DON to a nearby river during high-flow events.

5.5 Conclusion

In conclusion, this study showed low concentrations of N in the shallow groundwater and porewater of a managed nitrate-enriched groundwater-fed fen. The results indicated that groundwater abstraction appeared to have a limited effect on groundwater table heights, buffered by a large regional Chalk aquifer. NO_3-N was the dominant form of N at the site, originating from the Chalk aquifer, as observed in the consistently nitrate-enriched groundwater springs, surface waters, and Chalk groundwater sources; compared to the low NO_3-N shallow groundwater and porewater sites, except for discrete nitrate-rich sites. The low NO_3-N in shallow groundwater and porewater was likely maintained by NO_3-N cycling and the stable groundwater table height. However, the discrete nitrate-rich shallow groundwater and porewater sites were probably influenced by the inflow of nitrate-enriched groundwater, rather than internal NO_3-N production or N deposition. Furthermore, the fen appeared to have a limited effect on the NO_3-N concentrations in the adjacent surface water (River Whitewater); although, there was some evidence of hydrological flow from the fen to the river. In general, this study highlights the complexity of N concentrations in fens. For example, water table management and NO_3-N enrichment can increase N concentrations in peatlands by lowering water tables or exceeding N uptake capacity; however, a low N environment was maintained throughout most of this fen, except at the discrete nitrate-rich sites. Therefore, more research is required to understand the complex N transfer and cycling in fen peatlands, which is further investigated in Chapters 6 and 7.

Chapter 6: Nitrogen and Hydrochemical Transfer and Cycling in a Nitrate-enriched Calcareous Fen

In this chapter, the hydrochemical characteristics of the water sources were compared and analysed using multivariate statistical analyses to understand the hydrological transfer and cycling of NO_3-N in the fen. This develops and tries to determine the spatial variability of NO_3-N in the fen demonstrated in Chapter 5, particularly the discrete nitrate-rich porewater sites.

6.1 Introduction

Peatlands are unique environments that regulate local and global biogeochemical cycles, particularly nitrogen (N) (Fisher & Acreman, 2004; Verhoeven, et al., 2006; Cao, et al., 2016), which has led to widespread interest in their ability to control surface water and groundwater borne N pollution (for example, Brix, 1994; Hoffmann, et al., 2011; Lind, et al., 2013; Mwagona, et al., 2019; Han, et al., 2020). Nitrate (NO_3-N) enrichment of waters is a global issue, particularly affecting intensive agricultural landscapes; for example, European river N loads to coastal waters have been estimated to range between 4.1 and 4.8 Tg yr^{-1} from 1985 to 2005 (Grizzetti, et al., 2012). Consequently, increased NO_3-N availability can increase fresh and marine water eutrophication, which can result in intense blooms of toxic algae, polluting drinking water and fisheries (Howarth & Marino, 2006; Lewis, et al., 2011; Moal, et al., 2019).

Peatland N cycling is influenced by specific geomorphological effects on hydrological connectivity, soil texture, and soil organic matter, to suggest some (Pinay, et al., 1995; Johnston, et al., 1999; Hefting, et al., 2004). Consequently, geomorphology affects peatland physicochemical and vegetation properties, and wetting-drying cycles (Duren & Pegtel, 2000; Venterink, et al., 2002; Rezanezhad, et al., 2016). N cycling is further complicated in permeable catchments, where hydrological connectivity and hydrochemical transfer are high

between surface water and groundwater (Correll, 1996; Almendinger & Leete, 1998; Prior & Johnes, 2002; Duval & Waddington, 2018; Johnes, et al., 2020). Consequently, N cycling will not be evenly distributed throughout a peatland, rather distinct cycling hotspots develop and are highly variable over space and time. This is particularly influenced by the hydrology, hydrogeology, and hydrochemistry of inflowing waters; for example, flow paths, water residence times, and solute concentrations (Reddy & DeLaune, 2008; Johnes, et al., 2020). This heterogeneity of hydrology, hydrogeology, and hydrochemistry in peatlands has resulted in the reporting of highly variable N cycling rates, defined as the difference in a mass or concentration of an N species over a period that is scaled to an areal estimate using a unit converter, such as the dry weight of a soil sample or a flow rate (Tietema, et al., 1993; Lind, et al., 2013; Yao, et al., 2018); for example, N cycling rates have ranged from 2.4 kg N ha^{-1} year^{-1} (Drewer, et al., 2010), 52 to 337 kg N ha^{-1} year^{-1} (Hoffmann, et al., 2011), and 1887 to 4046 kg N ha^{-1} y^{-1} (Lind, et al., 2013). Therefore, there is a requirement to improve the understanding of peatland N cycling, in particular, the influence of hydrology and hydrochemical transfer in managed peatlands, to interpret the apparent N cycling variability and how N is transferred from different water sources.

Hydrology and hydrochemical transfer are particularly important in riparian fen peatlands, saturated by groundwater and hydrologically connected to surface water (Paulissen, et al., 2004). Groundwater hydrochemistry, and thus fen hydrochemistry, is heavily influenced by the catchment bedrock through chemical weathering (Han & Liu, 2004; Gan, et al., 2018), by climatic conditions through temperature and runoff (Rogora, et al., 2003; West, 2012), and anthropogenic activities; for example, intensive fertilisation application (Amano, et al., 2018; Su, et al., 2020). Furthermore, as groundwater moves through the peatland, biogeochemical cycles will influence groundwater hydrochemistry. Consequently, the hydrochemical evolution of waters has previously been used to evaluate external hydrological inputs, hydrological connectivity, and biogeochemical cycling in groundwaters, surface waters, and peatlands; for example, using ionic ratios or multivariate statistical analyses such as principal component

analysis (PCA) or hierarchal cluster analysis (HCA) (for example, Mazlum, et al., 1999; Helena, et al., 2000; Güler, et al., 2002; Cao, et al., 2016; Amano, et al., 2018; Gan, et al., 2018; Johnes, et al., 2020; Su, et al., 2020; Gupta, et al., 2021).

Mazlum et al. (1999) used PCA analysis to successfully identify several hydrochemical influences of a riverine water quality monitoring station in Turkey, such as a small domestic waste discharge, an industrial waste discharge, nitrification, and seasonality. Cloutier et al. (2008) used both HCA and PCA to better identify the processes that control the geochemical evolution of groundwater in a Canadian catchment, defining the main groups of groundwater associated with specific geochemical regions, distinguished by geological formations, hydrogeological context, hydraulic gradients, and geochemical processes. However, Güler et al. (2002) found that combining HCA and PCA did not improve their analysis of surface water and groundwater types in a catchment when reviewing graphical and multivariate analysis methods. Instead, Güler et al. (2002) concluded that the combination of graphical methods, such as Piper diagrams, and HCA offered a robust methodology to classify large water quality data sets, providing the hydrochemical characteristics of the statistical groups for comparison; whereas, the PCA did not improve the cluster results provided by the HCA, which were relatively similar.

Multivariate statistical methods have been used in wetland and peatland studies to investigate numerous fields, such as hydrodynamics (Cole & Brooks, 2000; Stein, et al., 2004), heavy metal contamination (Zhao, et al., 2021), and biogeochemical cycling (Weyer, et al., 2014; He, et al., 2016). Furthermore, researchers have used dissolved solutes and ionic ratios of metals to determine hydrological sources and biogeochemical cycling in peatlands. For example, Johnes et al. (2020) investigated the hydrological effects on wetland nutrient cycling, using incongruent dissolution in calcareous groundwaters to infer water residence times, mainly strontium/calcium (Sr:Ca) and magnesium/calcium (Mg:Ca) ratios. The depleted ratios of Sr:Ca and Mg:Ca in the porewaters of the wetland represented groundwater that had been

subjected to modification in the wetland soil matrix through biogeochemical processes, such as cation exchange. Consequently, multivariate statistical analysis and ionic ratio determination, in combination with the knowledge of the geological, hydrological, and hydrogeological environment (Cloutier, et al., 2008), are potentially very powerful tools to study the effects of hydrogeochemistry on N transfer and cycling in peatlands.

This study undertakes a rigorous multivariate approach to understanding N transfer and cycling as a result of hydrology and hydrogeochemistry in a calcareous nitrogen-enriched peatland. Respectively, the objectives are to (1) determine the hydrological connectivity of the fen porewater with the other site water sources; (2) evaluate the transfer of N in the system through the porewater and other site water sources; and (3) determine where and how N cycling may occur as a result of hydrological connectivity and hydrochemical controls.

6.2 Methodology

A detailed explanation of the field site (Greywell Fen), sample collection, and laboratory measurements that formed the hydrochemical dataset used in this chapter are presented in Chapter 4.

6.2.1 Hydrochemical Dataset

The hydrochemical characterisation of Greywell Fen was carried out between May 2021 and May 2022 (Table 6.1), collecting groundwater springs ($n = 13$), surface water ($n = 5$), Chalk groundwater ($n = 2$), shallow groundwater ($n = 2$), and porewater samples ($n = 12$) from 34 locations throughout the study site on a fortnightly basis. In total, 11 hydrochemical variables were measured: nutrients (NH_3-N, NO_3-N, DON, and P), selected cations (Ca^{2+}, Mg^{2+}, K^+, Na^+, Al^{3+}, and $Fe^{2+/3+}$) and DOC ($n = 673$ for each variable).

Table 6.1: Descriptive hydrochemical statistics for the 673 water samples between May 2021 and May 2022 (concentrations in mg l^{-1}, except * in µg l^{-1}). 'TFe' represents total dissolved Fe.

Parameter	Min.	Max.	Median	Mean	SD	Skewness
NH$_3$-N	0.03	1.35	0.09	0.13	0.31	19.29
NO$_3$-N	0.10	15.70	6.36	5.94	4.56	0.11
DON	0.00	6.81	1.83	1.75	1.45	-
P	0.02	1.22	0.02	0.04	0.08	-
Ca^{2+}	53.48	151.44	118.51	115.97	12.55	-1.70
K$^+$	0.04	10.48	1.20	1.32	0.92	4.18
Mg^{2+}	0.69	2.67	1.92	1.92	0.22	-0.17
Na$^+$	5.25	14.53	9.36	9.40	0.92	-1.62
Al*	6.74	44.96	19.94	19.50	3.97	0.78
Tfe*	0.06	624.22	3.86	12.88	38.59	10.7
DOC	2.70	49.98	5.61	7.49	5.49	3.28
Mg:Ca	0.02	0.04	0.03	0.03	0.004	-

6.2.2 Data Preparation and Transformation

Before completing the multivariate statistical analyses, preparatory and transformational steps were completed; for example, removing variables due to certain conditions or ensuring Normal distribution of variables (Güler, et al., 2002; Cloutier, et al., 2008; Gan, et al., 2018). First, P and DON were removed from the data set, since most values were near or below detection limits, which resulted in the use of 9 variables (NH$_3$-N, NO$_3$-N, Ca^{2+}, Mg^{2+}, K$^+$, Na$^+$, Al^{3+}, Fe$^{2+/3+}$ and DOC). Then, any censored values, that is, values reported as near or below the detection limits, were replaced by multiplying the detection limit by 0.55, a value based on theoretical replacement factors produced by Sanford et al. (1993) to mitigate the effect of censored values in these analysis types. This concerned mainly NH$_3$-N and NO$_3$-N because censored values are not suitable for multivariate statistical analyses (Güler, et al., 2002)

PCA is a nonparametric statistical analysis (Kaiser, 1960; Jacintha, et al., 2017); however, the analysis is improved if the variables are normally distributed and standardised (Tabachnick & Fidell, 2007; Mertler, et al., 2021). Consequently, log transformation and standardisation are

commonly applied to hydrochemical/hydrogeochemical datasets. This reduces the influence of high standard deviations on the Euclidean distance, an important mechanism in multivariate statistical analyses (Judd, 1980; Berry, 1996), and data transformations can homogenise the distribution variance (Rummel, 1980). Therefore, highly positively skewed variables were log transformed to have Normal distributions, except for NO_3-N, Mg^{2+}, and Al as their distributions were close to Normal (Mazlum, et al., 1999; Güler, et al., 2002; Cloutier, et al., 2008; Gan, et al., 2018). Then, the log transformed and Normal distribution variables were all standardised to ensure equal weighting using the Z-score equation (1):

$$Z_i = \frac{(X_i - mean)}{s} \qquad (1)$$

where Z_i is the standardised value (based on a zero mean), X_i is the individual variable datum, and s is the standard deviation of the variable.

6.2.3 Multivariate Statistical Procedure

PCA reduces the variables in a data set to uncorrelated components (Gan, et al., 2018). In this study, the components chosen for analysis were selected using the Kaiser criterion, where components with eigenvalues > 1 are retained; eigenvalues explain the variance of each principal component (Holland, 2008). However, the Kaiser criterion has no theoretical basis, but the principal components with the highest eigenvalues explain the most variance in the data and therefore can be considered important for data analysis (Chatfield, 1980; Cloutier, et al., 2008).

HCA was performed to classify the data set into various hydrochemical clusters. Güler et al. (2002) found that the best distance measure and linkage methods to produce the most distinctive clusters were the Euclidean distance and Ward's linkage method. Euclidean

distance categorises the groups with the highest similarity first, linking the samples together with Ward's linkage method until all samples have been categorised; this is a unique linkage method as it uses variance analysis to evaluate group distances (Cloutier, et al., 2008; Gan, et al., 2018). The samples are visualised in a dendrogram, and the groups are selected visually by drawing a 'phenon line'; samples below this line are grouped. This makes HCA a semiobjective method (Cloutier, et al., 2008). Spearman's rho correlation analysis was used for all correlation analyses, as most of the measured variables did not meet normality. All statistical analyses were performed in RStudio® Version 1.4.1103.

6.3 Results

6.3.1 Hydrochemical Characteristics

The hydrochemical characteristics of the groundwater springs (GS), surface water (SW), Chalk groundwater (CG), shallow groundwater (SG), and porewater (PW) are presented in Table 6.2. Ca^{2+} and Na^+ were the most dominant cations in the water sources. Generally, groundwater springs showed the highest concentrations of Ca^{2+} (120.75 ± 4.30 mg l^{-1}, ± is the standard deviation) and NO_3-N (10.62 ± 3.10 mg l^{-1}). While the porewater showed the lowest concentrations of Ca^{2+} (114.03 ± 17.96 mg l^{-1}) and NO_3-N (0.40 ± 1.76 mg l^{-1}), and expressed the highest concentrations of Fe (11.49 ± 61.43 µg l^{-1}) and DOC (9.07 ± 7.43 mg l^{-1}). Generally, the hydrochemistry of the water sources was similar, except for NO_3-N, Fe, and DOC. Median NO_3-N concentrations showed that shallow groundwater and porewater were depleted compared to groundwater springs, surface water, and Chalk groundwater. However, there were differences between shallow groundwater and porewaters, the latter being enriched with Fe and DOC.

The Mg:Ca ratio was not included in the PCA or HCA, but was used in the correlation matrices (Section 6.3.4). The Mg:Ca ratio was used to indicate the water residence time of

95

calcareous groundwater and the influence of noncalcareous waters. Initially, calcareous groundwater is calcium-rich, but as the groundwater moves through the Chalk, incongruent dissolution of calcite occurs which releases Mg^{2+} (Kloppmann, et al., 1998; Edmunds, et al., 2003). Thus, higher Mg:Ca ratios can represent longer water residence times, while lower ratios can indicate noncalcareous water inputs, such as rainwater or surface runoff (Johnes, et al., 2020). The water sources with the highest median ratios were Chalk groundwater (0.030), shallow groundwater (0.028), and porewaters (0.029), which did not differ significantly (*p*-values ranging from 0.30 to 1.00). However, Chalk groundwater, shallow groundwater, and porewaters differed significantly from both groundwater springs and surface waters (*p*-values < 0.001). Groundwater springs (0.025) and surface waters had the lowest ratios (0.025) and did not differ significantly (*p*-value = 1.00) (Table 6.2).

Table 6.2: Summary of hydrochemical characteristics for each water source (median concentrations in mg l^{-1}, except * in µg l^{-1}). Concentrations in bold or underlined denote the highest and lowest concentrations, respectively, in the water sources. 'TFe' represents total dissolved iron.

	GS					SW					CG					SG					PW				
	n	Min.	Max.	Med.	SD	*n*	Min.	Max.	Med.	SD	*n*	Min.	Max.	Med.	SD	*n*	Min.	Max.	Med.	SD	*n*	Min.	Max.	Med.	SD
NH₃-N	259	0.03	0.63	0.09	0.07	95	0.03	0.26	<u>0.08</u>	0.05	39	0.03	0.56	<u>0.08</u>	0.09	39	0.03	0.97	**0.11**	0.25	239	0.03	1.35	0.09	0.49
NO₃-N	259	1.53	15.7	**10.62**	3.10	95	0.21	11.03	8.67	2.25	39	0.10	9.29	7.46	2.06	39	0.10	8.18	1.28	3.05	239	0.10	8.67	<u>0.40</u>	1.79
Ca²⁺	259	97.38	130.8	**120.75**	4.30	95	109.06	127.4	119.87	4.10	39	91.74	125.67	114.71	6.87	39	64.05	124.74	111.74	13.35	239	53.48	151.44	<u>114.03</u>	17.96
K⁺	259	0.57	6.33	<u>0.95</u>	0.54	95	1.11	2.42	1.28	0.21	39	1.38	2.67	**1.66**	0.37	39	0.75	3.92	1.17	0.79	239	0.04	10.48	1.13	1.36
Mg²⁺	259	1.58	2.28	<u>1.79</u>	0.16	95	1.73	2.06	1.87	0.08	39	1.11	2.35	2.05	0.19	39	0.69	2.14	1.94	0.3	239	1.13	2.67	**2.04**	0.25
Na⁺	259	7.98	12.89	9.42	0.73	95	8.71	12.76	**9.62**	0.62	39	7.53	10.23	9.32	0.5	39	6.41	9.5	<u>8.99</u>	0.71	239	5.25	14.53	9.27	1.16
Al*	259	6.93	41.13	**20.08**	3.96	95	6.9	38.59	19.83	3.81	39	8.6	33.62	<u>19.5</u>	4.03	39	6.74	22.4	19.6	3.6	239	8	44.96	20.01	4.09
TFe*	259	0.06	56.79	<u>2.82</u>	5.55	95	0.24	34.02	3.7	5.67	39	0.16	38.5	2.11	6.1	39	0.63	44.98	3.16	7.24	239	0.21	624.22	**11.49**	61.43
DOC	259	3.04	10.92	5.11	11.22	95	33.06	8.87	4.92	1.32	39	22.7	17.82	<u>4.6</u>	2.26	39	33.23	20.78	5.22	2.69	239	2.96	49.98	**9.07**	7.43
Mg:Ca	259	0.022	0.031	0.025	0.002	95	0.024	0.030	0.025	0.002	39	0.020	0.035	0.030	0.003	39	0.024	0.031	0.028	0.002	239	0.025	0.045	0.029	0.004

6.3.2 Hierarchical Cluster Analysis (HCA)

Sample classification into clusters was based on visual observation of the HCA dendrogram (Figure 6.1). In this study, the phenon line, the line that divides the dendrogram into clusters, was drawn at a linkage distance of 27 (Figure 6.1, line not shown). Therefore, the samples below this phenon line are grouped into the same cluster, resulting in three clusters (Figure 6.1). To reiterate, the placement of the phenon line is objective, and changing the position changes the cluster number; however, in this study, the three clusters were considered satisfactory to explain the distinct hydrochemical differences between the water sources, and increasing the number of clusters would have added unnecessary complexity to the data analysis.
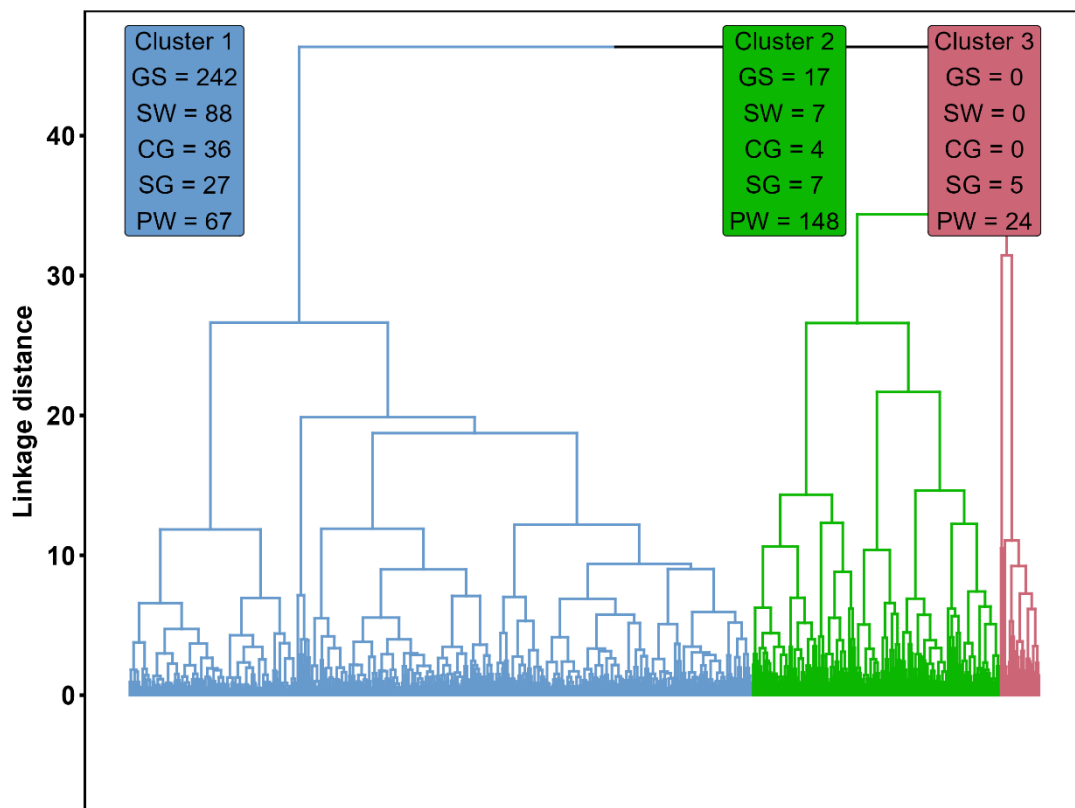
Figure 6.1: HCA dendrogram for the water source samples. Cluster 1 = light blue, Cluster 2 = green, and Cluster 3 = red. The box annotations show the number of water source samples in each cluster.

Cluster 1 was the largest and included samples from each water source, containing most of the groundwater springs, surface water, Chalk groundwater, and shallow groundwater samples (Figure 6.1). Cluster 1 displayed the highest concentrations of NO_3-N, Ca^{2+}, Na^+, and Al and the lowest concentrations of NH_3-N, Fe, and DOC (Table 6.3). Furthermore, cluster 1 mostly included porewater sites (PW0.2, PW2.4, and PW4.4) which consistently had the highest NO_3-N concentrations, compared to the porewater sites in clusters 2 and 3, which were generally near or below detection limits. Cluster 2 also included samples from each water source, but porewater samples were dominant (Figure 6.1). Cluster 2 was characterised by high concentrations of Mg^{2+}, Fe, and Al, although Mg^{2+} was relatively similar to cluster 1, and Al was similar in all three clusters (Table 6.3). Cluster 2 also showed the lowest concentrations of K^+. Cluster 3 was the smallest, only containing shallow groundwater and porewater samples. This cluster showed the highest concentrations of NH_3-N, K^+, Fe, and DOC, and the lowest concentrations of NO_3-N, Ca^{2+}, Mg^{2+}, Al, and Na^+ (Table 6.3). Cluster 1 and 2 Fe concentrations were relatively similar.

Table 6.3: Hydrochemical characteristics of each HCA cluster (median concentrations in mg l^{-1}, except * in µg l^{-1}). Concentrations in bold or underlined denote the highest and lowest concentrations, respectively, in the three clusters. 'TFe' represents total dissolved iron.

Parameter	C1	C2	C3
n	460	183	29
NH_3-N	<u>0.08</u>	0.11	**0.13**
NO_3-N	**8.03**	0.40	<u>0.24</u>
Ca^{2+}	**119.14**	114.78	<u>78.58</u>
K^+	1.22	<u>0.95</u>	**3.39**
Mg^{2+}	1.91	**2.03**	<u>1.64</u>
Na^+	**9.42**	9.26	<u>8.15</u>
Al*	**20.21**	19.26	<u>18.11</u>
TFe*	<u>2.85</u>	13.01	**13.20**
DOC	<u>5.00</u>	9.26	**16.45**

6.3.3 Principal Component Analysis (PCA)

The principal components with eigenvalues > 1 are presented in Table 6.4 with their respective explained variances. The four principal components accounted for 72.0% of the total variance in the data. Principal components 1 and 2 explained 28.1% and 20.4% of the variance, respectively; whereas, components 3 and 4 were less important, explaining 13.0% and 10.6% of the variance, respectively.

Table 6.4: Principal component loadings and explained variance for the four components. Loadings ≥ 0.4 or ≤ -0.4 are shown in bold. 'TFe' represents total dissolved iron.

Parameter	PC1	PC2	PC3	PC4
NH_3-N	-0.15	0.23	**0.61**	-0.11
NO_3-N	**0.52**	0.22	-0.11	-0.08
Ca^{2+}	**0.40**	**-0.46**	0.21	-0.15
K^+	-0.11	**0.47**	0.03	**0.46**
Mg^{2+}	-0.06	**-0.56**	0.33	0.15
Na^+	0.20	-0.07	**0.40**	**0.68**
Al	0.02	-0.28	**-0.52**	**0.50**
TFe	**-0.46**	-0.26	-0.13	-0.09
DOC	**-0.53**	-0.05	0.09	0.08
Explained Variance	2.5	1.8	1.2	1.0
Explained variance (%)	28.1	20.4	13.0	10.6
Cumulative % of the variance	28.1	48.5	61.5	72.0

Principal component 1 explained the most variance, expressing high positive loadings of NO_3-N and Ca^{2+} and high negative loadings of Fe and DOC (Table 6.4). This corresponded to the HCA that divided cluster 1 and clusters 2 and 3 into high NO_3-N and low DOC samples and lower NO_3-N and higher DOC samples (Table 6.3). Although principal component 2 showed high negative loadings of Ca^{2+} and Mg^{2+}. Principal components 3 and 4 represented 13.0% and 10.6% of the variance, respectively. Principal component 3 showed high positive

loadings of NH_3-N and Na^+ and high negative loadings of Al; whereas, principal component 4 expressed high positive loadings of K^+, Na^+, and Al (Table 6.4).

Principal components 1 and 2 are summarised in Figure 6.2, which presents the position of the hydrochemical solute loadings and the water source samples within the PCA axes. Generally, groundwater springs, surface water, and Chalk groundwater samples were distributed within the positive loading of principal component 1, large amounts of overlap were observed between groundwater springs, surface water, Chalk groundwater, and shallow groundwater samples; these overlaps suggest a common source. Although shallow groundwater and porewater samples were distributed within the negative loading of principal component 1. Despite the large variability observed in the porewater samples, a large number were similar to other site water sources, indicating that groundwater entering the peatland was modified.
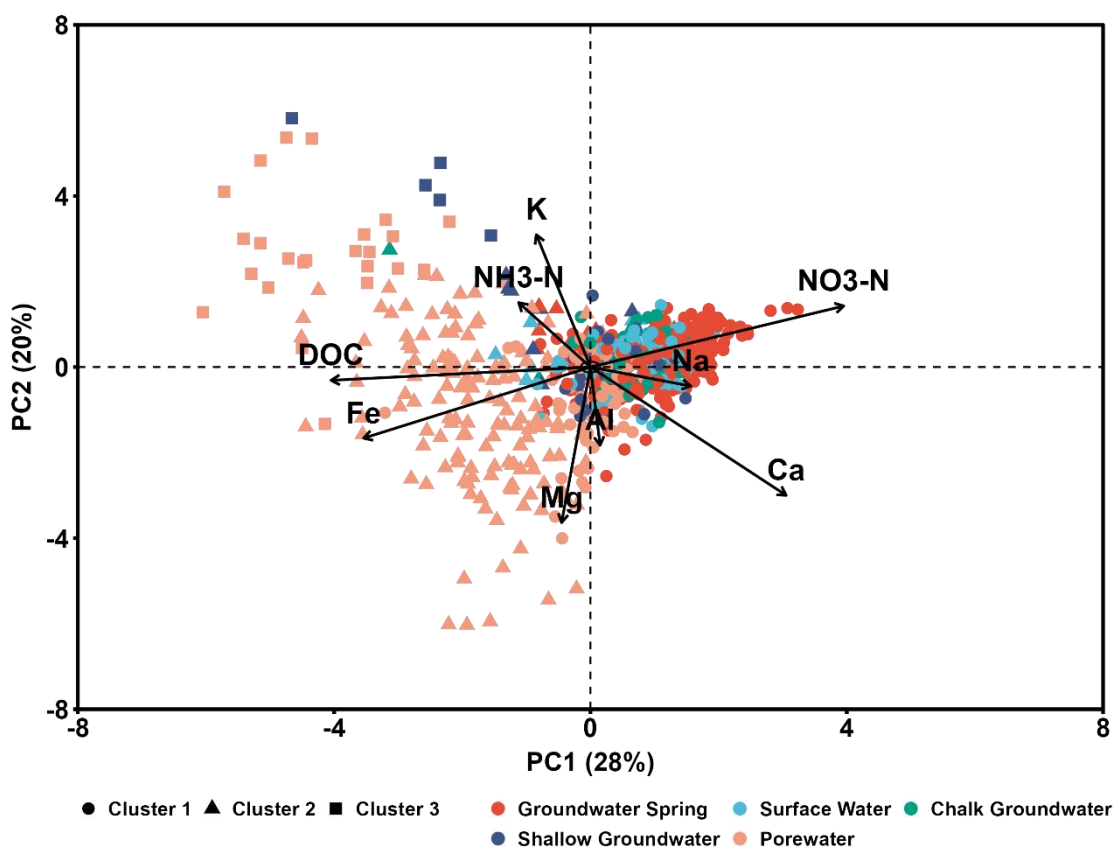
Figure 6.2: PCA biplot of the principal components 1 and 2. The three clusters according to the HCA are represented by the symbols: ●, ▲, and ■.

6.3.4 Correlation Matrices

A Spearman's correlation matrix between values for hydrochemical parameters determined across all water sources is presented in Table 6.5. NO_3-N showed the strongest correlations with DON (rho = 0.91, p-value < 0.001), Mg:Ca ratio (rho = -0.59, p-value < 0.001), Fe (rho = -0.56, p-value < 0.001), and DOC (rho = -0.56, p-value < 0.001). The correlation between NO_3-N and DOC provides further evidence of the distinction between high NO_3-N and low DOC and lower NO_3-N and higher DOC. DON showed similar correlation strengths with the same solutes and ratios. This suggests that NO_3-N and DON have similar hydrogeochemical behaviours or are linked through N cycling. Additionally, Fe and DOC were relatively well correlated with each other (rho = 0.48, p-value < 0.001).

Table 6.5: Spearman's correlation (rho) matrix of hydrochemical solutes including all water source samples. Bold values denote correlation coefficients (rho) ≥ 0.5 or ≤ -0.5. 'TFe' represents total dissolved iron.

Parameters	NH_3-N	NO_3-N	DON	P	Ca	K	Mg	Na	Al	Fe	DOC	Mg:Ca
NH_3-N	1											
NO_3-N	-0.11**	1										
DON	-0.09*	**0.91*****	1									
P	-0.16***	-0.05	-0.02	1								
Ca^{2+}	-0.03	0.33***	0.24***	0.05	1							
K^+	0.14***	-0.13**	-0.07	0.03	-0.31***	1						
Mg^{2+}	0	-0.44***	-0.40***	0.04	0.25***	0.12**	1					
Na^+	-0.03	0.37***	0.29***	0.05	0.36***	-0.16***	0	1				
Al	-0.19***	-0.01	-0.02	0.05	0.09*	-0.10**	0.11**	0	1			
TFe	-0.04	**-0.56*****	**-0.56*****	0.01	-0.14***	-0.03	0.13***	-0.25***	0.11**	1		
DOC	0.14***	**-0.56*****	**-0.51*****	0.12**	-0.26***	-0.03	0.10**	-0.11**	0	0.48***	1	
Mg:Ca	0.03	**-0.69*****	**-0.59*****	0.04	-0.48***	0.35***	0.57***	-0.33***	-0.06	0.31***	0.36***	1

* p-value < 0.05, ** p-value < 0.01, *** p-value < 0.001

A Spearman's correlation matrix between the values for hydrochemical parameters determined in the fen porewaters only is presented in Table 6.6. NO_3-N displayed many of the same correlations as in Table 6.5, albeit weaker, including DON (rho = 0.73, p-value < 0.001), Fe (rho = -0.42, p-value < 0.001), and DOC (rho = -0.47, p-value < 0.001); however, the NO_3-N correlation with the Mg:Ca ratio was much weaker (rho = -0.15, p-value > 0.01). Similarly, DON expressed similar correlation strengths with dissolved solutes to that of NO_3-N. Although several other correlations became stronger, including Fe with DOC (rho = 0.62, p-value < 0.001), Ca^{2+} with Mg^{2+} (rho = 0.74, p-value < 0.001), and Ca^{2+} with Na^+ (rho = 0.52, p-value < 0.001).

Table 6.6: Spearman's correlation (rho) of hydrochemical solutes including only porewater source samples. Bold values denote correlation coefficients (rho) ≥ 0.5 or ≤ -0.5. 'TFe' represents total dissolved iron.

Parameters	NH₃-N	NO₃-N	DON	P	Ca	K	Mg	Na	Al	Fe	DOC	Mg:Ca
NH₃-N	1											
NO₃-N	-0.09	1										
DON	0.04	**0.73*****	1									
P	-0.09	0.01	0.02	1								
Ca²⁺	-0.17**	0.18**	0.12*	0.09	1							
K⁺	0.26***	0.11	0.11	0	-0.47***	1						
Mg²⁺	-0.08	0.01	-0.06	0.03	**0.74*****	-0.36***	1					
Na⁺	-0.18**	0.09	0.02	0.08	**0.52*****	-0.20***	0.48***	1				
Al	-0.20***	0.04	-0.09	0.07	0.29***	-0.22***	0.30***	0.13*	1			
TFe	0.01	-0.42***	-0.47***	0.01	-0.05	-0.18**	0.06	-0.1	0.1	1		
DOC	0.14*	-0.47***	-0.49***	0.15*	-0.28***	0.08	-0.04	0.04	-0.05	0.62***	1	
Mg:Ca	0.07	-0.15*	-0.22***	-0.05	-0.44***	0.31***	0.15*	-0.17**	-0.02	0.13*	0.33***	1

* p-value < 0.05, ** p-value < 0.01, *** p-value < 0.001

6.4 Discussion and Interpretation

Peatland N cycling is highly complex and variable, and is affected by many interacting and compounding biogeochemical, hydrological, geological, and hydrogeological processes. Various processes affect the solute concentrations in water, resulting in specific hydrochemical signatures. In this study, multivariate and correlation analyses revealed particular hydrochemical groups and relationships. These observations were used to interpret the processes that may have generated the hydrochemical signatures.

6.4.1 Hydrochemical Clusters

HCA categorised the water source samples into two branches with three main clusters (Figure 6.1). Cluster 1 included all water sources, but mainly groundwater springs, surface water, Chalk groundwater, and shallow groundwater samples, characterised by elevated NO_3-N and Ca^{2+} (Table 6.3). Elevated Ca^{2+} reflects the dominance of mineral dissolution of the calcareous bedrock on the groundwater hydrochemical composition (Reeve, et al., 1996; Su, et al., 2020). Elevated NO_3-N indicated that the Chalk aquifer was the main N source at the site, probably resulting from the storage and slow release of NO_3-N in Chalks, commonly referred to as 'legacy nitrate storage' (Stuart & Lapworth, 2016; Wang, et al., 2016). Furthermore, the shallow groundwater and porewater samples (22% of the total porewater samples) included in cluster 1 mainly showed high NO_3-N concentrations (SG01, PW0.2, PW2.4, and PW4.4), suggesting a greater influence of nitrate-enriched groundwater in these samples. There was a possibility that this resulted from nitrification or biological N fixation; however, NH_3-N was near or below the detection limits across all shallow groundwater and porewater sites (Table 6.3), and the NO_3-N concentrations measured at these sites are probably too high to represent conversion from nitrification or biological N fixation.

Clusters 2 and 3 were predominantly composed of shallow groundwater and porewater samples (78% of the total porewater samples) (Figure 6.1), characterised by depleted NO_3-N and Ca^{2+} and elevated Fe and DOC (Table 6.3). Peat porewaters are often associated with high DOC reflecting the high organic matter content of peat (Reeve, et al., 1996; Webster & McLaughlin, 2010), as well as dissolved Fe, which is only active under reducing conditions (Todorov, et al., 2005; Boomer & Bedford, 2008). Furthermore, the shallow groundwater sample represented in clusters 2 and 3 was primarily SG05, suggesting that the hydrochemical composition of shallow groundwater was influenced spatially. The hydrochemical differences between clusters 2 and 3 were primarily related to cations (Ca^{2+}, K^+, Na^+, and Al) and DOC (Table 6.3), indicating the influence of ion exchange or adsorption processes.

6.4.2 Nitrate Transfer and Cycling

Principal component 1, which explained 28.1% of the variance, was related to high loadings of NO_3-N and Ca^{2+} (positive) and Fe and DOC (negative) (Figure 6.2). Cluster 1 probably represented direct nitrate-enriched inflows from the Chalk aquifer as the water source for the site, dominating the hydrochemical compositions of the groundwater springs and surface water sites. Clusters 2 and 3, on the other hand, likely represented nitrate-enriched groundwaters transformed by biogeochemical processes within the peat (that is, N cycling or ion exchange/adsorption) (Figure 6.2). This was supported by the strong negative correlation of the Mg:Ca ratio with NO_3-N (rho = -0.59, p-value < 0.001) observed when all water samples were considered (Table 6.5). The depleted Mg:Ca values indicated longer water residence times of calcareous water in the peat compared to the other water sources (Johnes, et al., 2020). This suggested that longer water residence times provided more time for NO_3-N cycling. However, when considering only porewater, this correlation was considerably weaker (rho = -0.15, p-value > 0.01).

The high loadings of Fe and DOC in PC1 and their positive correlation (rho = 0.62, *p*-value < 0.001), may reflect highly reducing conditions, where anaerobic organic carbon decomposition occurs and ferric iron (Fe^{3+}) is reduced to the more soluble ferrous iron (Fe^{2+}) form (Lovley & Phillips, 1986; Lovley & Phillips, 1988). Reducing conditions are conducive to NO_3-N cycling, indicated by a negative correlation between NO_3-N and DOC in the porewater samples (rho = -0.47, *p*-value < 0.001). DOC is required for microbial growth and is used as an electron donor and oxidised via heterotrophic denitrification (Wetzel, 1992; Rivett, et al., 2008; Rajta, et al., 2019). As such, high organic matter content and high NO_3-N cycling rates are often associated with one another (for example, Burford & Bremner, 1975; Hedin, et al., 1998; Davidsson & Ståhl, 2000; Bernard-Jannin, et al., 2017). Denitrification, which uses ferrous iron (Fe^{2+}) (Rivett, et al., 2008; Zhang & Furman, 2021), may explain the negative correlation of NO_3-N with Fe in the porewater samples (rho = -0.42, *p*-value < 0.001). However, Lucassen et al. (2004) observed similar porewater Fe concentrations (28 µg l^{-1}) as in this study (Table 6.3). The low Fe concentrations were associated with nitrate-enriched groundwater inflows, where Fe reduction was prevented by the elevated NO_3-N in the groundwater inflows. As NO_3-N is a more energetically favourable electron acceptor in anaerobic sediments, the high porewater NO_3-N acted as a redox buffer and maintained low porewater Fe. In comparison to other peatlands, porewater Fe in this study was considerably lower; for example, a range of < 279.2 to 8376.8 µg l^{-1} was observed in three northern peatlands (Blodau & Moore, 2002). Furthermore, in this study, higher porewater Fe was observed where porewater NO_3-N was depleted. Therefore, the negative correlation of NO_3-N with Fe and porewater sites (PW0.2, PW2.4, and PW4.4) included in cluster 1 (Figure 6.1), may reflect discrete nitrate-enriched groundwater inflows within the fen, where NO_3-N cycling probably occurred in adjacent areas.

6.4.3 Hydrological Residence Time

Principal component 2, which explained 20.4% of the variance, was related to the high loading of K^+ (positive) and Ca^{2+} and Mg^{2+} (negative) (Figure 6.2), which explained the variability between clusters 2 and 3, and therefore, primarily the porewater samples. Peat cation exchange capacity (CEC), the ability to adsorb exchangeable cations, is known to be high (Rippy & Nelson, 2007; Maher, et al., 2008). Moreover, divalent ion adsorption can be particularly strong compared to monovalent ions (Salmon, 2006). This being the case, cluster 3 could reflect high Mg^{2+} and Ca^{2+} absorption, where ion exchange processes release K^+ into porewaters, which was considerably lower in clusters 1 and 2 (Table 6.3). Consequently, principal component 2 probably reflected the water residence time variability of the porewater samples, with cluster 3 reflecting the longest residence times. This may explain the weaker negative correlation of NO_3-N with the Mg:Ca ratio in the porewaters (rho = -0.15, p-value > 0.01) compared to the correlation when considering all water sources (Table 6.5). Furthermore, the weaker negative correlation was probably affected by the positive correlation between Ca^{2+} and Mg^{2+} in the porewater samples (rho = 0.74, p-value < 0.001). Reeve et al. (1996) suggested that a high correlation between Ca^{2+} and Mg^{2+} indicated groundwater inflows in lowland peatlands. However, Ca^{2+} did not correlate with NO_3-N in the porewaters (Table 6.6), which would be expected if the Chalk aquifer was the main source of NO_3-N in the fen. The high correlation between Ca^{2+} and Mg^{2+} could reflect a high amount of porewater mixing with variable water residence times. Previous studies have used Ca^{2+} and Mg^{2+} concentrations to indicate water residence times in peatlands (Chapman, et al., 1997; Worrall, et al., 2003). In this study, the calcium-rich porewaters, which are more recently derived from the Chalk aquifer, with a shorter residence time in the peat, may mix frequently with magnesium-richer porewaters with a longer residence time in the peat, resulting in a high association between Ca^{2+} and Mg^{2+} in the porewaters samples. Furthermore, this absence of correlation between NO_3-N and hydrochemical solutes considered to be derived from the Chalk aquifer; for

example, Mg^{2+} and Ca^{2+} suggested that any hydrological connection between the fen and the underlying aquifer was limited.

6.4.4 Episodic or Seasonal Events

Principal components 3 and 4 explained considerably less variance (13.0% and 10.6%, respectively), possibly reflecting episodic events, seasonal changes, or random variability in the water samples. Principal component 3 was related to high loadings of NH_3-N and Na^+ (positive) and Al (negative) (Table 6.4). Elevated NH_4-N and Na^+ concentrations have been associated with rainwater inputs (Proctor, 1994; Adamson, et al., 2001). Furthermore, elevated NH_3-N could be associated with internal organic matter cycling, where higher porewater NH_3-N was observed in spring and summer (data not shown), possibly resulting from increased evapotranspiration and lower water saturation in the fen (Boomer & Bedford, 2008; Weyer, et al., 2014). Principal component 4 was related to high positive loadings of K^+, Na^+, and Al (Table 6.4), which was difficult to interpret, but could also be associated with evaporation processes in groundwater springs and surface water samples (Cao, et al., 2016). However, this could also be the result of random variability.

6.4.5 Hydrogeological Transfer and Cycling of Nitrate

NO_3-N transfer and cycling within the fen were primarily determined by the spatial variability of discrete nitrate-enriched groundwater inflows, as well as the concentrations of redox-sensitive solutes (Fe and DOC). Hydrogeological variability is an important control of biogeochemical cycling in calcareous peat wetlands (Abesser, et al., 2008; Lapworth, et al., 2009; House, et al., 2015). Previous study site specific reports have suggested that groundwater inflows to the fen occur through discrete groundwater springs and slow-moving diffuse flows (Jacobs, 2019). Groundwater inflow through diffuse flow was suggested as a minor contribution, controlled by a relatively impermeable clay deposit overlying

unconsolidated gravel and the Chalk aquifer, which partitioned the Chalk aquifer from direct contact with fen peat (Section 3.5.1, Figure 3.3). Therefore, when the clay deposit thinned or was absent, more direct groundwater inflows into the fen were possible. High porewater NO_3-N may represent direct nitrate-enriched groundwater inflows (Figure 6.3). Fen areas with direct nitrate-enriched groundwater inflows are likely N saturated, where there is reduced NO_3-N cycling (Hanson, et al., 1994; Hefting, et al., 2006), due to the consistent inflow of nitrate-enriched groundwater, lower water residence times, and lower concentrations of DOC (Figure 6.3). This more direct groundwater inflow was probably limited, which is consistent with the original conceptual model (Section 3.5.1, Figure 3.3); however, this study cannot confirm the actual amount of these direct groundwater inflows. NO_3-N cycling is possibly greater in areas adjacent to the nitrate-enriched groundwater inflows, where the water residence time and the concentration of DOC increase (Figure 6.4). As the fen was partitioned from the Chalk aquifer by the relatively impermeable clay layer (Figure 6.3), most of the nitrate-enriched groundwater bypasses the fen and has minimal interaction with the active NO_3-N cycling zones. Additionally, this prevented high inflows of nitrate-enriched groundwater into the fen. Furthermore, the results suggested limited hydrological connectivity between the fen and adjacent surface water (River Whitewater); however, a potential hydraulic gradient from the fen to the river was observed (Section 5.3.1). The hydrochemical differences between the porewater and surface water would suggest that the amount of water movement between the two was small.

However, the study was limited to some extent, as it could only conceptualise the processes that occur in the fen using grab samples that represented a distinct time and hydrochemical composition of porewater, a common issue in field studies (Facchi, et al., 2007; Matamoros, 2012). Furthermore, the porewater sampling technique (Section 4.2) relies on a bulk porewater sample from various soil depths, which meant that the processes that affect groundwater-borne NO_3-N as it moved through the soil profile could not be interrupted. NO_3-N cycling was further investigated at high resolutions across space and time in Chapter 7 using peat columns

from two sites in the fen. The two sites represented high and low NO_3-N porewater sites to compare and further investigate the observations and conceptualisations in this study.

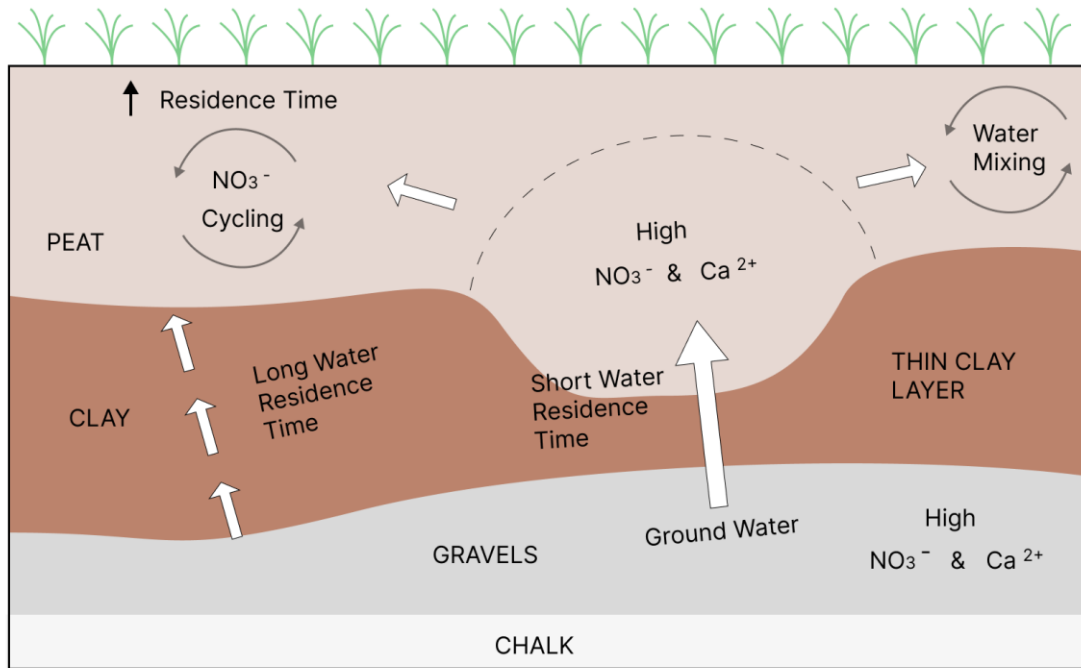**Figure 6.3:** Conceptual diagram of the hydrogeological and hydrochemical transfer and cycling of NO_3-N at Greywell Fen.
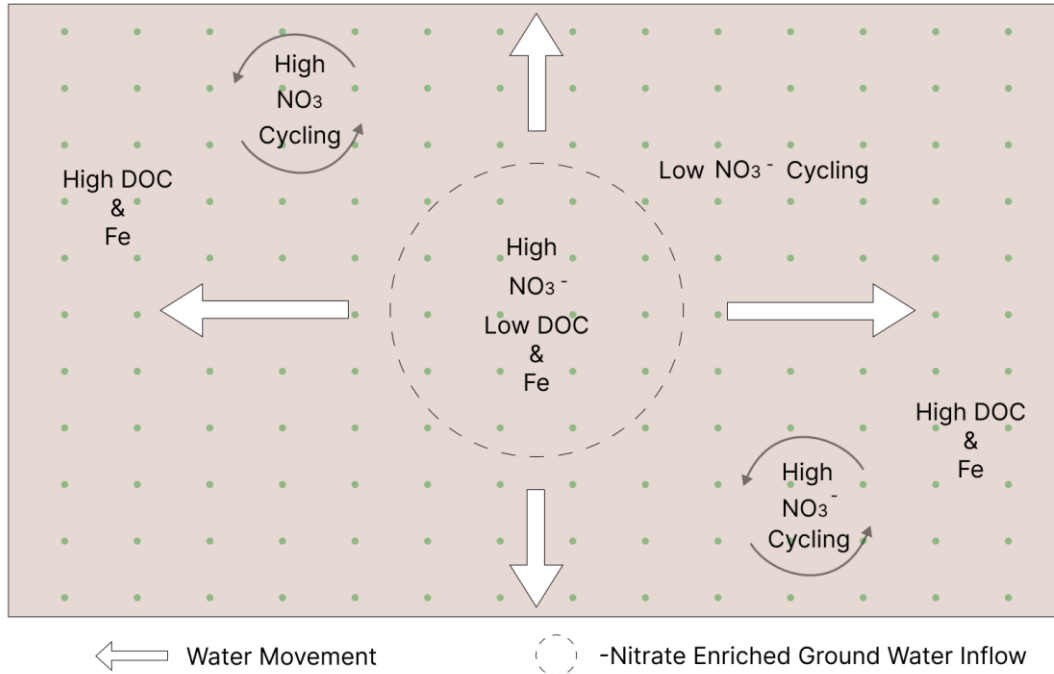

Figure 6.4: Aerial view of the movement and NO_3-N cycling of nitrate-enriched groundwater near the peat surface.

6.5 Conclusion

Multivariate and correlation analyses demonstrated that discrete nitrate-enriched groundwater inflows influenced the spatial patterns of NO_3-N concentrations in the porewaters. Furthermore, the hydrochemical differences between the porewater and surface water indicated that the limited hydrological connectivity between the fen, the Chalk aquifer, and the adjacent river facilitated much of the nitrate-enriched groundwater to bypass the fen. HCA identified several porewater sites with similar hydrochemistry to waters directly derived from the Chalk aquifer, such as groundwater springs, surface water, and Chalk groundwater. However, the hydrochemistry of most porewater samples differed considerably from those water sources, representing groundwater that had been transformed by biogeochemical reactions in the soil matrix. PCA and correlation analysis further developed this observation, suggesting that the inflowing nitrate-enriched groundwater was transformed by NO_3-N cycling, particularly the negative correlations of NO_3-N with the Mg:Ca ratio, DOC, and Fe. Furthermore, the hydrochemical variability of the porewater sites, presented by HCA and PCA, was influenced by the water residence times in the peat, resulting from cation exchange processes and increased concentrations of DOC and Fe. The porewater with the lowest residence time was the most hydrochemically similar to the nitrate-enriched groundwater, and the porewater became more hydrochemically distinct as the residence time increased.

This evidence suggested that discrete nitrate-enriched groundwater inflows throughout the fen were limited. This is consistent with a previous conceptual hydrogeological model of the fen (Section 3.5.1, Figure 3.3), which suggested that groundwater inflow was controlled by an impermeable clay layer that divided the fen and the Chalk aquifer, decreasing the hydrological connection. Where the clay layer thinned, the hydrological connection increased and discrete groundwater inflows occurred, resulting in high porewater NO_3-N. Due to this impermeable clay layer, most of the nitrate-enriched groundwater probably had limited hydrological contact with the fen and bypassed it. Research investigating the control of waterborne N pollution

114

should consider bypassing nitrate-enriched groundwater as a reason for apparent N 'removal'. Consequently, hydrogeology has an important influence on N transfer and cycling in fens, affecting the suitability of peatlands to control waterborne N pollution by limiting hydrological connection and N transfer to the active NO_3-N cycling zones.

7.0 Nitrogen Buffering Capacity and Nitrous Oxide Release in Nitrate-enriched Fen Peat

Chapter 7 outlines a laboratory experiment that builds on the key findings of Chapters 5 and 6, which were used to measure variation and hypothesise processes occurring in the field. Chapter 5 demonstrated that NO_3-N was variable across space in the fen, rather than over time, where discrete nitrate-rich porewater sites existed. Chapter 6 further explored this, hypothesising that the discrete nitrate-rich porewater sites in the fen were controlled by the thinning of a clay layer that divides the fen peat from the underlying nitrate-enriched Chalk aquifer; where the clay thinned, a direct inflow of nitrate-enriched groundwater occurred. Furthermore, the experiment outlined in this chapter enabled high resolution spatial and temporal sampling in intact soil columns, particularly porewater hydrochemistry and greenhouse gas release measurements that were not readily achievable in the field. This work provides further evidence of the processes operating in the fen, in particular, through the simulation of increased groundwater table heights, which might be expected from the groundwater abstraction shutdown.

7.1 Introduction

Excessive use of nitrogen (N) fertilisers over decades have resulted in N enrichment of surface water and groundwater, mainly in the nitrate form (NO_3-N) (Ardón, et al., 2010; Cusell, et al., 2013; Weber, et al., 2020). This is a major contributor to fresh and marine water eutrophication, contributing to intensive and harmful algal blooms (Howarth & Marino, 2006; Lewis, et al., 2011; Hou, et al., 2015; Wang, et al., 2016). To mitigate this issue, there has been considerable interest in using riparian and groundwater-fed peatlands (or fens) as NO_3-N buffers, as they are important N sinks in the terrestrial environment (Venterink, et al., 2002; Zak & Gelbrecht, 2007; Cabezas, et al., 2012; Riet, et al., 2013; Han, et al., 2020); however,

their efficacy as NO_3-N buffers can be highly variable and is controlled by several factors (Section 2.2) (Drewer, et al., 2010; Hoffmann, et al., 2011; Lind, et al., 2013), particularly groundwater table height (Reddy & DeLaune, 2008).

In general, the groundwater table height of a fen peatland controls the diffusion of oxygen (O_2) into the soil, thus defining the aerobic/anaerobic boundary (Rivett, et al., 2008). Naturally, groundwater tables are mainly near the surface, maintaining a low oxygen and redox reducing environment, and facilitating reactions that can reduce NO_3-N concentrations (Pinay, et al., 1993; Hoffmann, et al., 2006). However, many fen peatlands are affected by water table lowering due to drainage or groundwater abstraction, which increases soil oxygen concentrations (Beltman, et al., 1996; Rückauf, et al., 2004). Increased oxygen concentrations can affect NO_3-N reduction processes and increase porewater N concentrations through organic matter mineralisation and nitrification (De Mars, et al., 1996; Venterink, et al., 2002; Mettrop, et al., 2014). Furthermore, lower and more variable water tables have been observed to increase nitrous oxide release, a potent greenhouse gas, as a result of increased N concentrations from mineralisation and increased denitrification and nitrification, resulting from alternating wetting and drying conditions. Furthermore, incomplete NO_3-N cycling reactions at lower pH levels can increase nitrous oxide release (Martikainen, et al., 1993; Regina, et al., 1996; Regina, et al., 1999; Roobroeck, et al., 2010). Therefore, rewetting is considered an effective method of restoring peatlands to reduce nitrous oxide release and facilitate NO_3-N buffering functions (Haycock & Pinay, 1993; Zak, et al., 2011).

Rewetting aims to restore NO_3-N reducing reactions. Denitrification is believed to be a primary nitrate reduction reaction in peatlands; an anoxic stepwise process that converts nitrate to nitrogen gas (N_2), with nitric oxide (NO) and nitrous oxide (N_2O) as intermediates (Lind, et al., 2013). Dissimilatory nitrate reduction to ammonium (DNRA) is another NO_3-N reduction reaction, but it is considered less important in peatlands (Burgin & Hamilton, 2007; Scott, et al., 2008). These reactions are mainly influenced by oxygen and DOC concentrations,

117

the latter acting as an electron donor (Burgin & Hamilton, 2007; Rivett, et al., 2008; Baldwin & Mitchell, 2012; Pan, et al., 2016). Fe concentration can also influence NO_3-N reducing reactions, as it is used as an electron acceptor during autotrophic denitrification and can signify reducing conditions (Rivett, et al., 2008).

Rewetting of peatlands with nitrate-enriched groundwater has raised concerns about increased N concentrations and N saturation, leading to reduced NO_3-N buffering, NO_3-N enrichment, and increased nitrous oxide release (Aber, 1992; Sabater, et al., 2003; Hefting, et al., 2006). Cabezas et al. (2012) found increased NH_4-N and DON concentrations in the porewaters of rewetted nitrate-enriched peat columns. Hefting et al. (2003) reported an increase in NO_3-N porewater and nitrous oxide release in an N saturated riparian wetland. Lind et al. (2013) observed high NO_3-N removal rates of up to 95% in peat columns receiving nitrate-enriched water, but noted a potential increase in nitrous oxide release. However, Mwagona et al. (2019) reported a 98% NO_3-N removal and negative nitrous oxide fluxes in some nitrate-enriched soil columns. Nykänen et al. (2002) reported minimal nitrous oxide fluxes in a bog over a 5-year NO_3-N enrichment field experiment. Despite the interest in peatlands to control NO_3-N enrichment, questions remain about N saturation, nitrous oxide release, and the impact of changes in water table heights, which is particularly relevant for peatland restoration with nitrate-enriched waters. The literature in this area is limited and generally does not consider porewater N dynamics and nitrous oxide release at high spatial and temporal resolutions (Cabezas, et al., 2012; Han, et al., 2020). Furthermore, as a result of the key findings aforementioned in Chapters 5 and 6, there is a requirement to simulate the rise of nitrate-enriched groundwater tables due to groundwater abstraction cessation. This experimental study simulates the potential impacts of groundwater abstraction shutdown on porewater hydrochemistry and nitrous oxide release.

This work aims to evaluate the nature of porewater NO_3-N cycling and nitrous oxide release in nitrogen-enriched peat at different water table heights. Specifically, the objectives are to (1)

simulate the effect of groundwater abstraction shutdown at two fen sites with contrasting NO_3-N concentrations; (2) determine the effect of water table height and NO_3-N enrichment on N dynamics; (3) determine the effect of different water table heights and NO_3-N enrichment on nitrous oxide release; and (4) investigate the influence of DOC and Fe chemistry on N dynamics.

7.2 Methodology

7.2.1 Study site

Greywell Fen (51.251°N 0.971°W) is located in Hampshire, United Kingdom. It is a calcareous, groundwater-dependent peatland (pH = 6.5 to 8.3) that covers a 38-ha area and is a designated Site of Special Scientific Interest (SSSI) due to its ecological value (Figure 7.1). The surrounding area is used for intensive mixed arable production. Bedrock geology is dominated by Seaford and Newhaven Chalk formations, overlain by superficial permeable and semipermeable deposits of gravel (River Terrace Deposits), clay, and peat. Alluvial deposits (gravel and clay) are up to 10 m deep and the peat deposits are up to 3 m deep. Furthermore, the clay deposits underlying the peat are believed to be thin or absent in some areas (Jacobs, 2019). Chalk groundwater at the site is known to be contaminated with NO_3-N (mean = 7.00 mg NO_3-N l^{-1}, between 1997 and 2021).
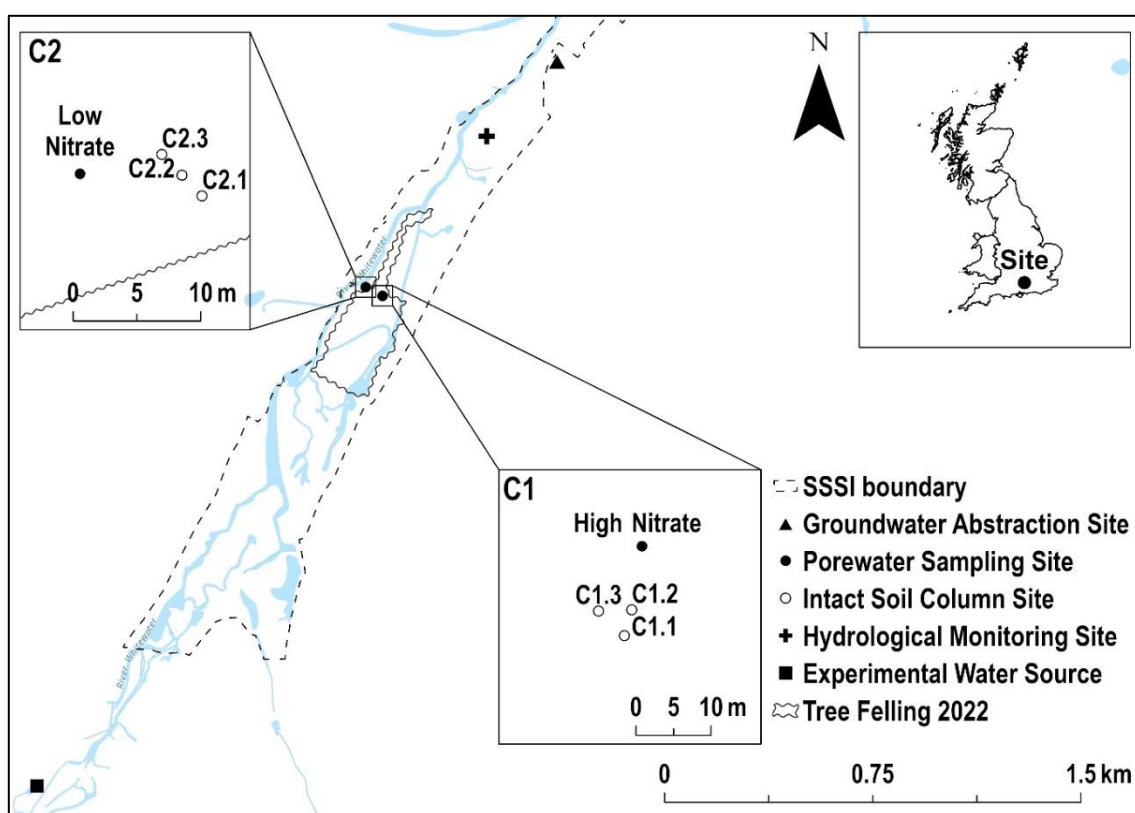
Figure 7.1: Greywell Fen sampling map. The high (median = 5.18 mg NO_3-N l^{-1}) and low (median = 0.34 mg NO_3-N l^{-1}) NO_3-N porewater sites refer to the hydrochemical analysis completed in Chapters 5 and 6. Destructive cores were taken adjacent (< 1 m) to the porewater sampling sites. The tree felling occurred in the winter of 2022.

7.2.2 Soil Sampling

A total of six intact soil columns (C1.1, C1.2, C1.3, C2.1, C2.2, C2.3) were collected from two sites (C1 and C2, each with 3 replicates) at Greywell Fen (Figure 7.1). Two sites were selected based on field monitoring studies (Chapters 5 and 6), which showed one site with high NO_3-N concentrations (C1) and the other (C2) with NO_3-N near or below the detection limits (Figure 7.1). Soil column sampling was carried out using a purpose designed steel corer (ID = 16 cm, L = 100 cm) based on Buttler et al. (1998). The corer featured a close-fitting tube arrangement consisting of an outer serrated steel tube and an inner PVC tube with a leading bevelled edge to reduce soil compaction (Figure 7.2 & Supplementary Information, Figure S1). Column sampling involved rotating the serrated steel tube on the soil surface, 'cutting' into the soil by a few centimetres, and recovering the 'cut' soil with the inner PVC tube stepwise until the desired depth (Figure 7.2 & Supplementary Information, Figure S1). The column was lifted from the ground, facilitated by the suction created during sampling, and PVC end caps were attached to both ends. The soil columns were stored vertically at 4 °C, allowing some gravitational drainage to occur. Although attempts were made to prevent soil compaction during coring, some occurred, leading to varying column heights (ranging from 65 to 81 cm; Table 7.1).
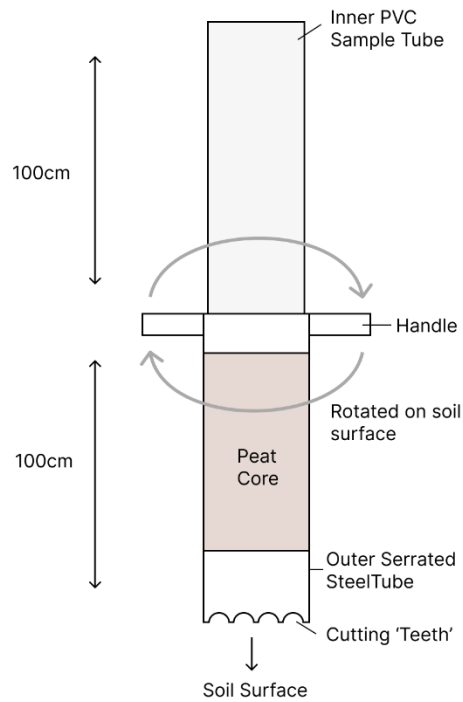
Figure 7.2: Peat column corer design.

Table 7.1: The heights of the six intact columns and the soil column labels of the two sites in Greywell Fen.

Site C1		Site C2	
Column	Height (cm)	Column	Height (cm)
C1.1	75	C2.1	73
C1.2	78	C2.2	65
C1.3	81	C2.3	77

Separately, to characterise the soil profile of the intact soil columns mentioned above, two 'destructive' soil cores were extracted from each of the two sampling sites (C1 and C2) adjacent to the soil columns used in the experiment. A Russian corer (ID = 0.09 cm, L = 100 cm) was used for these soil extractions. The 'destructive' soil cores were stored at 4 °C for approximately four months before analysis.

7.2.3 Experimental Design

Experimental water, to be used for the simulated groundwater table heights, was collected from a nitrate-contaminated groundwater spring (approximately 14.40 mg NO_3-N l^{-1}) located outside of the fen and considered one of the sources of the adjacent River Whitewater (Figure 7.1). The groundwater spring hydrochemical characteristics are presented in Table 7.2. The experimental water was vacuum filtered (Fisherbrand Grade 1 Qualitative filter paper) immediately after collection and stored at 4 °C.

Table 7.2: Summary of experimental water hydrochemical characteristics (mean concentrations in mg l^{-1}, except * in µg l^{-1}). 'TFe' represents total dissolved iron.

NH_3-N	NO_3-N	DON	P	Ca^{2+}	K^+	Mg^{2+}	Na^+	Al*	TFe*	DOC
0.08	14.40	3.55	0.02	116.26	0.81	1.71	10.26	19.37	4.50	1.10

The experimental design aimed to simulate vertical groundwater movement in the six soil columns (Figure 7.4 & Supplementary Information, Figure S2a). To measure the soil porewater, six Rhizon soil moisture samplers (SMS) (2.5 × 100 mm, Rhizosphere Research Products, Wageningen, The Netherlands) were inserted and sealed in six holes along each PVC tube to analyse the porewater for dissolved inorganic and organic N, cations, and DOC. Porewater samples were taken using a 10 ml syringe. The spacing between the Rhizon samplers was determined by the column height and the distance from the uppermost Rhizon sampler to the soil surface (Figure 7.3). For example, if the distance was > 5 cm between the uppermost Rhizon sampler and the soil surface, a 12 cm spacing was used; whereas, if the distance was < 5 cm, a 10 cm spacing was used. Only two columns (C2.1 and C2.2) had 10 cm spacing. The height of the Rhizon samplers was always measured from the bottom of the

columns. Furthermore, Rhizon samplers were installed so that the 10 cm porous membrane of the Rhizon was in the middle of the soil columns, reducing potential 'edge effects' (Stephenson, et al., 1984; Szalay, et al., 1996; MacNally, 1997; Ahn & Mitsch, 2002; Alexander, et al., 2016). The open tops of the columns were fitted with rubber-vented static chambers (with a stainless-steel jubilee strap) that allowed gas sampling through a PTFE/butyl septum (20 mm) using a 20 ml syringe, based on a design by Sullivan (2015) (Figure 7.4 & Supplementary Information, Figure S2c).
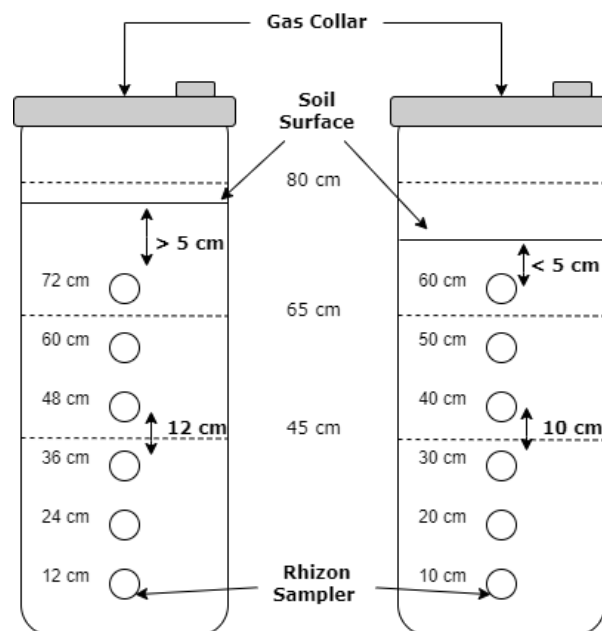
Figure 7.3: Spacing between the Rhizon Soil Moisture Samplers (SMS) according to the column height in the soil columns (explained in the text). The dotted lines represent the water tables (45 cm, 65 cm, and 80 cm).

The inflow of experimental groundwater was regulated via the base of the columns as follows. Sealed inside the bottom of the columns was a layer of acid-washed glass beads (approximately 2 cm in diameter) to ensure an even distribution of inflowing experimental water (Shuai & Jaffé, 2019) (Figure 7.4 & Supplementary Information, Figure S2b). This aimed to prevent nonuniform saturation of the soil columns, which could produce highly variable

porewater saturations. All water connections were made with gastight tubing (Masterflex® Tygon® 16 L/S® Precision Pump Tubing, Cole-Parmer[TM], Illinois, United States), and the columns were made watertight with silicone sealant (Geobond Marine Sealant, Geocel®, Chapeltown, United Kingdom). The water inflows were connected to an experimental water reservoir (25-litre HDPE container) that was deoxygenated using argon gas to simulate anoxic groundwater (Lind, et al., 2012). The dissolved oxygen concentration (DO) was maintained at < 1 mg l^{-1} throughout the experiment, as measured with an oxygen probe (ProDIGITAL DO Metre, YSI Incorporated, Ohio, United States). The deoxygenated water was then pumped into the columns to the desired water table height using a peristaltic pump (Masterflex® L/S® Variable-Speed Console Drive, Cole-Parmer[TM], Illinois, United States). The experiment was carried out in a temperature-controlled room at 20 °C.

Three successive water table heights were simulated (45 cm, 65 cm, and 80 cm), measured from the column bottoms. These were based on historical water table measurements (2016 – 2020) from a hydrological monitoring site closest to the groundwater abstraction site (Figure 7.1). These three water table heights are representative of the minimum, mean, and maximum water table heights measured at this site. Each water table height was allowed to equilibrate for 4 to 7 days before a 10-day sampling period. This sequence of water table equilibration and sampling was repeated for each successive water table height in the columns, totalling 30 days of porewater and gas sampling and analysis. Further details on the sampling and analysis protocols are reported in Section 7.2.4.

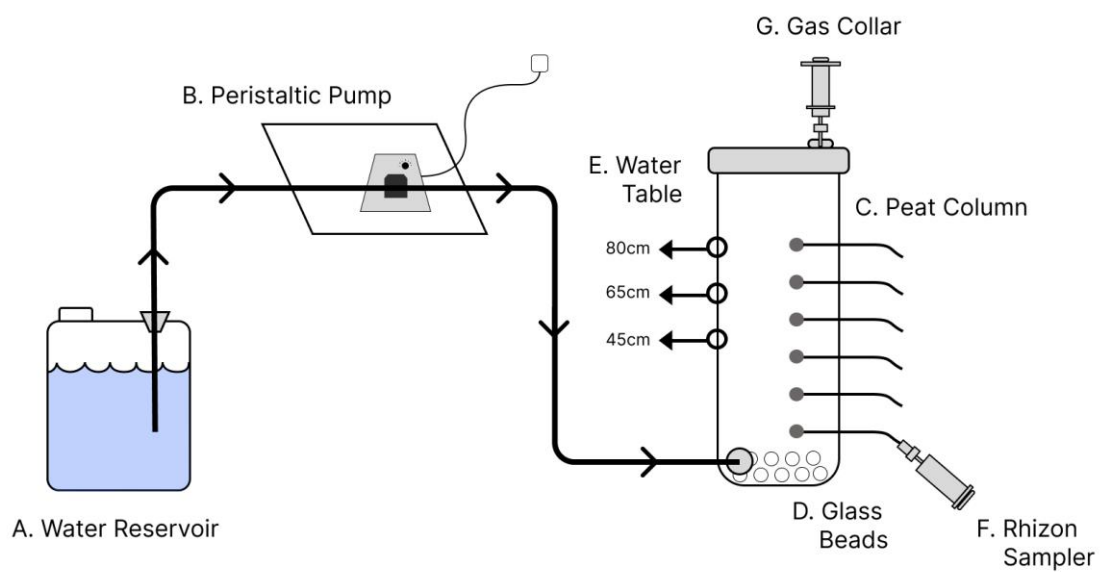**Figure 7.4:** Experimental design of the mesocosms showing the experimental water container (A) where water was pumped (B) through the column (C) from the bottom into the glass beads (D) and out through an outlet once the desired water table height was reached (E). In each soil column, porewater sampling was performed at different heights using Rhizon SMS samplers (F) and gas sampling was performed through a vented gas collar (G).

The control treatment for this experiment involved the use of ultrapure water for three water table height simulations, using three replicate soil columns extracted from sites C1 and C2 with the same method described in Section 7.2.2. For each control column, the porewater sampling was carried out on the first and final (5th) day over a 5-day period after the equilibrium period (4 to 7 days).

7.2.4 Porewater and Headspace Nitrous Oxide Analyses

During the 10-day sampling period, for each of the three successive water table heights, column porewater and headspace gas were sampled from Rhizons and static chambers for each of the respective columns. On all sampling occasions, the gas was sampled first to minimise the potential gas release from porewaters during Rhizon sampling (Riet, et al., 2013). The porewater samples were analysed for dissolved solutes, including dissolved inorganic and organic N, cations, and DOC. However, occasionally, porewater sample volumes were too low for collection, particularly during the 45 cm water table.

During the 10-day sampling period, NH_3-N, NO_3-N, and P were sampled for analysis daily, while cations, dissolved organic nitrogen (DON), and dissolved organic carbon (DOC) were measured on days 1, 2, 4, 6, and 10. As the experiment became a closed system after each pumping phase to reach the desired water table height, this sampling regime was designed to conserve the water volume within the columns, as well as the porewater sampling volume. NH_3-N, NO_3-N, and P were measured using an automated colourimetric analyser (Skalar San[++] Continuous Flow Analyser, Breda, The Netherlands), with detection limits of 0.03 to 0.34 mg l^{-1}, 0.13 to 0.49 mg l^{-1}, and 0.02 to 0.024 mg l^{-1}. The reason for the detection limit range is explained in Section 4.2. Total dissolved N (TDN) was determined using sodium persulfate ($Na_2S_2O_8$) and a digestion oven (CEM, MARS 5 Digestion Microwave). The digested samples were analysed using an automated colourimetric analyser (Skalar San[++] Continuous Flow Analyser, Breda, The Netherlands). DON was calculated based on the

difference between total dissolved N and total inorganic N (TIN) (DON = TDN – TIN). The cations, calcium (Ca^{2+}), magnesium (Mg^{2+}), potassium (K^+), sodium (Na^+), total iron ($Fe^{2+/3+}$), and aluminium (Al^{3+}), were determined using ICP-OES (Perkin Elmer Optima 7300 ICP-OES, Waltham, MA, United States). DOC was determined using a total organic carbon (TOC) analyser (Shimadzu TOC-L, Kyoto, Japan). DOC was calculated based on the difference between total carbon (TC) and dissolved inorganic carbon (DOC = TC – DIC).

Nitrous oxide (N_2O) was sampled daily and analysed using gas chromatography (7890B GC system with Flame Ionisation Detector (FID) and Electronic Capture Detector (ECD), Agilent Technologies, California, United States). All porewater and greenhouse gas analyses were carried out within 72 hours after sampling. It should be noted that two days of nitrous oxide measurements during the 80 cm water table treatment (days 24 and 25) were removed from the dataset, as the measurements were thought to be a systematic error during the analysis.

7.2.5 Soil Core Analysis

The four soil cores used for destructive analysis were divided into 10 cm subsamples and homogenised, air-dried, ground, and sieved (< 2 mm). Further, the peat subsamples were dried (105 °C for 24 hours) and milled (Laval Lab Inc. Planetary Ball Mill, Pulverisette 5, Laval, Canada), before determining total carbon (C_t) and total nitrogen (N_t), and calculating the C:N ratio. The subsamples were analysed with a CN elemental analyser (Thermo Scientific™ Flash 2000 Elemental Analyser, Waltham, MA, US).

7.2.6 Statistical Analysis

The study design was a complete randomised block design (RCBD). The Kruskal-Wallis test and Scheirer–Ray–Hare test are two nonparametric statistical tests, which were used to assess the hydrochemical and gaseous differences between different soil columns and water table treatments, with a threshold of 0.05 used for significance. In addition, principal component analysis (PCA) was applied. The mean nitrous oxide and porewater variables measured for each column and associated water table heights were used for the PCA analysis. Before completing the PCA analysis, some data transformations were carried out on the dataset. Highly positively skewed variables were logarithmically transformed, except for Ca^{2+}, Mg^{2+}, and Na^+, since their distributions were close to Normal. Subsequently, all variables were standardised to ensure equal weighting. P and DON were removed from the data set, as most of the mean values were near or below detection limits. Spearman's rho correlation analysis was used for all correlation analyses, as most of the measured variables did not meet normality. All statistical analyses were performed in RStudio® Version 1.4.1103.

7.3 Results

7.3.1 Porewater Hydrochemistry

In this section, the concentrations of dissolved solutes for each water table height treatment are presented as the means of the values obtained from all rhizon samplers throughout the 10-day sampling period of each treatment ($n = 60$ for NH_3-N, NO_3-N, and P; $n = 30$ for cations, DON, and DOC). These data are presented in Table 7.3 for each of the three replicate columns at sites C1 ('high N' site) and C2 ('low N' site).

In all columns, Ca^{2+} and Na^+ were the dominant cations in the porewater, ranging from 119.2 ± 19.20 (SD) to 152.44 ± 32.81 mg l^{-1} and 9.08 ± 0.90 to 21.74 ± 12.01 mg l^{-1}, respectively. Interestingly, significant differences in solute concentrations were found between the two sampling sites (p-values < 0.001), except for NO_3-N (p-value = 0.033) and P (p-value = 0.23). NO_3-N was higher in the C1 columns than the C2 columns throughout the successive water table heights, with the highest concentrations occurring during the 65 cm water table height. Similarly, DOC was higher in the C1 columns, with the highest concentrations occurring during the 80 cm water table height. Fe was higher in the C2 columns compared to the C1 columns, with particularly high mean concentrations measured during the 45 cm and 80 cm water table height treatments (Table 7.3).

Table 7.3: Selected hydrochemistry of the porewater in all soil columns for each successive water table height maintained by the experimental groundwater (mean concentrations in mg l^{-1}, except * in µg l^{-1}). 'TFe' represents total iron. Values in parentheses indicate the standard deviation of the mean (*n* values are explained in the text).

Water Table	Soil Column	NH$_3$-N	NO$_3$-N	DON	P	Ca^{2+}	K$^+$	Mg^{2+}	Na$^+$	Al*	TFe*	DOC
45 cm	**C1.1**	0.90 (0.56)	1.14 (2.95)	0 (3.46)	0.20 (0.16)	133.30 (12.65)	1.11 (0.23)	2.09 (0.25)	14.59 (3.86)	26.89 (3.93)	39.58 (60.22)	14.03 (4.95)
	C1.2	0.53 (0.55)	0.36 (0.30)	0 (0.58)	0.06 (0.07)	142.82 (20.31)	3.19 (3.09)	2.32 (0.41)	19.03 (8.69)	38.42 (17.95)	36.08 (38.62)	19.93 (16.22)
	C1.3	0.39 (0.23)	0.57 (0.77)	0 (0.92)	0.05 (0.04)	152.44 (32.82)	0.66 (0.40)	2.48 (0.47)	19.53 (9.64)	33.99 (12.51)	24.90 (34.77)	23.02 (14.71)
	C2.1	0.31 (0.17)	0.42 (0.32)	0 (0.26)	0.06 (0.07)	139.80 (37.51)	3.56 (1.41)	2.08 (0.59)	9.60 (0.51)	25.06 (2.73)	269.70 (363.06)	11.15 (6.48)
	C2.2	0.43 (0.23)	0.32 (0.07)	0.27 (0.38)	0.47 (1.05)	126.93 (19.83)	4.74 (5.98)	1.98 (0.22)	9.75 (0.92)	26.74 (8.00)	94.59 (107.39)	11.36 (7.33)
	C2.3	0.34 (0.25)	1.02 (1.02)	0 (0.89)	0.03 (0.02)	128.50 (22.84)	4.82 (4.34)	1.96 (0.41)	9.08 (0.90)	27.09 (7.14)	37.25 (32.57)	14.63 (15.59)
65 cm	**C1.1**	0.41 (0.31)	1.88 (3.74)	0 (3.68)	0.09 (0.08)	134.12 (22.02)	1.11 (0.49)	2.07 (0.35)	16.43 (5.64)	23.57 (8.09)	13.97 (12.23)	21.75 (14.64)
	C1.2	0.24 (0.17)	2.11 (4.17)	0 (1.50)	0.03 (0.01)	143.11 (22.39)	4.09 (3.85)	2.31 (0.45)	21.74 (12.01)	25.50 (8.48)	31.81 (48.92)	30.08 (21.49)
	C1.3	0.32 (0.23)	1.80 (3.51)	0 (0.72)	0.03 (0.01)	144.51 (35.89)	1.03 (0.94)	2.35 (0.53)	18.86 (9.89)	24.67 (9.54)	9.32 (8.60)	24.66 (16.61)
	C2.1	0.20 (0.12)	0.27 (0.16)	0 (0.13)	0.02 (0.01)	138.33 (26.89)	3.79 (1.88)	2.03 (0.41)	9.94 (0.76)	20.08 (2.41)	55.91 (78.89)	12.69 (3.56)
	C2.2	0.30 (0.19)	0.27 (0.17)	0.14 (0.20)	0.28 (0.56)	120.23 (19.62)	4.02 (4.37)	1.91 (0.26)	9.81 (1.04)	20.07 (3.12)	40.03 (41.26)	15.46 (7.57)
	C2.3	0.18 (0.17)	2.25 (4.54)	0 (3.43)	0.03 (0.02)	131.97 (22.84)	5.55 (5.80)	2.00 (0.45)	9.67 (1.40)	22.21 (9.03)	18.17 (18.23)	14.98 (7.18)
80 cm	**C1.1**	0.54 (0.42)	2.51 (5.77)	0 (5.55)	0.05 (0.04)	120.60 (28.61)	3.40 (4.43)	1.93 (0.40)	19.92 (9.40)	26.38 (6.19)	30.50 (33.47)	31.04 (23.46)
	C1.2	0.64 (0.89)	0.34 (0.34)	0 (0.96)	0.10 (0.34)	138.74 (24.89)	4.79 (4.66)	2.34 (0.58)	20.65 (9.92)	26.10 (6.29)	162.29 (207.74)	34.40 (29.58)
	C1.3	0.36 (0.26)	1.02 (2.08)	0 (1.20)	0.03 (0.02)	139.04 (24.37)	1.56 (1.73)	2.31 (0.40)	19.73 (10.48)	28.89 (14.84)	22.37 (32.24)	25.66 (17.44)
	C2.1	0.34 (0.22)	0.30 (0.13)	0 (0.25)	0.06 (0.11)	134.38 (22.99)	4.29 (2.36)	2.05 (0.29)	10.11 (0.78)	22.07 (1.54)	120.04 (140.80)	13.70 (3.51)
	C2.2	0.30 (0.18)	0.30 (0.13)	0.14 (0.26)	0.18 (0.29)	119.26 (19.20)	4.00 (3.65)	1.93 (0.22)	9.71 (0.94)	22.45 (3.12)	59.80 (69.29)	14.17 (7.31)
	C2.3	0.23 (0.21)	0.61 (0.91)	0 (0.57)	0.06 (0.07)	123.03 (18.24)	6.18 (5.40)	1.94 (0.28)	9.53 (1.07)	23.12 (2.29)	29.21 (23.06)	15.49 (7.79)

7.3.2 Porewater Nitrogen Dynamics

The mean porewater concentrations of NO_3-N and NH_3-N for the 10-day sampling periods at the different porewater sampling heights are plotted for the three successive water table treatments (45, 65 and 80 cm) in Figure 7.5. Generally, in all columns and for all water table treatments, the NO_3-N concentrations remained low at all porewater heights, ranging from 0.26 ± 0.16 (SD) to 1.31 ± 0.30 mg NO_3-N l^{-1} and did not differ significantly across the columns (*p*-values = 1.00). However, NO_3-N concentrations at the highest porewater sampling height (60/72 cm) were highly variable between the columns and the water tables, ranging from 0.26 ± 0.16 to 13.56 ± 7.42 mg NO_3-N l^{-1} (Figure 7.5). Interestingly, NO_3-N concentrations in all columns at 60/72 cm, except C2.1 and C2.2, increased from the 45 cm water table to the 65 cm water table. At the 80 cm water table, NO_3-N concentrations decreased in these columns, except in C1.1 (Figure 7.3). Columns C2.1 and C2.2 consistently showed NO_3-N concentrations near or below detection (0.13 to 0.49 mg NO_3-N l^{-1}) throughout the experiment. NO_3-N differed significantly between the column sites (*p*-value = 0.003) and at different water table heights (*p*-value = 0.029). However, NO_3-N did not differ significantly between the column sites (C1 and C2) during different water table heights (*p*-value = 0.93), indicating a similar behaviour between the C1 and C2 sites throughout the sequence of water tables (Table 7.4).

Mean concentrations of NH_3-N (over 10 days), ranging from 0.08 ± 0.05 to 2.11 ± 1.45 mg NH_3-N l^{-1}, were considerably lower than those of NO_3-N (Figure 7.5). Generally, NH_3-N decreased between the 10/12 cm and 50/60 cm porewater heights in the soil columns during the different water table treatments, but some columns showed an increase at the 60/72 cm height (Figure 7.5). NH_3-N concentrations were highest in C1.1 during the 45 cm water table. NH_3-N differed significantly between the column sites (*p*-value < 0.001) and at different water table heights (*p*-value < 0.001). Furthermore, NH_3-N differed significantly between column

sites during the different water tables (*p*-value = 0.018). DON was not further investigated because its mean porewater concentrations were near zero in most soil columns (Table 7.4).
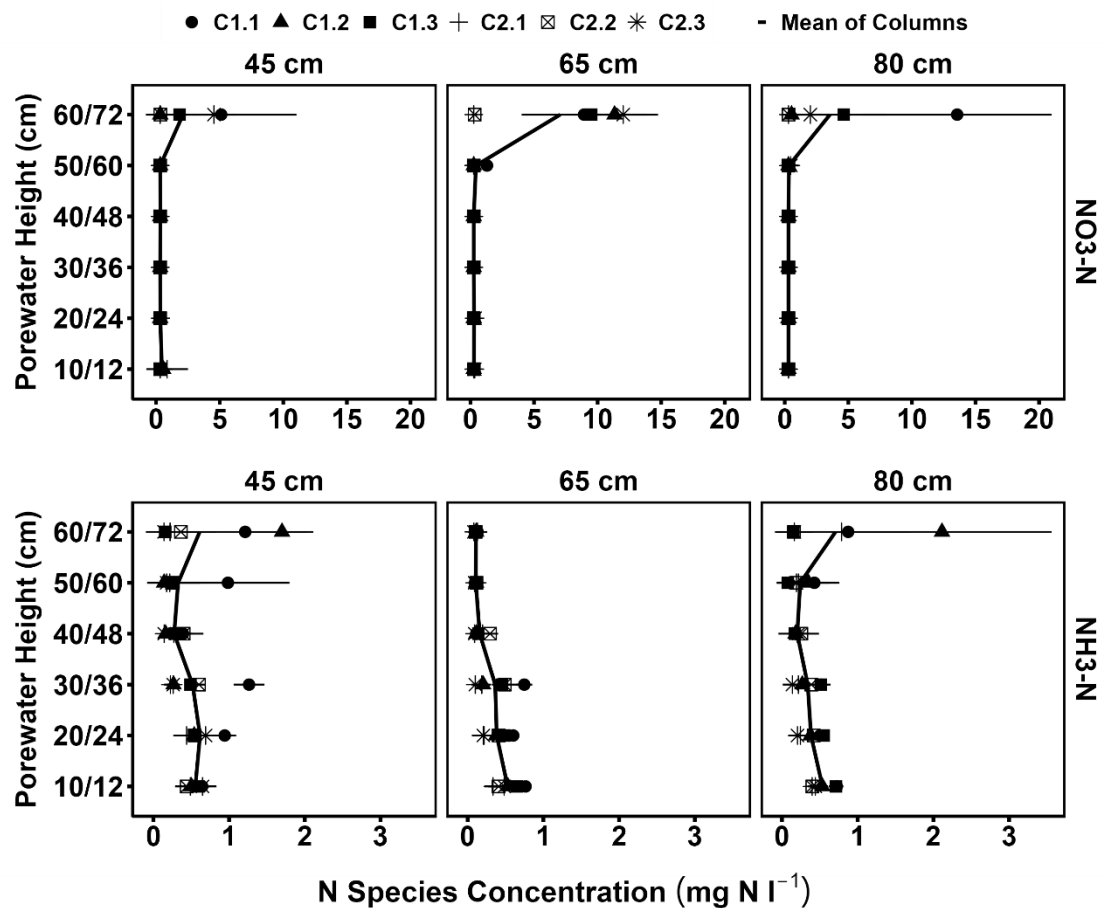

Figure 7.5: Mean concentrations of soil column porewater NH_3-N and NO_3-N at the different rhizon sampling heights over the 10-day sampling periods for the three successive water table treatments (45 cm, 65 cm, and 80 cm). The black line represents the mean of the six columns ($n = 6$) and the error bars show the standard deviation.

Table 7.4: Scheirer–Ray–Hare test on the differences between porewater NO_3-N and NH_3-N between the soil column sites (C1 and C2) at different water table heights (45 cm, 65 cm, and 80 cm).

	NH₃-N		NO₃-N	
Effect	*p*	*p* <.05	*p*	*p* <.05
Column Site	<0.001	*	0.032	*
Water Table Height	<0.001	*	0.029	*
Column Site:Water Table Height	0.66		0.28	

7.3.3 Porewater DOC and Fe Dynamics

Generally, the mean DOC over the 10-day sampling periods increased with increasing porewater sampling heights in all columns and with the water table height treatments (Figure 7.6). There were insufficient porewater volumes in C1.1 at 60 cm and 72 cm at the 45 cm water table height and 72 cm at the 65 cm water table height, and in C1.3 at 60 cm at the 65 cm water table height. In all columns, the DOC concentrations between 10/12 cm and 30/36 cm ranged from 6.10 ± 3.73 (SD) to 17.86 ± 13.59 mg l^{-1}, compared to the concentrations between 40/48 cm and 60/72 cm, which ranged from 8.37 ± 2.90 to 78.39 ± 12.32 mg l^{-1} (Figure 7.6). Furthermore, the concentrations at the 50/60 cm and 60/72 cm heights in C1.1, C1.2, and C1.3 were much higher compared to the C2 columns, ranging from 29.65 ± 8.47 to 78.39 ± 12.32 mg l^{-1}, and increased with water table height (Figure 7.6). In general, DOC did not differ significantly between 10/12 cm and 30/36 cm (*p*-value = 0.05 to 1.00), but differed significantly between 40/48 cm and 60/72 cm (*p*-value = 0.008 to < 0.001) in the soil columns. Furthermore, DOC concentrations differed significantly between the two column sites (C1 and C2) (*p*-value < 0.001) and with water table height (*p*-value < 0.001), but the effect of the water table heights did not differ significantly between the soil column sites (*p*-value = 0.54) (Table 7.5).

Mean Fe concentrations (over 10 days) in the soil columns increased with increasing porewater heights (Figure 7.6). Fe concentrations were particularly variable at the 45 cm and 80 cm water table heights, with ranges of 2.24 ± 0.48 (SD) to 541.75 ± 611.04 µg l^{-1} and 2.30 ± 0.35 to 503.04 ± 249.30 µg l^{-1}, respectively, particularly in columns C1.2 and C2.1. With the water table at 65 cm, the concentrations ranged from 7.87 ± 4.44 to 145.21 ± 137.42 µg l^{-1} across all porewater heights, with the highest concentrations found in C2.1 at 10/12 cm (106.15 ± 53.92 µg l^{-1}) and 60/72 cm (145.21 ± 137.42 µg l^{-1}) (Figure 7.6). Similarly to DOC, Fe differed significantly between soil column sites (p-value < 0.001) and in each water table (p-value < 0.001), but the effect of the water tables was similar in the column sites (p-value = 0.99) (Table 7.5).
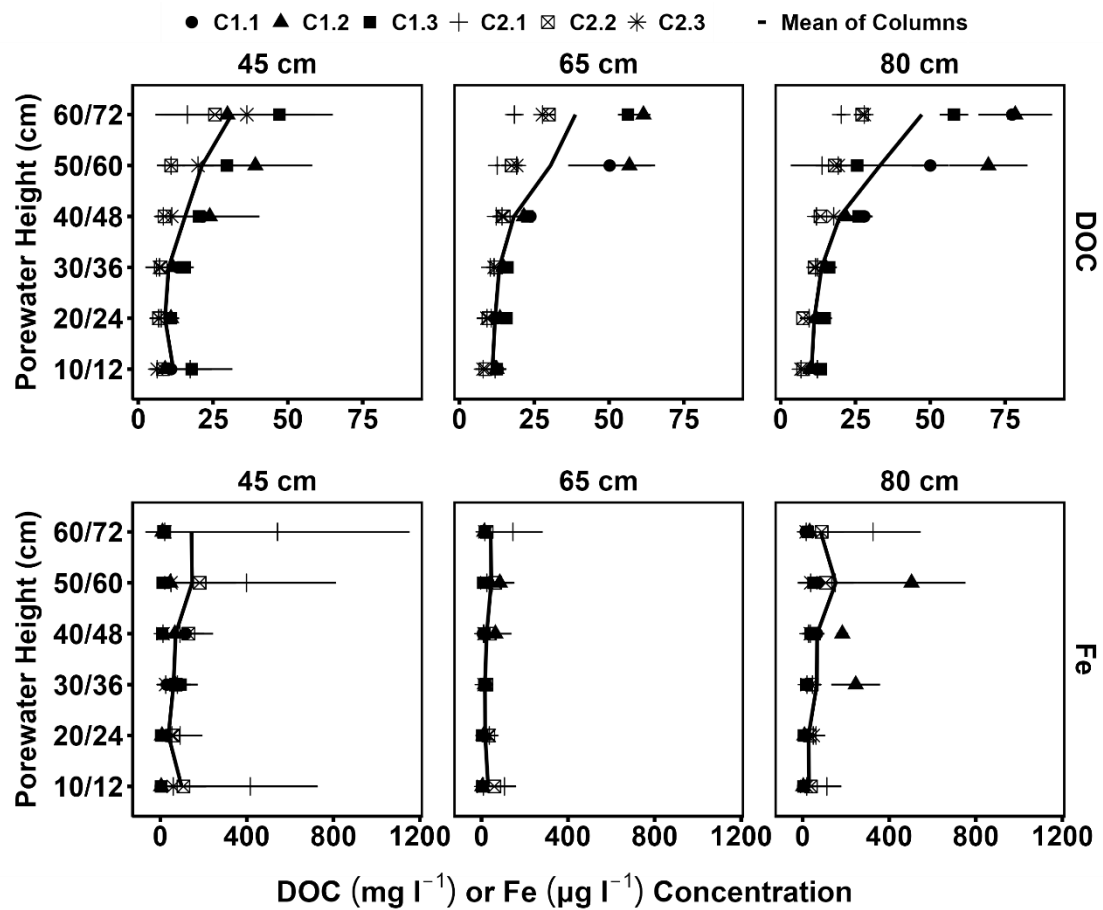
Figure 7.6: Mean concentrations of soil column porewater DOC (mg l⁻¹) and Fe (µg l⁻¹) at different rhizon sampling heights over 10-day sampling periods for the three successive water table treatments (45 cm, 65 cm, and 80 cm). The black line represents the mean of the six columns ($n = 6$) and the error bars show the standard deviation.

Table 7.5: Scheirer–Ray–Hare test on the differences between porewater DOC and Fe between the soil column sites (C1 and C2) at different water table heights (45 cm, 65 cm, and 80 cm).

	DOC		Fe	
Effect	**p**	**$p < .05$**	**p**	**$p < .05$**
Column Site	<0.001	*	<0.001	*
Water Table Height	<0.001	*	<0.001	*
Column Site:Water Table Height	0.54		0.99	

136

7.3.4 Porewater Hydrochemistry - Control Experiment

The mean porewater concentrations of NO_3-N, NH_3-N, DOC, and Fe for the 5-day sampling periods at different porewater sampling heights in the soil columns during the control treatments are presented in Table 7.6. The water tables were maintained at 45 cm, 65 cm, and 80 cm using ultrapure water. Generally, the porewater NH_3-N concentrations in the control water tables were similar to the nitrate-enriched experiment; however, at the 45 cm and 80 cm water table heights in the nitrate-enriched experiments, two columns (C1.1 and C1.2) showed an increase of NH_3-N at the uppermost porewater height (Figure 7.5), which was not observed in the corresponding control water tables (Table 7.6). Porewater NO_3-N concentrations were also similar to the nitrate-enriched water tables, which were low throughout most of the columns (Table 7.6). NO_3-N concentrations remained low even at the upper porewater height (60/72 cm), which contrasted with the NO_3-N concentrations in several columns at the nitrate-enriched water table 65 cm (C1.1, C1.2, C1.3, and C2.3) and 80 cm (C1.1, C1.3, and C2.3), which showed elevated porewater concentrations (Figure 7.5).

Porewater DOC concentrations in the control water tables showed a similar increase through the porewater heights as the nitrate-enriched water tables (Figure 7.6); however, this could not be confirmed for the control 45 cm water table, as no data were available for the 50/60 and 60/72 cm porewater heights (Table 7.6). Generally, the porewater Fe concentrations for the control water tables were considerably higher throughout the lower porewater heights (Table 7.6), compared to the nitrate-enriched water tables (Figure 7.6). For example, porewater Fe concentrations ranged from 97.00 to 626.77 µg l^{-1} at the 65 cm control water table, compared to the nitrate-enriched water table, which ranged from 7.91 to 145.21 µg l^{-1}.

Table 7.6: Summary of porewater hydrochemical characteristics for the control experiment at each water table height (mean concentrations in mg l^{-1}, except * in µg l^{-1}). 'TFe' represents total iron and '-' indicates unavailable data.

Water Table	Height (cm)	NH$_3$-N	NO$_3$-N	TFe*	DOC
45 cm	10/12	0.50	0.61	277.24	12.33
	20/24	0.71	0.61	486.84	23.76
	30/36	0.19	0.61	353.34	14.21
	40/48	0.10	0.61	6.61	14.19
	50/60	0.10	0.61	-	-
	60/72	0.12	13.47	-	-
65 cm	10/12	0.73	0.61	626.77	16.09
	20/24	0.80	0.61	205.20	11.53
	30/36	0.35	0.61	341.42	18.73
	40/48	0.29	0.61	355.94	23.65
	50/60	0.53	0.61	471.43	24.83
	60/72	0.23	0.61	97.00	-
80 cm	10/12	0.85	0.61	575.44	12.13
	20/24	1.02	0.61	492.43	14.20
	30/36	0.69	0.61	127.16	14.87
	40/48	0.25	0.61	25.08	17.94
	50/60	0.58	0.61	118.39	21.81
	60/72	0.68	0.61	110.85	31.00

7.3.5 Nitrous Oxide Dynamics

The mean headspace concentrations of nitrous oxide for each of the three successive 10-day sampling periods are presented for all six columns in Figure 7.7. Generally, all soil columns were found to be sources of nitrous oxide, which generally increased with the water table height from 45 to 80 cm. The highest increases were observed in C1.1 and C1.2 during the 80 cm water table height, with C1.1 reaching 227.78 ± 265.38 (SD) ppm and C1.2 reaching 32.90 ± 15.44 ppm. Nitrous oxide release in the other columns (C1.3, C2.1, C2.2, and C2.3) was generally lower, with maximum concentrations at the 80 cm water table ranging from 5.40 ± 5.46 to 20.63 ± 14.63 ppm. However, C2.2 and C2.3 did not increase through the successive water table treatments, with mean concentrations remaining relatively consistent, ranging from

5.40 ± 5.46 to 7.76 ± 2.80 ppm. The mean nitrous oxide concentrations differed significantly between the column sites (*p*-values < 0.001) and between the water tables (*p*-values < 0.001) (Table 7.7). Furthermore, nitrous oxide differed significantly between the two column sites at each water table (*p*-values = 0.008).
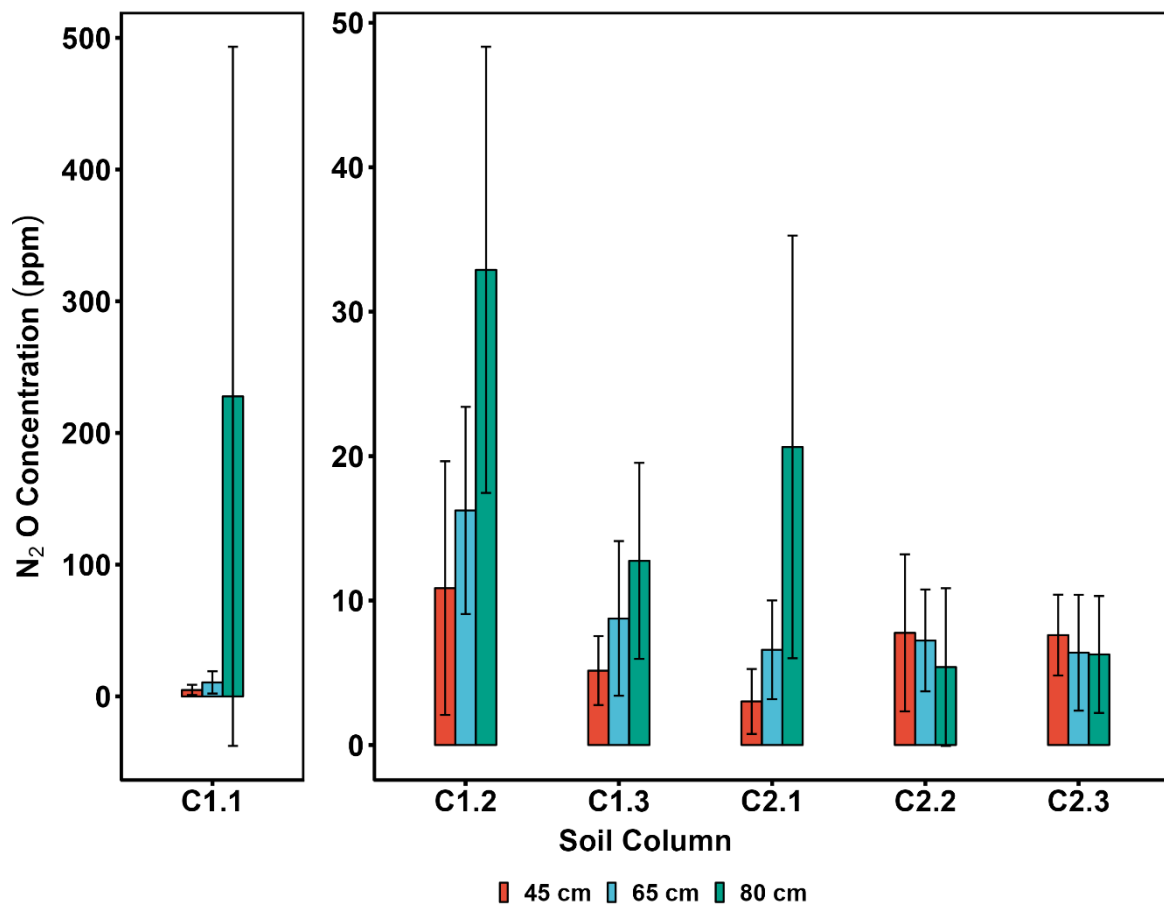

Figure 7.7: The mean nitrous oxide concentrations over the 10-day sample period for each of the three successive water table heights. Error bars show the standard deviation.

Table 7.7: Scheirer–Ray–Hare test on the differences between nitrous oxide release between the soil column sites (C1 and C2) at different water table heights (45 cm, 65 cm, and 80 cm).

	N_2O	
Effect	***p***	***p* <.05**
Column Site	<0.001	*
Water Table Height	<0.001	*
Column Site:Water Table Height	0.008	*

7.3.6 Principal Component Analysis (PCA) and Correlation Matrix

PCA analysis was used to summarise the interrelationships between porewater hydrochemistry and gaseous release of the soil columns at the different water tables (Figure 7.8). PCA extracted four components that explained 89% of the total variance (Supplementary Information, Table S1). For this study, only principal components 1 and 2 were considered, which explained 63% of the total variance and provided sufficient information. The strength of the effect a variable has on a principal component is represented by positive and negative loadings (Legendre & Legendre, 1998)

Principal component 1 explained 44% of the variance (Figure 7.8), characterised by high positive loadings of Fe and K^+ and high negative loadings of nitrous oxide, NO_3-N, DOC, Na^+, Mg^{2+}, and Ca^{2+}. Principal component 2 explained less variance (19%), which showed high negative loadings of Fe, Ca^{2+}, and Mg^{2+} and high positive loadings of Na^+, DOC, NO_3-N, nitrous oxide, and K^+. The C2 soil columns were distributed along the positive loading of principal component 1, while the C1 columns were distributed within the negative loadings of principal component 1, indicating distinct hydrochemical and gaseous characteristics at the two sampling sites (Figure 7.8).

The effect of each water table height (45 cm, 65 cm, and 80 cm) was similar at the respective column sampling sites (C1 and C2) (Figure 7.8). The 45 cm water table height was distributed along the negative loading of principal component 2, associated with Fe, Ca^{2+}, Mg^{2+}, and NH_3-N. However, the 65 cm and 80 cm water table heights were distributed mainly along the positive loadings of principal component 2, associated with Na^+, DOC, NO_3-N, nitrous oxide, and K^+ (Figure 7.8). This suggests that higher water tables were associated with higher porewater NO_3-N and nitrous oxide release.
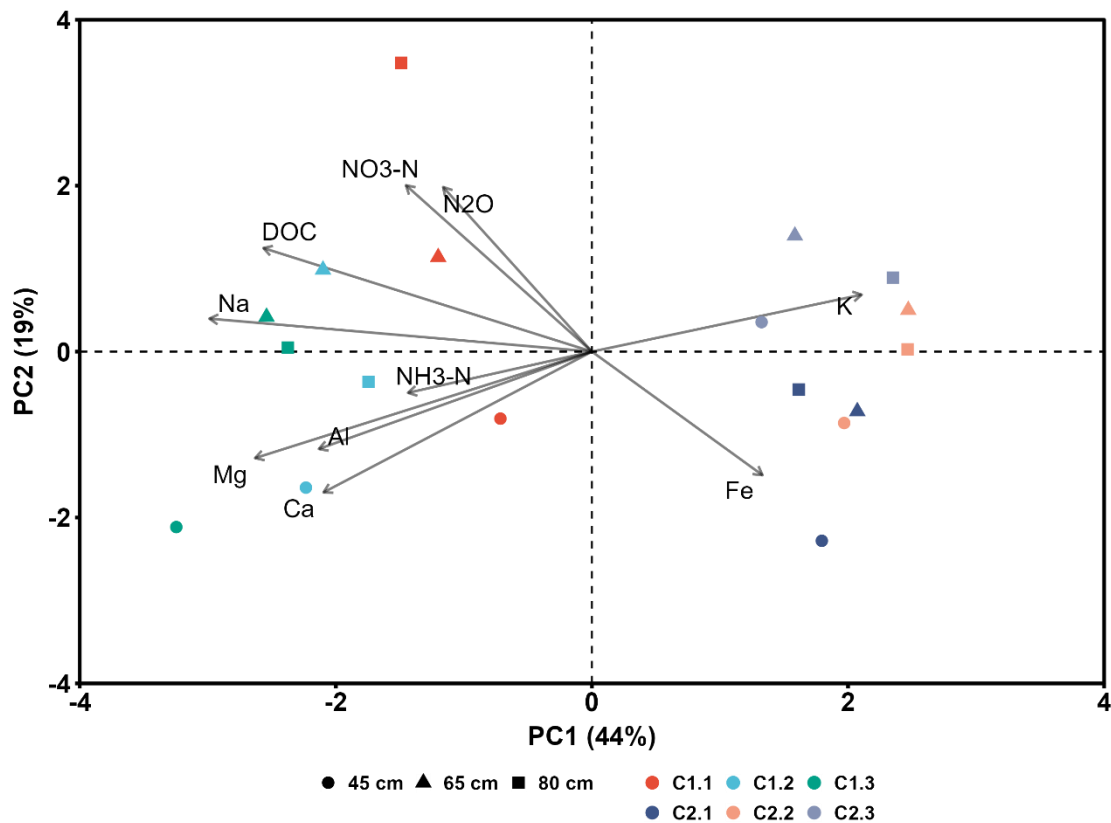

Figure 7.8: PCA biplot for porewater hydrochemistry and nitrous oxide release among the six soil columns subjected to three successive water table heights. Mean values from Table 7.3 were used for this analysis.

A Spearman's correlation matrix between all measured hydrochemical solutes and nitrous oxide release is presented in Table 7.8. NO_3-N showed the strongest correlations with Fe (rho = -0.70, p-value < 0.01) and DOC (rho = 0.50, p-value < 0.05). Nitrous oxide was strongly correlated with DOC (rho = 0.61, p-value < 0.01). Additionally, Fe and DOC were negatively correlated with each other (rho = -0.53, p-value < 0.05).

Table 7.8: Spearman's correlation (rho) matrix of hydrochemical solutes and nitrous oxide release in the soil column sites (C1 and C2). Mean values from Table 7.3 and the nitrous oxide release were used for this analysis. Bold values denote correlation coefficients (rho) ≥ 0.5 or ≤ -0.5. 'TFe' represents total dissolved iron.

Parameter	NH_3-N	NO_3-N	Ca^{2+}	K^+	Mg^{2+}	Na^+	Al*	TFe*	DOC	N_2O
NH_3-N	1									
NO_3-N	0.10	1								
Ca^{2+}	0.11	0.13	1							
K^+	-0.41	-0.16	-0.48*	1						
Mg^{2+}	0.34	0.18	**0.94***	**-0.51***	1					
Na^+	0.49*	0.25	**0.52***	-0.48*	**0.61****	1				
Al*	**0.66****	0.31	0.39	-0.36	**0.50***	0.38	1			
TFe*	0.11	**-0.70****	-0.2	0.35	-0.21	-0.22	-0.16	1		
DOC	0.26	**0.50***	0.28	-0.2	0.38	**0.76***	0.31	**-0.53***	1	
N_2O	0.25	0.11	-0.07	0.2	-0.01	**0.52***	0.06	-0.06	**0.61****	1

* p-value < 0.05, ** p-value < 0.01, *** p-value < 0.001

7.3.7 Sampling Site Soil Characteristics

The C:N ratios were used to characterise the soil profile of the two sample sites (Figure 7.9), C1 and C2 (Figure 7.1). The ratios were similar between depths of 0 and 60 cm (13.9 to 18.1), which was confirmed to be peat by visual examination. However, the ratios between the two sites began to differ considerably below 60 cm. The ratio for site C1 remained low until 80 cm and then rapidly increased between 80 and 100 cm, reaching 68.2 (Figure 7.9). In contrast, the C2 site ratio increased between 60 and 80 cm, reaching 38.4, and then increased further between 80 and 100 cm, reaching 50.3 (Figure 7.9). Visual inspection of the soil cores showed that the change in the C:N values was due to a transition from peat to clay in the soil substrate. Therefore, the main difference between the two columns was the thickness of the clay layer, 20 cm at site C1 compared to 40 cm at site C2 (Figure 7.9).
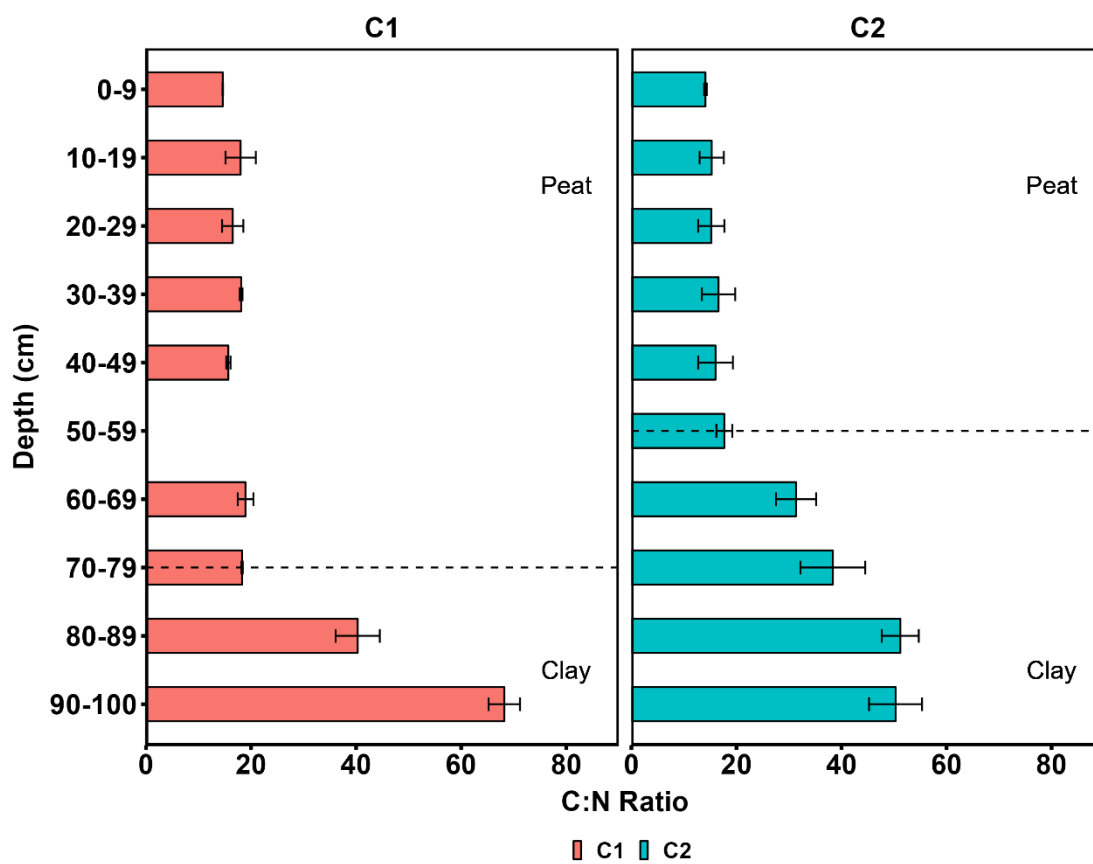
Figure 7.9: Soil characteristics (mean C:N values) of the two sampling sites ($n = 2$) in Greywell Fen. The dotted line indicates the marked change in the soil profile, and the error bars show the standard deviation ($n = 2$). C1 50-60 cm is missing data as there was not enough sample in the soil core for analysis.

7.4 Discussion

Peatlands have been widely reported to mitigate the NO_3-N enrichment of water (Venterink, et al., 2002; Lind, et al., 2013; Mwagona, et al., 2019; Han, et al., 2020), through various NO_3-N reduction processes, such as denitrification or dissimilatory reduction to nitrate (Bachand & Horne, 1999; Burgin & Hamilton, 2007; Messer, et al., 2017). However, NO_3-N enrichment and/or fluctuating water tables have been shown to decrease the efficiency of NO_3-N reduction and increase nitrous oxide release (Aber, 1992; Martikainen, et al., 1993; Regina, et al., 1996; Hefting, et al., 2003; Roobroeck, et al., 2010); however, NO_3-N enrichment and different water tables are rarely studied together (Han, et al., 2020). Furthermore, NO_3-N enrichment effects on NO_3-N cycling efficiency and nitrous oxide release are conflicting, with reports of limited or no observable effects (Nykänen, et al., 2002; Mwagona, et al., 2019). This study aimed to further evaluate the nature of porewater NO_3-N cycling and nitrous oxide release in nitrogen-enriched peat at different water table heights, particularly in rewetting scenarios.

7.4.1 Spatial Dynamics of NO_3-N, NH_3-N, DOC, and Fe

For all water table treatments (45 cm, 65 cm and 80 cm), among all soil columns, the porewater concentrations of NO_3-N at most of the porewater heights (10/12 cm to 50/60 cm) were considerably lower than in the experimental groundwater source (14.40 mg NO_3-N l^{-1}), with values generally near or below the detection limit (Figure 7.5). This suggested that NO_3-N from the experimental water was transformed from one N species to another, that is, effectively 'removed' from the soil columns during the successive water table treatments. Generally, denitrification is considered a dominant NO_3-N cycling reaction in peatlands (Cabezas, et al., 2012; Lind, et al., 2013; Mwagona, et al., 2019). The increased nitrous oxide emissions with increasing water tables of nitrate-enriched water provided evidence of denitrification during the water table treatments (Figure 7.7), with previous studies reporting increased nitrous oxide release with increasing denitrification rates (Yu, et al., 2006; Lind, et

al., 2013). Furthermore, the low porewater concentrations of NH_3-N suggested that dissimilatory nitrate reduction to ammonium was not a major contributor to NO_3-N cycling in the soil columns (Figure 7.5). However, there were elevated NH_3-N concentrations at the lower porewater sampling heights (between 10/12 cm and 30/36 cm) in the soil columns over the water table treatments, suggesting some dissimilatory nitrate reduction to ammonium. After equilibrating for 4 to 7 days, most porewater heights had NO_3-N concentrations near or below detection during sampling (Figure 7.5), suggesting relatively rapid NO_3-N cycling. For example, previous studies have reported complete cycling of added NO_3-N within days and hours (Williams, et al., 1999; Rückauf, et al., 2004; Lind, et al., 2013; Robertson & Thamdrup, 2017).

The water table had a considerable impact on porewater NO_3-N concentrations at the 60/72 cm height, which showed high variability between the soil columns. Unlike previous reports (for example, Venterink, et al., 2002; Holden, et al., 2004; Cusell, et al., 2013), NO_3-N concentrations increased with increasing water tables, particularly from 45 cm to 65 cm (Figure 7.5). The higher NO_3-N and NH_3-N concentrations during the 45 cm water table in some of the soil columns (C1.1, C1.3, and C2.3) probably resulted from the increased oxygen concentrations in the near surface peat due to undersaturated water conditions; leading to increased organic matter decomposition and nitrification, increasing porewater NO_3-N and NH_3-N concentrations (Knorr & Blodau, 2009).

The porewater NO_3-N concentrations increased in response to the subsequent elevation of the water table height to 65 cm; conversely, NH_3-N concentrations decreased (Figure 7.5). This may have been due to the upward diffusion of nitrate-enriched water to the 60/72 cm porewater sampling height (Rezanezhad, et al., 2016), which would explain this localised increase in NO_3-N concentration. Peat soils are known to have thresholds for critical moisture content for denitrification (Klein & Logtestijn, 1994; Amha & Bohne, 2011), and the threshold for denitrification may not have been reached at this water table height (65 cm). This condition

would lead to NO_3-N saturation, which refers to the reduced ability of peat to effectively cycle NO_3-N, resulting in NO_3-N accumulation (Aber, 1992; Hefting, et al., 2003; Sabater, et al., 2003; Hefting, et al., 2006). NO_3-N saturation was particularly evident in columns with an upper porewater height of 72 cm (C1.1, C1.2, C1.3, and C2.3), ranging from 8.93 ± 4.91 (SD) to 12.01 ± 2.74 mg NO_3-N l^{-1}, where the porewaters were probably not fully water saturated; compared to the columns with an upper porewater height of 60 cm (C2.1 and C2.2), both of which showed concentrations of 0.26 ± 0.16 mg NO_3-N l^{-1}, which were fully saturated at the 65 cm water table. This suggests that a sufficient moisture threshold was not reached for denitrification in C1.1, C1.2, C1.3, and C2.3. However, the moisture content was not measured in this study, so this cannot be confirmed. The control experiment for this water table height found NO_3-N near or below the detection limits at the 60/72 height (Table 7.6), suggesting that NO_3-N concentrations were influenced by the nitrate-enriched water.

Generally, porewater NO_3-N concentrations decreased with the rise in the water table from 65 cm to 80 cm; however, three columns (C1.1, C1.3, and C2.3) maintained relatively high NO_3-N concentrations: 13.56 ± 7.42 mg NO_3-N l^{-1}, 4.64 ± 3.31 mg NO_3-N l^{-1}, and 2.01 ± 1.53 mg NO_3-N l^{-1} (Figure 7.5), respectively. This suggests NO_3-N saturation at the 60/72 cm porewater height of these columns despite the increasing water table height and the columns being fully water saturated. The control experiment for this water table height, in which ultrapure water was used to simulate the water tables, showed NO_3-N concentrations near or below the detection limits at the 60/72 cm height (Table 7.6); this demonstrates the marked influence of the nitrate-enriched water on porewater NO_3-N cycling.

The high amount of porewater NO_3-N variability at the 60/72 cm porewater sampling heights among the different water tables may have resulted from the variability of DOC and Fe, both of which can affect NO_3-N cycling(Saunders & Kalff, 2001; Ambus & Christensen, 1993; Cabezas, et al., 2012) (Ambus & Christensen, 1993; Saunders & Kalff, 2001; Cabezas, et al., 2012).

For example, Burford & Bremner (1975) found soil denitrification to be significantly correlated with DOC (r = 0.99, *p*-value = <.001). Similar results were obtained in this experiment, where nitrous oxide was strongly correlated with DOC (rho = 0.61, *p*-value < 0.01). In general, DOC concentrations were highest at the 60/72 cm porewater height in all columns, particularly in the C1 ('high N' site) columns (Figure 7.6). However, the C1 columns also showed the highest porewater NO_3-N at 60/72 cm height (Figure 7.5), suggesting that the higher concentrations of DOC did not affect NO_3-N cycling. The limited effect of organic carbon concentrations on NO_3-N cycling in organic-rich soils is consistent with some previous reports (Gordon, et al., 1986; Merrill & Zak, 1992; Seitzinger, 1994).

Overall, the results showed a strong positive correlation between NO_3-N and DOC (rho = 0.50, *p*-value < 0.05). This contradicts previous reports, where increasing DOC concentrations are associated with higher NO_3-N cycling rates (for example, Burford & Bremner, 1975; Hedin, et al., 1998; Davidsson & Ståhl, 2000; Bernard-Jannin, et al., 2017). The positive correlation exhibited in the current research may have been influenced by the differences in the concentrations of DOC and NO_3-N between the two field sites (C1 and C2) where the columns were extracted, with C1 columns showing higher mean concentrations of both DOC and NO_3-N (Table 7.3). The variability of DOC could be due to the varying peat depths and clay thickness at the two sites (Figure 7.9), with C1 columns having a greater peat depth and a thin clay layer compared to C2 columns. For example, Kalbitz (2001) reported a decrease in DOC concentrations with increasing depth in unmanaged peatlands, resulting from dissolved organic matter (DOM) adsorption in the mineral soil horizons. Therefore, the lower peat depth and thicker clay layer in the C2 soil columns may have lowered the DOC concentrations due to less organic-rich peat and greater DOC adsorption in the clay mineral soil. Furthermore, the current results showed that the dissolved Fe and NO_3-N had a strong negative correlation (rho = -0.70, *p*-value < 0.01), which indicates strongly reducing conditions in the peat porewaters (Boomer & Bedford, 2008).

Generally, DOC and dissolved Fe are considered highly correlated in peat soils (Lovley & Phillips, 1986; Hall, et al., 2016; Chen, et al., 2020). However, in this study, they were found to be strongly negatively correlated (rho = -0.53, p-value < 0.05). Curtinrich et al. (2022) also found significant negative correlations (p-value < 0.05 and p-value < 0.001) between Fe(III) and DOC in two mineral poor peatlands as a result of Fe complexation with organic carbon; however, Fe(III) complexation could not be confirmed because total dissolved Fe was measured, rather than individual Fe species. Fe concentrations in the columns were irregular and highly variable, but generally low, ranging from 2.24 ± 0.48 (SD) to 541.75 ± 611.04 µg l^{-1}. As Fe concentrations in experimental water were low (4.50 ug l^{-1}), Fe was believed to be produced in situ from various Fe redox processes, commonly reported in peatlands, such as Fe(III) reduction to Fe(II) (Lovley & Phillips, 1986; Lovley & Phillips, 1988; Bhattacharyya, et al., 2018; Chen, et al., 2020).

Overall, the porewater NO_3-N variability at the 60/72 cm height between the different soil columns may be due to the difference in the clay layer thickness (Figure 7.9), with the C2 columns having a thicker clay layer. Hydrogeology is an important control of biogeochemical cycling in peatlands (Abesser, et al., 2008; Lapworth, et al., 2009; House, et al., 2015); and this agrees with the findings reported by House et al. (2015) and Chapter 6, which hypothesised that the thickness of a clay layer controlled the spatial variability of NO_3-N, where a thin clay layer provided a direct inflow of nitrate-enriched groundwater, resulting in high porewater concentrations of NO_3-N.

7.4.2 Nitrous Oxide Release

Nitrous oxide concentration was highly variable throughout the experiment, ranging from 3.02 ± 2.25 to 227.78 ± 265.38 ppm (Figure 7.7). Generally, studies investigating nitrous oxide release in peatlands convert nitrous oxide measurements from parts per million (ppm) to a flux (often g N m^{-2} y^{-1}). However, given the methodology used in this study, it was decided that

the measurements would remain in parts per million. This meant that nitrous oxide measurements were not directly compared with those of other studies.

Unlike previous studies in which nitrous oxide release decreased with a rising water table height (Regina, et al., 1996; Glatzel, et al., 2008; Jørgensen, et al., 2012), nitrous oxide release in the current research increased significantly (p-values = 0.001) with increasing water table heights, but varied considerably among the soil columns (Figure 7.7). The current findings are in line with previous reports that found increased nitrous oxide release with increasing soil moisture in nitrate-enriched conditions (Davidson, et al., 2000; Ruser, et al., 2006; Jungkunst, et al., 2008). For example, in intact soil columns enriched with NO_3-N (150 kg N ha^{-1}), Ruser et al. (2006) found a high nitrous oxide release at a water-filled pore space of > 70%, resulting from denitrification.

The C1 columns had the highest porewater NO_3-N concentrations at the 60/72 cm porewater height, as well as nitrous oxide release (Figure 7.5 & Figure 7.7); however, NO_3-N was not significantly correlated with nitrous oxide release (rho = 0.11, p-value > 0.05), which contrasts with previous reports (Tauchnitz, et al., 2008; Ye & Horwath, 2016). However, Meng et al. (2023) found lower R-squared values between porewater NO_3-N and nitrous oxide release (p-value < 0.01) in two nitrogen-enriched peat microcosms compared to the R-squared in control microcosms, which was hypothesised to be a result of higher 'pulses' of nitrous oxide release in the two nitrogen-enriched microcosms. Anthony & Silver (2021) also reported a similar phenomenon in nitrate-enriched agricultural peatlands, described as 'hot moments' of nitrous oxide release, accounting for 45% of the annual nitrous oxide emissions. Therefore, these 'pulses' of nitrous oxide release may explain the high variability of nitrous oxide observed in the fen soil columns. Specifically, the increase in nitrous oxide release could be due to NO_3-N saturation, where high NO_3-N concentrations persist. For example, Hefting et al. (2003) reported greater nitrous oxide release in a nitrate-enriched riparian area (20 kg N ha^{-1} yr^{-1}) compared to a less nitrate-enriched area (2–4 kg N ha^{-1} yr^{-1}), where denitrification rates did

not differ significantly. Furthermore, the positive correlation between DOC and nitrous oxide release (rho = 0.61, p-value < 0.01) found here, agrees with the findings of Liimatainen et al. (2018), who reported a positive correlation between DOC and nitrous oxide release (p-value < 0.05); where readily available organic compounds are used for heterotrophic denitrification.

7.4.3 The Relationship between Porewater Hydrochemistry, Nitrous Oxide Release, and Soil Geology

The PCA for porewater hydrochemistry and nitrous oxide release among the six soil columns showed a large contrast in these measurements between the two sampling sites, C1 and C2 (Figure 7.8). The C1 columns were associated with higher NO_3-N and DOC concentrations and nitrous oxide release (principal component 1), suggesting NO_3-N saturation. This was indicated by the increased NO_3-N concentration and nitrous oxide release with rising water tables (Figure 7.5 & Figure 7.7). In contrast, the C2 columns were mainly associated with Fe and K^+ (principal component 1) (Figure 7.8), which may suggest the influence of the thicker clay layer at the C2 site (Figure 7.9). Clay is known to have an affinity for K^+ due to its high cation exchange capacity (CEC) and can release K^+ to porewaters (Binner, et al., 2017). Furthermore, the higher association with Fe in the C2 columns suggests more chemically reduced environmental conditions (Figure 7.8). Consequently, despite the weak correlation between NO_3-N concentrations and nitrous oxide release (rho = 0.11, p-value < 0.01), PCA suggested that higher concentrations of porewater NO_3-N and DOC were associated with increased nitrous oxide release.

The clear distinction between the two column sites (C1 and C2) in both porewater hydrochemistry and nitrous oxide release suggests that the thickness of the clay layer may have influenced both factors. This strongly supports the findings presented in Chapter 6 and House et al. (2015), where NO_3-N concentration and cycling were mainly controlled by the thickness of a clay layer overlying the Chalk aquifer. As clay is relatively impermeable

(Klimentos & McCann, 1990), a thicker clay layer could have decreased the flow of the experimental water during pumping and increased the contact time between the nitrate-enriched water and peat. This increased contact time may have prevented NO_3-N saturation in the near surface of the C2 soil columns compared to the C1 soil columns. Furthermore, hydrogeology has been shown to affect nitrous oxide release in riparian wetlands (Sánchez-Pérez, et al., 2003) and calcareous river systems (Cooper, et al., 2017). For example, Cooper et al. (2017) found that rivers overlying unconfined Chalk bedrock had higher nitrous oxide release compared to bedrock confined by glacial deposits.

7.5 Conclusion

In conclusion, the NO_3-N buffering in the rewetted nitrate-enriched peat was high; however, NO_3-N saturation occurred in the near surface porewaters, particularly in the not fully water saturated conditions, and nitrous oxide release increased in some columns. These findings are explained as follows:

- High NO_3-N buffering occurred throughout the soil profile in most of the fen soil columns. This was indicated by negligible NO_3-N concentrations at most porewater heights, which were probably water saturated throughout the sequence of water table treatments; which suggested high denitrification rates, with some evidence of dissimilatory nitrate reduction to ammonium.

- However, NO_3-N saturation was observed in the near surface porewaters (60/72 cm porewater height) in some soil columns. Where high porewater NO_3-N persisted and increased with rising water table heights, particularly from 45 cm to 65 cm, suggesting that insufficient moisture content may have reduced NO_3-N cycling efficiency, probably denitrification, in the near surface peat.

- Nitrous oxide release increased with rising nitrate-enriched water tables in most columns, which was greatest at the highest water table (80 cm). However, there was a limited correlation between porewater NO_3-N and nitrous oxide release, where nitrous oxide release was highly variable. This suggested that nitrous oxide was released in 'pulses' and stimulated by higher porewater NO_3-N, rather than linearly increasing with porewater NO_3-N.

- The occurrence of NO_3-N saturation in soil columns appeared to be controlled by the thickness of a clay layer. PCA revealed that higher porewater NO_3-N concentrations and nitrous oxide release were associated with a thin clay layer in the soil columns. This was believed to reduce the contact time between nitrate-enriched water and peat compared to soil columns with a thicker clay layer, increasing the occurrence of NO_3-N saturation in the near surface porewater.

Despite these findings, further research should focus on the nitrous oxide release from high porewater NO_3-N sites in field settings to confirm the observations in this laboratory study, as well as the higher temporal resolution in the measurement of N dynamics (that is, hours rather than days). This study highlights the importance of hydrogeology in peatlands, where if the peat overlies a relatively impermeable layer such as clay, it can reduce the risk of NO_3-N saturation and nitrous oxide release.

8.0 Conclusions

This final chapter provides an overview of the study and the key findings reported in the three research chapters (5, 6, and 7). Based on these, a conceptual model of NO_3-N cycling in the fen is presented (Figure 8.1), together with the wider implications of the study for research and fen management, as well as recommendations for future research. Specific consideration is given to the implications of this study for the management of Greywell Fen in terms of groundwater abstraction.

The objective of this research was to evaluate N dynamics in a calcareous nitrate-enriched groundwater-fed fen and assess the impacts of groundwater restoration and propose mitigation options if needed. A continuous field monitoring programme was used to determine groundwater table heights, N concentrations, and hydrochemical variability in the fen over space and time (Chapters 5 and 6). The data collected from this programme was then used to inform a laboratory soil column experiment with high spatial and temporal sampling resolutions, which further investigated N cycling and nitrous oxide release in rewetted nitrate-enriched fen peat (Chapter 7).

The field monitoring programme was carried out over a year (2021 to 2022) with water samples collected every two weeks from various water sources at the Greywell Fen study site, including groundwater springs, surface water, Chalk groundwater, shallow groundwater, and porewater. These water samples were analysed using colourimetric analysis (N species), MARs digestion (organic N), ICP-OES (cations), and TOC analysis (organic carbon). The laboratory experiment involved sampling six large intact soil columns, which were subjected to nitrate-enriched water and different water table heights. Gas and porewater samples were taken daily for 30 days and analysed using gas chromatography and the same water quality techniques as the field monitoring programme. However, the epidemic of COVID-19 affected

the research and reduced the available time for practical and experimental work, particularly the intact soil column experiments. Time was limited for methodological development or resource procurement to further explore certain research topics.

Continuous field monitoring of NH_3-N, NO_3-N, and DON in Chapter 5 showed that NO_3-N concentrations in the fen varied spatially more than temporally. Most of the fen porewaters showed low NO_3-N concentrations (median range = 0.13 to 0.49 mg NO_3-N l^{-1}) compared to the nitrate-enriched groundwater and surface water (median range = 5.55 to 14.01 mg NO_3-N l^{-1}), but discrete nitrate-rich porewater sites were observed (median range = 1.37 to 6.86 mg NO_3-N l^{-1}). These elevated sporadic NO_3-N concentrations in the porewaters were not caused by variability in groundwater table height, which was not affected by the nearby groundwater abstraction. Instead, they were believed to be influenced by the inflows of nitrate-enriched groundwater into the fen. The low NO_3-N concentrations in the fen were probably sustained through NO_3-N cycling and a stable groundwater table height. The fen had a limited effect on NO_3-N concentrations in the adjacent surface water (River Whitewater), suggesting a limited hydrological connection. However, there was some evidence of a potential hydrological flow from the fen to the river. The observation of discrete nitrate-rich porewater sites led to further research on the hydrological transport and cycling of NO_3-N, using hydrochemical solutes in the fen and various water sources (Chapter 6). Overall, Chapter 5 highlighted the complexity of N variability in fens, where despite water table management or nitrate enrichment – both of which can increase N concentrations – a low N environment was maintained throughout most of the fen porewaters, except for the discrete nitrate-rich porewater sites.

The work in Chapter 6 investigated the hydrological transport and cycling of N using multivariate statistical analyses (HCA and PCA) and dissolved solute correlations. The application of HCA found that the nitrate-rich porewater sites were hydrochemically similar to the nitrate-enriched groundwater and surface water, and this was interpreted as corresponding to discrete inflows of nitrate-rich groundwater into the fen. Furthermore, the

hydrochemical similarity between the nitrate-enriched groundwater and surface water suggested that the Chalk aquifer was the main water source of the fen. However, most of the porewater was hydrochemically different from that of the nitrate-enriched groundwater and surface water, with DOC and Fe concentrations up to 3 and 4 times higher, respectively, and NO_3-N concentrations up to 40 times lower at these porewater sites. This suggested the biogeochemical cycling of the nitrate-enriched groundwater entering the fen. The PCA and solute correlations demonstrated that NO_3-N cycling in the porewaters was controlled by water residence time, as identified by cation exchange processes and increased concentrations of DOC and Fe, particularly Ca^{2+} and Mg^{2+} concentrations, ranging from 53.48 to 151.44 mg l^{-1} and 1.13 to 2.67 mg l^{-1}. A previous conceptual model of fen hydrogeology hypothesised that an impermeable clay layer overlying the Chalk aquifer controlled groundwater flow into the fen and variations in the clay layer thickness would allow greater or lesser flow. Therefore, it was thought that the hydrochemical transfer and cycling of NO_3-N were controlled by the thinning or absence of this impermeable clay layer, which reduced the hydrological connection between the fen and the Chalk aquifer. Where the clay layer thinned, the hydrological connection increased and a direct inflow of nitrate-enriched groundwater occurred, resulting in higher porewater NO_3-N concentrations, with median concentrations up to 14 times higher than other porewater sites. Therefore, most of the nitrate-enriched groundwater probably bypassed the fen as a result of being divided from the Chalk aquifer by this impermeable clay layer. Chapter 6 demonstrated that bypassing nitrate-enriched waters should be considered as a potential explanation of NO_3-N 'removal' in peatlands. In addition, it highlighted the important influence of hydrogeology on N cycling by limiting hydrological connectivity and N transfer. The key findings of Chapters 5 and 6 were further investigated in Chapter 7, a laboratory-based soil column experiment.

The work in Chapter 7 investigated the effect of rewetting with nitrate-enriched groundwater on N cycling in intact soil columns from 'high' and 'low' NO_3-N porewater sites at Greywell Fen (median concentrations = 5.18 and 0.34 mg NO_3-N l^{-1}). The results indicated that the cycling

of NO$_3$-N, probably denitrification, was high throughout most of the soil profile in the columns during the water table sequence (45 cm, 65 cm, and 80 cm), with mean concentrations ranging from 0.26 to 1.31 mg NO$_3$-N l^{-1}. However, NO$_3$-N concentrations near the peat surface and nitrous oxide release increased with the successive water table heights in some columns. NO$_3$-N concentrations near the peat surface were highest in most soil columns, ranging from 0.26 to 13.56 mg NO$_3$-N l^{-1}, during the mid-water table (65 cm) and not fully water saturated conditions. This suggested an insufficient moisture content for efficient NO$_3$-N cycling, resulting in NO$_3$-N accumulation. Nitrous oxide release was highest during the above surface water table height (80 cm) and fully water saturated conditions, ranging from 5.46 to 227.78 ppm. However, nitrous oxide release was highly variable and did not correlate with porewater NO$_3$-N. This suggested that nitrous oxide was released in 'pulses' and stimulated by increased NO$_3$-N concentrations, rather than linearly increasing with porewater NO$_3$-N. Furthermore, PCA demonstrated that NO$_3$-N concentrations and nitrous oxide release were higher in the soil columns from the nitrate-rich porewater site. This site had a thin clay layer compared to the low porewater NO$_3$-N site (20 cm compared to 40 cm); the thicker clay layer in the columns from the low NO$_3$-N site may have slowed the inflow of the experimental water, increasing the water residence time and NO$_3$-N cycling. Further evidence of the hydrogeological control of NO$_3$-N transfer and cycling that was hypothesised in Chapter 6. Chapter 7 showed that there is a risk of N saturation, which is the accumulation of NO$_3$-N and increased nitrous oxide release when rewetting with nitrate-enriched groundwater, particularly if fen areas have a greater hydrological connection to a nitrate-enriched water source.

The observations of the three studies (Chapters 5, 6, and 7) and a previous conceptual hydrogeological model (Section 3.5.1, Figure 3.3) developed a conceptual model of NO$_3$-N cycling at Greywell Fen, presented in Figure 8.1. The spatial variability of porewater NO$_3$-N in the fen was mainly controlled by the thickness of an impermeable clay layer, which covered an unconsolidated gravel layer on top of the Chalk aquifer. If the clay layer was thin or absent, a direct inflow of nitrate-enriched groundwater occurred. As a result of a higher hydrological

connection to the nitrate-enriched Chalk aquifer, shorter water residence time, and a consistent near surface groundwater table, discrete nitrate-saturated porewater sites culminated. At these discrete sites, high NO_3-N concentrations persisted and there was the possibility of 'pulses' of high nitrous oxide release (Figure 8.1). Subsequently, the nitrate-rich porewater travelled horizontally to nearby low porewater NO_3-N areas, where NO_3-N cycling occurred as the water residence time increased, the concentrations of DOC increased, and the reducing conditions were higher (Figure 8.1). Furthermore, because the thin or absent clay layer occurred only at discrete locations, most of the nitrate-enriched groundwater flow was slowed by thicker clay layers, decreasing the hydrological connection to the Chalk aquifer, and increasing water residence time and contact time with the peat (Figure 8.1). This probably prevented the fen from becoming completely NO_3-N saturated by the nitrate-enriched groundwater. Consequently, this limited hydrological connectivity between the fen and the Chalk aquifer, divided by the impermeable clay layer, suggests that most groundwater bypasses the fen and does not come into contact with the active NO_3-N cycling in the peat layer. Furthermore, this limited hydrological connectivity extended to the nearby surface water (River Whitewater), although it is not known what controlled this. It is assumed that hydrogeology had some influence. Therefore, the limited hydrological connectivity prevented complete NO_3-N enrichment of the fen and maintained a low N environment. However, it culminated in discrete nitrate-rich locations in the fen, which could be sites of high nitrous oxide release, and meant that nitrate-enriched groundwater and surface water bypassed the fen, maintaining high NO_3-N concentrations in these water sources.

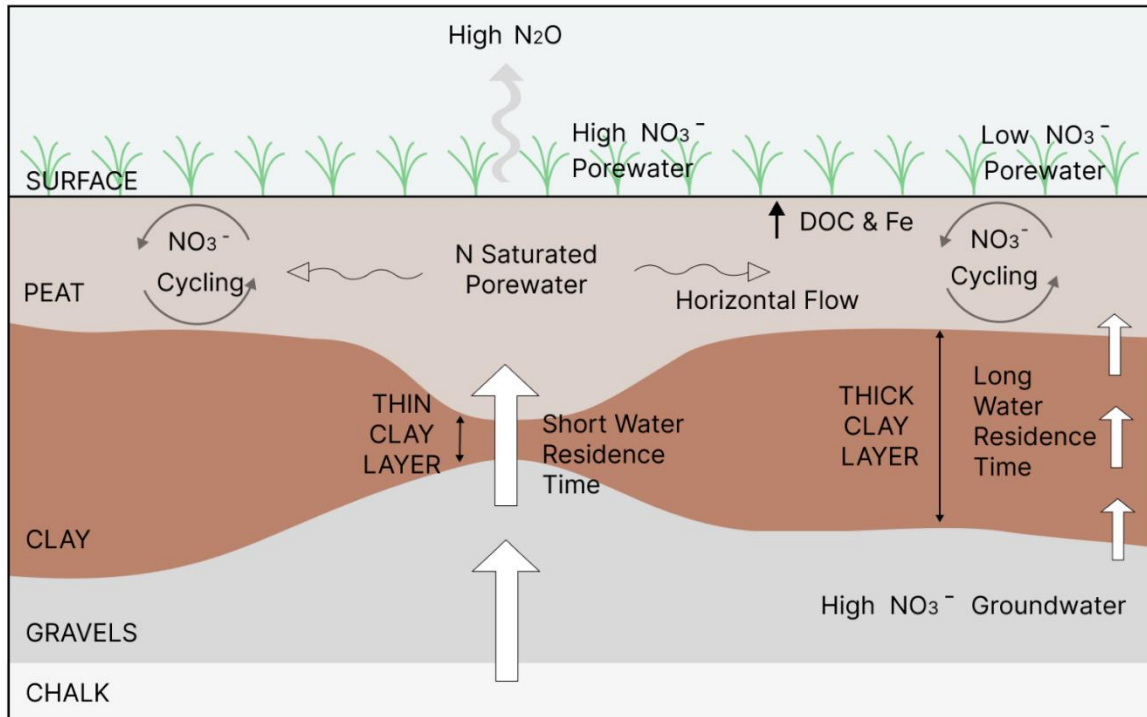**Figure 8.1:** Conceptual hydrological transfer and cycling of NO_3-N at Greywell Fen

Consequently, this thesis highlights the importance of continuing research on N cycling in peatlands subjected to nitrate-enriched waters, particularly the impact of hydrogeology and hydrology on N cycling and the release of nitrous oxide from nitrate-rich peatland areas. The study recommends measuring soil temperature across the fen at high spatial resolutions. Warmer soil/sediment temperatures have been used to identify groundwater inflows (Conant, 2004; Anderson, 2005; House, et al., 2015). Areas with warmer temperatures could be measured for hydrochemistry and thickness of the underlying clay layer. This would determine the amount of nitrate-enriched groundwater inflows across the fen and the importance of clay deposit thickness in controlling the spatial variability of porewater NO_3-N.

Furthermore, this would help to develop the conceptual hydrogeological model into a process-based model, which would provide explicit biogeochemical assumptions of the system and improve fen management both here and in other fen systems (Cuddington et al.,

159

2013). The process-based model could improve the understanding of the relationship between hydrology, hydrochemistry, and vegetation in fens. In addition, the study recommends measuring nitrous oxide release and comparing the results of field porewater sites exhibiting different NO_3-N concentrations. Furthermore, nitrous oxide measurements are difficult, as the release can be episodic and highly temporal (Rapson & Dacres, 2014). Therefore, in the future, there is a need to improve measurements with more sophisticated analytical equipment, for better accuracy and precision; for example, Fourier-transform infrared spectroscopy (FTIR) or laser absorption spectroscopy (Griffith, 2002; Edwards, et al., 2003; Chen & Fisher, 2013). A better understanding of these processes will better inform waterborne N management decisions in fen peatlands and minimise negative impacts on a global scale.

These findings improve our understanding of N cycling in nitrate-enriched fen peatlands, particularly calcareous environments, and have broader implications for the management of the study site and the use and restoration of peatlands as NO_3-N buffers. This research was intended to inform South East Water, the owner of the groundwater abstraction site at the fen, of the hydrochemical impact of a planned groundwater abstraction shutdown in 2025. The evidence from this research suggests that a groundwater abstraction shutdown is not necessary to prevent further fen degradation, as groundwater abstraction did not have a significant impact on groundwater table heights or NO_3-N concentrations in the fen. Consequently, the ecological management already carried out on the site should continue, for example, the grazing, shrub removal, and tree fellings (Section 3.4.2). Furthermore, the most recent ecological condition survey conducted by Natural England (2022) has noted the reduction of the area of unfavourable – declining conditions in the fen from 97% to 37%, as a result of ecological management. If groundwater abstraction is ceased, this should not increase the NO_3-N enrichment of the fen because the nitrate-enriched groundwater in the Chalk aquifer is divided from the fen by a clay layer, which controls the amount and rate of the nitrate-enriched groundwater inflow. However, in both scenarios, caution should be exercised.

First, if groundwater abstraction is continued, hydrological and hydrochemical monitoring should continue at selected locations, such as those with different NO_3-N concentrations. This is particularly important because although the effects of groundwater abstraction are limited at present, the increasing intensity of drought predicted in Europe due to climate change could increase hydrological pressure in the fen, lowering groundwater table heights and increasing N concentrations due to increased organic matter mineralisation (Martinl, et al., 1997; Holden, et al., 2004; Niedermeier & Robinson, 2007; Cabezas, et al., 2014; Füssel, et al., 2017; Spinoni, et al., 2018). This could increase N flushing into adjacent surface waters (Ulén, 1995; Kull, et al., 2008; Johnes, et al., 2020) or internal eutrophication and change the vegetation community (Bridgham & Richardson, 1993; Bridgham, et al., 1998; Venterink, et al., 2002). In order to mitigate these negative impacts, the groundwater abstraction pumping regime could vary seasonally; for example, following the peaks and troughs of the groundwater recharge processes to minimise hydrological pressure on the aquifer. Second, if groundwater abstraction is ceased, it should be considered that the hydrological connectivity between the fen and the Chalk aquifer could change; for example, the amount of discrete nitrate-enriched groundwater inflows could increase due to the reduced hydrological pressure imposed by groundwater abstraction on the Chalk aquifer. However, this would be limited to the fen areas closest to the groundwater abstraction. It is recommended that future research examines and develops groundwater hydrology flow patterns in the fen, particularly if this is modelled under different groundwater abstraction scenarios.

In a broader context, the thesis showed the important influence of hydrogeology on N cycling in fen peatlands. Hydrogeological conditions should be considered when trying to restore fen peatlands with the specific use as a NO_3-N buffer, as it could reduce the contact between the nitrate-polluted water source and the active N cycling zones of the peatland. Furthermore, there is a risk of NO_3-N saturation and increased nitrous oxide release in the surface peat layers that receive a direct inflow of nitrate-enriched waters, even under partial or complete

water saturation. This is particularly concerning since nitrous oxide is a powerful greenhouse gas.

Overall, the thesis completed a one-year field monitoring programme and an intensive 30-day experiment, despite the COVID-19 pandemic. In addition, a conceptual hydrogeochemical and biogeochemical model was developed that advances our understanding of NO_3-N enrichment in calcareous fen peatlands on both local and broader scales.
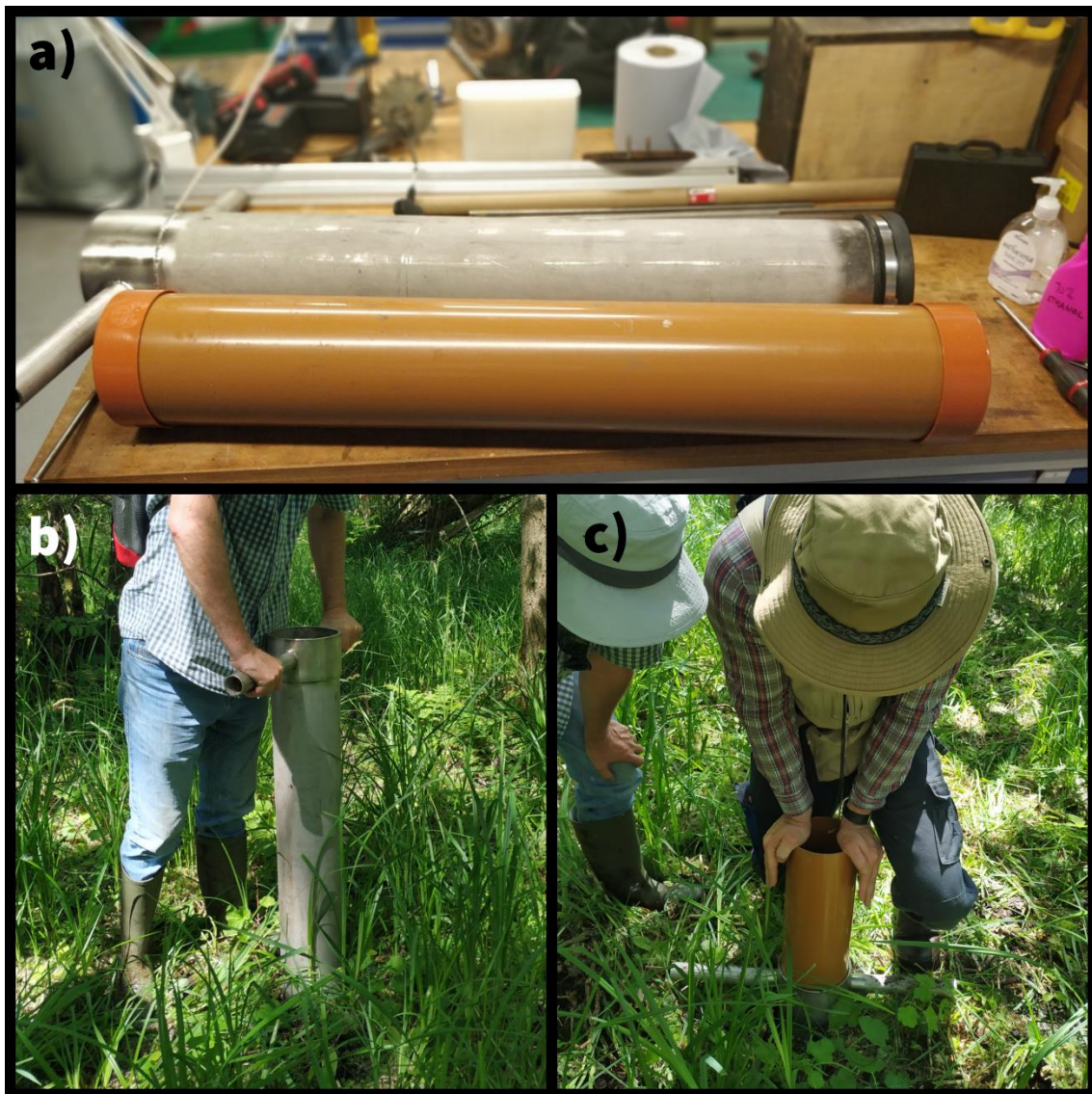
Figure S1: Photos of a) steel 'cutter' tube and PVC sampling tube; b) steel 'cutter' core rotated on ground surface; and c) PVC sampling tube 'recovering' soil column.
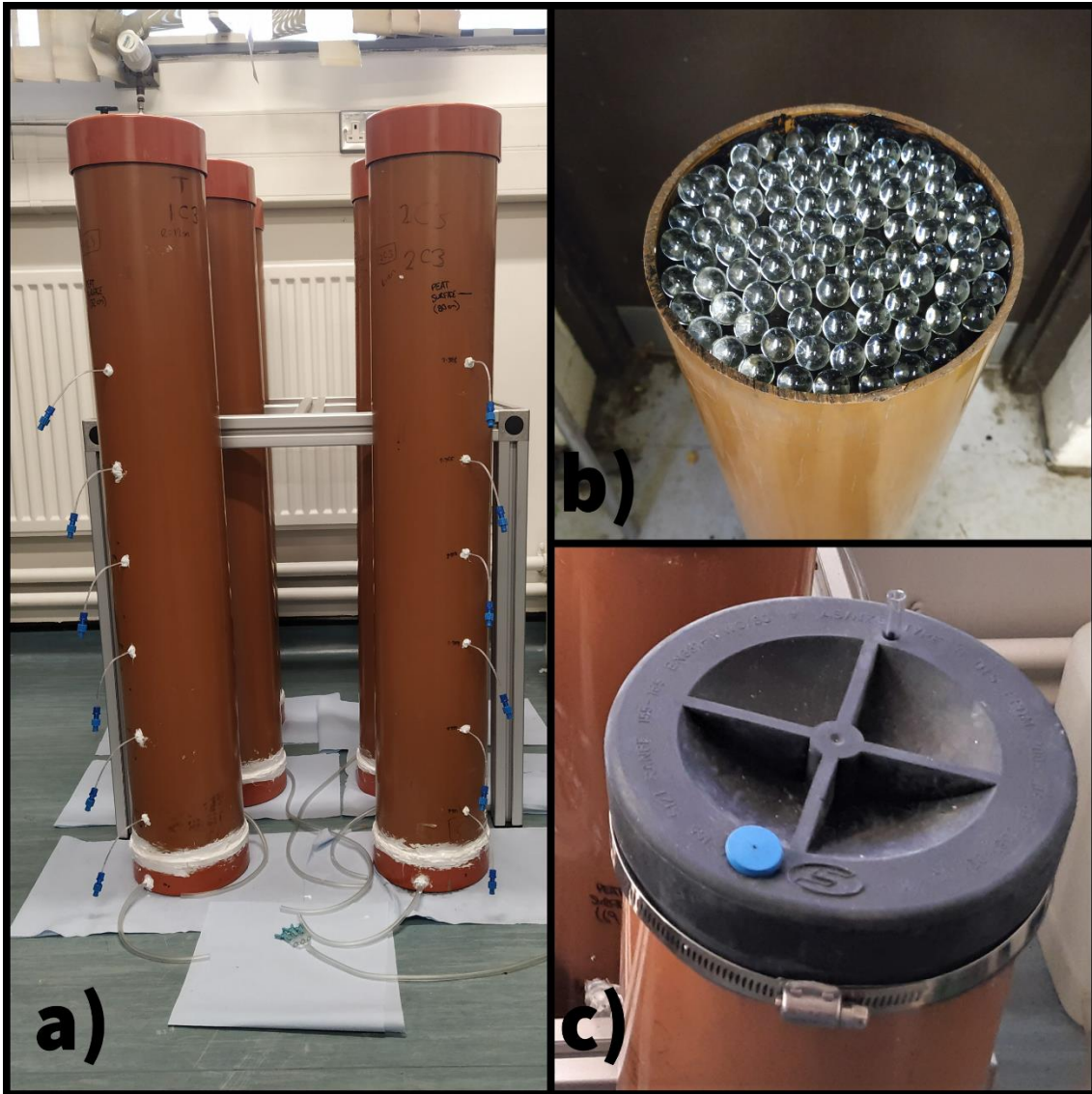
Figure S2: Photos of a) intact soil column experimental design; b) acid-washed glass beads in the column bottom; and c) rubber-vented static chamber for gas sampling.

Table S1: Principal component loadings and explained variance for the four components with eigenvalues ≥ 1.

Parameter	PC1	PC2	PC3	PC4
NH_3-N	-0.22	-0.07	0.51	-0.58
NO_3-N	-0.22	0.44	-0.35	-0.16
Ca	-0.33	-0.41	-0.19	0.30
K	0.33	0.16	0.19	0.50
Mg	-0.41	-0.29	-0.05	0.30
Na	-0.46	0.11	0.12	0.14
Al	-0.33	-0.24	0.19	-0.15
Fe	0.21	-0.31	0.54	0.23
DOC	-0.39	0.31	0.12	0.29
N2O	-0.14	0.50	0.47	0.17
Explained Variance	4.4	1.9	1.6	1.0
Explained Variance (%)	43.7	19.4	15.9	9.7
Cumulative % of the variance	43.7	63.1	79.1	88.8

References

Aber, J. D., 1992. Nitrogen cycling and nitrogen saturation in temperate forest ecosystems. *Trends in Ecology & Evolution ,* 7(7), pp. 220-224 doi: https://doi.org/10.1016/0169-5347(92)90048-G.

Abesser, C., Shand, P., Gooddy, D. & Peach, D., 2008. *The role of alluvial valley deposits in groundwater–surface water exchange in a Chalk river,* Wallingford, United Kingdom: IAHS.

Acreman, M. et al., 2011. Chapter 9: Freshwaters – Openwaters, Wetlands and Floodplains. In: E. Maltby & S. Ormerod, eds. *UK National Ecosystem Assessment: Technical Report .* United Kingdom: UK National Ecosystem Assessment, pp. 296-360.

Adamson, J. K., Scott, W. A., Rowland, A. P. & Beard, G. R., 2001. Ionic concentrations in a blanket peat bog in northern England and correlations with deposition and climate variables. *European Journal of Soil Science ,* 52(1), pp. 69-79 doi: https://doi.org/10.1046/j.1365-2389.2001.t01-1-00350.x.

Ahn, C. & Mitsch, W. J., 2002. Scaling considerations of mesocosm wetlands in simulating large created freshwater marshes. *Ecological Engineering ,* 18(3), pp. 327-342.

Alexander, A. C., Luiker, E., Finley, M. & Culp, J. M., 2016. Chapter 8 - Mesocosm and Field Toxicity Testing in the Marine Context. In: J. Blasco, P. M. Chapman, O. Campana & M. Hampel, eds. *Marine Ecotoxicology: Current Knowledge and Future Issues.* Cambridge, Massachusetts, United States: Academic Press, pp. 239-256.

Allen Associates, 1992. *The three counties wetland monitoring scheme,* s.l.: Allen Associates. Report for HWT..

Allen, D. J. et al., 2010. Interaction between groundwater, the hyporheic zone and a Chalk stream: a case study from the River Lambourn, UK. *Hydrogeology Journal ,* Volume 18, p. 1125–1141.

Almasri, M. N. & Kaluarachchi, J. J., 2007. Modeling nitrate contamination of groundwater in agricultural watersheds. *Journal of Hydrology ,* 343(3-4), pp. 211-229.

Almendinger, J. E. & Leete, J. H., 1998. Peat characteristics and groundwater geochemistry of calcareous fens in the Minnesota River Basin, U.S.A.. *Biogeochemistry ,* Volume volume 43, pp. 17-41 https://doi.org/10.1023/A:1005905431071.

Amano, H., Nakagawa, K. & Berndtsson, R., 2018. Surface water chemistry and nitrate pollution in Shimabara, Nagasaki, Japan. *Environmental Earth Sciences,* Volume 77, pp. Article number: 354 doi: https://doi.org/10.1007/s12665-018-7529-9.

Ambus, P. & Christensen, S., 1993. Denitrification variability and control in a riparian fen irrigated with agricultural drainage water. *Soil Biology and Biochemistry,* 25(7), pp. 915-923 doi: https://doi.org/10.1016/0038-0717(93)90094-R.

Amer, F., Bouldin, D. R., Black, C. A. & Duke, F. R., 1955. Characterization of soil phosphorus by anion exchange resin adsorption and 32P equilibration.. *Plant Soil,* Volume 6, p. 391–408.

Amha, Y. & Bohne, H., 2011. Denitrification from the horticultural peats: effects of pH, nitrogen, carbon, and moisture contents. *Biology and Fertility of Soils,* Volume 47, pp. 293-302 doi: https://doi.org/10.1007/s00374-010-0536-y.

Amon, J. P., Thompson, C. A., Carpenter, Q. J. & Miner, J., 2002. Temperate zone fens of the glaciated Midwestern USA. *Wetlands ,* Volume 22, pp. 301–317 doi: https://doi.org/10.1672/0277-5212(2002)022[0301:TZFOTG]2.0.CO;2.

Ander, L. et al., 2004. *Baseline Series Report 13: The Great Ouse Chalk aquifer, East Anglia,* s.l.: British Geological Survey Commissioned Report CR/04/236 N & Environment Agency Report NC/99/74/13.

Ander, L., Shand, P. & Wood, S., 2006. *Baseline Series Report 21: The Chalk and Crag of North Norfolk and the Waveney Catchment,* s.l.: British Geological Survey Commissioned Report CR/05/043N & Environment Agency Report NC/99/74/21.

Anderson, M. P., 2005. Heat as a Ground Water Tracer. *Groundwater,* 43(6), pp. 951-968 doi: https://doi.org/10.1111/j.1745-6584.2005.00052.x.

Anthony, T. L. & Silver, W. L., 2021. Hot moments drive extreme nitrous oxide and methane emissions from agricultural peatlands. *Global Change Biology,* 27(20), pp. 5141-5153 doi: https://doi.org/10.1111/gcb.15802.

Ardón, M., Morse, J. L., Doyle, M. W. & Bernhardt, E. S., 2010. The Water Quality Consequences of Restoring Wetland Hydrology to a Large Agricultural Watershed in the Southeastern Coastal Plain. *Ecosystems,* Volume 13, p. 1060–1078.

Argo, W. R. et al., 1997. Evaluating Rhizon Soil Solution Samplers as a Method for Extracting Nutrient Solution and Analyzing Media for Container-grown Crops. *HortTechnology,* 7(4), p. 404–408.

Audet, J. et al., 2014. Nitrous oxide fluxes in undisturbed riparian wetlands located in agricultural catchments: Emission, uptake and controlling factors. *Soil Biology and Biochemistry,* Volume 68, pp. 291-299 doi: https://doi.org/10.1016/j.soilbio.2013.10.011.

Babiker, I. S. et al., 2004. Assessment of groundwater contamination by nitrate leaching from intensive vegetable cultivation using geographical information system. *Environmental International,* 29(8), pp. 1009-1017.

Bachand, P. A. M. & Horne, A. J., 1999. Denitrification in constructed free-water surface wetlands: II. Effects of vegetation and temperature. *Ecological Engineering,* 14(1-2), pp. 17-32.

Bain, C. G. et al., 2019. *IUCN UK Commission of Inquiry on Peatlands,* Edinburgh: IUCN UK Peatland Programme.

Baldwin, D. S. & Mitchell, A., 2012. Impact of sulfate pollution on anaerobic biogeochemical cycles in a wetland sediment. *Water Research,* 46(4), pp. 965-974.

Bart, D., Booth, E., II, S. P. L. & Bernthal, T., 2020. Impacts of groundwater extraction on calcareous fen floristic quality. *Journal of Environmental Quality ,* 49(3), pp. 723-734.

Bedford, B. L. & Godwin, K. S., 2003. Fens of the United States: Distribution, characteristics, and scientific connection versus legal isolation. *Wetlands ,* Volume 23 , pp. 608–629 doi: https://doi.org/10.1672/0277-5212(2003)023[0608:FOTUSD]2.0.CO;2.

Beltman, B., Broek, T. V. D., Bloemen, S. & Witsel, C., 1996. Effects of restoration measures on nutrient availability in a formerly nutrient-poor floating fen after acidification and eutrophication. *Biological Conservation ,* 78(3), pp. 271-277.

Berry, J. K., 1996. *Spatial Reasoning for Effective GIS.* Hoeboken, New Jersey: John Wiley & Sons.

Bhattacharyya, A., Schmidt, M. P., Stavitski, E. & Martínez, C. E., 2018. Iron speciation in peats: Chemical and spectroscopic evidence for the co-occurrence of ferric and ferrous iron in organic complexes and mineral precipitates. *Organic Geochemistry,* Volume 115, pp. 124-137 doi: https://doi.org/10.1016/j.orggeochem.2017.10.012.

Biddau, R. et al., 2019. Source and fate of nitrate in contaminated groundwater systems: Assessing spatial and temporal variations by hydrogeochemistry and multiple stable isotope tools. *Science of the Total Environment,* Volume 647, pp. 1121-1136.

Binner, I., Dultz, S., Schellhorn, M. & Schenk, M. K., 2017. Potassium adsorption and release properties of clays in peat-based horticultural substrates for increasing the cultivation safety of plants. *Applied Clay Science,* Volume 145, pp. 28-36 doi: https://doi.org/10.1016/j.clay.2017.05.013.

Birgander, J., Olsson, P. A. & Rousk, J., 2018. The responses of microbial temperature relationships to seasonal change and winter warming in a temperate grassland. *Global Change Biology,* 24(8), pp. 3357-3367 doi: https://doi.org/10.1111/gcb.14060.

Blodau, C. & Moore, C. L. R. T. R., 2002. Iron, sulfur, and dissolved carbon dynamics in a northern peatland. *Fundamental and Applied Limnology ,* 154(4), pp. 561-583 doi: 10.1127/archiv-hydrobiol/154/2002/561 .

Boelter, D., 1968. *Important physical properties of peat materials.* Quebec, Department of Engery, Minds and Resources and National Research Council of Canada: Proceedings of the 3rd International Peat Congress, 150-154 .

Boomer, K. M. B. & Bedford, B. L., 2008. Influence of nested groundwater systems on reduction–oxidation and alkalinity gradients with implications for plant nutrient availability in four New York fens. *Journal of Hydrology,* 351(1-2), pp. 107-125 doi: https://doi.org/10.1016/j.jhydrol.2007.12.003.

Böttcher, J., Strebel, O., Voerkelius, S. & Schmidt, H. L., 1990. Using isotope fractionation of nitrate-nitrogen and nitrate-oxygen for evaluation of microbial denitrification in a sandy aquifer. *Journal of Hydrology,* 114(3-4), pp. 413-424 doi: https://doi.org/10.1016/0022-1694(90)90068-9.

Bouskill, N. J. et al., 2019. Evidence for Microbial Mediated NO3– Cycling Within Floodplain Sediments During Groundwater Fluctuations. *Frontiers in Earth Science,* p. https://doi.org/10.3389/feart.2019.00189.

Bridgham, S. D., Updegraff, K. & Pastor, J., 1998. Carbon, Nitrogen, and Phosphorus Mineralization in Northern Wetlands. *Ecology ,* 79(5), pp. 1545-1561.

British Geological Survey, 1999. *Denitrification in the unsaturated zones of the British, Technical Report WD/99/2,* Keyworth: British Geological Survey.

Buckingham, S., Tipping, E. & Hamilton-Taylor, J., 2008. Dissolved organic carbon in soil solutions: a comparison of collection methods. *Soil Use and Management ,* 24(1), pp. 29-36.

Bu, J., Liu, W., Pan, Z. & Ling, K., 2020. Comparative Study of Hydrochemical Classification Based on Different Hierarchical Cluster Analysis Methods. *Internation Journal of Environmental Research & Public Health ,* 17(24), p. 9515 doi: https://doi.org/10.3390/ijerph17249515.

Burford, J. R. & Bremner, J. M., 1975. Relationships between the denitrification capacities of soils and total, water-soluble and readily decomposable soil organic matter. *Soil Biology and Biochemistry,* 7(6), pp. 389-394 doi: https://doi.org/10.1016/0038-0717(75)90055-3.

Burgin, A. J. & Hamilton, S. K., 2007. Have we overemphasized the role of denitrification in aquatic ecosystems? A review of nitrate removal pathways. *Frontiers in Ecology and the Environment ,* 5(2), pp. 89-96 doi: https://doi.org/10.1890/1540-9295(2007)5[89:HWOTRO]2.0.CO;2.

Buttler, A., Grosvernier, P. & Matthey, Y., 1998. A new sampler for extracting undisturbed surface peat cores for growth pot experiments. *New Phytologist,* 140(2), pp. 355-360.

Cabezas, A. et al., 2012. Effects of degree of peat decomposition, loading rate and temperature on dissolved nitrogen turnover in rewetted fens. *Soil Biology and Biochemistry,* Volume 48, pp. 182-191 doi: https://doi.org/10.1016/j.soilbio.2012.01.027.

Calver, T., Yarmuch, M., Conway, A. J. & Stewart, K., 2019. Strong legacy effect of peat composition on physicochemical properties of reclamation coversoil. *Canadian Journal of Soil Science ,* 99(3), pp. 244-253 https://doi.org/10.1139/cjss-2018-0160.

Cao, X. et al., 2016. Sources, Spatial Distribution, and Seasonal Variation of Major Ions in the Caohai Wetland Catchment, Southwest China. *Wetlands ,* Volume 36, pp. 1069–1085 doi: https://doi.org/10.1007/s13157-016-0822-z.

Caron, J., Létourneau, G. & Fortin, J., 2015. Electrical Conductivity Breakthrough Experiment and Immobile Water Estimation in Organic Substrates: Is R = 1 a Realistic Assumption?. *Vadose Zone Journal ,* 14(9), pp. 1-8.

Cey, E. E., Rudolph, D. L., Aravena, R. & Parkin, G., 1999. Role of the riparian zone in controlling the distribution and fate of agricultural nitrogen near a small stream in southern Ontario. *Journal of Contaminant Hydrology,* 37(1-2), pp. 45-67 doi: https://doi.org/10.1016/S0169-7722(98)00162-4.

Chapman, P. J., Reynolds, B. & Wheater, H. S., 1997. Sources and controls of calcium and magnesium in storm runoff: the role of groundwater and ion exchange reactions along water flowpaths. *Hydrology and Earth System Sciences ,* 1(3), pp. 671–685 doi: https://doi.org/10.5194/hess-1-671-1997.

Charman, D., 2003. Peatlands and environmental change. *Journal of Quaternary Science,* 18(5), pp. 466-466.

Chatfield, C., 1980. *Introduction to Multivariate Analysis.* New York : Routledge.

Chen, C., Hall, S. J., Coward, E. & Thompson, A., 2020. Iron-mediated organic matter decomposition in humid soils can counteract protection. *Nature Communnications ,* Volume 11, pp. 2255 doi: https://doi.org/10.1038/s41467-020-16071-5.

Chen, H. et al., 2012. Spatiotemporal Variations in Nitrous Oxide Emissions from an Open Fen on the Qinghai–Tibetan Plateau: a 3-Year Study. *Water, Air & Soil Pollution ,* Volume 223, pp. 6025–6034 doi: https://doi.org/10.1007/s11270-012-1336-9.

Chen, J. S. L. W. & Fisher, H., 2013. Quantum Cascade Laser Spectrometry Techniques: A New Trend in Atmospheric Chemistry. *Applied Spectroscopy Reviews ,* 48(7), pp. 523-559 doi: https://doi.org/10.1080/05704928.2012.757232.

Chen, M., Lee, J.-H. & Hur, J., 2015. Effects of Sampling Methods on the Quantity and Quality of Dissolved Organic Matter in Sediment Pore Waters as Revealed by Absorption and Fluorescence Spectroscopy. *Environmental Science and Pollution Research,* Volume 19, pp. 14841-14851.

Cirmo, C. P. & McDonnell, J. J., 1997. Linking the hydrologic and biogeochemical controls of nitrogen transport in near-stream zones of temperate-forested catchments: a review. *Journal of Hydrology,* 199(1-2), pp. 88-120 doi: https://doi.org/10.1016/S0022-1694(96)03286-6.

Clark, J. M., Chapman, P. J., Heathwaite, A. L. & Adamson, J. K., 2006. Suppression of Dissolved Organic Carbon by Sulfate Induced Acidification during Simulated Droughts. *Environmental Science & Technology,* 40(6), p. 1776–1783 doi: https://doi.org/10.1016/j.geoderma.2005.06.003.

Clements, W. H., Cherry, D. S. & Jr., J. C., 1988. Impact of Heavy Metals on Insect Communities in Streams: A Comparison of Observational and Experimental Results. *Canadian Journal of Fisheries and Aquatic Sciences,* 45(11), pp. 2017-2025.

Cloutier, V., Lefebvre, R., Therrien, R. & Savard, M. M., 2008. Multivariate statistical analysis of geochemical data as indicative of the hydrogeochemical evolution of groundwater in a sedimentary rock aquifer system. *Journal of Hydrology,* 353(3-4), pp. 294-313 doi: https://doi.org/10.1016/j.jhydrol.2008.02.015.

Cole, C. A. & Brooks, R. P., 2000. Patterns of wetland hydrology in the Ridge and Valley province, Pennsylvania, USA. *Wetlands ,* Volume 20, pp. 438–447 doi: https://doi.org/10.1672/0277-5212(2000)020<0438:POWHIT>2.0.CO;2.

Conant, B., 2004. Delineating and Quantifying Ground Water Discharge Zones Using Streambed Temperatures. *Groundwater ,* 42(2), pp. 243-257 doi: https://doi.org/10.1111/j.1745-6584.2004.tb02671.x.

Cooper, R. J., Wexler, S. K., Adams, C. A. & Hiscock, K. M., 2017. Hydrogeological Controls on Regional-Scale Indirect Nitrous Oxide Emission Factors for Rivers. *Environmental Science & Technology ,* 51 (18), p. 10440–10448 doi: https://doi.org/10.1021/acs.est.7b02135.

Correll, D. L., 1996. *Buffer zones: Their processes and potential in water protection - Buffer zones: Their processes and potential in water protection.* Harpenden , Quest Environmental .

Cuddington, K. et al., 2013. Process-based models are required to manage ecological systems in a changing world. *Ecosphere ,* 4(2), pp. 1-12 doi: https://doi.org/10.1890/ES12-00178.1.

Curtinrich, H. J., Sebestyen, S. D., Griffiths, N. A. & Hall, S. J., 2022. Warming Stimulates Iron-Mediated Carbon and Nutrient Cycling in Mineral-Poor Peatlands. *Ecosystems ,* Volume 25, pp. 44–60 doi: https://doi.org/10.1007/s10021-021-00639-3.

Cusell, C., Lamers, L. P. M., Wirdum, G. v. & Kooijman, A., 2013. Impacts of water level fluctuation on mesotrophic rich fens: acidification vs. eutrophication. *Journal of Applied Ecology ,* 50(4), pp. 998-1009.

Daims, H. et al., 2015. Complete nitrification by Nitrospira bacteria. *Nature ,* Volume 528, pp. 504-509.

D'Angelo, E. & Reddy, K., 1993. Ammonium oxidation and nitrate reduction in sediments of a hypereutrophic lake. *Soil Science Society of America Journal ,* Volume 57, pp. 1156-1163.

Davidson, E. et al., 2000. Testing a conceptual model of soil emissions of nitrous and nitric oxides. *Bioscience,* 50(8), pp. 667-680 doi: https://doi.org/10.1641/0006-3568(2000)050[0667:TACMOS]2.0.CO;2.

Davies, G., 2012. *Greywell Fen – WFD Groundwater Quality Study. Unpublished,* Bristol: Environment Agency .

De Mars, H., Wassen, M. J. & Peeters, W. H. M., 1996. The effect of drainage and management on peat chemistry and nutrient deficiency in the former Jegrznia-floodplain (NE-Poland). *Vegetatio,* Volume 126, p. 59–72 doi: https://doi.org/10.1007/BF00047762.

Dijk, J. v. et al., 2004. Restoring natural seepage conditions on former agricultural grasslands does not lead to reduction of organic matter decomposition and soil nutrient dynamics. *Biogeochemistry ,* Volume 71, p. 317–337.

Dowrick, D. J., Freeman, C., Lock, M. A. & Reynolds, B., 2006. Sulphate reduction and the suppression of peatland methane emissions following summer drought. *Geoderma,* 132(3-4), pp. 384-390 doi: https://doi.org/10.1016/j.geoderma.2005.06.003.

Dowrick, D. J. et al., 1999. Nitrous oxide emissions from a gully mire in mid-Wales, UK, under simulated summer drought. *Biogeochemistry ,* Volume 44, p. 151–162 doi: https://doi.org/10.1023/A:1006031731037.

Drewer, J. et al., 2010. Comparison of greenhouse gas fluxes and nitrogen budgets from an ombotrophic bog in Scotland and a minerotrophic sedge fen in Finland. *European Journal of Soil Science,* 61(5), pp. 640-650 doi: https://doi.org/10.1111/j.1365-2389.2010.01267.x.

Duren, I. V. & Pegtel, D., 2000. Nutrient limitations in wet, drained and rewetted fen meadows: evaluation of methods and results. *Plant and Soil,* Volume 220, p. 35–47 doi: https://doi.org/10.1023/A:1004735618905.

Duval, T. P. & Waddington, J. M., 2018. Effect of hydrogeomorphic setting on calcareous fen hydrology. *Hydrological Processes ,* 32(11), pp. 1695-1708 doi: https://doi.org/10.1002/hyp.11625.

Edmunds, W. M. et al., 1987. Baseline geochemical conditions in the Chalk aquifer, Berkshire, U.K.: a basis for groundwater quality management. *Applied Geochemistry,* 2(3), pp. 251-274 doi: https://doi.org/10.1016/0883-2927(87)90042-4.

Edmunds, W. M., Shand, P., Hart, P. & Ward, R. S., 2003. The natural (baseline) quality of groundwater: a UK pilot study. *Science of the Total Environment ,* 310(1-3), pp. 25-35 doi: https://doi.org/10.1016/S0048-9697(02)00620-4.

Edwards, G. C. et al., 2003. A diode laser based gas monitor suitable for measurement of trace gas exchange using micrometeorological techniques. *Agricultural and Forest Meteorology,* 115(1-2), pp. 71-89 doi: https://doi.org/10.1016/S0168-1923(02)00166-1.

Facchi, A., Gandolfi, C. & Whelan, M. J., 2007. A comparison of river water quality sampling methodologies under highly variable load conditions. *Chemosphere,* 66(4), pp. 746-756 doi: https://doi.org/10.1016/j.chemosphere.2006.07.050.

Fairchild, I. J., Bradby, L., Sharp, M. & Tison, J.-L., 1994. Hydrochemistry of carbonate terrains in alpine glacial settings. *Earth Surface Processes and Landforms,* 19(1), pp. 33-54 doi: https://doi.org/10.1002/esp.3290190104.

Falcon-Suarez, I., Rammlmair, D., Juncosa-Rivera, R. & Delgado-Martin, J., 2014. Application of Rhizon SMS for the assessment of the hydrodynamic properties of unconsolidated fine grained materials. *Engineering Geology,* Volume 172, pp. 69-76.

Farrant, A. R., 2012. *Geology of the Greywell area, Basingstoke, Hampshire,* Nottingham, UK: British Geological Survey (Unpublished.

Feast, N. A., Hiscock, K. M., Dennis, P. F. & Bottrell, S. H., 1997. Controls on stable isotope profiles in the Chalk aquifer of north-east Norfolk, UK, with special reference to dissolved sulphate. *Applied Geochemistry,* 12(6), pp. 803-812.

Fenech, C. et al., 2012. The potential for a suite of isotope and chemical markers to differentiate sources of nitrate contamination: A review. *Water Research,* 46(7), pp. 2023-2041.

Fisher, J. & Acreman, M. C., 2004. Wetland nutrient removal: a review of the evidence. *Hydrology and Earth Science Systems ,* Volume 8, pp. 673–685 https://doi.org/10.5194/hess-8-673-2004, 2004..

Fisher, M. & Reddy, K., 2013. Soil Pore Water Sampling Methods . In: R. DeLaune, K. Reddy, C. Richardson & J. Megonigal, eds. *Methods in Biogeochemistry of Wetlands, Volume 10.* Maidson, Wisconsin : Soil Science Society of America Book Series , pp. 55-70.

Flechard, C. R. et al., 2007. Effects of climate and management intensity on nitrous oxide emissions in grassland systems across Europe. *Agriculture, Ecosystems & Environment,* 121(1-2), pp. 135-152 doi: https://doi.org/10.1016/j.agee.2006.12.024.

Fojt, W. J., 1994. Dehydration and the threat to East Anglian fens, England. *Biological Conservation,* 69(2), pp. 163-175 doi: https://doi.org/10.1016/0006-3207(94)90056-6.

Forster, S. S. D., Cripps, A. C. & Smith-Carington, A., 1982. Nitrate leaching to groundwater. *Philosophical Transactions of the Royal Society B,* 296(1082), p. 477–489.

Foster, S. S. D. & Bath, A. H., 1983. The distribution of agricultural soil leachates in the unsaturated zone of the British Chalk. *Environmental Geology ,* Volume 5, pp. 53-59..

Freeman, C., Ostle, N. & Kang, H., 2001. An enzymic 'latch' on a global carbon store. *Nature ,* Volume 409, p. 149 doi: https://doi.org/10.1038/35051650.

Füssel, H.-M., Jol, A., Marx, A. & Hilden, M., 2017. *Climate change, impacts and vulnerability in Europe 2016,* Copenhagen: European Environment Agency doi: 10.2800/534806.

Galloway, J. N. et al., 2003. The Nitrogen Cascade. *BioScience,* 53(4), pp. 341–356 doi: https://doi.org/10.1641/0006-3568(2003)053[0341:TNC]2.0.CO;2.

Gan, Y. et al., 2018. Groundwater flow and hydrogeochemical evolution in the Jianghan Plain, central China. *Hydrogeology Journal,* Volume 26, pp. 1609–1623 doi: https://doi.org/10.1007/s10040-018-1778-2.

Gao, F. et al., 2012. A new collector for in situ pore water sampling in wetland sediment. *Environmental Technology ,* 33(3), pp. 257-264.

Giddings, J. M. & Eddlemon, G. K., 1979. Some ecological and experimental properties of complex aquatic microcosms. *International Journal of Environmental Studies,* 13(2), pp. 119-123, DOI: 10.1080/00207237908709812.

Gilliam, J. W., 1994. Riparian Wetlands and Water Quality. *Journal of Environmental Quality,* 23(5), pp. 896-900 doi: https://doi.org/10.2134/jeq1994.00472425002300050007x.

Glatzel, S. et al., 2008. Small scale controls of greenhouse gas release under elevated N deposition rates in a restoring peat bog in NW Germany. *Biogeosciences,* Volume 5, pp. 925-935 doi: https://doi.org/10.5194/bg-5-925-2008.

Gooddy, D. C. et al., 2007. The significance of colloids in the transport of pesticides through Chalk. *Science of the Total Environment ,* 385(1-3), pp. 262-271.

Goodroad, L. L. & Keeney, D. R., 1984. Nitrous Oxide Emission from Forest, Marsh, and Prairie Ecosystems. *Journal of Environmental Quality ,* 13(3), pp. 448-452 doi: https://doi.org/10.2134/jeq1984.00472425001300030024x.

Gordon, A. S., Cooper, W. J. & Scheidt, D. J., 1986. Denitrification in marl and peat sediments in the Florida everglades. *Applied and Environmental Microbiology,* 52(5), pp. 987-91 doi: 10.1128/aem.52.5.987-991.

Granli, T. & Boeckman, O., 1994. Nitrous Oxide from Agriculture. *Norwegian Journal of Agricultural Sciences,* Volume 12, pp. 1-128 .

Griffiths, N. A., Sebestyen, S. D. & Oleheiser, K. C., 2019. Variation in peatland porewater chemistry over time and space along a bog to fen gradient. *Science of The Total Environment,* Volume 697, p. 134152 doi: https://doi.org/10.1016/j.scitotenv.2019.134152.

Grizzetti, B., Bouraoui, F. & Aloe, A., 2012. Changes of nitrogen and phosphorus loads to European seas. *Global Change Biology ,* 18(2), pp. 769-782 doi: https://doi.org/10.1111/j.1365-2486.2011.02576.x.

Groffman, P. M., Gold, A. J. & Jacinthe, P.-A., 1998. Nitrous oxide production in riparian zones and groundwater. *Nutrient Cycling in Agroecosystems ,* 52(2-3), pp. 179-186 doi: 10.1023/a:1009719923861.

Güler, C., Thyne, G. D., McCray, J. E. & Turner, K. A., 2002. Evaluation of graphical and multivariate statistical methods for classification of water chemistry data. *Hydrogeology Journal,* Volume 10, pp. 455–474 doi: https://doi.org/10.1007/s10040-002-0196-6.

Gutknecht, J. L. M., Goodman, R. M. & Balser, T. C., 2006. Linking soil process and microbial ecology in freshwater wetland ecosystems. *Plant and Soil,* Volume 289, pp. 17–34 https://doi.org/10.1007/s11104-006-9105-4.

Hagemann, N., Harter, J. & Behrens, S., 2016. Chapter 7: Elucidating the Impacts of Biochar Applications on Nitrogen Cycling Microbial Communities. In: T. K. Ralebitso & C. H. Orr, eds. *Biochar Application: Essential Soil Microbial Ecology.* Amsterdam, The Netherlands: Elsevier, pp. 163-198.

Hall, S. J. et al., 2016. Drivers and patterns of iron redox cycling from surface to bedrock in a deep tropical forest soil: a new conceptual model. *Biogeochemistry,* Volume 130, pp. 177–190 doi: https://doi.org/10.1007/s10533-016-0251-3.

Han, G. & Liu, C.-Q., 2004. Water geochemistry controlled by carbonate dissolution: a study of the river waters draining karst-dominated terrain, Guizhou Province, China. *Chemical Geology ,* 204(1-2), pp. 1-21 doi: https://doi.org/10.1016/j.chemgeo.2003.09.009.

Han, J. Y., Kim, D.-H., Oh, S. & Moon, H. S., 2020. Effects of water level and vegetation on nitrate dynamics at varying sediment depths in laboratory-scale wetland mesocosms. *Science of the Total Environment,* Volume 703, p. 134741 doi: https://doi.org/10.1016/j.scitotenv.2019.134741.

Hansen, B. et al., 2017. Groundwater nitrate response to sustainable nitrogen management. *Scientific Reports ,* Volume 7, p. Article number: 8566.

Hanson, G. C., Groffman, P. M. & Gold, A. J., 1994. Denitrification in Riparian Wetlands Receiving High and Low Groundwater Nitrate Inputs. *Journal of Environmental Quality ,* 23(5), pp. 917-922.

Hanson, G. C., Groffman, P. M. & Gold, A. J., 1994. Symptoms of nitrogen saturation in a riparian wetland. *Ecological Applications,* Volume 4, pp. 750-756.

Haria, A. H., Hodnett, M. G. & Johnson, A. C., 2003. Mechanisms of groundwater recharge and pesticide penetrationto a chalk aquifer in southern England. *Journal of Hydrology ,* Volume 275, p. 122–137.

Harris, E. et al., 2021. Denitrifying pathways dominate nitrous oxide emissions from managed grassland during drought and rewetting. *Science Advances ,* 7(6), p. doi: 10.1126/sciadv.abb7118.

Hartsock, J. A. & Bremer, E., 2018. Nutrient supply rates in a boreal extreme-rich fen using ion exchange membranes. *Ecohydrology ,* 11(7), p. https://doi.org/10.1002/eco.1995.

Haycock, N. & Pinay, G., 1993. Groundwater Nitrate Dynamics in Grass and Poplar Vegetated Riparian Buffer Strips during the Winter. *Journal of Environmental Quality,* 22(2), pp. 273-278 doi: https://doi.org/10.2134/jeq1993.00472425002200020007x.

Haycock, N., Pinay, G. & Walker, C., 1993. Nitrogen retention in river corridors: European perspective. *Ambio,* 22(6), pp. 340-346 doi: .

Hefting, M. et al., 2006. Water quality dynamics and hydrology in nitrate loaded riparian zones in the Netherlands. *Environmental Pollution,* 139(1), pp. 143-156 doi: https://doi.org/10.1016/j.envpol.2005.04.023.

Hefting, M. et al., 2004. Water table elevation controls on soil nitrogen cycling in riparian wetlands along a European climatic gradient. *Biogeochemistry ,* Volume 67, p. 113–134 doi: https://doi.org/10.1023/B:BIOG.0000015320.69868.33.

Hefting, M. M., Bobbink, R. & Caluwe, H. d., 2003. Nitrous Oxide Emission and Denitrification in Chronically Nitrate-Loaded Riparian Buffer Zones. *Journal of Environmental Quality,* 32(4), pp. 1194-1203 doi: https://doi.org/10.2134/jeq2003.1194.

Helena, B. et al., 2000. Temporal evolution of groundwater composition in an alluvial aquifer (Pisuerga River, Spain) by principal component analysis. *Water Research ,* 34(3), pp. 807-816 doi: https://doi.org/10.1016/S0043-1354(99)00225-0.

Henault, C. et al., 2012. Nitrous Oxide Emission by Agricultural Soils: A Review of Spatial and Temporal Variability for Mitigation. *Pedosphere,* 22(4), pp. 426-433 doi: https://doi.org/10.1016/S1002-0160(12)60029-0.

Hensen, A., Skiba, U. & Famulari, D., 2013. Low cost and state of the art methods to measure nitrous oxide emissions. *Environmental Research Letters ,* 8(2), pp. 025022 doi: 10.1088/1748-9326/8/2/025022.

He, W., Choi, I., Lee, J.-J. & Hur, J., 2016. Coupling effects of abiotic and biotic factors on molecular composition of dissolved organic matter in a freshwater wetland. *Science of the Total Environment ,* Volume 544, pp. 525-534 doi: https://doi.org/10.1016/j.scitotenv.2015.12.008.

Hill, A. R., 2019. Groundwater nitrate removal in riparian buffer zones: a review of research progress in the past 20 years. *Biogeochemistry,* Volume 143, pp. 347–369 doi: https://doi.org/10.1007/s10533-019-00566-5.

Hill, A. R. & Devito, K. J., 1997. Hydrological-Chemical Interactions in Headwater Forest Wetlands. In: C. C. Trettin, ed. *Northern Forested Wetlands Ecology and Management.* Milton Park, United Kingdom: Routledge, pp. 213-230 doi: https://doi.org/10.1201/9780203745380.

Hoag, R. S. & Price, J. S., 1997. The effects of matrix diffusion on solute transport and retardation in undisturbed peat in laboratory columns. *Journal of Containment Hydrology ,* 28(3), pp. 193-205.

Hoewyk, D. V. et al., 2000. Soil Nitrogen Dynamics in Organic and Mineral Soil Calcareous Wetlands in Eastern New York. *Soil Science Society of America Journal,* 64(6), pp. 2168-2173 doi: https://doi.org/10.2136/sssaj2000.6462168x.

Hoffmann, C. C. et al., 2006. Groundwater flow and transport of nutrients through a riparian meadow – Field data and modelling. *Journal of Hydrology,* 331(1-2), pp. 315-335 doi: https://doi.org/10.1016/j.jhydrol.2006.05.019.

Hoffmann, C. C., Kronvang, B. & Audet, J., 2011. Evaluation of nutrient retention in four restored Danish riparian wetlands. *Hydrobiologia,* Volume 674, pp. 5–24 doi: https://doi.org/10.1007/s10750-011-0734-0.

Holden, J., 2005. Peatland hydrology and carbon release: why small-scale process matters. *Philosophical Transactions of the Royal Society A ,* 363(1837), p. 2891–2913 doi: https://doi.org/10.1098/rsta.2005.1671.

Holland, S. M., 2008. *Holland, Steven M. "Principal components analysis (PCA),* Athens, GA: Department of Geology, University of Georgia 30602-2501.

Hou, L. et al., 2015. Anaerobic ammonium oxidation and its contribution to nitrogen removal in China's coastal wetlands. *Scientific Reports,* Volume 5, p. Article number: 15621 (2015).

House, A. R. et al., 2015. Discrete wetland groundwater discharges revealed with a three-dimensional temperature model and botanical indicators (Boxford, UK). *Hydrogeology Journal,* Volume 23, pp. 775–787 doi: https://doi.org/10.1007/s10040-015-1242-5.

Howarth, R. W. et al., 1996. Regional nitrogen budgets and riverine N & P fluxes for the drainages to the North Atlantic Ocean: Natural and human influences. *Biogeochemistry,* Volume 35 , pp. 75-139 doi: 10.1007/978-94-009-1776-7_3.

Howarth, R. W. & Marino, R., 2006. Nitrogen as the limiting nutrient for eutrophication in coastal marine ecosystems: Evolving views over three decades. *Limonology and Oceanography ,* 51(1 Part 2), pp. 364-376 https://doi.org/10.4319/lo.2006.51.1_part_2.0364.

Howden, N. J. K. & Burt, T. P., 2008. Temporal and spatial analysis of nitrate concentrations from the Frome and Piddle catchments in Dorset (UK) for water years 1978 to 2007: Evidence for nitrate breakthrough?. *Science of the Total Environment ,* 407(1), pp. 507-526.

Howden, N. J. K., Neal, C., Wheater, H. S. & Kirk, S., 2010. Water quality of lowland, permeable Chalk rivers: the Frome and Piddle catchments, west Dorset, UK. *Hydrology Research,* 41(2), p. 75–91.

Huang, H. et al., 2018. Sources Identification of Nitrogen Using Major Ions and Isotopic Tracers in Shenyang, China. *Geofluids,* Volume 2018, p. Article ID 8683904 https://doi.org/10.1155/2018/8683904.

Huang, J. et al., 2016a. Development and evaluation of a diffusive gradients in a thin film technique for measuring ammonium in freshwaters. *Analytica Chimica Acta,* Volume 094, pp. 83-91.

Huang, J., Bennett, W. W., Welsh, D. T. & Teasdale, P. R., 2016c. Determining time-weighted average concentrations of nitrate and ammonium in freshwaters using DGT with ion exchange membrane-based binding layers. *Environmental Science: Processes & Impacts,* Volume 18, pp. 1530-1539 DOI: 10.1039/C6EM00260A.

Hutchinson, G. L. & Mosier, A. R., 1981. Improved Soil Cover Method for Field Measurement of Nitrous Oxide Fluxes. *Soil Science Society of America Journal ,* 45(2), pp. 311-316 doi: https://doi.org/10.2136/sssaj1981.03615995004500020017x.

Ibánhez, J. S. P. & Rocha, C., 2014. Porewater sampling for NH4+ with Rhizon Soil Moisture Samplers (SMS): potential artifacts induced by NH4+ sorption. *Freshwater Science,* 33(4), pp. 1195-1203.

Inobeme, A. et al., 2022. Chemometric approach in environmental pollution analysis: A critical review. *Journal of Environmental Management,* Volume 309, p. 114653 doi: https://doi.org/10.1016/j.jenvman.2022.114653.

IPCC, 2007. *Climate Change 2007: the Physical Science Basis Contribution of Working Group I to the Fourth Assessment. Report of the Intergovernmental Panel on Climate Change,* Cambridge: Cambridge University Press.

Ireson, A. M. & Butler, A. P., 2011. Controls on preferential recharge to Chalk aquifers. *Journal of Hydrology ,* 398(1-2), pp. 109-123.

IUCN, 2018. *UK Peatland Strategy ,* Cambridge, United Kingdom: IUCN UK Peatland Programme.

Jacintha, T. G. A., Rawat, K. S., Mishra, A. & Singh, S. K., 2017. Hydrogeochemical characterization of groundwater of peninsular Indian region using multivariate statistical techniques. *Applied Water Science,* Volume 7, pp. 3001–3013 doi: https://doi.org/10.1007/s13201-016-0400-9.

Jacobs, 2019. *Greywell Fen SSSI: Interim Condition Analysis Report,* Birmingham, UK : Jacobs U.K. Limited, Unpublished .

Jain, S. & Singh, V., 2003. Chapter 2 - Acquisition and Processing of Water Resources Data. In: S. Jain & V. Singh, eds. *Developments in Water Science .* Amsterdam: Elsevier Science, pp. 47-121.

Jarvie, H. P. et al., 2005. Nutrient hydrochemistry for a groundwater-dominated catchment: The Hampshire Avon, UK. *Science of the Total Environment ,* 344(1-3), pp. 143-158.

Jarvie, H. P. et al., 2020. Biogeochemical and climate drivers of wetland phosphorus and nitrogen release: Implications for nutrient legacies and eutrophication risk. Journal of *Environmental Quality ,* 49(6), pp. 1703-1716.

Jin, Z. et al., 2015. Using dual isotopes to evaluate sources and transformations of nitrate in the West Lake watershed, eastern China. *Journal of Containment Hydrology ,* Volume 117-178, pp. 64-75.

Johnes, P. J. et al., 2020. Determining the Impact of Riparian Wetlands on Nutrient Cycling, Storage and Export in Permeable Agricultural Catchments. *Water,* 12(1), p. 167 doi: https://doi.org/10.3390/w12010167.

Johnston, C. A., Bridgham, S. D. & Schubauer-Berigan, J. P., 1999. Nutrient Dynamics in Relation to Geomorphology of Riverine Wetlands. *Soil Science Society of America Journal,* 65(2), pp. 557-577 doi: https://doi.org/10.2136/sssaj2001.652557x.

Jonge, V. N. d., Elliott, M. & Orive, E., 2002. Causes, historical development, effects and future challenges of a common environmental problem: eutrophication. In: V. N. d. Jonge, M. Elliott & E.

Orive, eds. *Nutrients and Eutrophication in Estuaries and Coastal Waters. Developments in Hydrobiology.* Dordrecht: Springer , pp. 1-19 doi: https://doi.org/10.1007/978-94-017-2464-7_1.

Joosten, H. et al., 2016. Chapter 4 - The role of peatlands in climate regulation. In: T. A. M. E. H. J. R. S. Aletta Bonn, ed. *Part I - Peatland ecosystems services.* Cambridge, United Kingdom : Cambridge University Press, pp. 63-76.

Jørgensen, C. J., Struwe, S. & Elberling, B., 2012. Temporal trends in N2O flux dynamics in a Danish wetland – effects of plant-mediated gas transport of N2O and O2 following changes in water level and soil mineral-N availability. *Global Change Biology,* 18(1), pp. 210-222 doi: https://doi.org/10.1111/j.1365-2486.2011.02485.x.

Judd, A. G., 1980. The Use of Cluster Analysis in the Derivation of Geotechnical Classifications. *Environmental & Engineering Geoscience ,* xvii(4), p. 193–211 doi: https://doi.org/10.2113/gseegeosci.xvii.4.193.

Jungkunst, H. F., Flessa, H., Scherber, C. & Fiedler, S., 2008. Groundwater level controls CO2, N2O and CH4 fluxes of three different hydromorphic soil types of a temperate forest ecosystem. *Soil Biology and Biochemistry ,* 40 (8), pp. 2047-2054 doi: https://doi.org/10.1016/j.soilbio.2008.04.015.

Kaiser, H. F., 1960. The Application of Electronic Computers to Factor Analysis. *Education and psychological measurement,* 20(1), pp. 141-151.

Kalbitz, K., 2001. Properties of organic matter in soil solution in a German fen area as dependent on land use and depth. *Geoderma,* 104(3-4), pp. 203-214 doi: https://doi.org/10.1016/S0016-7061(01)00081-7.

Kenzie, A. B. M., Farmer, J. G. & Sugden, C. L., 1997. Isotopic evidence of the relative retention and mobility of lead and radiocaesium in Scottish ombrotrophic peats. *Science of The Total Environment,* 203(2), pp. 115-127 doi: https://doi.org/10.1016/S0048-9697(97)00139-3.

Klavins, M., Sire, J., Purmalis, O. & Melecis, V., 2008. Approaches to estimating humification indicators for peat. *Mires & Peat,* Volume 3, pp. Article 07 doi: http://www.mires-and-peat.net/, ISSN 1819-754X.

Kleimeier, C., Liu, H., Rezanezhad, F. & Lennartz, B., 2018. Nitrate Attenuation in Degraded Peat Soil-Based Constructed Wetlands. *Water,* 10(4), p. 355 https://doi.org/10.3390/w10040355.

Kleimeier, C., Rezanezhad, F., Cappellen, P. V. & Lennartz, B., 2017. Influence of pore structure on solute transport in degraded and undegraded fen peat soils. *Mires and Peat,* 19(18), pp. 1-9 (Online: http://www.mires-and-peat.net/pages/volumes/map19/map1918.php); 10.19189/MaP.2017.OMB.282.

Klein, C. A. M. D. & Logtestijn, R. S. P. V., 1994. Denitrification in the top soil of managed grasslands in The Netherlands in relation to soil type and fertilizer level. *Plant and Soil ,* Volume 163, p. 33–44 doi: https://doi.org/10.1007/BF00033938.

Klimentos, T. & McCann, C., 1990. Relationships among compressional wave attenuation, porosity, clay content, and permeability in sandstones. *Geophysics,* 55(8), p. 998–1014 doi: https://doi.org/10.1190/1.1442928.

Kloppmann, W., Dever, L. & Edmunds, W. M., 1998. Residence time of Chalk groundwaters in the Paris Basin and the North German Basin: a geochemical approach. *Applied Geochemistry ,* 13(5), pp. 593-606 doi: https://doi.org/10.1016/S0883-2927(97)00110-8.

Knorr, K.-H. & Blodau, C., 2009. Impact of experimental drought and rewetting on redox transformations and methanogenesis in mesocosms of a northern fen soil. *Soil Biology and Biochemistry,* 41(6), pp. 1187-1198 doi: https://doi.org/10.1016/j.soilbio.2009.02.030.

Kooijman, A. & Hedenäs, L., 2009. Changes in nutrient availability from calcareous to acid wetland habitats with closely related brown moss species: increase instead of decrease in N and P. *Plant and Soil,* Volume 324, pp. 267-278.

Koreselamn, W., Verhoven, M. B. V. K. & A., J. T., 1993. Release of inorganic N, P and K in peat soils; effect of temperature, water chemistry and water level. *Biogeochemistry,* Volume 20, pp. 63-81.

Koskinen, M. et al., 2017. Restoration of nutrient-rich forestry-drained peatlands poses a risk for high exports of dissolved organic carbon, nitrogen, and phosphorus. *Science of the Total Environment ,* Volume 586, pp. 858-869.

Koskinen, M. et al., 2017. Restoration of nutrient-rich forestry-drained peatlands poses a risk for high exports of dissolved organic carbon, nitrogen, and phosphorus. *Science of the Total Environment ,* Volume 586, pp. 858-869.

Kreiling, R. M. et al., 2015. Effects of Flooding on Ion Exchange Rates in an Upper Mississippi River Floodplain Forest Impacted by Herbivory, Invasion, and Restoration. *Wetlands,* 35(5), p. 1005–1012.

Kull, A. et al., 2008. The effects of fluctuating climatic conditions and weather events on nutrient dynamics in a narrow mosaic riparian peatland. *Boreal Environmental Research ,* 13(3), pp. 243-263.

Kuusemets, V., Mander, Ü., Lõhmus, K. & Ivask, M., 2001. Nitrogen and phosphorus variation in shallow groundwater and assimilation in plants in complex riparian buffer zones. *Water Science & Technology,* 44(11-12), p. 615–622.

Lapworth, D. J., Gooddy, D. C., Allen, D. & Old, G. H., 2009. Understanding groundwater, surface water, and hyporheic zone biogeochemical processes in a Chalk catchment using fluorescence properties of dissolved and colloidal organic matter. *Journal of Geophysical Research ,* 114(G3), p. G00F02 doi: 10.1029/2009JG000921.

Lapworth, D. J. et al., 2008. Groundwater nitrogen composition and transformation within a moorland catchment, mid-Wales. *Science of The Total Environment,* 390(1), pp. 241-254 doi: https://doi.org/10.1016/j.scitotenv.2007.09.043.

Lee, L. J. E., Lawrence, D. S. L. & Price, M., 2006. Analysis of water-level response to rainfall and implications for recharge pathways in the Chalk aquifer, SE England. *Journal of Hydrology,* 330(3-4), pp. 604-620 doi: https://doi.org/10.1016/j.jhydrol.2006.04.025.

Leeson, S. R. et al., 2017. Nitrous oxide emissions from a peatbog after 13 years of experimental nitrogen deposition. *Biogeosciences,* 14(24), pp. 5753-5764 doi: 10.5194/bg-14-5753-2017.

Legendre, P. & Legendre, L., 1998. *Numerical Ecology.* 20 ed. Amsterdamn: Elsevier .

Lehmann, M. F., Sigman, D. M. & Berelson, W. M., 2004. Coupling the 15N/14N and 18O/16O of nitrate as a constraint on benthic nitrogen cycling. *Marine Chemistry,* 88(1-2), pp. 1-20 doi: https://doi.org/10.1016/j.marchem.2004.02.001.

Leroy, F. et al., 2019. Response of C and N cycles to N fertilization in Sphagnum and Molinia-dominated peat mesocosms. *Journal of Environmental Sciences ,* Volume 77, pp. 264-272 doi: https://doi.org/10.1016/j.jes.2018.08.003.

Levy, P. E. et al., 2020. *Sulphur and nitrogen atmospheric Concentration Based Estimated Deposition (CBED) data for the UK 2016-2018.,* Lancaster: NERC Environmental Information Data Centre https://doi.org/10.5285/5999d471-fe1d-45fa-889d-3156edb785a7.

Lewis, J. W. M., Wurtsbaugh, W. A. & Paerl, H. W., 2011. Rationale for Control of Anthropogenic Nitrogen and Phosphorus to Reduce Eutrophication of Inland Waters. *Environmental Science & Technology,* 45(24), pp. 10300-10305 doi: https://doi.org/10.1021/es202401p.

Li, D. et al., 2020. Source and Quality of Groundwater Surrounding the Qinghai Lake, NE Qinghai-Tibet Plateau. *Groundwater,* p. https://doi.org/10.1111/gwat.13042.

Liimatainen, M. et al., 2018. Factors controlling nitrous oxide emissions from managed northern peat soils with low carbon to nitrogen ratio. *Soil Biology and Biochemistry,* Volume 122, pp. 186-195 doi: https://doi.org/10.1016/j.soilbio.2018.04.006.

Lindau, C. W. et al., 1999. Modelling Urea, Ammonium, and Nitrate Transport and Transformations in Flooded Soil Columns. *Soil Science ,* 164(2), pp. 123-132.

Lind, L. P. D., Audet, J., Tonderski, K. & Hoffmann, C. C., 2013. Nitrate removal capacity and nitrous oxide production in soil profiles of nitrogen loaded riparian wetlands inferred by laboratory microcosms. *Soil Biology & Biochemistry,* Volume 60, pp. 156-164 doi: https://doi.org/10.1016/j.soilbio.2013.01.021.

Lohila, A. et al., 2010. Responses of N2O fluxes to temperature, water table and N deposition in a northern boreal fen. *European Journal of Soil Science, Special Issue: Nitrogen and greenhouse gas exchange,* 61(5), pp. 651-661 doi: https://doi.org/10.1111/j.1365-2389.2010.01265.x.

Lovley, D. R. & Phillips, E. J. P., 1986. Organic Matter Mineralization with Reduction of Ferric Iron in Anaerobic Sediments. *Applied and Environmental Microbiology,* 51(4), pp. 683-689 doi: https://doi.org/10.1128/aem.51.4.683-689.1986.

Lovley, D. R. & Phillips, E. J. P., 1988. Novel Mode of Microbial Energy Metabolism: Organic Carbon Oxidation Coupled to Dissimilatory Reduction of Iron or Manganese. *Applied and Environmental Microbiology ,* 54(6), pp. 1472-1480 doi: https://doi.org/10.1128/aem.54.6.1472-1480.1988.

Low, R. et al., 2012. *Groundwater abstraction impact and long-term vegetation community survival in Greywell Fen.* Birmingham and Midland Institute, Groundwater Dependent Ecosystems.

Low, R. et al., 2012. *Ecohydrological impact assessment, Greywell Fen, Hampshire.* Birmingham and Midland Institute, Birmingham, The Geological Society's 'Groundwater Dependent Ecosystems' conference.

Lucassen, E. C. H. E. T., Smolders, A. J. P., Salm, A. L. v. d. & Roelofs, J. G. M., 2004. High groundwater nitrate concentrations inhibit eutrophication of sulphate-rich freshwater wetlands. *Biogeochemistry,* Volume 67, p. 249–267 doi: https://doi.org/10.1023/B:BIOG.0000015342.40992.cb.

Lundin, L. et al., 2017. Impacts of rewetting on peat, hydrology and water chemical composition over 15 years in two finished peat extraction areas in Sweden. *Wetlands Ecology and Management,* Volume 25, p. 405–419.

MacDonald, A. M. & Allen, D. J., 2001. Aquifer properties of the Chalk of England. *Quarterly Journal of Engineering Geology and Hydrogeology,* Volume 34, pp. 371-384 doi: https://doi.org/10.1144/qjegh.34.4.371.

MacNally, R., 1997. Scaling artefacts in confinement experiments: a simulation model. *Ecological Modelling,* 99(2-3), pp. 229-245.

Macrae, M. L., Devito, K. J., Strack, M. & Waddington, J. M., 2013. Effect of water table drawdown on peatland nutrient dynamics: implications for climate change. *Biogeochemistry,* Volume 112, p. 661–676.

Maher, M., Prasad, M. & Raviv, M., 2008. Chapter 11 - Organic Soilless Media Components . In: M. Raviv, H. Lieth & A. Bar-Tal, eds. *Soilless Culture: Theory and Practice .* Cambridge, Massachusetts, United States: Academic Press, pp. 459-504 doi: https://doi.org/10.1016/B978-044452975-6.50013-7.

Martens, D. A., 2005. Denitrification. In: D. Hillel, ed. *Encyclopedia of Soils in the Environment.* Cambridge, United States: Academic Press, pp. 378-382.

Martikainen, P. J., Nykänen, H., Crill, P. & Silvola, J., 1993. Effect of a lowered water table on nitrous oxide fluxes from northern peatlands. *Nature,* Volume 366, p. 51–53 doi: https://doi.org/10.1038/366051a0.

Martinl, H., Ivanoff, D. B., Graetz, D. A. & Reddy, K. R., 1997. Water Table Effects on Histosol Drainage Water Carbon, Nitrogen, and Phosphorus. *Journal of Enivronmental Quality ,* 26(4), pp. 1062-1071 doi: https://doi.org/10.2134/jeq1997.00472425002600040018x.

Maslov, M. N. & Maslova, O. A., 2020. Temperate peatlands use-management effects on seasonal patterns of soil microbial activity and nitrogen availability. *CATENA,* Volume 190, p. 104548 doi: https://doi.org/10.1016/j.catena.2020.104548.

Matamoros, V., 2012. 1.13 - Equipment for Water Sampling Including Sensors. In: J. Pawliszyn, ed. *Comprehensive Sampling and Sample Preparation Vol.1 .* Cambridge, United States: Academic Press, pp. 247-263 doi: https://doi.org/10.1016/B978-0-12-381373-2.00013-2.

Matheson, F. E. et al., 2002. Fate of 15N-nitrate in unplanted, planted and harvested riparian wetland soil microcosms. *Ecological Engineering,* 19(4), pp. 249-264 doi: https://doi.org/10.1016/S0925-8574(02)00093-9.

Mazlum, N., Ozer, A. & Mazlum, S., 1999. Interpretation of Water Quality Data by Principal Components Analysis. *Turkish Journal of Engineering and Environmental Sciences,* Volume 23, p. 19–26.

McDermott-Kurtz, A., Bahr, J. M., Carpenter, Q. J. & Hunt, R. J., 2007. The importance of subsurface geology for water source and vegetation communities in Cherokee Marsh, Wisconsin. *Wetlands,* Volume 27, pp. 189–202 doi: https://doi.org/10.1672/0277-5212(2007)27[189:TIOSGF]2.0.CO;2.

Meng, X. et al., 2023. Methane and Nitrous Oxide Emissions from a Temperate Peatland under Simulated Enhanced Nitrogen Deposition. *Sustainability,* 15(2), p. 1010 doi: https://doi.org/10.3390/su15021010.

Merrill, A. G. & Zak, D. R., 1992. Factors controlling denitrification rates in upland and swamp forests. *Canadian Journal of Forest Research,* 22(11), pp. 1597-1604 doi: https://doi.org/10.1139/x92-212.

Mertler, C. A., Vannatta, R. A. & LaVenia, K. N., 2021. *Advanced and Multivariate Statistical Methods: Practical Application and Interpretation.* 7 ed. New York: Routledge.

Messer, T. L., Burchell, M. R., Böhlke, J. K. & R.Tobias, C., 2017. Tracking the fate of nitrate through pulse-flow wetlands: A mesocosm scale 15N enrichment tracer study. *Ecological Engineering ,* 106 (Part A), pp. 597-608 doi: https://doi.org/10.1016/j.ecoleng.2017.06.016.

Mettrop, I. S., Cusell, C., Kooijman, A. M. & Lamers, L. P. M., 2014. Nutrient and carbon dynamics in peat from rich fens and Sphagnum-fens during different gradations of drought. *Soil Biology and Biochemistry,* Volume 68, pp. 317-328 doi: https://doi.org/10.1016/j.soilbio.2013.10.023.

Miller, J. J., Bremer, E., Curtis, T. & Chanasyk, D. S., 2015. An assessment of nutrient dynamics in streambank soils of the Lower Little Bow River in southern Alberta using ion exchange membranes. *Water Quality Research Journal,* 52(3), p. 196–208.

Miner, G., 2006. *Standard Methods for the Examination of Water and Wastewater.* 21st ed. Denver: American Water Works Association. Journal.

Mitchell, C. P. J. & Branfireun, B. A., 2005. Hydrogeomorphic Controls on Reduction–Oxidation Conditions across Boreal Upland–Peatland Interfaces. *Ecosystems ,* Volume 8, pp. 731–747 doi: https://doi.org/10.1007/s10021-005-1792-9.

Moal, M. L. et al., 2019. Eutrophication: A new wine in an old bottle?. *Science of the Total Environment,* 651(Part 1), pp. 1-11 doi: https://doi.org/10.1016/j.scitotenv.2018.09.139.

Moon, J. B. et al., 2020. Variation in surface and subsurface nitrogen cycling in headwater floodplain wetlands due to soil type and wetland condition. *Wetlands Ecology and Management volume,* Volume 28, p. 727–751.

Moore, J., Bird, D. L., Dobbis, S. K. & Woodward, G., 2017. Nonpoint Source Contributions Drive Elevated Major Ion and Dissolved Inorganic Carbon Concentrations in Urban Watersheds. *Environmental Science & Technology Letters,* 4(6), p. 198–204.

Morris, P. J., Waddington, J. M., Benscoter, B. W. & Turetsky, M. R., 2011. Conceptual frameworks in peatland ecohydrology: looking beyond the two-layered (acrotelm–catotelm) model. *Ecohydrology,* 4(1), pp. 1-11 doi: https://doi.org/10.1002/eco.191.

Mugasha, A. G. & Pluth, D. J., 1995. Ammonia loss following surface application of urea fertilizer to undrained and drained forested minerotrophic peatland sites in central Alberta, Canada. *Forest Ecology and Management,* 78(1-3), pp. 139-145 doi: https://doi.org/10.1016/0378-1127(95)03585-7.

Mulot, M., Villard, A., Varidel, D. & Mitchell, E. A. D., 2015. A mesocosm approach to study the response of Sphagnum peatlands to hydrological changes: Setup, optimisation and performance. *Mires and Peat,* Volume 16, pp. 1-12 .

Muñoz-Leoz, B., Antigüedad, I., Garbisu, C. & Ruiz-Romera, E., 2011. Nitrogen transformations and greenhouse gas emissions from a riparian wetland soil: An undisturbed soil column study. *Science of The Total Environment ,* 409(4), pp. 763-770.

Mwagona, P. C., Yao, Y., Yuanqi, S. & Yu, H., 2019. Laboratory study on nitrate removal and nitrous oxide emission in intact soil columns collected from nitrogenous loaded riparian wetland, Northeast China. *PLOS one,* 14(3), p. e0214456. doi: https://doi.org/10.1371/journal.pone.0214456.

Natural England, 1984. *Greywell Fen SSSI.* [Online] Available at: https://designatedsites.naturalengland.org.uk/SiteDetail.aspx?SiteCode=S1000282&SiteName=grey

well&countyCode=&responsiblePerson=&SeaArea=&IFCAArea=
[Accessed 17 April 2020].

Natural England, 2018. *Designated Sites View, Greywell Fen SSSI.* [Online]
Available at:
https://designatedsites.naturalengland.org.uk/SiteDetail.aspx?SiteCode=S1000282&SiteName=grey
well&county
[Accessed 19 03 2021].

Natural England, 2021. *Favourable Conservation Status Definitions: Natural England Technical Information Note,* York: TIN180 Natural England.

Natural England, 2022. *Designated Sites View: SSSI Condition Summary.* [Online]
Available at:
https://designatedsites.naturalengland.org.uk/ReportUnitConditionSummary.aspx?SiteCode=S1000
282&ReportTitle=Greywell%20Fen%20SSSI
[Accessed 19 04 2023].

Neal, C. et al., 2006. Nitrate concentrations in river waters of the upper Thames and its tributaries. *Science of the Total Environment,* 365(1-3), pp. 15-32 doi: https://doi.org/10.1016/j.scitotenv.2006.02.031.

Nelson, W. M., Gold, A. J. & Groffman, P. M., 1995. Spatial and Temporal Variation in Groundwater Nitrate Removal in a Riparian Forest. *Journal of Environmental Quality ,* 24(4), pp. 691-699 doi: https://doi.org/10.2134/jeq1995.00472425002400040021x.

Niedermeier, A. & Robinson, J. S., 2007. Hydrological controls on soil redox dynamics in a peat-based, restored wetland. *Geoderma,* 137(3-4), pp. 318-326 doi: https://doi.org/10.1016/j.geoderma.2006.08.027.

Nykänen, H., Vasander, H., Huttunen, J. T. & Martikainen, P. J., 2002. Effect of experimental nitrogen load on methane and nitrous oxide fluxes on ombrotrophic boreal peatland. *Plant & Soil ,* Volume 242, p. 147–155 doi: https://doi.org/10.1023/A:1019658428402.

Paludan, C. & Blicher-Mathiesen, G., 1996. Losses of inorganic carbon and nitrous oxide from a temperate freshwater wetland in relation to nitrate loading. *Biogeochemistry ,* Volume 35, p. 305–326 doi: https://doi.org/10.1007/BF02179957.

Pan, H. et al., 2020. Biogeographical distribution of dissimilatory nitrate reduction to ammonium (DNRA) bacteria in wetland ecosystems around the world. *Journal of Soils and Sediments ,* Volume 20, p. 3769–3778.

Pan, W. et al., 2016. Dissimilatory microbial iron reduction release DOC (dissolved organic carbon) from carbon-ferrihydrite association. *Soil Biology and Biochemistry ,* Volume 103, pp. 232-240.

Paulissen, M. P. C. P., Ven, P. J. M. V. D., Dees, A. J. & Bobbink, R., 2004. Differential effects of nitrate and ammonium on three fen bryophyte species in relation to pollutant nitrogen input. *New Phytologist ,* 164(3), pp. 451-458 https://doi.org/10.1111/j.1469-8137.2004.01196.x.

Peach, D. W. et al., 2006. *Hydrogeology and hydrochemistry of the Pang and Lambourn catchments,* Nottingham: British Geological Survey Commissioned Report CR/06/46N.

Pieterse, N. M., Venterink, H. O., Schot, P. P. & Verkroost, A. W. M., 2005. Is nutrient contamination of groundwater causing eutrophication of groundwater-fed meadows. *Landscape Ecology,* Volume 20, pp. 743–753 doi: 10.1007/s10980-005-1436-7.

Pinay, G. & Decamps, H., 1988. The role of riparian woods in regulating nitrogen fluxes between the alluvial aquifer and surface water: A conceptual model. *Regulated Rivers: Research & Management,* 2(4), pp. 507-516 doi: https://doi.org/10.1002/rrr.3450020404.

Pinay, G., Roques, L. & Fabre, A., 1993. Spatial and Temporal Patterns of Denitrification in a Riparian Forest. *Journal of Applied Ecology,* 30(4), pp. 581-591 doi: https://doi.org/10.2307/2404238.

Pinay, G., Ruffinoni, C. & Fabre, A., 1995. Nitrogen cycling in two riparian forest soils under different geomorphic conditions. *Biogeochemistry,* Volume 30, p. 9–29 doi: https://doi.org/10.1007/BF02181038.

Potila, H. & Sarjal, T., 2004. Seasonal fluctuation in microbial biomass and activity along a natural nitrogen gradient in a drained peatland. *Soil Biology and Biochemistry ,* 36(7), pp. 1047-1055 doi: https://doi.org/10.1016/j.soilbio.2004.02.014.

Pratt, P. F., 1951. Potassium removal from Iowa soils by greenhouse and laboratory procedures. *Soil Science,* 72(2), pp. 107-118.

Price, M., Low, R. G. & McCann, C., 2000. Mechanisms of water storage and flow in the unsaturated zone of the Chalk aquifer. *Journal of Hyrology ,* 223(1-4), pp. 54-71.

Prior, H. & Johnes, P. J., 2002. Regulation of surface water quality in a Cretaceous Chalk catchment, UK: an assessment of the relative importance of instream and wetland processes. *Science of The Total Environment,* Volume 282-283, pp. 159-174 doi: https://doi.org/10.1016/S0048-9697(01)00950-0.

Proctor, M. C. F., 1994. Seasonal and Shorter-Term Changes in Surface-Water Chemistry on Four English. *Journal of Ecology,* 82(3), pp. 597-610 doi: https://doi.org/10.2307/2261267.

Qian, P. & Schoenau, J. J., 2002. Practical applications of ion exchange resins in agricultural and environmental soil research. *Candian Journal of Soil Science ,* 82(1), pp. 9-21, https://doi.org/10.4141/S00-091.

Quinton, W. L., Gray, D. M. & Marsh, P., 2000. Subsurface drainage from hummock-covered hillslopes in the Arctic tundra. *Journal of Hydrology ,* Volume 237, p. 113–125.

Rajta, A., Bhatia, R., Setia, H. & Pathania, P., 2019. Role of heterotrophic aerobic denitrifying bacteria in nitrate removal from wastewater. *Journal of Applied Microbiology,* 128(5), pp. 1261-1278 doi: https://doi.org/10.1111/jam.14476.

Ramsar Convention on Wetlands, 2018. *Global Wetland Outlook: State of the World's Wetlands and their Services to People.,* Gland, Switzerland: Ramsar Convention Secretariat.

Rapson, T. D. & Dacres, H., 2014. Analytical techniques for measuring nitrous oxide. *TrAC Trends in Analytical Chemistry,* Volume 54, pp. 65-74 doi: https://doi.org/10.1016/j.trac.2013.11.004.

Rascio, N. & Rocca, N. L., 2008. Biological Nitrogen Fixation. In: *Encyclopedia of Ecology.* Cambridge, United States : Academic Press, pp. 412-419.

Ratcliffe, D. A., 1977. *A Nature Conservation Review..* Cambridge: Cambridge University Press.

Reddy, K. R. & DeLaune, R. D., 2008. *Biogeochemistry of Wetlands.* 1st Edition ed. Boca Raton: Science and Applications doi: https://doi.org/10.1201/9780203491454.

Reeder, S. W., Hitchon, B. & Levinson, A. A., 1972. Hydrogeochemistry of the surface waters of the Mackenzie River drainage basin, Canada—I. Factors controlling inorganic composition. *Geochimica et Cosmochimica Acta,* 36(8), pp. 825-865 doi: https://doi.org/10.1016/0016-7037(72)90053-1.

Reeve, A. S., Siegel, D. I. & H.Glaser, P., 1996. Geochemical controls on peatland pore water from the Hudson Bay Lowland: a multivariate statistical approach. *Journal of Hydrology ,* 181(1-4), pp. 285-304 doi: https://doi.org/10.1016/0022-1694(95)02900-1.

Regina, K., Nykänen, H., Silvola, J. & Martikainen, P. J., 1996. Fluxes of nitrous oxide from boreal peatlands as affected by peatland type, water table level and nitrification capacity. *Biogeochemistry ,* Volume 35, p. 401–418 doi: https://doi.org/10.1007/BF02183033.

Regina, K., Silvola, J. & Martikainen, P. J., 1999. Short-term effects of changing water table on N2O fluxes from peat monoliths from natural and drained boreal peatlands. *Global Change Biology,* 5(2), pp. 183-189 doi: https://doi.org/10.1046/j.1365-2486.1999.00217.x.

Reynolds, B., Stevens, P. A., Hughes, S. & Brittain, S. A., 2004. Comparison of field techniques for sampling soil solution in an upland peatland. *Soil Use and Management ,* 20(4), pp. 454-456.

Rezanezhad, F. et al., 2017. The Role of Pore Structure on Nitrate Reduction in Peat Soil: A Physical Characterization of Pore Distribution and Solute Transport. *Wetlands,* Volume 37, p. 951–960.

Rezanezhad, F., Price, J. S. & Craig, J. R., 2012. The effects of dual porosity on transport and retardation in peat: A laboratory experiment. *Canadian Journal of Soil Science,* 92(5), pp. 723-732.

Rezanezhad, F. et al., 2016. Structure of peat soils and implications for water storage, flow and solute transport: A review update for geochemists. *Chemical Geology ,* Volume 429, pp. 75-84.

Rezanezhad, F. et al., 2016. Structure of peat soils and implications for water storage, flow and solute transport: A review update for geochemists. *Chemical Geology,* Volume 429, pp. 75-84 doi: https://doi.org/10.1016/j.chemgeo.2016.03.010.

Riet, B. P. v. d., Hefting, M. M. & Verhoeven, J. T. A., 2013. Rewetting Drained Peat Meadows: Risks and Benefits in Terms of Nutrient Release and Greenhouse Gas Exchange. *Water, Air, & Soil Pollution,* 224(4), pp. Article number: 1440 doi: 10.1007/s11270-013-1440-5.

Rippy, J. F. M. & Nelson, P. V., 2007. Cation Exchange Capacity and Base Saturation Variation among Alberta, Canada, Moss Peats. *HortScience,* 42(2), p. :349–352 doi: https://doi.org/10.21273/HORTSCI.42.2.349.

Rivett, M. O. et al., 2008. Nitrate attenuation in groundwater: A review of biogeochemical controlling processes. *Water Research,* 42(16), pp. 4215-4232 doi: https://doi.org/10.1016/j.watres.2008.07.020Get rights and content.

Robertson, E. K. & Thamdrup, B., 2017. The fate of nitrogen is linked to iron(II) availability in a freshwater lake sediment. *Geochimica et Cosmochimica Acta,* Volume 205, pp. 84-99 doi: https://doi.org/10.1016/j.gca.2017.02.014.

Rodwell, J. S., 1991. *British Plant Communities.* Vol. 1-5 ed. Peterborough, UK: Joint Nature Conservation Committe.

Rogora, M., Mosello, R. & Arisci, S., 2003. The Effect of Climate Warming on the Hydrochemistry of Alpine Lakes. *Water, Air, and Soil Pollution,* Volume 148, p. 347–361 doi: https://doi.org/10.1023/A:1025489215491.

Roobroeck, D., Butterbach-Bahl, K., Brüggemann, N. & Boeckx, P., 2010. Dinitrogen and nitrous oxide exchanges from an undrained monolith fen: short-term responses following nitrate addition. *European Journal of Soil Science, Special Issue: Nitrogen and greenhouse gas exchange,* 61(5), pp. 662-670 doi: https://doi.org/10.1111/j.1365-2389.2010.01269.x.

Roulet, N. T., 1990. Hydrology of a headwater basin wetland: Groundwater discharge and wetland maintenance. *Hydrological Processes ,* 4(4), pp. 387-400 doi: https://doi.org/10.1002/hyp.3360040408.

Rowland, C. et al., 2017. *Land Cover Map 2015 (vector, GB) ,* Swindon: NERC Environmental Information Data Centre.

Roy, E. D. & White, J. R., 2013. Methods in Biogeochemistry of Wetlands, Volume 10. In: R. DeLaune, K. Reddy, C. Richardson & J. Megonigal, eds. *Measurements of Nitrogen Mineralization Potential in Wetland Soils.* Madison: Soil Science Society of America, pp. 465-475.

Rückauf, U., Augustin, J., Russow, R. & Merbach, W., 2004. Nitrate removal from drained and reflooded fen soils affected by soil N transformation processes and plant uptake. *Soil Biology and Biochemistry,* 36(1), pp. 77-90 doi: https://doi.org/10.1016/j.soilbio.2003.08.021.

Rummel, R. J., 1980. *Applied factor analysis.* Evanston, Illnois : Northwestern University Press.

Ruser, R. et al., 2006. Emission of N2O, N2 and CO2 from soil fertilized with nitrate: effect of compaction, soil moisture and rewetting. *Soil Biology and Biochemistry,* 38(2), pp. 263-274 doi: https://doi.org/10.1016/j.soilbio.2005.05.005.

Sabater, S. et al., 2003. Nitrogen Removal by Riparian Buffers along a European Climatic Gradient: Patterns and Factors of Variation. *Ecosystems ,* Volume 6, pp. 0020–0030 doi: https://doi.org/10.1007/s10021-002-0183-8.

Salmon, R. C., 2006. Cation Exchange Reactions. *Journal of Soil Science,* 15(2), pp. 273-283 doi: https://doi.org/10.1111/j.1365-2389.1964.tb02225.x.

Sánchez-Pérez, J. M. et al., 2003. A standardised method for measuring in situ denitrification in shallow aquifers: numerical validation and measurements in riparian wetlands. *Hydrology and Earth System Science,* 7(1), pp. 87–96 doi: https://doi.org/10.5194/hess-7-87-2003.

Sanderson, N. A., 2003. *Vegetation Survey of Greywell Moors Reserve ,* Curdridge: Report for Hampshire and Isle of Wight Wildlife Trust. Unpublished .

Sandrin, T. R., Herman, D. C. & Maier, R. M., 2009. Chapter 11: Physiological Methods. In: R. M. Maier, I. L. Pepper & C. P. Gerba, eds. *Environmental Microbiology (Second Edition).* Cambridge, United States : Academic Press, pp. 191-223.

Sanford, R. F., Pierson, C. T. & Crovelli, R. A., 1993. An objective replacement method for censored geochemical data. *Mathematical Geology ,* Volume 25, p. 59–80 doi: https://doi.org/10.1007/BF00890676.

Sasikala, S., Tanaka, N., Wah, H. S. Y. W. & Jinadasa, K. B. S. N., 2009. Effects of water level fluctuation on radial oxygen loss, root porosity, and nitrogen removal in subsurface vertical flow wetland mesocosms. *Ecological Engineering ,* 35(3), pp. 410-417.

Saunders, D. & Kalff, J., 2001. Nitrogen retention in wetlands, lakes and rivers. *Hydrobiologia,* Volume 443, p. 205–212 doi: https://doi.org/10.1023/A:1017506914063.

Saxena, A. et al., 2017. A review of clustering techniques and developments. *Neurocomputing,* Volume 267, pp. 664-681 doi: https://doi.org/10.1016/j.neucom.2017.06.053.

Scott, J. T., McCarthy, M. J., Gardner, W. S. & Doyle, R. D., 2008. Denitrification, dissimilatory nitrate reduction to ammonium, and nitrogen fixation along a nitrate concentration gradient in a created freshwater wetland. *Biogeochemistry ,* Volume 87, pp. 99-111 doi: https://doi.org/10.1007/s10533-007-9171-6.

Seeberg-Elverfeldt, J., Schlüter, M., Feseker, T. & Kölling, M., 2005. Rhizon sampling of porewaters near the sediment-water interface of aquatic systems. *Limnology and Oceanography: Methods,* Volume 3, p. 361–371.

Seitzinger, S. P., 1994. Linkages between organic matter mineralization and denitrification in eight riparian wetlands. *Biogeochemistry ,* Volume 25, p. 19–39 doi: https://doi.org/10.1007/BF00000510.

Shand, P. et al., 2003. *Baseline Series Report 6: The Chalk of the Colne and Lee River catchments,* s.l.: British Geological Survey Commissioned Report CR/03/069N & Environment Agency Report NC/99/74/6.

Silvan, N. et al., 2002. Gaseous nitrogen loss from a restored peatland buffer zone. *Soil Biology and Biochemistry ,* 34(5), pp. 721-728 doi: https://doi.org/10.1016/S0038-0717(02)00002-0.

Šimek, M., Elhottová, D., Klimeš, F. & Hopkins, D. W., 2004. Emissions of N2O and CO2, denitrification measurements and soil properties in red clover and ryegrass stands. *Soil Biology and Biochemistry ,* 36(1), pp. 9-21 doi: https://doi.org/10.1016/j.soilbio.2003.08.010.

Smedley, P. L. et al., 2003. *Baseline Series Report 5: The Chalk of the North Downs, kent and East Surrey,* s.l.: British Geological Survey Commissioned Report CR/03/033N & Environment Agency Report NC/99/74/5.

Smedley, P., Neumann, I. & Farrell, R., 2004. *Baseline Series Report 10: The The Chalk aquifer of Yorkshire and Nortth Humberside,* s.l.: British Geological Survey Commissioned Report CR/04/128N & Environment Agency Report NC/99/74/10.

Smith, K. A. et al., 1995. The measurement of nitrous oxide emissions from soil by using chambers. *Philosophical Transactions of the Royal Society of London A ,* 351(1696), pp. 327-338 doi: https://doi.org/10.1098/rsta.1995.0037.

Smolders, A. J. P. et al., 2007. Internal eutrophication: How it works and what to do about it—a review. *Chemistry and Ecology ,* 22(2), pp. 93-111.

Song, J., Luo, Y. M., Zhao, Q. G. & Christie, P., 2003. Novel use of soil moisture samplers for studies on anaerobic ammonium fluxes across lake sediment-water interfaces. *Chemosphere,* 50(6), pp. 711-715.

Sorensen, J. P. R., Butcher, A. S., Stuart, M. E. & Townsend, B. R., 2015. Nitrate fluctuations at the water table: implications for recharge processes and solute transport in the Chalk aquifer. *Hydrological Processes,* 29(15), pp. 3355-3367.

South East Water, 2005. *Whitewater Environmental Studies AMP4 RSA Programme: Inception Report,* Snodland, Kent : South East Water, Unpublished .

South East Water, 2019. *Greywell Fen SSSI: Interim Condition Analysis Report,* Snodland: Unpublished .

South East Water, 2020. *Greywell Fen SSSI vegetation and botanical monitoring report,* Snodland: Unpublished .

Spinoni, J. et al., 2018. Will drought events become more frequent and severe in Europe?. *International Journal of Climatolgly ,* 38(4), pp. 1718-1736 doi: https://doi.org/10.1002/joc.5291.

Stefanakis, A., Akratos, C. S. & Tsihrintzis, V. A., 2014. Treatment Processes in VFCWs. In: A. Stefanakis, C. S. Akratos & V. A. Tsihrintzis, eds. *Vertical Flow Constructed Wetlands: Eco-engineering Systems for Wastewater and Sludge Treatment.* Amsterdam: Elsevier, pp. 57-84.

Stein, E. D., Mattson, M., Fetscher, A. E. & Halama, K. J., 2004. Influence of geologic setting on slope wetland hydrodynamics. *Wetlands ,* Volume 24, pp. 244–260 doi: https://doi.org/10.1672/0277-5212(2004)024[0244:IOGSOS]2.0.CO;2.

Stephenson, G. L. et al., 1984. Spatial Distribution of Plankton in Enclosures of Three Sizes. *Canadian Journal of Fisheries and Aquatic Sciences,* 41(7), pp. 1048-1054.

Stuart, M. E. & Lapworth, D. J., 2016. Macronutrient status of UK groundwater: Nitrogen, phosphorus and organic carbon. *Science of the Total Environment ,* Volume 572, pp. 1543-1560.

Stuart, M. & Smedley, P., 2009. *Baseline groundwater chemistry: the Chalk aquifer of Hampshire,* s.l.: British Geological Survey Open Report OR/09/052.

Su, C. et al., 2020. Source characterization of nitrate in groundwater using hydrogeochemical and multivariate statistical analysis in the Muling-Xingkai Plain, Northeast China. *Environmental Monitoring and Assessment,* Volume 192, pp. Article number: 456 doi: https://doi.org/10.1007/s10661-020-08347-6.

Sullivan, B., 2015. *Building a vented static chamber and collar,* Reno: University of Nevada Reno.

Szalay, F. A. D., Batzer, D. P. & Resh, V. H., 1996. Mesocosm and Macrocosm Experiments to Examine Effects of Mowing Emergent Vegetation on Wetland Invertebrates. *Environmental Entomology,* 25(2), p. 303–309.

Tabachnick, B. G. & Fidell, L. S., 2007. *Using multivariate statistics.* Vol. 5 ed. Boston: Pearson Education.

Tauchnitz, N., Brumme, R., Bernsdorf, S. & Meissner, R., 2008. Nitrous oxide and methane fluxes of a pristine slope mire in the German National Park Harz Mountains. *Plant and Soil,* Volume 303, pp. 131–138 doi: https://doi.org/10.1007/s11104-007-9493-0.

Teuben, A. & Verhoef, H. A., 1992. Relevance of micro- and mesocosm experiments for studying soil ecosystem processes. *Soil Biology and Biochemistry,* 24(11), pp. 1179-1183.

Tiemeyer, B. et al., 2007. A comprehensive study of nutrient losses, soil properties and groundwater concentrations in a degraded peatland used as an intensive meadow – Implications for re-wetting. *Journal of Hydrology,* 345(1-2), pp. 80-101 https://doi.org/10.1016/j.jhydrol.2007.08.002.

Tietema, A. et al., 1993. Nitrogen cycling in acid forest soils subject to increased atmospheric nitrogen input. *Forest Ecology and Management,* 57(1-4), pp. 29-44 doi: https://doi.org/10.1016/0378-1127(93)90160-O.

Tobias, C. R. et al., 2001. Tracking the fate of a high concentration groundwater nitrate plume through a fringing marsh: A combined groundwater tracer and in situ isotope enrichment study. *Limnology and Oceanography,* 46(8), pp. 1977-1989 doi: https://doi.org/10.4319/lo.2001.46.8.19777.

Todorov, S. G., Siegel, D. I. & Costello, A. M., 2005. Microbial Fe(III) reduction in a minerotrophic wetland – geochemical controls and involvement in organic matter decomposition. *Applied Geochemistry,* 20(6), pp. 1120-1130 doi: https://doi.org/10.1016/j.apgeochem.2005.02.005.

Trepel, M. & Palmeri, L., 2002. Quantifying nitrogen retention in surface flow wetlands for environmental planning at the landscape-scale. *Ecological Engineering,* 19(2), pp. 127-140 doi: https://doi.org/10.1016/S0925-8574(02)00038-1.

Ulén, B., 1995. Episodic precipitation and discharge events and their influence on losses of phosphorus and nitrogen from tile drained arable fields. *Swedish Journal of Agricultural Research ,* 25(1), pp. 25-31.

van Haesebroeck, V., Boeye, D., Verhagen, B. & Verheyen, R. F., 1997. Experimental investigation of drought induced acidification in a rich fen soil. *Biogeochemistry,* Volume 37, p. 15–32.

VanZomeren, C. M., White, J. R. & DeLaune, R. D., 2012. Fate of Nitrate in Vegetated Brackish Coastal Marsh. *Soil Science Society of America Journal ,* 76(5), pp. 1919-1927 doi: https://doi.org/10.2136/sssaj2011.0385.

Venterink, H. O., Davidsson, T., Kiehl, K. & Leonardson, L., 2002. Impact of drying and re-wetting on N, P and K dynamics in a wetland soil. *Plant and Soil ,* Volume 243, p. 119–130 doi: 10.1023/A:1019993510737.

Verhoeven, J. T. A., Arheimer, B., Yin, C. & Hefting, M. M., 2006. Regional and global concerns over wetlands and water quality. *Trends in Ecology and Evolution,* 21(2), pp. 96-103 doi: https://doi.org/10.1016/j.tree.2005.11.015.

Vitt, D. H. & Chee, W.-L., 1990. The relationships of vegetation to surface water chemistry and peat chemistry in fens of Alberta, Canada. *Vegetatio,* Volume 89, p. 87–106 doi: https://doi.org/10.1007/BF00032163.

Wang, L. et al., 2016. The changing trend in nitrate concentrations in major aquifers due to historical nitrate loading from agricultural land across England and Wales from 1925 to 2150. *Science of the Total Environment ,* 542 (Part A), pp. 694-705.

Wang, M., Talbot, J. & Moore, T. R., 2018. Drainage and fertilization effects on nutrient availability in an ombrotrophic peatland. *Science of The Total Environment,* Volume 621, pp. 1255-1263.

Wang, S. et al., 2020. Hotspot of dissimilatory nitrate reduction to ammonium (DNRA) process in freshwater sediments of riparian zones. *Water Research ,* Volume 173, p. 115539 doi: https://doi.org/10.1016/j.watres.2020.115539.

Ward, M. H. et al., 2018. Drinking Water Nitrate and Human Health: An Updated Review. *International Journal of Environmental Research and Public Health,* 15(7), p. 1557 doi: 10.3390/ijerph15071557.

Watt, M., Silk, W. K. & Passioura, J. B., 2006. Rates of Root and Organism Growth, Soil Conditions, and Temporal and Spatial Development of the Rhizosphere. *Annals of Botany,* 97(5), p. 839–855.

Weber, G., Honecker, U., Jochen & Kubiniok, 2020. Nitrate dynamics in springs and headwater streams with agricultural catchments in southwestern Germany. *Science of the Total Enivronment ,* Volume 722, p. https://doi.org/10.1016/j.scitotenv.2020.137858.

Webster, K. L. & McLaughlin, J. W., 2010. Importance of the Water Table in Controlling Dissolved Carbon along a Fen Nutrient Gradient. *Soil Science Society of America ,* 74(6), pp. 2254-2266 doi: https://doi.org/10.2136/sssaj2009.0111.

Weller, D., Correll, D. & Jordan, T., 1994. Denitrification in riparian forests receiving agricultural discharges. In: W. J. Mitsch, ed. *Global Wetlands: Old World and New .* Amsterdam: Elsevier Science B.V., pp. 117-131.

Wellings, S. R. & Bell, J. P., 1980. Movement of water and nitrate in the unsaturated zone of Upper Chalk near Winchester, Hants., England. *Journal of Hydrology,* 48(1-2), pp. 119-136 doi: https://doi.org/10.1016/0022-1694(80)90070-0.

Weltzin, J. F. et al., 2001. Production and microtopography of bog bryophytes: response to warming and water-table manipulations. *Oecologia,* Volume 128, p. 557–565 doi: https://doi.org/10.1007/s004420100691.

West, A. J., 2012. Thickness of the chemical weathering zone and implications for erosional and climatic drivers of weathering and for carbon-cycle feedbacks. *Geology ,* 40(9), p. 811–814 doi: https://doi.org/10.1130/G33041.1.

Wetzel, R. G., 1992. Gradient-dominated ecosystems: sources and regulatory functions of dissolved organic matter in freshwater ecosystems. In: K. Salonen & R. I. J. T. Kairesalo, eds. *Dissolved Organic Matter in Lacustrine Ecosystems. Developments in Hydrobiology, vol 73..* Dordrecht: Springer, pp. 181–198 doi: https://doi.org/10.1007/978-94-011-2474-4_14.

Wetzel, R. G., 2001. Chapter 12: The Nitrogen Cycle. In: *Limnology (Third Edition) .* Cambridge, United States: Academic Press, pp. 205-237.

Wexler, S. K., Hiscock, K. M. & Dennis, P. F., 2012. Microbial and hydrological influences on nitrate isotopic composition in an agricultural lowland catchment. *Journal of Hydrology ,* Volume 468-469, pp. 85-93.

Weyer, C. et al., 2014. Catchments as heterogeneous and multi-species reactors: An integral approach for identifying biogeochemical hot-spots at the catchment scale. *Journal of Hydrology ,* 519(Part B), pp. 1560-1571 doi: https://doi.org/10.1016/j.jhydrol.2014.09.005.

Wheeler, B., Shaw, S. & Robertson, R., 1995. In: *Restoration of Temperate Wetlands.* Chichester: Wiley, p. 562.

Wieder, R. K. et al., 2019. Experimental nitrogen addition alters structure and function of a boreal bog: critical load and thresholds revealed. *Ecological Monographs,* 89(3), p. e01371 doi: https://doi.org/10.1002/ecm.1371.

Williams, B., Silcock, D. & Young, M., 1999. Seasonal dynamics of N in twoSphagnum moss species and the underlying peat treated with15NH4 15NO3. *Biogeochemistry ,* Volume 45, p. 285–302 doi: https://doi.org/10.1007/BF00993004.

Wood, M. E. et al., 2015. Spatial variation in nutrient dynamics among five different peatland types in the Alberta oil sands region. *Ecodrology ,* 9(4), pp. 688-699.

Worrall, F., Burt, T. & Adamson, J., 2003. Controls on the chemistry of runoff from an upland peat catchment. *Hydrological Processes ,* 17(10), pp. 1887-2098 doi: https://doi.org/10.1002/hyp.1244.

Xu, J., Morris, P. J., Liu, J. & Holden, J., 2018. PEATMAP: Refining estimates of global peatland distribution based on a meta-analysis. *CATENA,* Volume 160, pp. 134-140.

Xu, S., Kang, P. & Sun, Y., 2016. A stable isotope approach and its application for identifying nitrate source and transformation process in water. *Environmental Science and Pollution Research,* Volume 23, p. 1133–1148.

Yao, L., Chen, C., Liu, G. & Liu, W., 2018. Sediment nitrogen cycling rates and microbial abundance along a submerged vegetation gradient in a eutrophic lake. *Science of the Total Environment,* Volume 616-617, pp. 899-907 doi: https://doi.org/10.1016/j.scitotenv.2017.10.230.

Yates, C. A. et al., 2022. Determining patterns in the composition of dissolved organic matter in fresh waters according to land use and management. *Biogeochemistry,* pp. doi: https://doi.org/10.1007/s10533-022-00964-2.

Ye, R. & Horwath, W. R., 2016. Nitrous oxide uptake in rewetted wetlands with contrasting soil organic carbon contents. *Soil Biology and Biochemistry,* Volume 100, pp. 110-117 doi: https://doi.org/10.1016/j.soilbio.2016.06.009.

Yu, K., Laune, R. D. D. & Boeck, P., 2006. Direct measurement of denitrification activity in a Gulf coast freshwater marsh receiving diverted Mississippi River water. *Chemosphere,* 65(11), pp. 2449-2455 doi: https://doi.org/10.1016/j.chemosphere.2006.04.046.

Zajac, K. & Blodau, C., 2016. The fate of 15N-nitrate in mesocosms from five European peatlands differing in long-term nitrogen deposition rate. *Biogeosciences ,* Volume 13, p. 707–722.

Zak, D. & Gelbrecht, J., 2007. The mobilisation of phosphorus, organic carbon and ammonium in the initial stage of fen rewetting (a case study from NE Germany). *Biogeochemistry ,* Volume 85, p. 141–151.

Zak, D., McInnes, R. & Gelbrecht, J., 2011. Preface: Restoration, biogeochemistry and ecological services of wetlands. *Hydrobiologia,* Volume 1-4, pp. 674 doi: https://doi.org/10.1007/s10750-011-0783-4.

Zhang, J. et al., 1995. Water geochemistry of the rivers around the Taklimakan Desert (NW China): Crustal weathering and evaporation processes in arid land. *Chemical Geology ,* 119(1-4), pp. 225-237 doi: https://doi.org/10.1016/0009-2541(94)00088-P.

Zhang, Y., Shi, P., Song, J. & Li, Q., 2019. Application of Nitrogen and Oxygen Isotopes for Source and Fate Identification of Nitrate Pollution in Surface Water: A Review. *Applied Sciences ,* 9(1), p. 18 doi: https://doi.org/10.3390/app9010018.

Zhang, Z. & Furman, A., 2021. Soil redox dynamics under dynamic hydrologic regimes - A review. *Science of the Total Environment ,* Volume 763, p. 143026 https://doi.org/10.1016/j.scitotenv.2020.143026.

Zhao, Q. et al., 2021. Heavy metal contamination in soils from freshwater wetlands to salt marshes in the Yellow River Estuary, China. *Science of the Total Environment,* Volume 774, p. 145072 doi: https://doi.org/10.1016/j.scitotenv.2021.145072.

Zomeren, C. M. V., White, J. R. & Laune, R. D. D., 2012. Fate of Nitrate in Vegetated Brackish Coastal Marsh. *Soil Science Society of America Journal,* 76(5), pp. 1919-1927.